https://theses.gla.ac.uk/

Theses Digitisation:

https://www.gla.ac.uk/myglasgow/research/enlighten/theses/digitisation/

This is a digitised version of the original print thesis.

Copyright and moral rights for this work are retained by the author

A copy can be downloaded for personal non-commercial research or study, without prior permission or charge

This work cannot be reproduced or quoted extensively from without first obtaining permission in writing from the author

The content must not be changed in any way or sold commercially in any format or medium without the formal permission of the author

When referring to this work, full bibliographic details including the author, title, awarding institution and date of the thesis must be given

Enlighten: Theses
https://theses.gla.ac.uk/
research-enlighten@glasgow.ac.uk

TRACER APPLICATIONS OF RADIOCAESIUM IN A COASTAL MARINE ENVIRONMENT

Thesis submitted to the University of Glasgow in fulfilment of the requirements for the degree of Doctor of Philosophy

By

IAN GERARD MC KINLEY

AUGUST 1979

CHEMISTRY DEPARTMENT
UNIVERSITY OF GLASGOW
GLASGOW G12 8QQ

ProQuest Number: 10984294

All rights reserved

INFORMATION TO ALL USERS
The quality of this reproduction is dependent upon the quality of the copy submitted.

In the unlikely event that the author did not send a complete manuscript
and there are missing pages, these will be noted. Also, if material had to be removed,
a note will indicate the deletion.

ProQuest 10984294

Published by ProQuest LLC (2018). Copyright of the Dissertation is held by the Author.

All rights reserved.
This work is protected against unauthorized copying under Title 17, United States Code
Microform Edition © ProQuest LLC.

ProQuest LLC.
789 East Eisenhower Parkway
P.O. Box 1346
Ann Arbor, MI 48106 – 1346

Acknowledgements

I gratefully acknowledge the invaluable supervision ,encouragement and advice given by Dr.M.S.Baxter throughout this project.Special mention must also be made of the continual assistance and provision of counting facilities by Dr.W.Jack and the considerable aid given by Dr.A.B.MacKenzie on whose initial work much of this thesis is based.Thanks for assistance during this research are extended to Dr.T.Leatherland,the crew of R.V. Endrick II and the Clyde River Purification Board for provision of ship time,hydrographic data and aid in sample collection;Dr.D.J.Ellett and the Scottish Marine Biological Association for collection of samples and provision of hydrographic data;A.G.Ballantyne,K.MacKay,D.McKie and D. Thompson for occasional technical assistance;J.McKinley,S.Flynn and D. Quigley for programming aid and the Chemistry Dept. Electronic,Mechanical and Glassblowing Workshops for construction and maintenance of equipment. The advice and help of past and present members (and associates) of the Nuclear Geochemistry Group has contributed greatly to this work,of whom special thanks to John Campbell,Ron Crawford,Josephine Docherty,Nina Drndarsky,Tony Fallick,John Farmer,Gus MacKenzie,Fred Mackie,Asizan Saad, Jane Smith-Briggs,Mike Stenhouse and Dave Swan who provided a most congenial social and scientific environment.I am grateful to I.Durant for typing this manuscript and especially so to Linda Kemp for preparation of tables,diagrams,references,proof-reading and continual help over the period of this project.

This work would not have been possible without the support of my parents, family and friends to whom I owe an inestimable debt of gratitude.

Finally,I acknowledge the support of a N.E.R.C. grant for this project.

ABSTRACT

In this study radiocaesium is confirmed as a versatile tracer and its use is demonstrated in the investigation of a wide range of processes occuring in the coastal marine environment. By utilising an analogue model, radiocaesium transport from Windscale to the North Channel may be characterised by a 'residence half-time' of ~12 months compounded with a 'lag time' of ~6 months. This transport is, however, shown to be variable - in 1977 a greatly increased Atlantic influx to the Irish Sea through the St. George's Channel was evident, resulting in an accelerated radiocaesium transport rate northwards through the North Channel. By further use of this model, the waters of the Clyde Sea Area may be shown to have a 'residence half-time' of ~3 months with the lag between the North Channel site and the Clyde being ~1 month. Additionally, ~40% of the northwards water flux from the Irish Sea may be shown to pass through the Clyde Sea Area. Transport from the North Channel to the Minch is also shown to change considerably between 1976 (advection rate~5km/day) and 1977 (advection rate ~1.5 km/day) associated with a marked widening of the coastal water plume in the Hebridean Sea Area during this period.

Consideration of the spatial radiocaesium distribution indicates that the Clyde Sea Area may be regarded as homogeneous both horizontally and vertically thus justifying the analogue model analysis. Exceptions to this generality are the deep waters of Lochs Fyne and Goil where significant residence of water in restricted basins of these fjords is proven by the measured radiocaesium profiles. Detailed study of radiocaesium / depth profiles in Loch Goil over a period of 2 years allows examination of the annual mixing cycle in this loch. By this method it is seen that L.Goil is characterised by fast surface ($\lesssim$30 m.) exchange at all times with a limited barrier to vertical mixing developing in late spring and more extreme stratification evident in late autumn / early winter. From a one dimensional vertical diffusion treatment, Cs-134 transport through the early winter pycnocline may be characterised by $7 \lesssim K_z \lesssim 25$ $cm^2 sec^{-1}$.

From analysis of the radiocaesium distribution in sediment cores, sedimentation rates of 200, 530 and 640 mg $cm^{-2} y^{-1}$ may be calculated for the Loch Goil deep, shallow and Gareloch sites respectively. From the Cs-134 profile in the upper layers of these cores, surface turbation (probably due to benthic organisms)may be characterised by $2 \lesssim K \lesssim 24$, $K \gtrsim 92$ and $K \gtrsim 45$ $cm^2 y^{-1}$ respectively at these three sites.

While the Cs-137 profile in Holyloch sediment indicates an accumulation rate of ~600 mg $cm^{-2} y^{-1}$ below a surface mixed zone of ~4 cm depth, this site is anomalous in that the sediment contains Co-60 and Cs-134 derived from the nearby U.S.N. nuclear submarine base.

As radiocaesium is shown to have a coastal water residence time of ~950 y its treatment as a conservative water tracer is justified on the timescale of nearshore oceanographic processes. In addition, however, the observed concentration factor onto sediment (~250) is sufficient for it to be used in a range of sedimentary tracer applications.

By constructing a budget for Windscale released Cs-137, it may be seen that the major reservoirs of this nuclide are the immediate Windscale vicinity (1.8%), the rest of the Irish Sea (17.3%), the North Channel/Clyde Sea Area (2.0%), the North Sea (19.7%) and marine sediment (2.6%). After reduction of the radiocaesium inventory to account for radioactive decay, the balance may be attributed to radiocaesium lost from the coastal water system into the North Atlantic (37.3%).

From measurements of radiocaesium concentration factors for fish in the Clyde Sea Area, a maximal dose to a member of the public is calculated as ~11% of the I.C.R.P. limits at the time of maximum measured Cs-137 concentration in this area (April 1977) although the dose to a general critical group would be much smaller - ~2% of I.C.R.P. limits.

Finally, as the hydrographic data obtained from radiocaesium tracer experiments is demonstrated to be useful in many other areas of research, future developments of this technique are proposed and alternative locations for study are suggested.

INDEX

CHAPTER 1. INTRODUCTION

1.1 Tracer Theory 1

1.2 Radiotracer Applications 11

1.3 Radiocaesium as a Marine Environmental Tracer 28

1.4 Areas of Study 40

1.5 Aims of Research 50

CHAPTER 2. EXPERIMENTAL

2.1 Introduction 52

2.2 Counting Systems 55

2.3 Water Samples 71

2.4 Sediment and Biological Samples 83

2.5 Errors, Reproducibility and Sample Calculations 88

CHAPTER 3. THE CLYDE SEA AREA

3.1 Introduction 102

3.2 Spacial Distribution of Radiocaesium in the C.S.A. 104

3.3 Temporal Variations in the Radiocaesium Content of the C.S.A. 118

3.4 Summary 141

CHAPTER 4. THE NORTHERN SEA LOCHS

4.1 Introduction 144

4.2 Qualitative Description of Mixing in L.Goil 146

4.3 Water Mixing and Transport in L.Long 161

4.4 Quantitative Analysis of Mixing in L.Goil 166

4.5 Gareloch and L.Fyne 186

4.6 General Overview 190

CHAPTER 5. THE HEBRIDEAN SEA AREA

5.1 Introduction 191

5.2 Data for Summer 1976 193

5.3 Data for Summer 1977 204

5.4 General Conclusions 215

CHAPTER 6. SEDIMENTS

6.1 Introduction 217

6.2 Coring Methodology 218

6.3 L.Goil - Site 1 234

6.4 L.Goil - Site 2 and Gareloch 249

6.5 Holyloch 253

6.6 Practical Applications and General Results 257

6.7 Summary 260

CHAPTER 7. SYNTHETIC OVERVIEW

7.1 Introduction 263

7.2 Summary of Results 263

7.3 Geochemical Budget for Windscale-released ^{137}Cs 266

7.4 Practical Applications 275

7.5 Further Developments 284

REFERENCES 286

APPENDICES 304

APPENDIX I RESULTS TABULATION A1

I.1 Clyde Sea Area A2

I.2 L.Goil/L.Long Deep Sites A7

I.3 Additional Sea Loch Sites A44

I.4 Hebridean Sea Area A59

I.5 Sediment A78

I.6 Miscellaneous A88

APPENDIX II COMPUTER PROGRAMS A92

II.1 Box Model Program A92

II.2 Calculation and Presentation Program A98

LIST OF FIGURES

1.1 Simple 3 Box Chain Model 8

1.2 C-14 Ages of Deep Ocean Water 20

1.3 Temporal and Latitudinal Variations in Fallout 24

1.4 Windscale Radiocaesium Plume 33

1.5 Annual Cs-137 Output from Windscale 35

1.6 Monthly Radiocaesium Output from Windscale 36

1.7 Map of the Clyde Sea Area 41

1.8 Monthly Variation of D.O. in the Bottom Waters of L.Goil 44

1.9 Surface Sediments in the Northern Section of the C.S.A. 45

1.10 The Hebridean Sea Area 48

1.11 Summer Surface Currents in the Hebridean Sea 49

2.1 Block Diagram of Counting System 56

2.2 Direct Counting Spectra 61

2.3 NaI(Tl) Spectrum of 'KCFC' 62

2.4 Cs-137 Calibration Spectrum 64

2.5 Ge(Li) Spectrum of 'KCFC' 66

2.6 Water Filtration Rig 78

2.7 Craib Corer 84

2.8 Gravity Corer 84

2.9 X-Radiograph of Frozen Core 86

2.10 Ge(Li) Energy/Efficiency Curve 89

3.1 Location of Stations in the C.S.A. 103

3.2 Spacial Distribution of Radiocaesium in the C.S.A. 106

3.3 Vertical Profiles from Stations in the C.S.A. 107

3.4 Temporal Variations of Radiocaesium in the C.S.A. 109

3.5 Radiocaesium Data for the North Channel 112

3.6 Proposed Deep Currents in the C.S.A. 115

3.7 Radiocaesium Output from Windscale 125

3.8 1 Box Mixing Model Analogue Circuit 126

3.9 1 Box Model Output for Windscale Cs-137 127

3.10 Smoothed N.C. Radiocaesium Curve 129

3.11 Comparison of Observed and Modelled Curves for N.C. Cs-137 130

3.12 1 Box Model Output for Windscale Ratio 132

3.13 2 Box Model Output for Windscale Radiocaesium 136

3.14 1 Box Model for the North Channel 138

3.15 Comparison of Observed and Modelled Curves for the C.S.A. 140

4.1 Map of the Northern Sea Lochs 145

4.2 L.Goil Profiles 1/4/76 147

4.3 LG1 Profiles - Winter 1975/76 149

4.4 LG2 Profiles - Winter 1975/76 150

4.5 LG1 Profiles - Summer 1976 152

4.6 LG1 Profiles - Autumn/Winter 1976 153

4.7 LG1 Profiles - Spring 1977 154

4.8 LG1 Profiles - Summer 1977 155

4.9 LG1 Profiles - Autumn 1977 156

4.10 LG1 Profiles - Winter 1977/78 157

4.11 LG1 Isopleths - Cs-137 160

4.12 L.Long Surface Radiocaesium Concentrations 162

4.13 L.Long Profiles 27/9/77 164

4.14 L.Long Isopleths - Cs-137 167

4.15 L.Goil Bathymetry 168

4.16 L.Goil/L.Long Ratio Isopleths 169

4.17 L.Goil/L.Long Density Isopleths 175

4.18 L.Goil/L.Long Density Comparison 176

4.19 L.Goil Mixing Model 177

4.20 Gareloch Profile 3/8/76 187

4.21 L.Fyne Profile 12/2/76 187

5.1 Hebridean Sea Area Sampling Stations 192

5.2 Summer 1976 Radiocaesium Data 194

5.3 Summer 1976 Cs-137 Isopleths 195

5.4 Islay/Malin Radiocaesium Data 198

5.5 Summer 1977 Radiocaesium Data 205

5.6 Summer 1977 Cs-137 Isopleths 206

5.7 Radiocaesium along H.S.A. Transect 210

5.8 Source Water Radiocaesium Curves 212

6.1 Sediment Sampling Site Locations 220

6.2 L.G.G.5 Profile 222

6.3 L.G.C.9 Profile 223

6.4 L.G.G.7 Profile 224

6.5 L.G.C.4 Profile 225

6.6 G.L.G.1 Profile 226

6.7 G.L.C.3 Profile 227

6.8 L.G.C.11 Profile 229

6.9 L.G.C.12 Profile 230

6.10 G.L.C.1 Profile 232

6.11 L.G.C.2 Profile 237

6.12 Windscale Output (Decay Corrected) 238

6.13 Cs-137 Profile Comparison 241

6.14 L.L.R.P.M.1 Profile 245

6.15 H.L.C.1 Profile 254

7.1 Irish Sea Regions for Budget Calculations 267

LIST OF TABLES

1.1	Primordial Radionuclides	12
1.2	Natural Decay Series	14
1.3	Applications of Natural Series Radionuclides	16
1.4	Cosmogenic Radionuclides	18
1.5	Artificial Radionuclides	22
1.6	Inventory of Radioactivity in the Oceans	27
2.1	Counting Facilities	57
2.2	Peaks in the Gamma Spectrum of 'KCFC'	67
2.3	Sediment Replicates	69
2.4	Water Sampling Programme	72
2.5	Evaluation of Filtration Effects	75
2.6	Comparison of Ion-Exchangers	75
2.7	Distribution of Cs-137 in 'KCFC'	80
2.8	Calculation of 'KCFC' Chemical Efficiency	80
2.9	Drying Effects Observed in 'KCFC' Cartridges	81
2.10	Replicate Results	92
2.11	Demonstration of Geometric Effects	93
2.12	Errors in Radiocaesium Quantification (Water)	95
2.13	Replicate 1-1 System (Well NaI)	95
2.14	G.U./M.A.F.F. Intercalibration	98
2.15	Errors in Radiocaesium Quantification (Sediment)	98
2.16	Summary of System Constants	101
3.1	Station Positions for Areal Study	105
3.2	Depth Weightings for Cs-137 Concentrations in the C.S.A.	118
4.1	Box Model Solutions (L.Goil)	171

5.1 Source Waters to the H.S.A. 200

6.1 Sediment Coring Locations 219

6.2 Radiocaesium Desorption Results 235

7.1 Relative Cs-137 Concentrations in Regions of the Irish Sea 268

7.2 Measured Radiocaesium Concentration Factors for Fish 272

7.3 Organic Reservoir Inventory of Cs-137 274

7.4 Windscale Radiocaesium Budget 276

7.5 Derived Coastal 'Dissolved Pu' Concentrations 281

Chapter One

Introduction

1.1 Tracer Theory

Since the marine environment is a dynamic system of some complexity, one of the major challenges in its study is the measurement of rates of processes occurring within it. For example, rate determination is of obvious importance in studies of water movement, sedimentation, air-sea interaction and biological growth. There are two distinct approaches to timescale elucidation - direct measurement and tracer techniques.

While direct rate measurement may be the most obvious approach, and has indeed provided useful data, it is inherently limited by factors such as a) the highly localised nature of direct measurements relative to the spatial and temporal inhomogeneity of most oceanic processes and b) the slow rate of many oceanic processes - often on a timescale of hundreds or thousands of years (McLellan, 1965; Pickard, 1975). Thus direct measurement techniques tend to be applied only to studies of relatively localised areas and short timescale processes, e.g. drifters or current meters to study coastal water transport (Best, 1970; Pritchard et al, 1971; Molcard, 1972; Ellett, 1978) and sediment traps for evaluation of sedimentation rates in inshore marine and lacustrine areas (Håkanson, 1976; Anderson, 1977; Kinnel et al, 1977). Exceptionally, given sufficient resources

larger scale processes may be studied, usually as part of collaborative projects (Pollard, 1973).

The alternative to direct measurement via tracers involves study of species which, by their distribution, allow the dynamic processes controlling them to be quantified. The simplest application is the 'dye-type' study in which a tracer material is intentionally introduced and its redistribution used to derive rate information (Pritchard et al, 1966; 1971). This method generally suffers from the spatial and timescale limitations common to direct measurements and thus, again, finds most application in restricted areas (Ito et al, 1966; Best, 1970). A more elegant version utilises long term releases, usually of industrial pollutants, to extend the temporal baseline (Jernelöv, 1974; Goldberg, 1975). Thus, pesticides with known introduction dates and input rates may be used as water tracers and, by their measurement within marine organisms, as tracers of transport rates to and within the biological food-chain (Nisbet and Sarofin, 1972; Duursma and Marchand, 1974; Young et al, 1975). Heavy metal 'horizons', based on local industrial history, may also be used in determination of near-shore and lacustrine sedimentation rates (Bruland et al, 1974) and for general environmental tracing (Halcrow et al, 1973; Brinckman and Iverson, 1975; Rutherford and Church, 1975; de Groot et al, 1976; Brannon et al, 1977; Bowen, 1978).

For the longer timescales generally associated with the open ocean, ambient natural tracers must be employed, as, in most cases, the impact of man on the oceans was not significant before the industrial revolution (with the possible exception of the effects of such processes as

anthropogenic deforestation and desertification). Two major parameters, usually used in conjunction, for the labelling of water bodies are salinity and temperature by which the major oceanic water masses can be characterised (Wallace, 1974; Pickard, 1975; Turekian, 1976). Salinity or temperature, with known freshwater input rates or heat fluxes, may be used as rate tracers (e.g. Saunders, 1973; Edwards and Edelsten, 1976a; 1976b; Mackay and Leatherland, 1976) but, more usually, the degree of mixing of two water bodies can be derived by this pair, allowing the change in a third, time-dependent parameter (e.g. the concentration of a low residence time species) to be used as a mixing rate tracer (Wilson, 1975).

In deep sea sedimentation studies, the very long time-scales involved allow palaeontological or palaeomagnetic markers to be used (Broecker, 1974; Turekian, 1976). Such markers, however, must first be dated via some additional time-dependent process and, even so, may show only gross temporal accumulation structures, as constant sedimentation rates between horizons must be assumed.

Thus far it has been indicated that tracers can form the basis of powerful techniques for provision of rate data, much of which would be difficult to obtain by other methods. However, in many applications, it is necessary or advantageous for the tracer to possess an internal time-dependency. In specific applications, processes such as the precipitation of reactive species, degradation of organic compounds, racemisation of amino acids or mineralisation of

sedimentary constituents may each in theory provide an in-built chemical 'clock' but an inherent limitation of these approaches lies in their sensitivity to environmental changes, e.g. temperature, pH, pE etc. (Price, 1976; Degans and Mopper, 1976). The requirement for time-dependent tracers possessing rate constants effectively independent of all physical and chemical perturbations is perhaps best met within the family of marine radionuclides.

Radioactivity can be defined as the spontaneous transformation of nuclear structure accompanied by the corresponding release (or, in rarer cases, incorporation) of particles and/or electromagnetic radiation. Radioactive species are thus particularly useful as tracers since the characteristic radiations emitted can often be used to identify the nuclide present, while the decay process itself removes the species at a definable rate, providing an in-built 'clock' which is unaffected by environmental change. Identification of radionuclides by their radiations is especially relevant in the case of α- or γ - emitters where the monoenergetic nature of the emissions allows quantitative characterisation by high resolution spectroscopy. In assay of γ- emitters (and, to some extent, X-ray emitters) the penetrating character of the electromagnetic radiation often allows pretreatment to be minimised, in some cases to the extent of direct, in-situ, quantitative measurement (e.g. Barnes and Gross, 1966).

The sensitivity of radioactivity measurement is determined by a) the selectivity and efficiency of the

techniques and apparatus used, b) the counting time and c) the half-life ($t_{\frac{1}{2}}$) of the species involved. The importance of the latter parameter is indicated by the simple first-order rate equation for radioactive decay:-

$$A = N\lambda \qquad \ldots.(1.1)$$

equivalent to $$A = \frac{N\ln 2}{t_{\frac{1}{2}}} \qquad \ldots.(1.2)$$

where A is the activity of the sample in disintegrations per unit time, N the number of atoms of radioactive species present and λ the appropriate decay constant.

The determination of radionuclides to concentrations of 10^{-12} g l^{-1} in water or 10^{-3} p.p.m. in sediments or organics is frequently achievable so that analytical sensitivity is generally superior to that of conventional methods based on stable species.

Activity is, by definition, the rate of decrease, through radioactive decay, of the number of atoms of a species and can therefore be expressed mathematically as:-

$$A = -\frac{\partial N}{\partial \tau} \qquad \ldots.(1.3)$$

where τ is time. Thus, integration of (1.1) from $\tau = 0$ to $\tau = t$ gives, on rearrangement:-

$$N_t = N_o e^{-t} \qquad \ldots.(1.4)$$

or, equivalently $$A_t = A_o e^{-t} \qquad \ldots.(1.5)$$

where the suffices on N and A indicate the time at which each parameter is measured. These equations, or simple

variations of them, provide the primary relationship between the number of radionuclide atoms (or activity or concentration) and time in an isolated system and thus form the basis of most radioactivity-based rate determinations (Aldrich and Wetherill, 1958; Friedlander et al, 1964; Prospero and Koczy, 1966).

For all useful tracers, a necessary condition is that input to the system studied should be non-uniform, either spatially or temporally. In most applications, input can be approximated as being either from a point source or from a source uniformly distributed over a system boundary (more complex cases being considered as a series of sub-systems where such approximations can be made). Examples of 'point' sources are river inputs of fresh water, sediment and soluble species in a coastal context (Barnes and Gross, 1966; Goldberg, 1975), waste from submarine dumps in a localised or bottom water context (Greve, 1971; Gross, 1972; Halcrow et al, 1973) and heat, metals and 'dead' carbon from submarine volcanoes in an oceanic system (Chester and Aston, 1976). Boundary inputs include 'fallout' metals, pesticides and radionuclides through the air / ocean interface (Volchok et al, 1971; Goldberg, 1975), detrital materials from water and gases from sediment through the water / sediment interface (Hammond et al, 1975; Price, 1976) and nutrients and biogenic debris from surface to deep water through the main ocean thermocline (Spencer, 1975; Williams, 1975). The importance of scaling in source classification must be

emphasized, as an input which may be regarded as 'boundary' in a localised context may be regarded as a point source on a coastal or global scale, while boundary inputs which are inhomogeneous on a small scale may be approximated as averaging to homogeneity in a much larger system (Baxter and McKinley, 1978).

When input (or, in some cases, output) is clearly defined, tracer distribution or redistribution can be analysed mathematically. Two common mathematical methods for this purpose are box-modelling and advection/diffusion treatments, the particular approach adopted being dependent on the system under study. Indeed, both methods can be used in complementary parts of a single, larger study (Prichard et al, 1971; Bowden, 1975; Oeschger et al, 1975).

Box-modelling involves approximation of the total system as a number of sub-systems which can be characterised by a single value of the tracer parameter. Interchange between boxes is then described in terms of simple functions, values of the interchange rates being calculated by solution of a set of simultaneous equations. Figure 1.1 illustrates a simple 3- box model in which each box (i) has a characteristic tracer concentration (C_i), volume (V_i) and rate of in-situ tracer destruction (Ri). In the case of in-situ production R_i assumes a negative value. Input rate (F_{in}), output rate constant (k_s) and box relationships are defined by the system under study, as are the interchange rate constants. The change in tracer content of each box over a time period from t = 0, $(V_iC_i)^o$, to

FIG 1.1 SIMPLE 3 BOX CHAIN MODEL

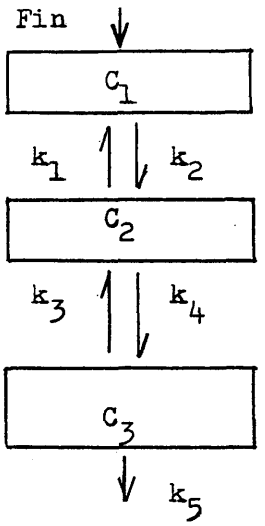

BOX	TRACER CONCENTRATION	VOLUME
1	C_1	V_1
2	C_2	V_2
3	C_3	V_3

$$(V_1C_1)^t = (V_1C_1)^o + (Fin + k_1C_2 - k_2C_1 - R_1)t \quad ..(A_1)$$

$$(V_2C_2)^t = (V_2C_2)^o + (k_2C_1 - k_1C_2 - k_4C_2 + k_3C_3 - R_2)t \quad ..(A_2)$$

$$(V_3C_3)^t = (V_3C_3)^o + (k_4C_2 - k_3C_3 - k_5C_3 - R_3)t \quad ..(A_3)$$

Steady State $(Vi\ Ci)^t = (Vi\ Ci)^o$

$$Fin + k_1C_2 = k_2C_1 + R_1 \quad ....(B_1)$$

$$k_2C_1 + k_3C_3 = k_1C_2 + k_4C_2 + R_2 \quad ....(B_2)$$

$$k_4C_2 = k_3C_3 + C_3k_5 + R_3 \quad ....(B_3)$$

if concentration gradient due to radioactive decay $Ri = Ci\lambda$
(λ decay constant of tracer)

measure Fin, C_1, C_2, C_3 ; postulate $k_1 = k_2$, $k_3 = k_4$

equations solvable for k_{1-5}

$t = t$, $(V_iC_i)^t$, can then be expressed in terms of a set of simple equations when first order exchange rates are postulated ((A_1) - (A_3) in Figure 1.1). By considering a steady state situation, where $(V_iC_i)^o = (V_iC_i)^t$, these equations can be simplified further (giving (B_1) - (B_3) in Figure 1.1). Further examination of the real system may allow these equations to be solved, e.g. if in-situ removal is due only to radioactive decay, $R_i = C_i \lambda$ where λ is the tracer decay constant. If it is realistic to assume $k_1 = k_2$ and $k_3 = k_4$, measurement of C_1, C_2, C_3 and F_{in} allows calculation of all rate constants.

The advection/diffusion treatment considers tracer variations as the result of a combination of advective and diffusive processes, where advection involves alteration in tracer concentrations associated with mass transfer of the containing medium, while diffusion allows tracer transport without mass transfer. The general three dimensional equation describing the variation in tracer concentration (c) with time (t) is thus:-

$$\frac{\partial c}{\partial t} = \underset{\alpha}{u\frac{\partial c}{\partial x}} + \underset{\beta}{v\frac{\partial c}{\partial y}} + \underset{\gamma}{w\frac{\partial c}{\partial z}} + \underset{\delta}{\frac{\partial}{\partial x}\left(K_x\frac{\partial c}{\partial x}\right)} + \underset{\varepsilon}{\frac{\partial}{\partial y}\left(K_y\frac{\partial c}{\partial y}\right)} + \underset{\zeta}{\frac{\partial}{\partial z}\left(K_z\frac{\partial c}{\partial z}\right)} + R \qquad \ldots.(1.6)$$

where terms α, β, γ are due to advection resolved into components along the three axes of Cartsian space, terms $\delta, \varepsilon, \zeta$ allow for similarly resolved diffusion and R is a term to compensate for in-situ destruction (or production) of tracer. Consideration of the real system often allows considerable simplification of this equation by neglecting

terms expected to be relatively small. Thus, in a steady state system, $\left(\frac{\partial c}{\partial t} = 0 \right)$, which can be regarded as one dimensional, e.g. a water or sediment column, equation (1.6) reduces to:-

$$0 = w \frac{\partial c}{\partial z} + \frac{\partial}{\partial z}\left(K_z \frac{\partial c}{\partial z}\right) + R \qquad \ldots (1.7)$$

which may be solved for w and K_z by measuring the distribution of two independent tracers. If in-situ removal is entirely by radioactive decay, $R = C\lambda$ and equation (1.7) reduces to a linear second order differential equation (given that K_z is independent of z) which may be readily solved by applying appropriate boundary conditions.

The mathematical methods considered above hold generally for all tracers, the time dependency of radioactive tracers being included in the in-situ removal (or production) term (R). The initially complex sets of equations generated in both approaches can generally be reduced significantly by considering the simplifying properties of the particular system under study. In complex systems, however, for which several independent tracers may be used, analytical solution may prove extremely difficult and laborious. Many of these intricate systems may now be handled via the 'number-crunching' abilities of modern computers which can routinely solve systems of hundreds of simultaneous equations. In addition to the common use of digital computers for straightforward evaluation of complex equations, a range of analogue computing methods is now available. Analogue

computing is particularly appropriate to box-modelling as each box may be represented as an electronic circuit where concentrations are represented as voltages, exchange rates by time constants and inputs are synthesized by function generators (Hardy, 1969). As highly complex box-models can be handled by this method, increasingly realistic models can be devised and solved (Ishiguro, 1972).

1.2. Radiotracer Applications

As mentioned previously, applications of radionuclides as tracers depend on their mode of introduction into the marine system and this, in turn, is often dependent on their mechanism of production. Generally radionuclides are grouped by production as primordial, cosmogenic or anthropogenic, although it must be noted that a particular nuclide may belong to more than one class.

Primordial radionuclides are species whose concentrations are controlled by sufficiently long half-lives to have survived, to a measurable extent, since the production of the source elements of the solar system ($\sim 6 \times 10^9$ years B.P.). Marine tracer applications of the parent radionuclides, some of which are listed in Table 1.1, are severely limited by their long half-lives as, for many of these species, decay is insignificant on marine timescales. Use of the shorter-lived parent species within this group (^{40}K, ^{87}Rb, ^{232}Th, ^{235}U, ^{238}U) is generally limited to deep ocean geochronological applications, where the extent of radioactive decay of the species, assessed by build-up of daughter

TABLE 1.1 PRIMORDIAL RADIONUCLIDES.

NUCLIDE	TYPE OF DISINTEGRATION	$t_{\frac{1}{2}}$(y)	% ISOTOPIC ABUNDANCE
K-40	BETA, E.C.	1.27×10^{9}	0.012
V-50	BETA, E.C.	6×10^{15}	0.24
Rb-87	BETA	5.7×10^{10}	27.8
In-115	BETA	5×10^{14}	95.7
Te-123	E.C.	1.2×10^{13}	0.87
La-138	E.C., BETA	1.1×10^{11}	0.089
Ce-142	ALPHA	5×10^{15}	11.07
Nd-144	ALPHA	2.4×10^{15}	23.85
Sm-147	ALPHA	1.1×10^{11}	14.97
Gd-152	ALPHA	1.1×10^{14}	0.20
La-176	BETA	3×10^{10}	2.59
Hf-174	ALPHA	2×10^{15}	0.18
Re-187	BETA	6×10^{10}	62.9
Pt-180	ALPHA	7×10^{11}	0.013
Th-232	ALPHA	1.4×10^{10}	100
U-235	ALPHA	7.1×10^{8}	0.7205
U-238	ALPHA	4.5×10^{9}	99.274

FROM FRIEDLANDER ET AL (1964)

(e.g. ^{40}Ar) or change in atomic ratio (e.g. $^{235}U/^{238}U$), can be related to the elapsed time since deposition of a particular sediment layer, via analogues of equation (1.4) (Aldrich and Wetherill, 1958; Friedlander et al, 1964; Prospero and Koczy, 1966; Burton, 1975). This class also includes, however, the radioactive daughters of these long-lived parents. Of these, the members of the three natural decay series are particularly important (Table 1.2).

In an isolated system, a pure parent species (^{238}U, ^{232}Th or ^{235}U) decays to produce daughters which eventually grow in to a steady-state of 'secular equilibrium' at which the activity of the parent equals that of each daughter in the chain; thus for each radioactive daughter its rate of production equals its rate of decay (full mathematical treatment in Friedlander et al, 1964). Within the decay chains, however, nuclear transformation is accompanied by changes in atomic number and hence in chemical properties and these, in a real marine system, tend to cause chemical fragmentation within the chain and thus to induce dis-equilibria which can be useful in a considerable range of tracer applications.

The first comprehensive measurements of radioactivity in marine materials were made by Joly (e.g. Joly, 1908; 1912), who examined ^{226}Ra concentrations via the 'emanation' of its daughter ^{222}Rn. High concentrations of ^{226}Ra measured in sediments relative to those in continental rocks were assumed to indicate the presence in excess of one of its parent nuclides within the ^{238}U series, but it was not until

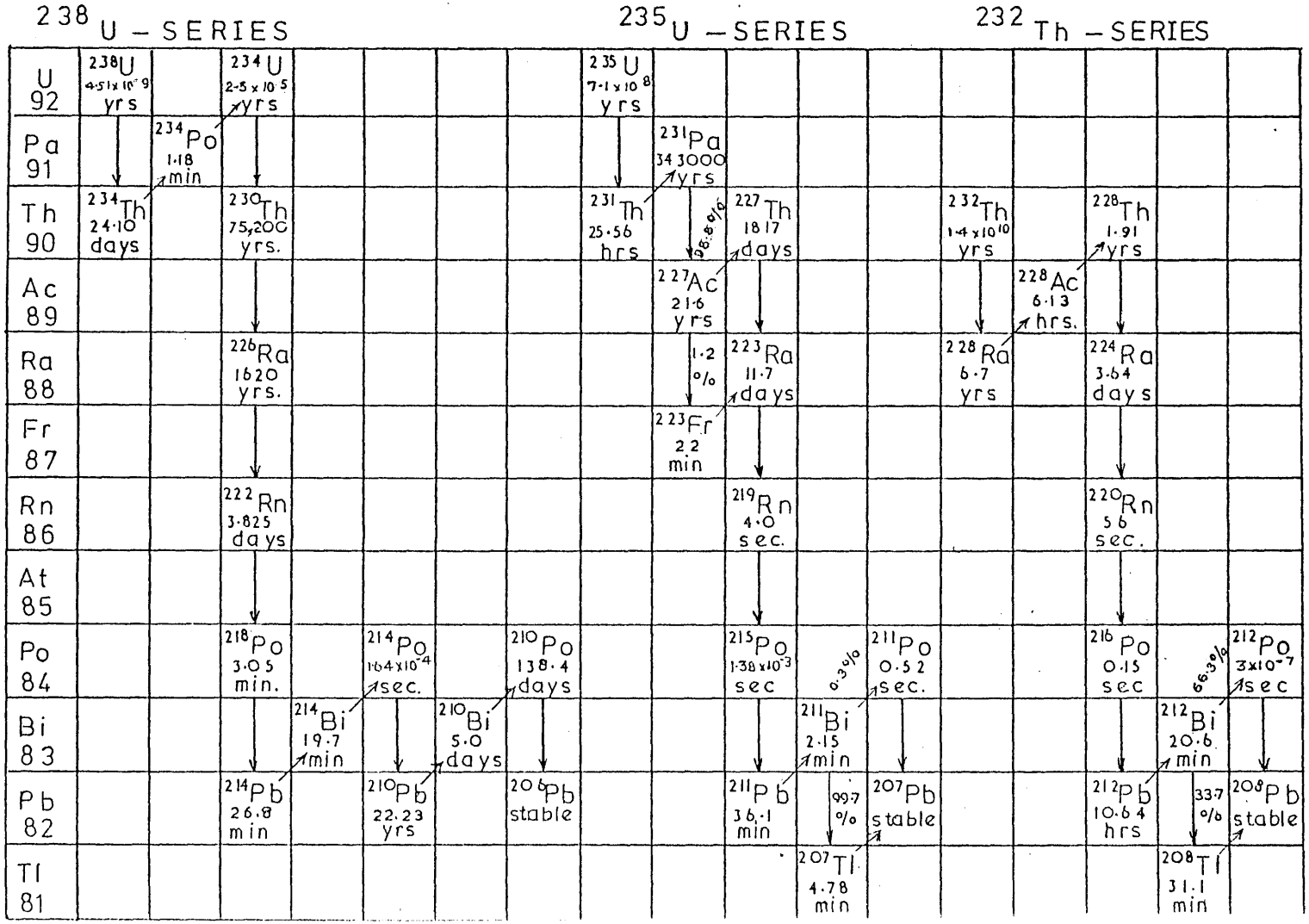

Table 1.2 Natural Decay Series

thirty years later that instrumental and analytical developments allowed identification of ^{230}Th as the parent responsible (Pettersson, 1937; Piggot and Urry, 1939; 1941). Since the mid-forties, an increased sensitivity of analytical methods has resulted in a significant expansion in the range of possible applications of natural series radionuclides. Thus, assay of excess ^{230}Th in the sediment column forms the basis of a major dating method which can be modified by measurements of similar radionuclides, e.g. ^{232}Th and ^{231}Pa (Prospero and Koczy, 1966; Thomson and Walton, 1972; Burton, 1975). The timescales which can be covered by natural series methods range from days to hundreds of thousands of years (Table 1.3) although it must be noted that the applicable time range of a radioactive tracer is determined not only by its half-life but also by its geochemical stability as indicated by its diffusion rate in sediments and its residence time in water. Actual applications range from geochronological measurements in deep sea sediments (Goldberg and Koide, 1962) to studies of fast mixing rates and diffusive processes in coastal deposits (Aller and Cochran, 1976) and, in the water column, from studies of mixing over the main ocean thermocline (Chung and Craig, 1973) to studies of rapid mixing processes in near-bottom waters (Chung, 1976) and surface waters (Bhat et al, 1965).

Applications of natural series radionuclides as biological tracers utilise the shorter-lived members of these series, e.g. ^{228}Ra (via $^{228}Ra/^{226}Ra$ ratio) for determining coral growth rates over $\sim$30 years (Moore and Krishnaswami,

TABLE 1.3 APPLICATIONS OF NATURAL SERIES RADIONUCLIDES.

METHOD	TIMESCALE	REFERENCE
a) Sediment		
$^{230}Th/^{232}Th$	4000- 40,000y.	Goldberg & Koide 1962
^{226}Ra	800-8,000y.	Koide & al ,1976
^{210}Pb	10-100y.	Koide & al ,1972
$^{228}Th/^{232}Th$	1-10y.	Koide & al ,1973
$^{234}Th/^{238}U$	10-100 days	Aller & Cochran,1976
b) Water		
^{226}Ra	400-4000y.	Chung & Craig ,1973
^{228}Ra	3-30y.	Moore ,1972
^{228}Th	1-10y.	Cherry & al ,1969
$^{234}Th/^{238}Th$	10-100 days	Bhat & al ,1969
^{222}Rn	2-20 days	Chung ,1974
c) Organics		
$^{228}Ra/^{226}Ra$	~ 30y.	Moore & Krishnaswami ,1972
^{210}Po	~ 1y.	Shannon ,1973

1972) and unsupported ^{210}Po as an indicator of concentration in food chains over shorter timescales (Shannon, 1973). While, in general, experimental difficulties have limited research in this field, the elemental specificity involved in biological incorporation of trace materials allows biogenic remains - generally corals and shells - to be suitable materials for geochronological study. For example, biogenic calcareous deposits are often gently enriched in uranium isotopes relative to their decay daughters, so that growth of ^{230}Th or ^{231}Pa to secular equilibrium can provide the basis of long-term chronologies ($\sim 10^5$ years), a method which seems particularly applicable to fossil corals (Steans and Thurber, 1967; Kaufman et al, 1971).

In 1946, Libby postulated the existence of cosmogenic radionuclides - species produced by activation of stable terrestrial material by cosmic rays (Libby, 1946). As this process occurs primarily in the upper atmosphere, the location of the production process for a range of species with a variety of half-lives is well specified. Radiotracer applications are dependent on the chemistry of the tracer species, but most depend primarily on the boundary-type input, through the atmosphere/ocean interface, into the marine environment. The radioactive decay of particulate-bound cosmogenic radionuclides provides a range of sedimentary tracers which tend to be complementary to natural series species. Radiocarbon, ^{14}C, is probably one of the most reliable and frequently used nuclides for dating marine sediments up to 40,000 years old (Broecker et al, 1960).

TABLE 1.4 COSMOGENIC RADIONUCLIDES.

NUCLIDE	RADIATION	$t_{\frac{1}{2}}$	AVERAGE SEA WATER ACTIVITY ($dpml^{-1}$)
^{3}H	β^-	12.3y.	3.6×10^{-2}
^{7}Be	EC	54d.	—
^{10}Be	β^-	2.5×10^{6}y.	10^{-6}
^{14}C	β^-	5730y.	2.6×10^{-1}
^{26}Al	β^+, EC	7.4×10^{5}y.	1.2×10^{-8}
^{32}Si	β^-	500y.	2.4×10^{-5}

(Data from BURTON,1975)

^{14}C dating is, indeed, often used to provide a master chronology against which the assumptions of other dating methods can be checked, deviations from an ideal match often yielding useful information about long-term perturbations in sediment structure (Ku and Broecker, 1967). The main limitation of ^{14}C dating is probably its limited age range as 4×10^4 years is a relatively short geological timespan. Reduction of experimental difficulties in assay of ^{10}Be and ^{26}Al is, however, resulting in their increasing use as longer timescale sedimentary tracers (Lal, 1962; Krishnaswami and Lal, 1972; Finkel et al, 1977; Somayajulu, 1977). Alternatively, research on increasing the sensitivity of ^{14}C detection by isotopic enrichment and/or measurement via cyclotron or particle accelerator methods may allow routine extension of ^{14}C chronologies to 10^5 years B.P. (Hedges, 1978).

Applications to water studies are also dominated by the wide use of ^{14}C which has a half-life suitable for investigation of oceanic circulation. Oceanic mixing studies via radiotracers are typified by the classic work of Bien et al (1965) in which the decay of radiocarbon during thermohaline circulation immediately shows the flow of the 'youngest' deep water, North Atlantic Deep Water, in a southwards direction whereafter it provides the main component of north-flowing Indian and Pacific Deep Waters (Fig 1.2). Although removal mechanisms and mixing with surface waters must be considered in a truly quantitative study, estimations of average deep water velocities can be derived. Tritium, ^3H, is in some ways, however, the ideal water tracer, particularly as it is incorporated directly

FIGURE 1.2 C-14 AGES OF DEEP OCEAN WATER

(After Bien et al, 1965)

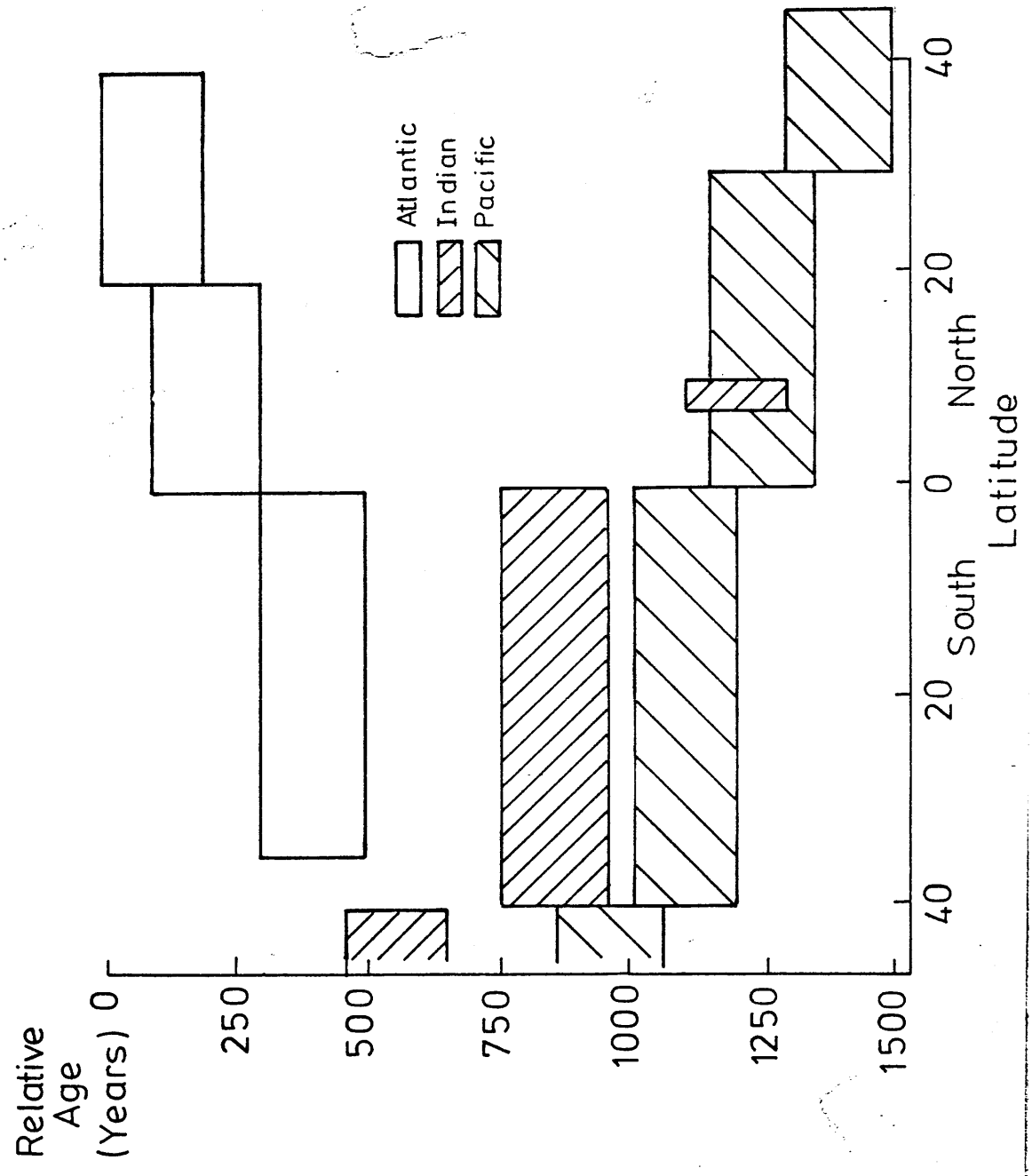

into the water molecule itself and thus may provide a measure of water movement over a timescale of $\sim$ 100 years. Direct application of ^{3}H as a cosmogenic tracer is, nevertheless, limited by the influence of anthropogenic contributions which have increased concentrations by two orders of magnitude over natural levels (Blaur, 1977).

Anthropogenic radionuclides are produced by the activities of man in both controlled and explosive fission and fusion processes. In most considerations, 'bomb' radionuclides, produced during the testing and use of nuclear explosives, and 'waste' radionuclides, released in effluents from the nuclear industry, are differentiated by their dissimilar modes of introduction into the marine environment (Joseph et al, 1971). A list of common artificial radionuclides (Table 1.5) shows the major components of both 'waste' and 'bomb' radioactivity. It is noticeable that many of the artificially produced species have negligible natural concentrations in the marine environment and thus have no pre-nuclear era background.

'Bomb' radionuclides are, in general, released into the marine environment as airborne particulates or gases so that marine input from 'fallout' tends to be both spatially and temporally diffuse as a result of extensive atmospheric transportation and residence time. Exceptions to this generalisation are the immediate fallout of radioactivity associated with large particulates in the vicinity of an explosion and the radioactive emissions associated with underwater detonations. In both these cases the

TABLE 1.5 ARTIFICIAL RADIONUCLIDES

ISOTOPE	HALF-LIFE	ORIGINATING FROM WEAPONS	ORIGINATING FROM WASTE	OCCURRING NATURALLY
H-3	12.26y	*	*	*
C-14	5568y	*		*
P-32	14.22d	*		
Sc-46	83.9d		*	
Cr-51	27.8d		*	
Mn-54	291d	*	*	
Fe-55	2.60y	*	*	
Fe-59	45.1d	*	*	
Co-57	270d	*		
Co-58	71.3d	*		
Co-60	5.24y	*	*	
Zn-65	245d	*	*	
As-76	26.4h		*	
Kr-85	10.3y	*		
Sr-89	50.5d	*	*	
Sr-90	27.7y	*	*	
Y-90	64.2h	*	*	
Y-91	57.5d	*		
Zr-95	65d	*	*	
Nb-95	35d	*	*	
Mo-99	66h	*		
Ru-103	39.8d	*	*	
Ru-106	1.00y	*	*	
Rh-106	130m	*	*	
Cd-113m	5.1y	*		
Cd-115m	43d	*		
Sb-125	2y		*	
Te-132	77.7h	*		
I-131	8.08d	*	*	
Cs-134	2.1y		*	
Cs-137	30.23y	*	*	
Ba-140	12.80d	*		
La-140	40.22h	*		
Ce-141	33.1d	*	*	
Ce-144	285d	*	*	
W-185	75.8d	*		
Bi-207	8.0y	*		
Po-210	138d		*	*
U-234	2.48E5y	*	*	*
U-235	7.10E8y	*	*	*
U-238	4.51E9y	*	*	*
Np-239	2.35d	*	*	
Pu-238	87.8y	*	*	
Pu-239	2.44E4y	*	*	
Pu-240	6537y	*	*	
Pu-241	14.9y	*	*	
Am-241	433y	*	*	
Cm-242	163d	*	*	
Cm-244	1.81E4y	*	*	

Adapted from Mauchline(1966)

radioactivity may often be regarded as having a point source and, during dispersion, may act as a localised, short-term dye-type tracer (Joseph et al, 1971).

The temporal variation of global fallout (Fig 1.3a) reflects the increase in nuclear weapons testing which occurred over the period 1945-1963 and was followed by the atmospheric nuclear testing moratorium in 1963. Latitudinal variations in the fallout pattern (Fig 1.3b) are the result of confinement of most nuclear testing to the northern hemisphere coupled with the effect of enhanced stratospheric input to the troposphere through the tropopause gap at mid-latitudes (Volchok et al, 1971).

Tracer applications of bomb radionuclides tend, like those of cosmogenic nuclides, to be dependent on the boundary-type input of species having a known fallout variation with time. Particular applications clearly depend on the chemistry of the tracers utilised. Thus, soluble species, e.g. ^{3}H, ^{14}C, ^{90}Sr and ^{137}Cs, are widely used in studies of mixing in the upper layers of the ocean (Broecker, 1974). Less soluble species, e.g. Pu and Np isotopes, are used as tracers of particulate settling in the oceans (Noshkin, 1972), while biologically active nuclides, e.g. ^{60}Co and ^{65}Zn, are employed as tracers of food-chain transfer and as indices of biological concentration factors (Lowman et al, 1966; Penreath, 1977). In many of these applications the radionuclides are effectively used as dye-type tracers since decay is insignificant over the study period, temporal marking being provided by the characteristic fallout maximum of 1963 and analysis being facilitated by radioactivity measurement.

FIGURE 1.3

a Temporal Variation in Bomb Fallout.

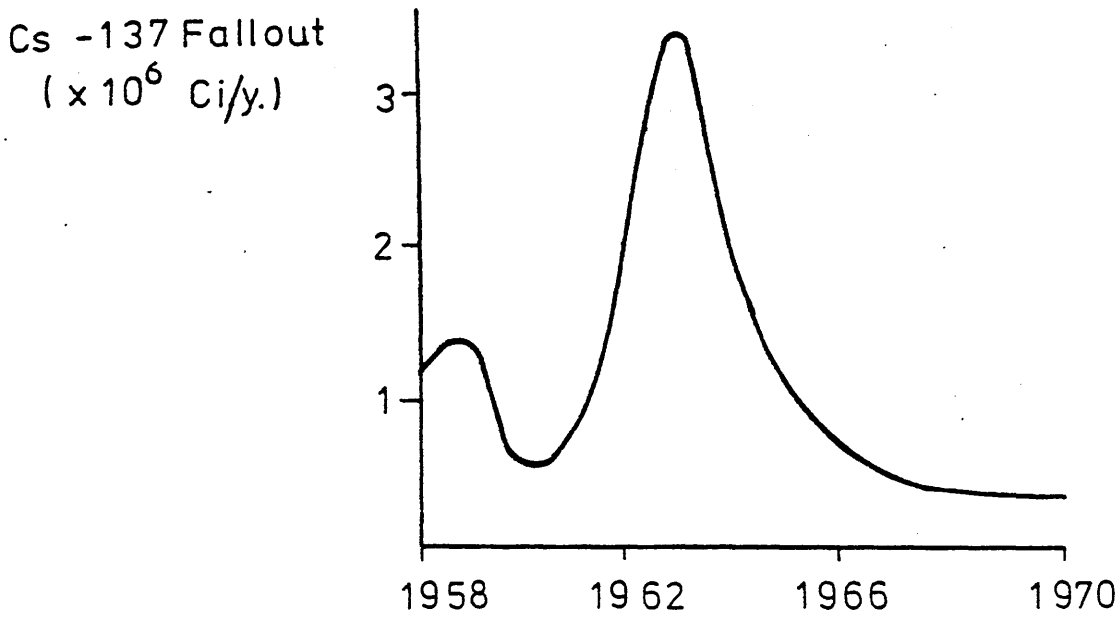

b Latitudinal Variation in Bomb Fallout

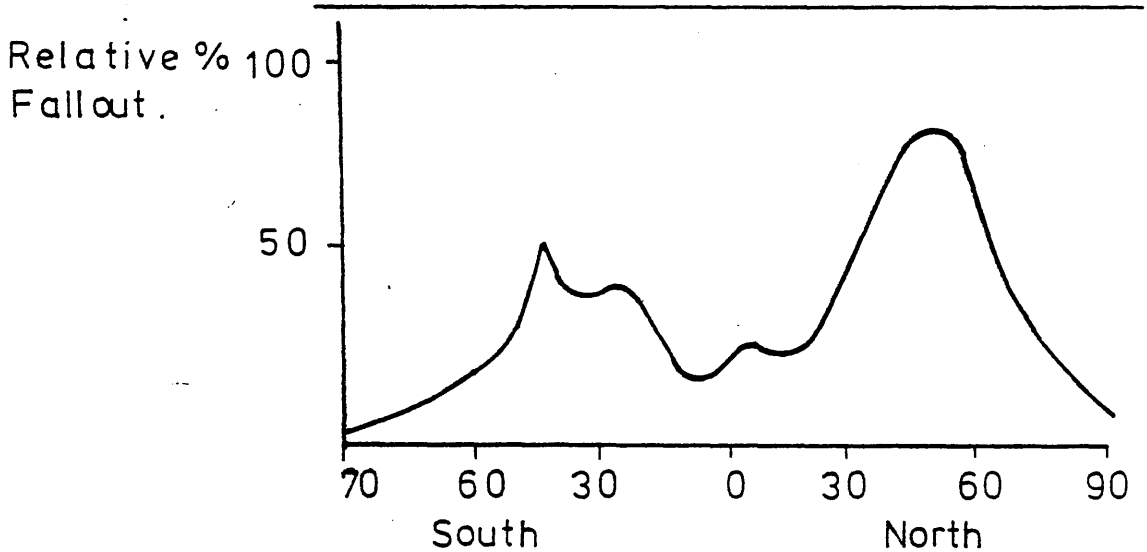

Waste releases into the marine environment from the nuclear industry tend to be highly localised and, as they are usually strictly monitored, may also be well specified in terms of radionuclides present and input variation with time. Waste releases may enter the marine environment as airbourne fallout, contaminated liquids or encapsulated solid material. Atmospheric fallout from the nuclear industry is, however, of limited value, as aerial dispersion tends to produce a diffuse and variablemarine input. In addition, encapsulated wastes tend to have a slow release rate, again limiting tracer applications (Joseph et al, 1971; Dunster, 1978). Liquid waste releases, on the other hand, may either be pumped directly into the sea or may enter via rivers but both cases tend to generate highly localised coastal inputs which are of major value in tracer applications. Liquid waste releases from naval reactors are only significant in restricted areas, e.g. harbours, and thus, in a tracer context, may be grouped with conventional coastal discharges.

The first major studies based on effluent-released radiotracers were centred on the plutonium production facility at Hanford (Washington State, U.S.A.) which, over a period of 27 years (1944-1971) discharged high activity effluent into the Columbia River (Robertson et al, 1973). This release provided a marine point source at the river mouth involving radionuclides such as ^{51}Cr, ^{239}Np, ^{32}P, ^{65}Zn, ^{152}Eu, ^{140}Ba and ^{46}Sc at concentrations well above 'fallout background' (Joseph et al, 1971). Dispersal of these radionuclides produced a characteristic 'plume' of radioactivity which allowed quantitative studies of coastal water movement along the west

coast of North America (Gross et al, 1965; Osterberg et al, 1965; Park et al, 1965; Barnes and Gross, 1966). In addition, changes in activity ratios of various components during dispersal and transport allowed speciation, adsorption onto particulates and precipitation reactions to be studied (Gross and Nelson, 1966; Osterberg et al, 1966; Evans and Cutshall, 1973). Measurement of the accumulation of radionuclides in the food chain also enabled calculation of metal concentration factors for many organisms. This process of biological concentration was itself utilised by using specific benthic species as radionuclide monitors (Osterberg et al, 1964; Carey et al, 1966; Young and Folson, 1973).

In Britain, radionuclide releases are dominated by those from the British Nuclear Fuels Ltd. (BNFL) reprocessing plant at Windscale in Cumbria. The Windscale plant is the largest of its type in the world and probably releases more nuclear waste into the marine environment than any other civil installation (Table 1.6). Radionuclides released from Windscale include ^{90}Sr, ^{95}Zr, ^{95}Nb, ^{106}Ru, ^{134}Cs, ^{137}Cs, Pu and ^{241}Am. While these species are extensively monitored in radiological hazard assessment programmes, they may also be used in a range of coastal tracer applications (Preston et al, 1972) as discussed hereafter.

Many smaller-scale tracer studies have exploited the releases from reactors and fuel-reprocessing plants as radionuclide sources (e.g. Best, 1970; Fukai and Murray, 1973; Patel et al, 1975; Hess et al, 1978). General reviews of radionuclides in the marine environment and tracer applications which usefully extend the brief summary presented here

TABLE 1.6

INVENTORY OF RADIOACTIVITY IN THE WORLDS OCEANS 1975

Nuclear Explosions (Worldwide Distribution)	Total Activity (Ci)
Fission Products ($-^{3}H$)	$2\text{-}6 \times 10^{8}$
^{3}H	10^{9}
Reactors & Fuel Reprocessing (restricted local distribution)	
Fission & Activation Products ($-^{3}H$)	10^{6}
^{3}H	10^{6}
TOTAL Natural ^{40}K	5×10^{11}
Total Artificial Radioactivity	10^{9}
WINDSCALE RELEASES	5×10^{5}

(Derived from PRESTON ,1972)

include:- Baxter and McKinley, 1978; Broecker, 1975; Burton, 1965; 1975; Duursma, 1972, 1976; Goldberg and Bruland, 1974; Mauchline, 1966; Mauchline and Templeton, 1964; National Academy of Sciences, 1971; Noshkin, 1972; Penreath, 1977; Preston, 1974; Preston et al 1972; Prospero and Koczy, 1966; Suess, 1958; Thomson and Walton, 1972.

1.3 Radiocaesium as a Marine Environmental Tracer

Caesium is the second heaviest member of group 1a of the periodic table, the alkali metals, and is the most electropositive and most alkaline element known (Weast, 1974). It exists in aqueous solution almost entirely as the solvated monovalent cation and is therefore characterised by a lack of chemical reactivity in solution and hence a long residence time in ocean waters (Brewer, 1975). Caesium in sea water, measured either by flame photometry or neutron activation, has a mean concentration of 0.4 g l^{-1} corrected to chlorinity 19‰ (Riley, 1975). Experimental values actually tend to fall into two groups, c. 0.5 g l^{-1} and c. 0.3 g l^{-1}, but this distribution probably reflects analytical discrepancies rather than real variability (Brewer, 1975). In any particular survey, caesium concentrations have been shown to be reasonably constant spatially, with the possible exception of high values reported in the Gulf of Mexico (Bolter et al, 1964). Levels are also constant with depth and season (Riley and Tongudai, 1966), the depth variations observed by Folsom et al (1964) being suspect (Turekian and Schutz, 1965). Estimates of caesium residence time in the deep ocean calculated by a steady state method depend on the assumed values

for caesium concentration and runoff input of caesium, a parameter which is poorly specified (Bolter et al, 1964; Noshkin and Bowen, 1973) but which is generally taken to be c. 6.3×10^9 g y^{-1} (Livingstone, 1963). Residence times quoted in the literature range from 6.5×10^4 y to 6.5×10^5 y (Bolter et al, 1964; Turekian and Schutz, 1965; Goldberg et al, 1971; Bro ecker, 1974, Brewer, 1975), allowing it to be classified, in any case, as semiconservative ("Biointermediate" in the nomenclature of Broecker, 1974).

Most research on caesium in the deep oceans has centred on the observed distribution of bomb fallout ^{137}Cs. ^{137}Cs, together with ^{90}Sr, comprises, after several years, a major component of residual fallout activity. Despite the considerable accumulation of data on these radionuclides in seawater, there is still no consensus of opinion on the reality of detection and interpretation of reported low concentrations of these species in deep ocean water (Volchok et al, 1971). Controversy has arisen over the detection of ^{137}Cs and ^{90}Sr in waters below 1500m and over the possibilities of differentiation of fallout input between particulate bound and ionic forms and of depth and spatial variations in $^{137}Cs/^{90}Sr$ ratio (Bowen, 1971; Broecker, 1971; Schubert, 1971). Assuming no ^{137}Cs or ^{90}Sr in deep water, the surface distributions of these species allow calculation of thermocline mixing rates consistent with those derived from natural radionuclide variations (Broecker, 1966). Extremely rigorous measurements of the $^{137}Cs/^{90}Sr$ ratio have failed to show any unambiguous variation with depth, although the ratio does appear to increase with decreasing radionuclide concentrations possibly reflecting difficulties in blank specification (Bowen et al, 1974). On the other hand, residence times for

^{90}Sr and ^{137}Cs, calculated from their concentrations in sediment, are orders of magnitude shorter than oceanic residence times calculated for their stable isotopes. This discrepancy may indicate an increased reactivity of the fall-out species or that the classical calculation of stable element residence times are skewed by uncertainties in river supply data or by near-shore effects (Noshkin and Bowen, 1973).

Extrapolation of deep ocean behaviour to an inshore context is difficult because of differences in the degree of interaction with sediment, particulate, biological and freshwater fluxes (Noshkin and Bowen, 1973; Turekian, 1977). This behavioural gradient has been manifested by a large decrease in the $^{137}Cs/^{90}Sr$ ratio in coastal waters, presumably as a result of selective removal of Cs by particulates relative to Sr, coupled with the very low $^{137}Cs/^{90}Sr$ ratios found in runoff, again due to selective Cs removal (Bowen et al, 1974). Despite this removal, on coastal timescales of months to several years, Cs can be regarded as sufficiently conservative for water tracer applications (Park et al, 1965; Preston et al, 1972; Noshkin and Bowen, 1973; Wilson, 1974). The fraction of Cs removed to sediment and marine organisms is, however, measureable and has a range of possible tracer applications (Baxter and McKinley, 1978; Hetherington and Harvey, 1978).

The major value of radiocaesium as a coastal marine tracer depends, however, mainly on its release in effluents from the nuclear industry. Caesium has 22 isotopes, all of which, with the exception of natural ^{133}Cs, are radioactive

with half-lives ranging from 25 secs to 3 x 10^6 y (Weast, 1974). The only isotopes useful as ambient tracers are ^{137}Cs ($t_{\frac{1}{2}}$ 30.23 $\pm$ 0.16 y) and ^{134}Cs ($t_{\frac{1}{2}}$ 2.05 y). ^{137}Cs, as mentioned previously, is a major product of uranium or plutonium fission and it is estimated that approximately 34MCi of this isotope had been introduced into the atmosphere from nuclear weapon testing by 1971 (Joseph et al, 1971). ^{137}Cs is also a major component of the fission fragments present in used reactor fuel rods and thus is also commonly released during fuel reprocessing (Woodhead, 1973). ^{134}Cs, is on the other hand, a 'shielded' nuclide, i.e. it possesses a stable isobar of atomic number one unit larger than its own. As fissile species are neutron-rich, fission is generally followed by a chain of β-decays till an isobar of reasonably long half-life is produced. Secondary production of ^{134}Cs by a β-decay chain is thus blocked by ^{134}Xe and the small amounts of primary ^{134}Cs produced by nuclear weapons can generally be regarded as negligible (Persson, 1968; Joseph et al, 1971; Livingstone and Bowen, 1977). In a nuclear reactor, however, secondary ^{134}Cs is produced by neutron activation of fission-produced ^{133}Cs (which is not shielded). As species produced by neutron activation 'grow-in' with their own half lives, this production process is only significant for ^{134}Cs on time-scales considerably greater than the microseconds involved in nuclear explosions. The major source of ^{134}Cs is thus waste release from fuel reprocessing operations.

As radiocaesium nuclides are produced in the cores of nuclear reactors, releases from the reactors themselves are negligible during normal operation and major releases occur only during fuel reprocessing (Williams and Davidge, 1962).

The largest source of waste radiocaesium to a coastal marine environment probably occurs at the Windscale fuel reprocessing plant in Cumbria, England, which presently releases $\sim 10^4$ Ci/month of ^{137}Cs and $\sim 2 \times 10^3$ Ci/month of ^{134}Cs (Howells, 1966; Woodhead, 1973; Howells, 1978). The only other significant sources of waste radiocaesium to N. European waters are the Experimental Reactor Establishment at Dounreay, Caithness which discharges $\sim$ 700 Ci/year (1973) (Jefferies et al, 1973) and the French reprocessing plant at Cap de la Hague. Releases from Dounreay are only significant in the locality of the output while ^{137}Cs from Cap de la Hague has been measured in the English Channel and southern North Sea (Jefferies et al, 1973; Kautsky, 1976; Mauchline, 1978). Fallout ^{137}Cs concentrations in the North Sea of $\sim$ 0.5 pCi l^{-1} in 1969 (Kautsky, 1976) have been calculated to result in a residual concentration of 0.2 pCi l^{-1} by 1973-4 and 0.1 pCi l^{-1} by 1976 (Livingstone and Bowen, 1977). Thus the fallout contribution can generally be regarded as insignificant in British coastal waters relative to ^{137}Cs concentrations resulting from waste releases.

The discharge of radiocaesium from Windscale into the Irish Sea, followed by the effects of coastal circulation, gives rise to a 'caesium plume' round the British coast (Fig 1.4) and this immediately yields useful information on dispersal and dilution of the coastal water body. The $^{134}Cs/^{137}Cs$ ratio provides an additional parameter for use as a dilution-independent 'clock' in calculating rates of coastal water movement (Jefferies et al, 1973; Dutton, 1977; Livingstone and Bowen, 1977; Baxter and McKinley, 1978; Baxter et al, 1978).

FIGURE 1.4 THE WINDSCALE RADIOCAESIUM PLUME

(After Jefferies et al, 1973)

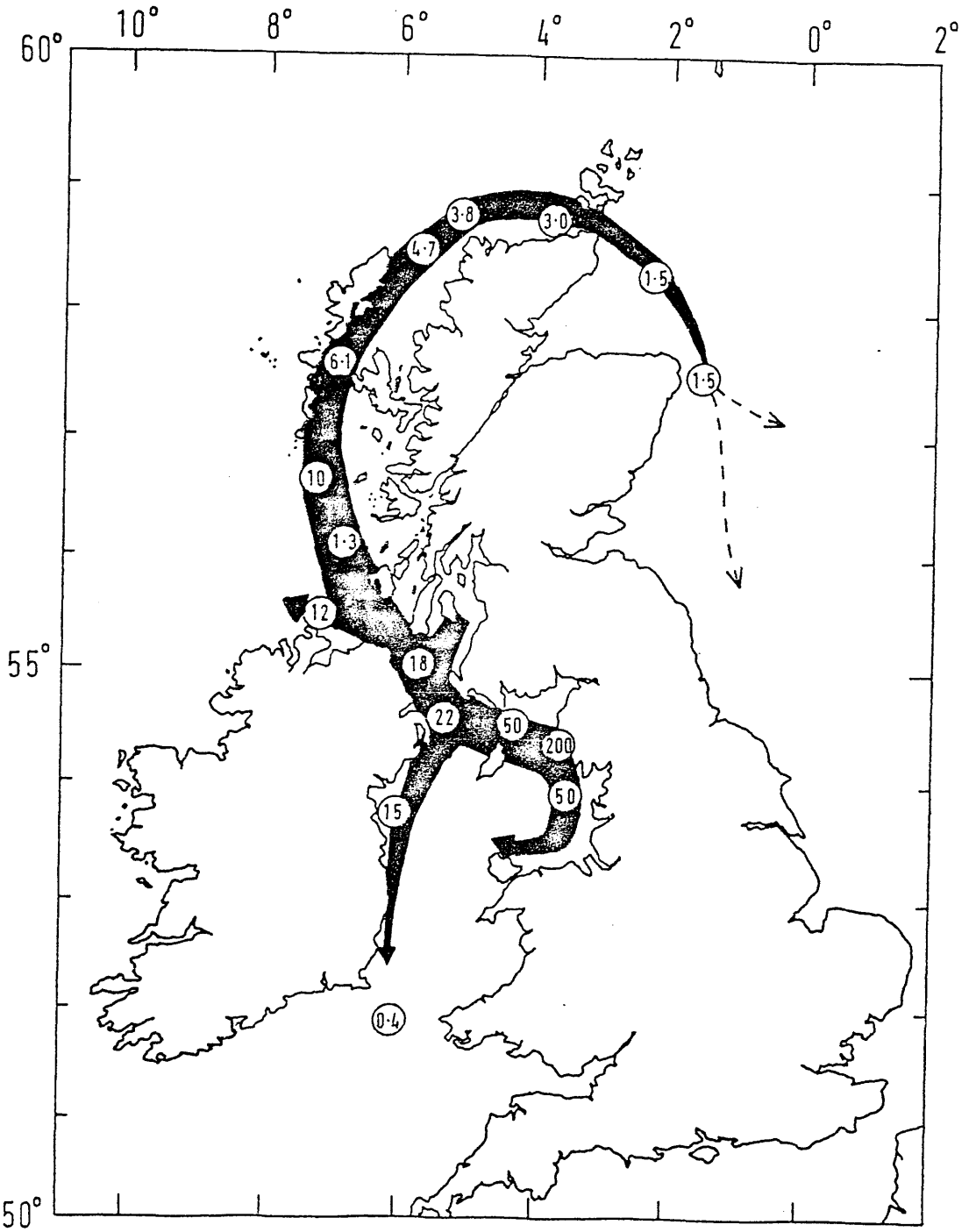

Numbers are Cs-137 concentrations in pCi/l (1972 values).

Simple interpretation of the observed radiocaesium distribution in coastal waters is, however, complicated by temporal variations in Windscale output. The general trend in increasing annual output until 1975 (Fig 1.5) limits the application of steady state treatments but allows the large increase in output between 1973 and 1975 to be used as a definitive marker by which lag times (or, equivalently, transit times) between Windscale output and coastal sampling stations can be derived (MacKenzie, 1977; Mauchline, 1978).

On a shorter timescale there is monthly variability in the ^{137}Cs output and in the $^{134}Cs/^{137}Cs$ ratio (Fig 1.6). This generates a series of 'pulses' of high output for several months' duration (Dutton, 1977; 1978; Howells, 1978). Although there is considerable damping of these short duration pulses by mixing within the Irish Sea and during transport, they again provide a set of temporal markers which can be matched between sampling sites (MacKenzie, 1977; Baxter et al, 1978; Baxter and McKinley, 1978; Dutton, 1978).

While radiocaesium is regarded as fairly conservative in coastal water tracer applications, a small but significant percentage of the water-borne radiocaesium is removed into the sediment column or taken up by marine organisms. The main removal process onto particulates involves ion-exchange on clays, mainly illite, by replacement of K^+ ions (Tamura and Jacobs, 1960; Pickering et al, 1966; Auffret et al, 1971; Duursma and Eisma, 1973). Although the extent of caesium removal is limited, the removal process itself is fast with a half-time of (0.7 ± 0.4) days (Duursma and Eisma, 1973). In-sediment diffusion coefficients of 10^{-9} to 10^{-8} cm^2 sec^{-1}

FIGURE 1.5

Cs-137 releases from Windscale

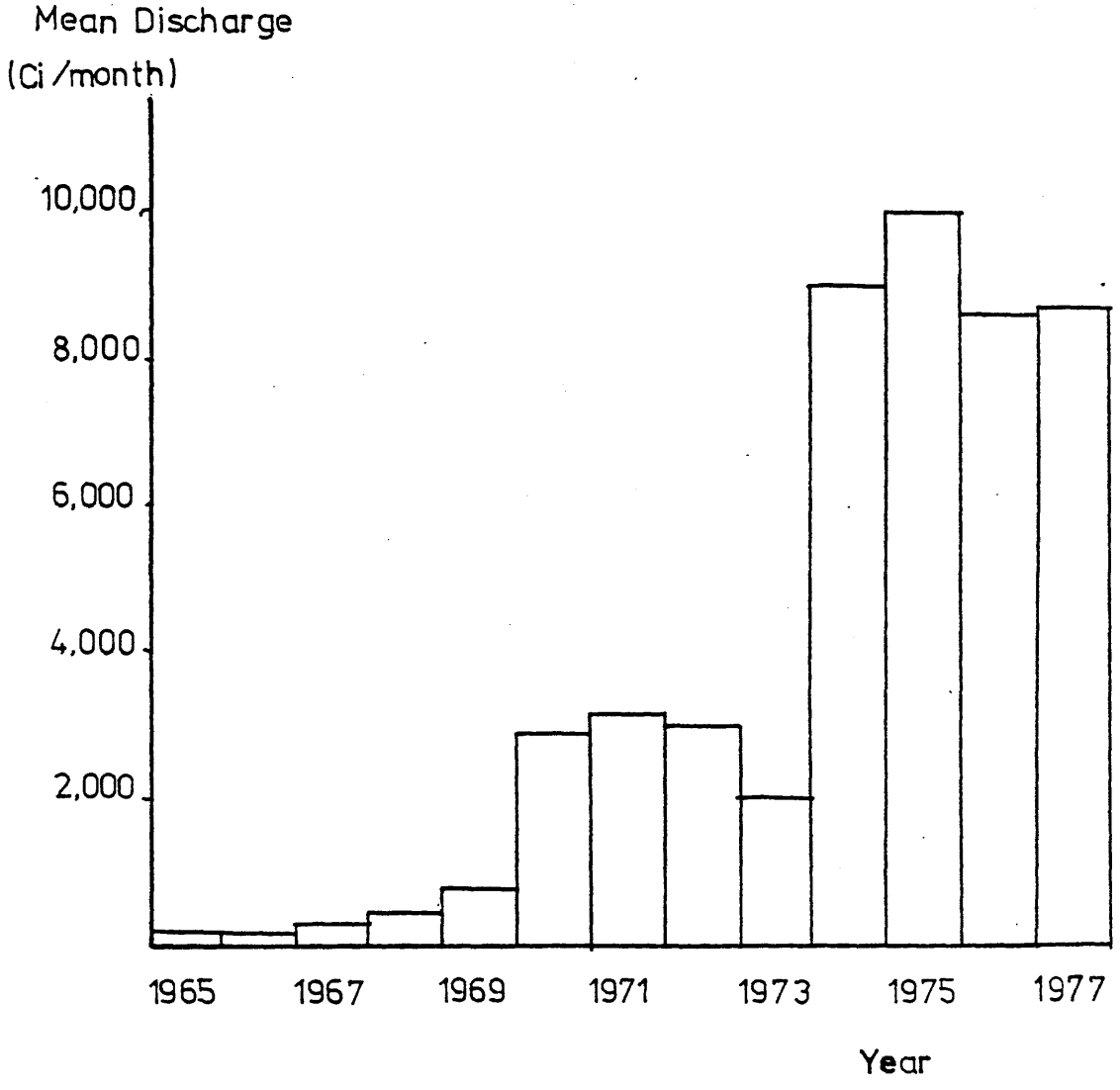

FIGURE 1.6 MONTHLY VARIATIONS IN WINDSCALE RADIOCAESIUM OUTPUT

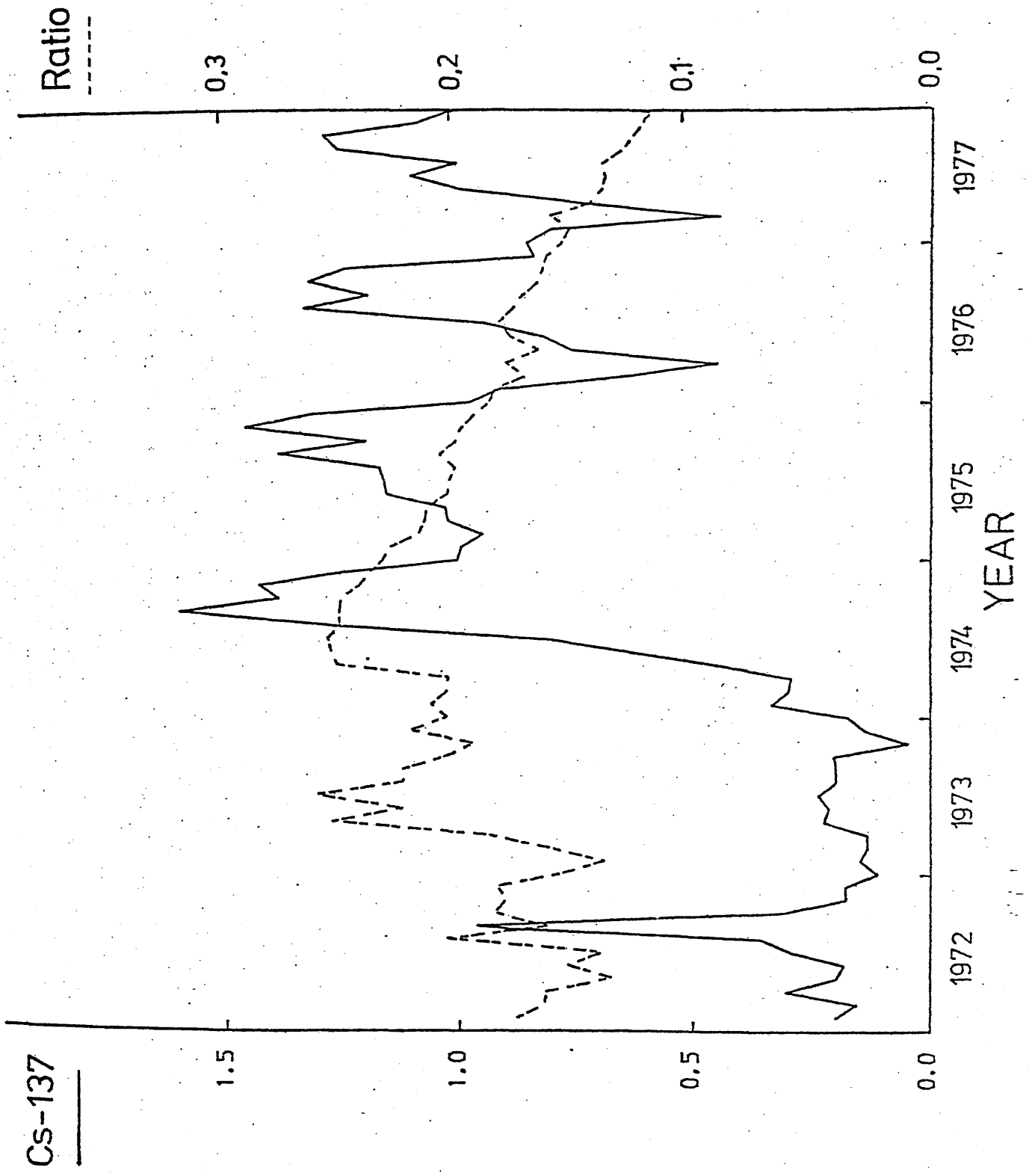

for ^{137}Cs(Duursma and Bosch, 1970; Duursma and Gross, 1971) may limit sediment geochronological applications (Goldberg and Bruland, 1974). As this effect would induce a depth penetration by diffusion of 2 - 4 cm in 10 years (Duursma and Gross, 1971), fallout geochronology may, nevertheless, be applicable in areas with large sedimentation rates, especially in view of the observation that post-depositional diffusion of ^{137}Cs would not change the depth of a peak maximum in the sediment, but would simply modify its magnitude (Krishnaswami et al, 1971).

In fresh water systems, caesium is more strongly sorbed (Duursma and Gross, 1971), due perhaps to diffusion of Cs further into the clay lattice, resulting in complete caesium immobilisation (Pickering et al, 1966). This fact, coupled with the effects of longer water residence times and increased particulate fluxes, gives rise to a more marked removal of fallout ^{137}Cs into the sediment column in lacustrine systems. This reasonably effective removal, coupled with the temporal variation in bomb fallout (Fig. 1.3a), has formed the basis of a convenient geochronological method for recent lacustrine sediments (Pennington et al, 1973; Ritchie et al, 1973; Robbins and Edgington, 1975). This method may, however, be limited by remobilisation and diffusion of Cs within the sediment column (Lietzke et al, 1973; Lerman and Lietzke, 1975) though, in practice, bioturbation may be a more significant post-depositional mobiliser of caesium. In such cases, the redistributed caesium may be used to calculate biogenic eddy diffusion coefficients (Robbins et al, 1977).

In the marine environment, therefore, removal of caesium into sediment is much less effective than in freshwater systems, corresponding to ~3% of the ^{137}Cs fallout delivered to the sea surface (Noshkin and Bowen, 1973). Thus, although removal rates may be higher (~7%) in shallow waters (Noshkin and Bowen, 1973), the total fallout radiocaesium content of marine sediments is generally low and, if distributed to depth by turbation processes, is often difficult to measure (Noshkin, 1972).

In the vicinity of radiocaesium waste releases, high radionuclide concentrations result in readily measureable activities in sediments. The extent of incorporation of radiocaesium onto particulates and its distribution with respect to mineralogy and particle size can be regarded as typical of stable caesium and thus useful marine chemical information may be derived (Duursma and Bosch, 1970; Duursma and Eisma, 1973). In addition, study of the removal of radionuclides into the sediment column may be extrapolated to other pollutants which may not be as readily examined due to multiplicity of sources (Turekian, 1977; Hetherington and Harvey, 1978). The depth distribution of ^{137}Cs in the sediment column may also be used and related to the Windscale output curve (Fig 1.5) to calculate sedimentation rates or examine sediment mixing or diffusion processes. The $^{134}Cs/^{137}Cs$ ratio may again be used as an additional independant tracer of half-life 2.2 years (Hetherington and Jefferies, 1974; Livingstone and Bowen, 1977; MacKenzie, 1977; Baxter et al, 1978; Swan, 1978).

From investigations of fallout radiocaesium in marine organics, organic concentration factors appear to be relatively low (5-50) and to show little increase in higher trophic levels (Bowen et al, 1971; Lowman et al, 1971; Penreath, 1977). Higher values (50-150) were, however, found in coastal areas (Gilat et al, 1975). Waste releases of radiocaesium into rivers and coastal waters have encouraged more detailed studies of biological concentration in restricted areas and these have implied much larger concentration factors in rivers (100-600) and freshwater lakes (Micholet-Cote et al, 1973; Bryan et al, 1966). Although, even in coastal areas, there is no apparent change in radiocaesium concentration factors during transfer between trophic levels, this transfer does result in increasing discrimination in favour of ^{137}Cs over K with increasing trophic level (Broom et al, 1975). Apart from the use of radiocaesium to 'tag' fish from contaminated areas, radiocaesium may be used as an indicator of the general pollutant content of marine organisms. In addition, radiocaesium contents of organisms may indicate time-averaged values for ambient radiocaesium levels in water (Baxter et al, 1978).

Radiological safety investigations have identified radiocaesium as a critical component of Windscale output (Preston, 1975). As such, routine monitoring required by the radiological hazard assessment programme provides a useful source of background data for oceanographic studies (Mitchell, 1973; 1975; 1977a; 1977b; Hetherington, 1976). Oceanographic determination of waste dispersal and distribution between water, sediment and marine organisms may,

in turn, be used to improve radiological hazard evaluation (Preston et al, 1972; Preston, 1975; Baxter et al, 1978).

1.4 Areas of Study

This project initially developed from natural tracer studies of water transport and sedimentation patterns in the Clyde Sea Area (MacKenzie, 1977; Swan, 1978) so that a major objective was to further understanding of marine processes in this region. The Clyde Sea Area, a term first introduced by Mill (1892), is a system of salt water bodies of total surface area 2500 km^2 lying to the north of a line from Girvan to the Mull of Kintyre, i.e. 55° 15' N (Fig 1.7). This embayment communicates with the Irish Sea and Atlantic Ocean via the narrow passages of the North Channel and consists of three distinct bathymetric regions:- a) the shallow drowned estuary of the Clyde river, b) a series of fjordic sea lochs to the north and c) the wider expanse of the Firth of Clyde (MacKenzie, 1977). The region has considerable importance for fishing, industrial, navigational, naval, sewage disposal and recreational purposes (NERC, 1974). The total catchment of the area sustains a population of about 2.5 million people and significant levels of pollution occur, notably in the estuary, off the Ayrshire coast, and at the sewage dumping ground at Garroch Head (CRPB, 1973; 1974a; 1975; 1976).

Water movement in the Clyde Sea Area has been studied via salinity and temperature surveys since the end of the 19th century (Mill, 1892; Milne, 1974). In recent years, extensive and regular surveys have been performed by the

FIGURE 1.7 MAP OF THE CLYDE SEA AREA

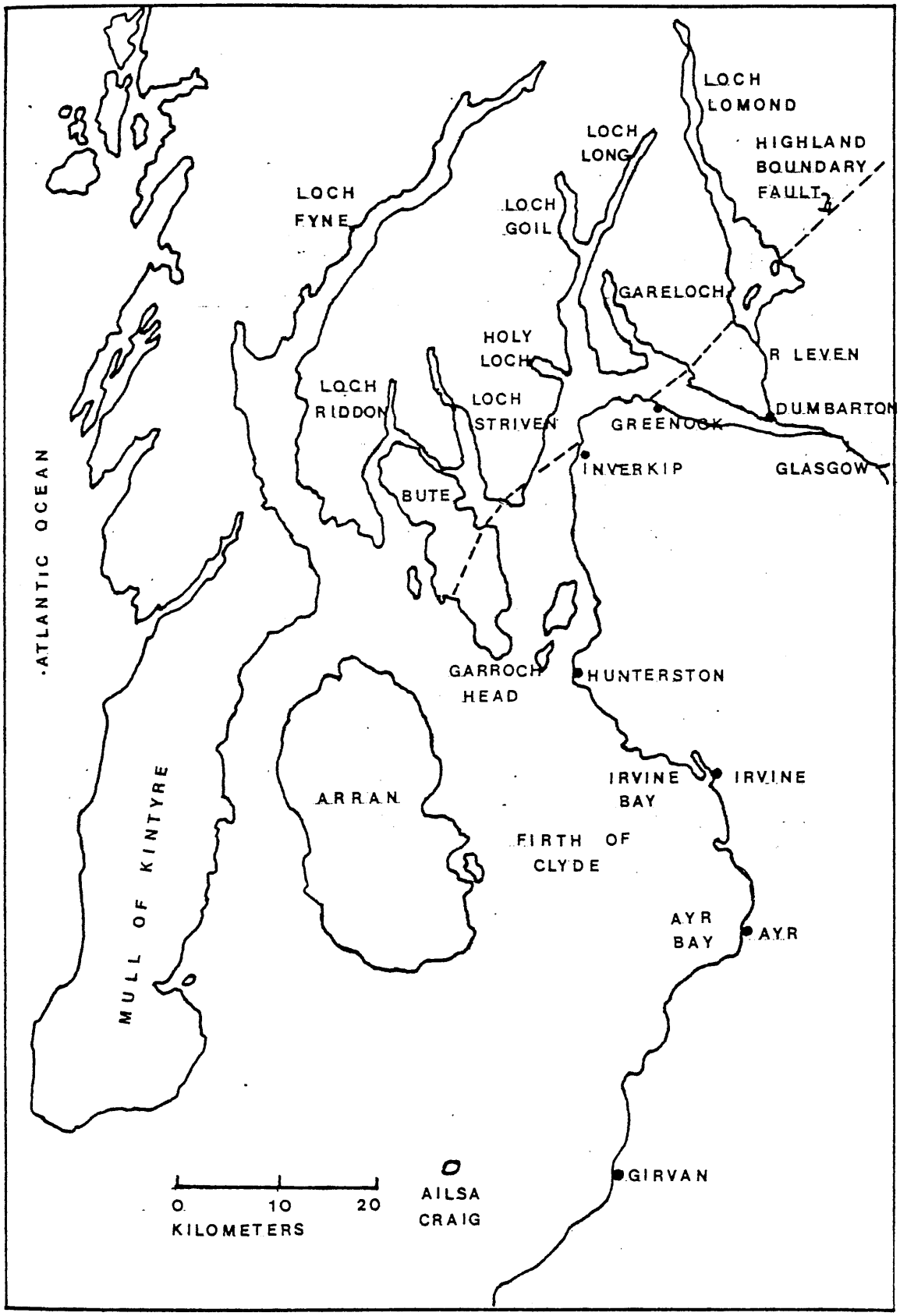

Clyde River Purification Board (CRPB). Salinities decrease from about 32‰ in the northern Firth to near zero values at the head of the estuary while vertical profiles show the estuary system to be intermediate between well and partially mixed (Collar, 1974). In the Firth, temperature and salinity show only small variations, largely due to freshwater input from the estuary and rivers of the Ayrshire coast. Direct measurements of currents by current meters, drifters etc. have been performed, mainly in areas receiving heavy pollution burdens or in shallow regions important for navigational purposes. The results of these surveys indicate that surface and near-shore currents are largely wind-induced while circulation in the open Firth is more complex with contributions generated by winds, tides and estuarine circulation (Barnes and Goodley, 1961; Johnston et al, 1974).

Salt water from both Irish Sea and Atlantic sources may enter the Clyde Sea Area. Trace metal studies have indicated that the Irish Sea-derived component is a major source of Cu, Zn, Cd and Pb to the area (Topping, 1974; Cambray et al, 1975). Radiocaesium peak-matching allowed MacKenzie (1977) to estimate that $\sim$ 92% of exchanging water is derived from the Irish Sea. The rate of this water exchange process was estimated from salinity data to be $\sim$ 9 months (the mean water replacement time in the Firth) (Craig, 1959) while from radiocaesium data, mean water residence times in the Clyde Sea Area of 2.1-8.2 months have been obtained (MacKenzie, 1977). Nevertheless the area remains ill-defined in terms of residence time, water origins and current velocities, as emphasised by the 1974 Clyde Study Group (Natural Environment

Research Council, 1974). The northern sea lochs are all typical glacial trenches with steep-sided, flat-bottomed, narrow profiles. Two of the lochs, Loch Goil and Gareloch, have been extensively studied and show an annual cycle in depth profile of salinity, temperature and dissolved oxygen. The dissolved oxygen profile is particularly marked in Loch Goil in autumn when deep water is virtually anoxic (Fig 1.8). These profiles have been interpreted as due to summer stratification followed by a 'winter overturn' and have been used to infer relatively long residence times for deep waters in the sea lochs (CRPB, 1974a; 1975b). Water in the deep basins of Loch Fyne has been shown to be virtually anoxic at all times of the year, implying a stagnant system (Leatherland 1977). Early radiocaesium measurements, however, have indicated continual mixing of Loch Goil with complete internal mixing occuring in less than 2.1 months, and, in addition, implied that both Loch Long and Loch Fyne could be classified as well mixed (MacKenzie, 1977).

Superficial sediments within the Clyde Sea Area have been classified into a distribution of three sediment facies, namely coarse littoral, transitional and deep silty clay (Fig 1.9). Sedimentation rates in the northern sea lochs have been estimated as 0.3 - 0.6 mmy^{-1} (pre-industrial) by ^{14}C dating (Baxter and Harkness, 1975), ~ 3 mmy^{-1} by radiocaesium and $\sim 1 mmy^{-1}$ by ^{210}Pb (MacKenzie, 1977). More recently, rates of ~ 6 mm y^{-1} for Loch Goil and ~ 20 mm y^{-1} for Gareloch have been obtained by ^{210}Pb measurements (Swan, 1978). By direct measurements of the sediment flux, Moore (1931) estimated a mean sedimentation rate for the Loch Strivan

FIGURE 1.8

Variation of Dissolved Oxygen in the Bottom Water of Loch Goil

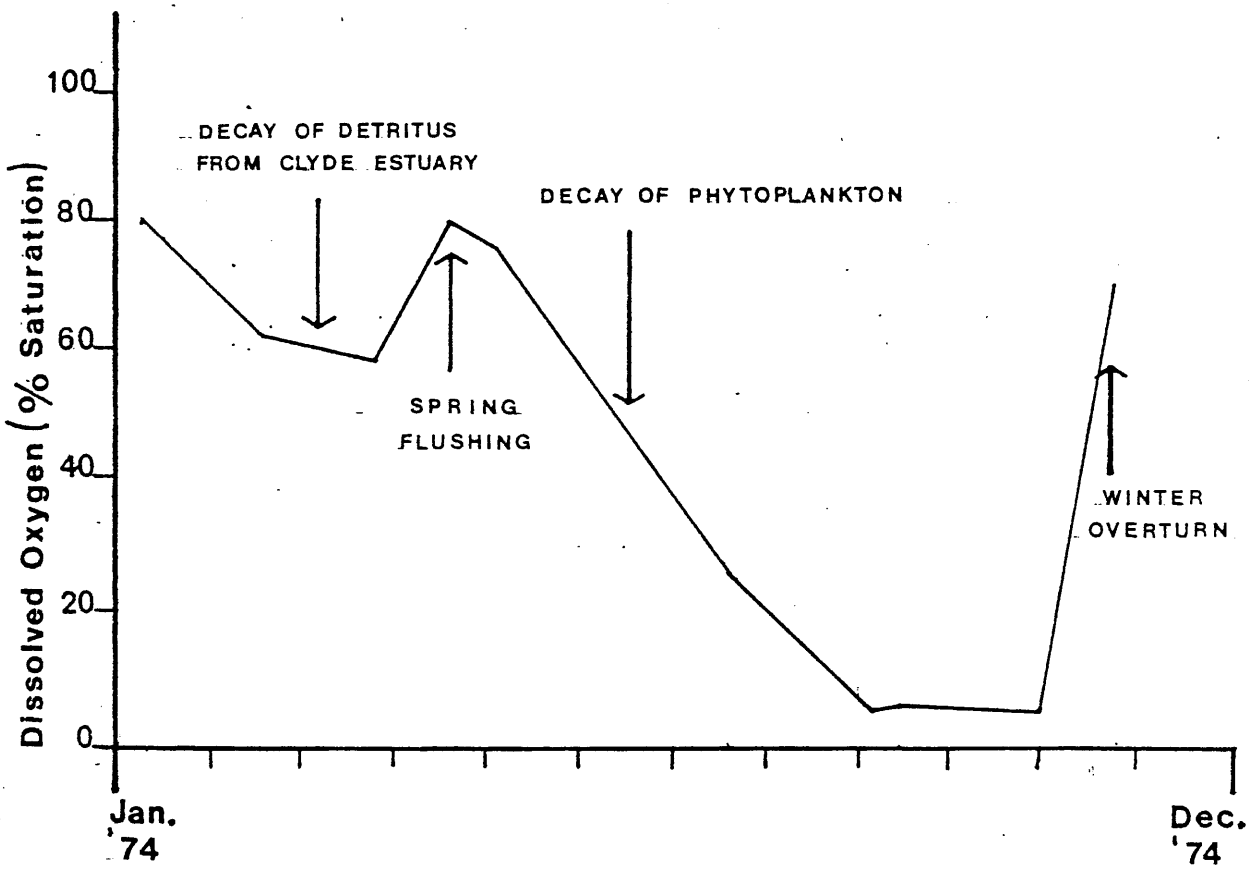

(Clyde River Purification Board, 1974.)

Figure 1.9 Surface sediments in the northern section of the Clyde Sea Area (Deegan et al., 1973)

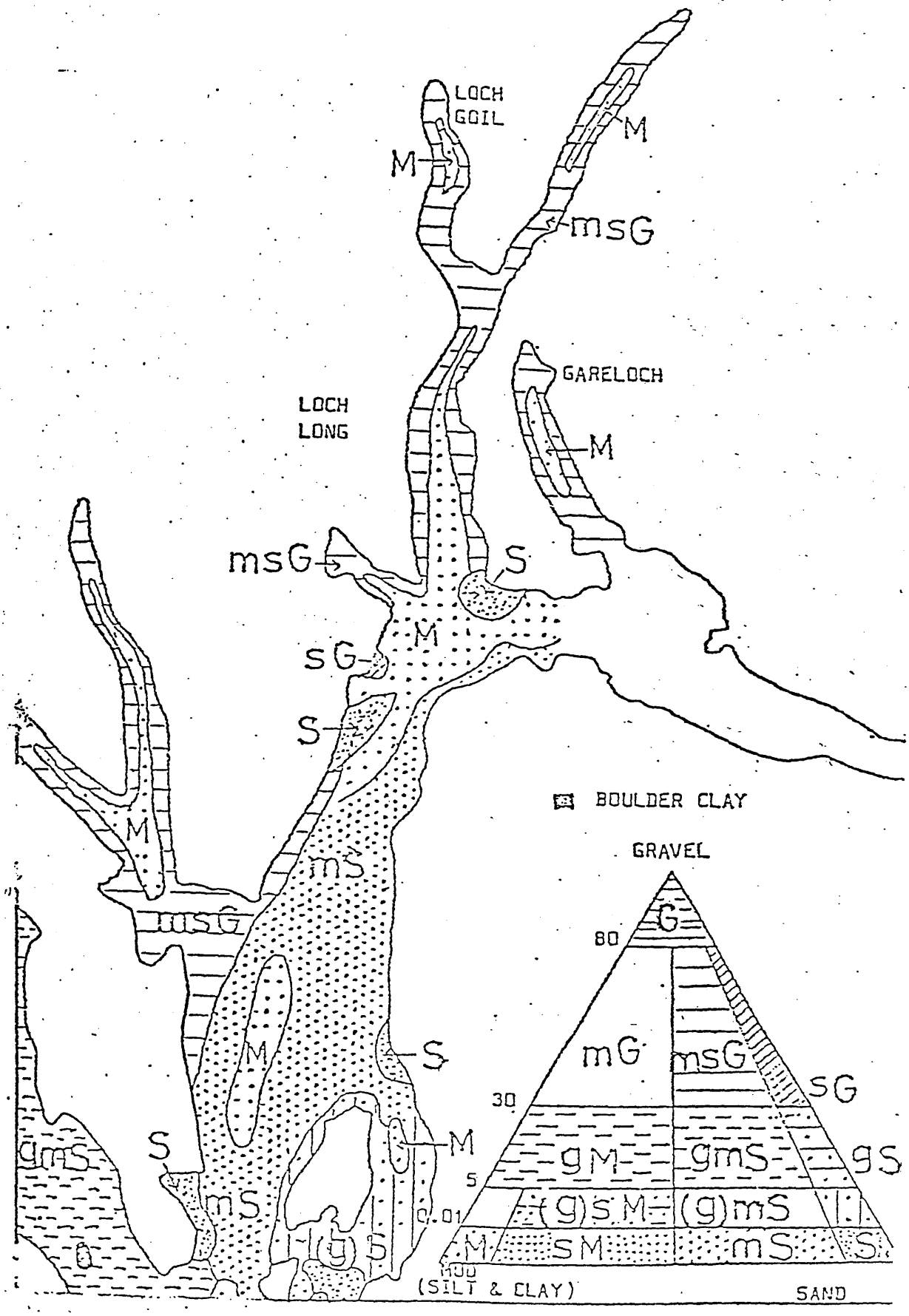

area of ~5 mm y^{-1} while Baxter and Harkness (1975), using $^{14}C/^{12}C$ measurements, deduced an artificial sedimentation rate of 7.5 $\pm$ 0.2 mm y^{-1} for the Garroch Head dumping site. Many of these past estimates of sedimentation rates are less than authoritative either through coring uncertainties (Swan, 1978) or interpretational ambiguity (Baxter and Harkness, 1975; Moore, 1931). It is therefore necessary to continue sedimentation studies in the area, a view supported by the Clyde Study Group (National Environment Research Council, 1974) who concluded 'Further information on sediment transport and deposition is needed before predictions about the distribution of effluents and the effects of dumping (of excavated material and sewage sludge) can be made'.

Water passing from the Clyde Sea Area mixes with north-flowing Irish Sea water and flows round the coast of Scotland (Jefferies et al, 1973; Ellett, 1977, 1978; Mauchline, 1978). This water body, contaminated by both stable and radioactive pollutants, is an obvious tracer of transport and mixing processes round the entire Scottish coast. One area of particular interest is the marine environment of the Outer Hebrides, as this area has been little studied by comparison with other coasts of the British Isles (Ellett, 1978).

This area, referred to as the Hebridean Sea Area, consists of the salt waters off the west coast of Scotland extending westwards ~ 100 miles from the coastline and from the north of Ireland to the north of the Outer Hebrides,

i.e. approximately 5.5 - 9° W by 55 - 58.5°N (Fig 1.10). Data collection in this area has been sparse and intermittant and the majority of hypotheses concerning processes at work in Hebridean seas have been obtained by inference and analogy (Ellett, 1978). Water transfer processes show marked seasonal variations. The surface circulation derives from the three main water types present - Atlantic, Clyde-Irish Sea and coastal fresh water runoff. By combining data from salinity and freshwater runoff measurements (Craig, 1954), drift bottle releases (Barnes and Goodley) and radiocaesium (Jefferies et al, 1973), Ellett has described summer surface current distribution (Fig 1.11). (Ellett, 1978). In winter, when water on the Hebridean Shelf is mixed throughout its depth by the frequent gales, Atlantic water invades the larger part of the shelf to the west of the islands. In spring this area is reoccupied by the spread of less dense coastal waters (Ellett, 1978). In addition to the general seasonal variation in circulation in this area, the coastal flow of Clyde-Irish Sea water shows marked yearly variations as indicated both by salinity/temperature measurements (Ellett, 1977; 1978) and radiocaesium measurements (Jefferies et al, 1973; Dutton, 1977; Mauchline, 1978). From measurements of $^{134}Cs/^{137}Cs$ ratio decrease, transit times from Windscale to the northern reaches of the North Channel of 1.1 - 1.8 y (Jefferies et al, 1973) and Windscale to the Minch of 0.7 - 1.6 y (Livingstone and Bowen, 1977) have been calculated. The discrepancy between these results has not, as yet, been unambiguously resolved.

Figure 1.10 The Hebridean Sea Area.

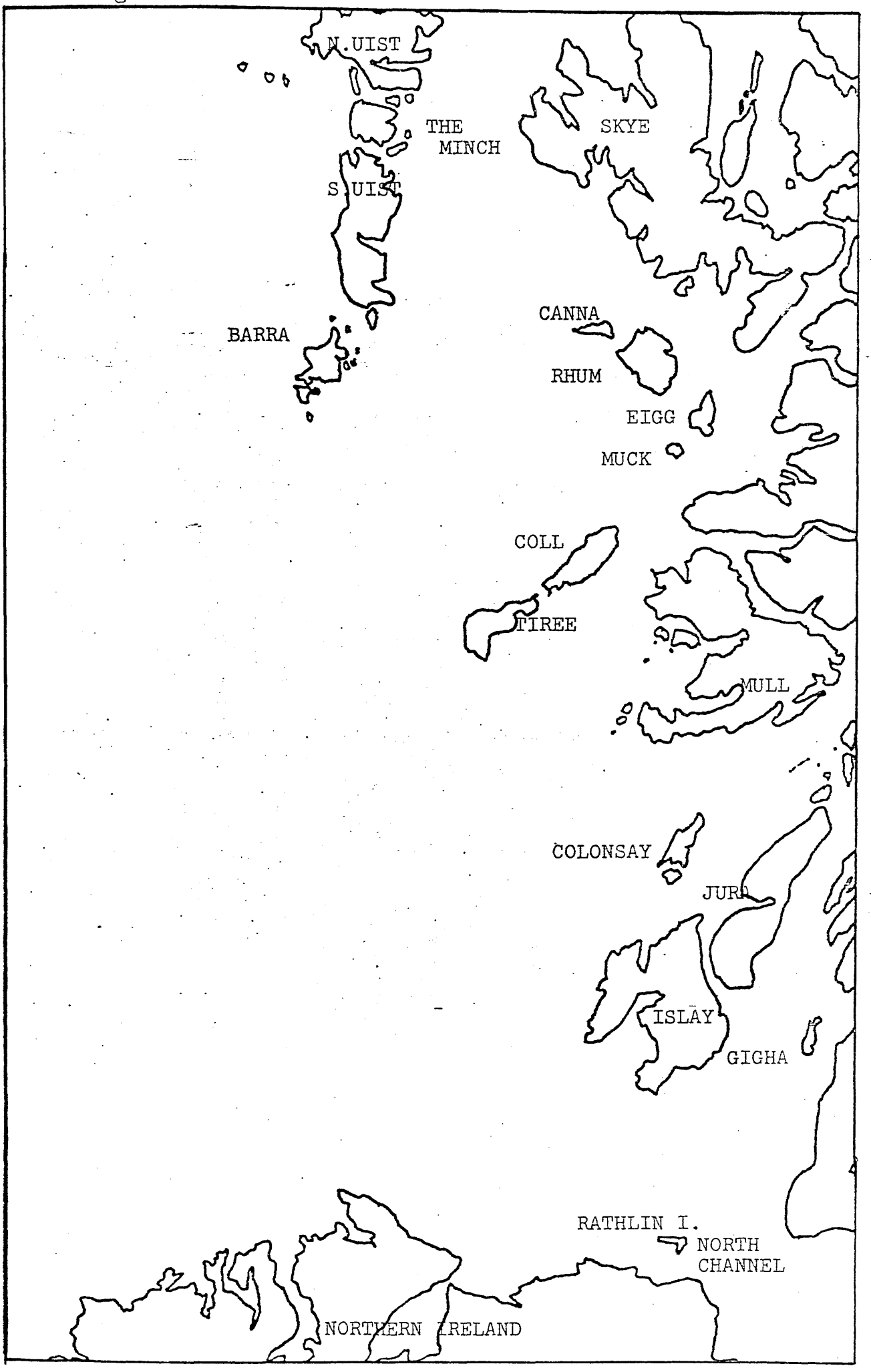

Figure 1.11 Summer surface currents in the Hebridean Sea.

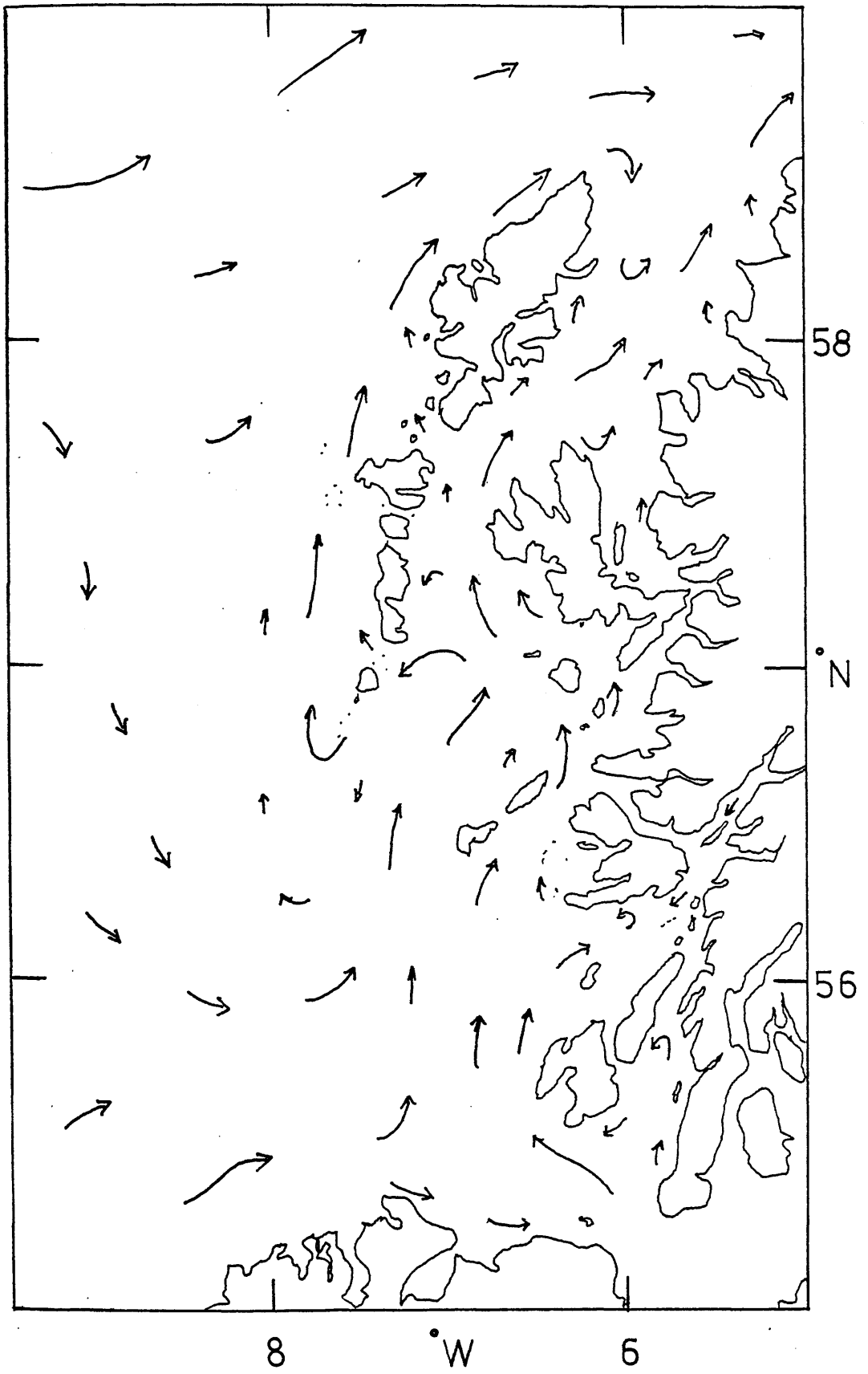

From Ellett(1978).

1.5 Aims of Research

The general aim of the project is to study water transport and sedimentation processes by applying radiocaesium as a tracer of both. Besides investigating specific areas within the western coastal area of Scotland, development of a general methodology is intended to allow more widespread application of this tracer. The project can be subdivided as follows:-

a) Development and simplification of radiocaesium measurement procedures for a variety of sample types, including water, sediment and biota, and evaluation of the errors involved in these measurements.

b) Evaluation of hydrographic parameters from radiocaesium distributions on a series of spatial and temporal scales, ranging from annual variation in coastal water flow in the Hebridean Sea Area to monthly variation in water exchange in Loch Goil. Associated construction of mathematical models of the systems involved will hopefully allow both calculation of relevant hydrographic parameters and assessment of the impact of other, non-radioactive pollutants.

c) Investigations of coastal marine sediments to evaluate radiocaesium as a tracer in geochronological and turbation studies. Comparison of analytical methods will allow optimisation of interpretation procedures for radiocaesium profiles.

d) Measurement of radiocaesium in marine organisms to allow examination of both concentration of radiocaesium through the food chain and bioconcentration of other both stable and

radioactive pollutants. From the activity of radiocaesium in water, sediment and seafoods, critical pathway analysis should enable some evaluation of the radiological health risks both to defined 'critical groups' and to the general population.

e) From an overview of accumulated data, to suggest further developments and areas to which the derived methodology could be applied.

The general structure of the following chapters will involve a) examination of experimental techniques, b) consideration of radiocaesium tracer applications in the waters of the Clyde Sea Area, Loch Goil and the Hebridean Sea Area, c) consideration of radiocaesium as a sediment tracer, with d) a final chapter covering biological applications, radiological hazards and a general overview. Each chapter will consist of an introduction, examination of results obtained (listed in Appendix 1) followed by mathematical analysis and interpretation. Whenever used, additional results obtained by other workers will be listed only in the discussion section of the relevant chapter.

Chapter Two

Experimental

2.1 Introduction

One of the major advantages of radiocaesium as a marine tracer is its convenience of measurement via high resolution γ-spectrometry. For full exploitation of this benefit, however, firstly sample pretreatment should be minimised and secondly the errors associated with sampling and analysis must be evaluated. A further practical requirement is for optimal use of counting time as the latter often becomes the rate determining factor in assessment of environmental radioactivity.

The overall general procedure for radiocaesium assay involves a) environmental sampling, b) sample preparation for counting, c) counting by γ-spectrometry and d) evaluation of radiocaesium content from the γ-spectrum. Each of these processes has associated errors, both random and systematic, which contribute to the total uncertainty in the final data.

As this project focusses on detailed examination of an existing method and on investigation of its range of applicability, a high throughput of samples is desired. Environmental sampling from the coastal areas considered is generally satisfied by a series of regular sampling trips taking 1 day/month, augmented by samples obtained by rarer additional or longer duration trips or samples collected by

other workers. Sample preparation for counting is performed, as far as possible, in a batch system in which a number of similar samples are treated simultaneously - if necessary by utilising duplicate sets of equipment. In the case of radiocaesium extraction from water, 8 filtration/extraction rigs are used in parallel while, for sediment samples, sections from a single core are generally prepared together. Through this procedure, a batch of water samples (8) may be prepared for counting in 2 days. A sediment core (generally ~15 samples) may be similarly prepared after 2 days' work with an intermediate gap of ~3 days for sample drying.

The time required for sample analysis by γ-spectrometry is a function of several parameters:- the radionuclides to be quantified, the radionuclide content of the original sample, the degree and efficiency of pretreatment, the detector efficiency and resolution, convenience of sample changeover and the desired degree of accuracy. For most samples the desired counting accuracy can, as discussed later, be obtained on the Glasgow University system using count times of either 400 or 800 mins., allowing a maximum throughput of 2 samples/day on a daily schedule of long (800 min.) overnight and short (400 min) daytime counts.

Analysis of resulting γ-spectra presently involves initial peak inte gration by hand and storage of data on punch cards, followed by calculation and analysis via a suite of Fortran computer programs. This procedure, although tedious, is again most efficiently handled by batch techniques by which ~40 spectra/day may be analysed.

Radioactivity counting is thus, generally, the rate determining process in the analytical technique, its optimisation being considered in the following section.

As in any study involving quantification of trace amounts of material, a number of practical experimental precautions must be observed. Two possible experimental biases must be considered - these potentially arising through contamination by extraneous material and removal by interfering species.

The purity of all reagents is maximised by sole use of research grade ('Analar') chemicals. Wherever possible, a single batch of reagent is used throughout the study. All water required for preparations is pre-distilled and stored in high density polythene containers. All glassware is 'pyrex' (Borosilicate glass), unused prior to the project. Before use and between runs, all non-disposable glassware is washed in dilute (2M) nitric acid or Pyroneg (Diversey Ltd), rinsed in decontaminating detergent solution (Decon 90) and then in distilled water. Re-usuable plastic tubing is similarly washed, although Pyroneg is invariably used in preference to nitric acid. In most cases, for repeated rinses of the large storage bulbs of the water filtration/ extraction rig, tap water may be used instead of distilled water. Glasgow tap water has been shown to be of insignificantly low radiocaesium concentration (McKinley, 1975) and its use in rinsing therefore has no measureable effect on either the efficiency of radiocaesium extraction or the system blank. Although these washings and decontamination

procedures undoubtedly constitute the most tedious and time-consuming stage in the preparation of water samples for counting, the range of activities measured (from ~ 1dpm l^{-1} to ~ 200 dpm l^{-1}) necessitates such precautions to prevent the occurence of memory effects.

In the following sections the counting facilities, the experimental procedures for water , sediment and biological materials and the calculation methods for results and errors are described.

2.2 Counting Systems

A γ-spectrometry system can be considered, at a basic level, to consist of a detector, an amplifier, an analyser and a readout. During this project a Nuclear Diodes Multichannel Pulse Height Analyser (Model 706) coupled to a Teletype remote printer via a Teletype interface (Model 856N) has been used for the analysis/readout stage, while three different detector/amplifier systems have been utilised (Fig 2.1, Table 2.1).

Between April 1975 and November 1976 a Nuclear Enterprises 3" x 3" cylindrical NaI (Tl) crystal/photomultiplier unit was used in conjunction with a Nuclear Enterprises 4660 High Voltage supply and a Canberra Spectroscopy Amplifier (Model 1417B). The resolution of this system is maintained over count-times of up to 800 minutes by a 'home made' temperature-compensating unit in which a thermistor senses temperature changes in the crystal/photomultiplier assembly and controls the amplifier gain to $<\pm \frac{1}{2}\%$. This system has a resolution of 9.3% FWHM at

FIGURE 2.1 BLOCK DIAGRAM OF COUNTING SYSTEM

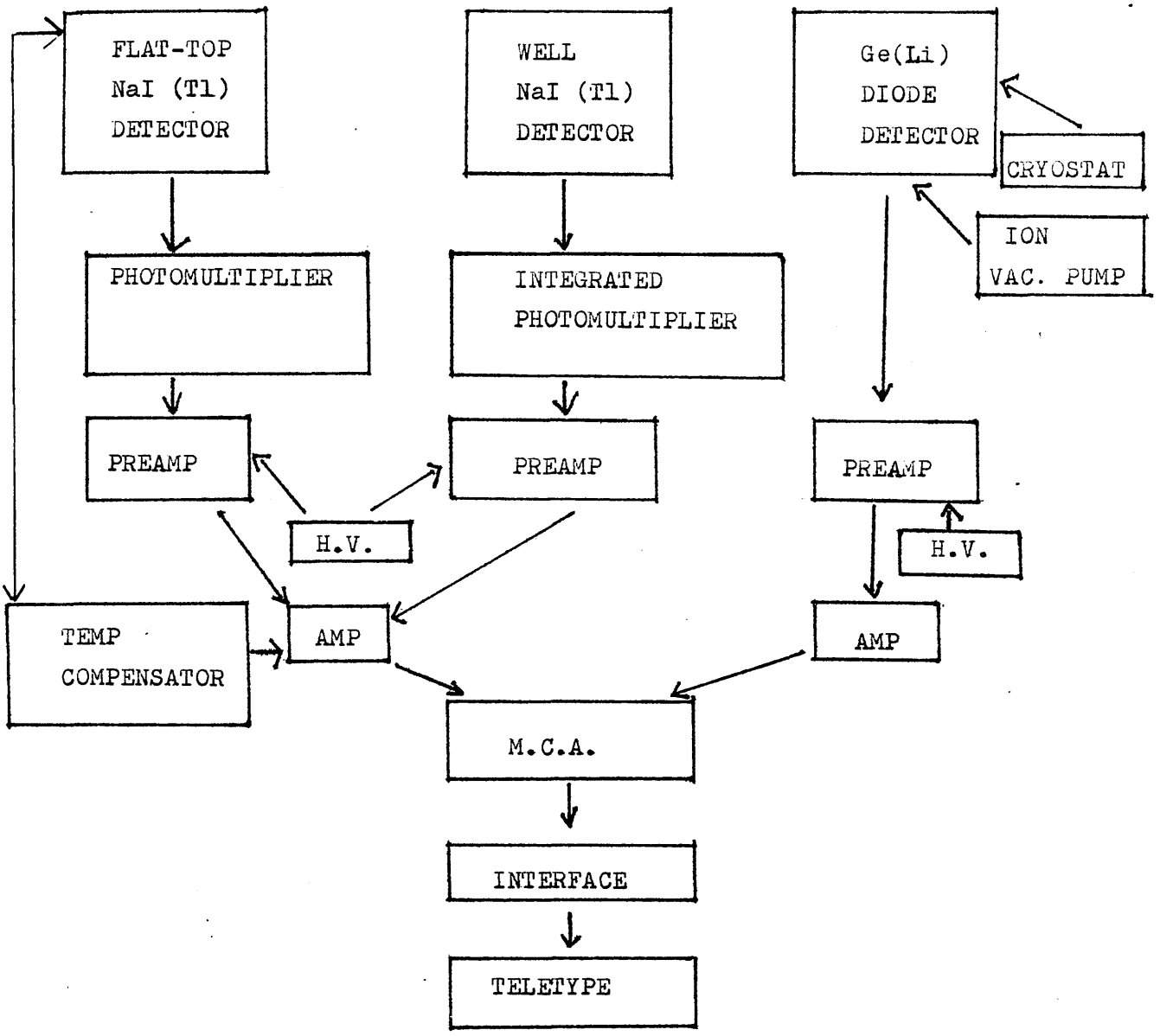

TABLE 2.1 COUNTING FACILITIES

DETECTOR	FLAT TOP NaI(Tl)	WELL NaI(Tl)	Ge(Li)
	3"x3" CYLINDRICAL	3"x3" CYLINDRICAL WELL ⅜"dia.x 1⅜" high	100c.c.
MAKE	NUCLEAR ENTERPRISES	BICRON (3MW3/P)	PHILIPS (APY 48)
DATES OF OPERATION	4/75-11/76	2/77-7/78	8/76-7/78
SPEC RESOLUTION	9.1% at 662 keV	8% at 662 keV	0.18% at1333 keV
ACTUAL RESOLUTION	9.3% at 662 keV	7% at 662 keV	0.27% at 662 keV
WORKING EFFICIENCY (Cs-137 on KCFC)	5.7%	20.8%	1.9%
BACKGROUND (EMPTY COUNTER Cs-137 WINDOW)	13.4cpm	5.7cpm	0.4cpm
COUNTER DETECTION LIMIT (Cs-137 on KCFC 800 mins)	6.9dpm	1.3dpm	3.9dpm
SAMPLES COUNTED (INCLUDING BLANKS, SPIKES etc)	×401	+370	+407

× INCLUDING ~150 BY MACKENZIE(1977)

+ INCLUDING ~20 IN CONJUNCTION WITH BALLANTYNE (1978)

the ^{137}Cs total capture 'photopeak' (662 keV) and a working efficiency for ^{137}Cs on KCFC of 5.7%. Empty counter background in the ^{137}Cs window is 13.4 cpm rising to 13.8 cpm when a blank KCFC cartridge is inserted. The limit of detection for this counter (3σ background) is thus 6.9 dpm for an 800 minute count of a KCFC cartridge.

The flat-top NaI (Tl) detector was replaced in February 1977 by a 3" x 3" cylindrical NaI (Tl) detector with a $\frac{5}{8}$" diameter x $1\frac{5}{8}$" deep well (Bicron, Model 3MW3/P). This unit, which includes an integral photomultiplier assembly, is sufficiently stable to give an increased resolution of 7% FWHM at 662 keV over an 800 minute count without an additional temperature compensator. With a working efficiency of 20.8% for ^{137}Cs on a KCFC cartridge in the well and a KCFC blank background of 6.3 cpm this system has a counting limit of detection of 1.3 dpm for an 800 min. counting period.

In addition to the NaI (Tl) system, a 100 cc Ge(Li) diode detector (Philips model APY48) has been available since August 1976. This unit, used in conjunction with a Nuclear Enterprises amplifier (NE 4603), gives a practical resolution of 0.27% at the ^{137}Cs photopeak. With a working efficiency of 1.9% for ^{137}Cs on a KCFC background of 0.49 cpm, a counter detection limit (3σ) of 3.9 dpm is obtained for an 800 min counting period.

All detectors are shielded on all sides by a 4" thick lead castle lined with 2mm cadmium sheet with an additional 2" of lead over the top of the detector.

The NaI (Tl) detector consists of a thallium-doped sodium iodide crystal which scintillates when exposed to γ-rays (Crouthamel et al, 1970). The resulting light pulse from each γ detected may be converted into a pulse of electrons and amplified by a photomultiplier to produce an output voltage pulse proportional in magnitude to the energy of the original γ-photon. A series of such voltage pulses may, after further amplification, be analysed and stored in a multichannel pulse-height analyser (M.C.A.) to produce a γ-spectrum. The overall detection efficiency depends on geometric factors but can be as high as 90% for energies below 200 keV, but drops to $\sim$ 20% by 1 MeV. The resolution of the NaI (Tl) is, however, limited by statistical fluctuations in output pulse heights as the conversion of the energy of ionising radiation to photons, electron emission at the photocathode and electron multiplication at each dynode are all subject to statistical variations. This effectively limits the resolution (Full Width Half Maximum) to $\sim$ 6% for the ^{137}Cs photopeak (or $\sim$ 40 keV).

The Ge(Li) solid state detector can be regarded as analogous to an ionisation chamber - where an impinging γ-ray causes the formation of electron-hole pairs in a semiconductor (Crouthamel et al, 1970). As a high potential is applied over this crystal in a cylindrical geometry, the electrons and 'holes' travel to the electrodes with high mobilities and again produce, after amplification, a voltage pulse which is proportional to the energy of the exciting γ-photon. This signal is then amplified by circuitry of low noise and high gain and is subsequently analysed by an

M.C.A. Efficiency is intrinsically lower than an equivalent NaI (Tl) system but this apparent disadvantage may be offset by the much higher resolution available.

The differences between these two detector types are probably best illustrated by comparing equivalent 'direct counting' spectra of environmental materials (Fig 2.2). It can be seen that while the Ge(Li) spectra show reasonably distinctive radiocaesium photopeaks, which may readily be used to assess nuclide content, the NaI (Tl) spectrum is insufficiently resolved for these photopeaks to be unambiguously defined and separated from background. The advantage of the higher NaI (Tl) efficiency may be exploited, however, if the caesium content of the sample is first extracted and purified radiochemically. This is most conveniently achieved for water samples by direct passage through a specific ion-exchanger onto which Cs is removed and concentrated in one step. The complete ion-exchange column can then itself be counted directly on a NaI (Tl) system and the resulting simple spectrum used for radiocaesium quantification (Fig 2.3)

The spectra from both detectors are output from the M.C.A. as arrays of numbers - 256 in the case of the NaI (Tl) and 1024 in the case of the Ge (Li) - in the form of a histogram of counts versus energy. Photopeaks are then integrated by hand over specific windows and these integrals further analysed by a suite of computer programs specifically developed during the project.

A basic problem in γ-spectral analysis is that an ideal spectrum from a monoenergetic point source yields not only a peak at an energy corresponding to the 'photopeak' but

FIGURE 2.2 DIRECT COUNTING SPECTRA (HOLYLOCH SEDIMENT)

a)NaI(Tl)

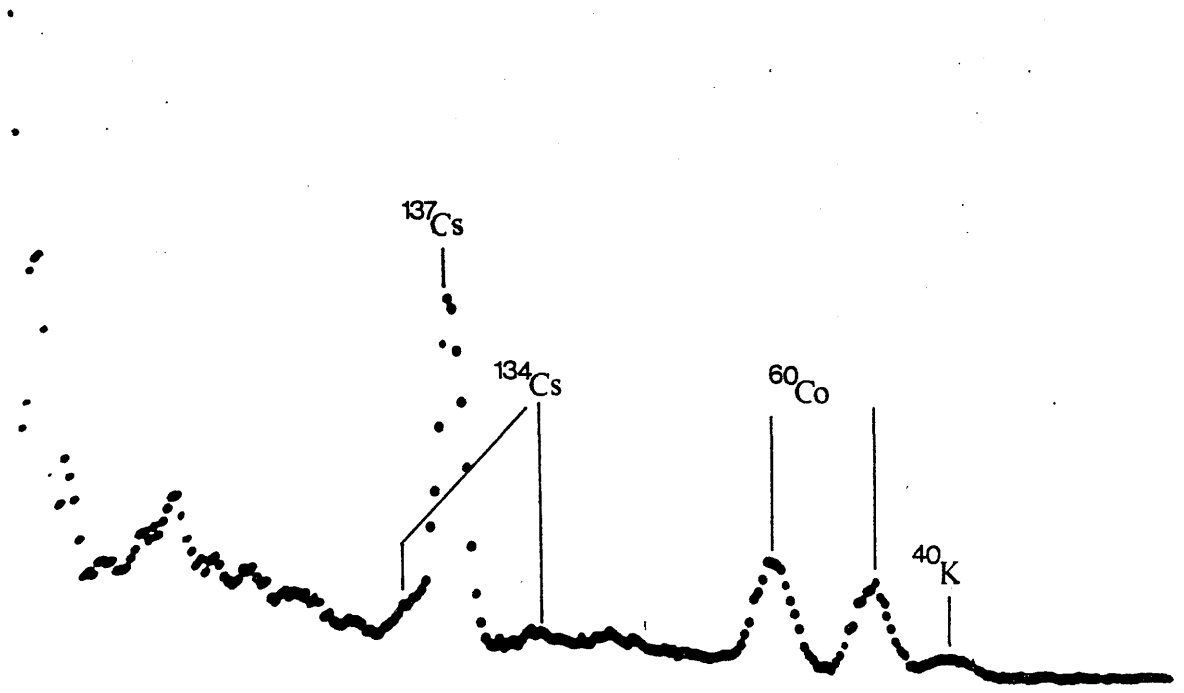

b)Ge(Li)

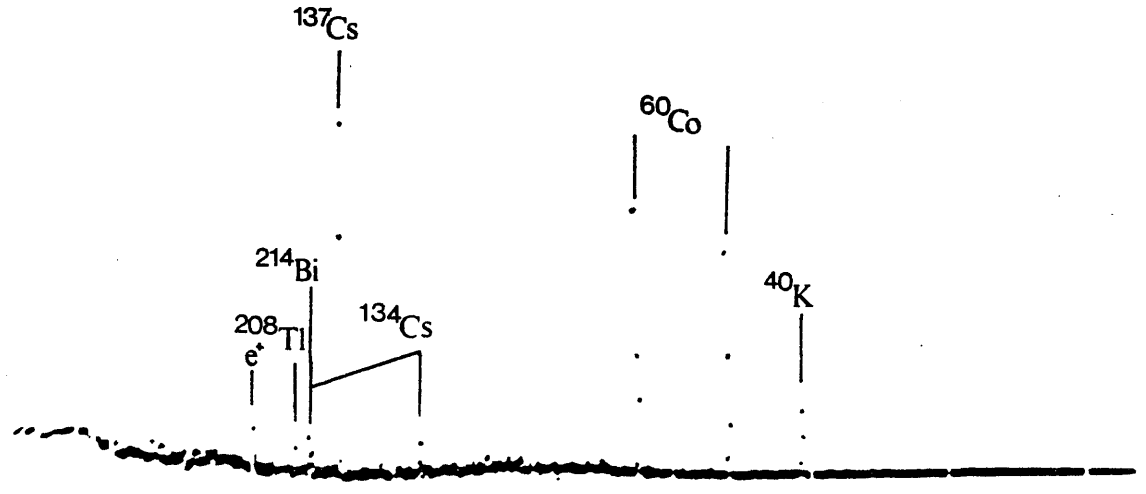

FIGURE 2.3 NaI(Tl) SPECTRUM OF USED "KCFC"

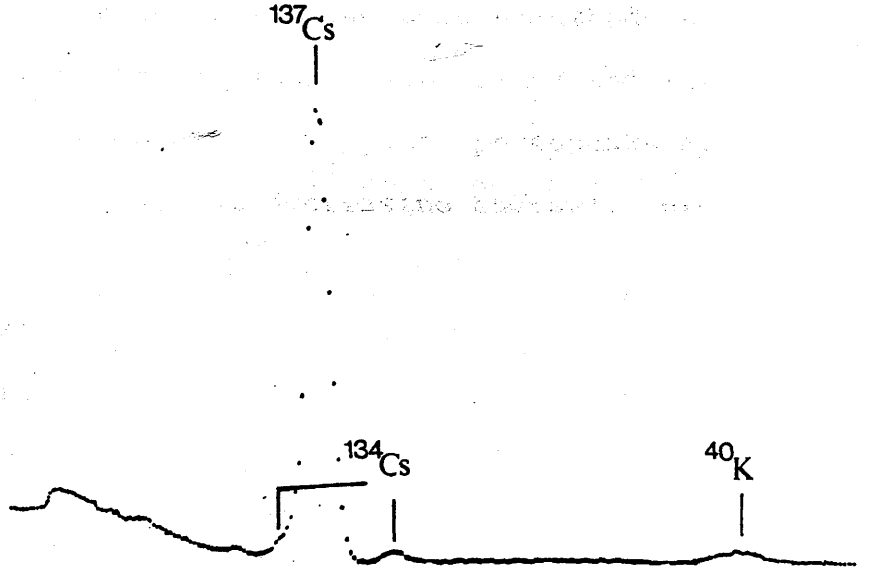

also shows a distribution of counts at lower energies (Fig 2.4) corresponding to energy loss processes, e.g. Compton scattering, backscatter, escape peaks etc. (explained fully in Friedlander et al (1964)). In the analysis of a complex spectrum containing several photopeaks, therefore, in addition to subtraction of an instrument 'empty counter' background, a further term must be deducted to account for base-line increases from the low energy distributions from higher energy photopeaks. Two common methods used to analyse complex spectra are 'spectrum-stripping' and 'peak shape analysis'. In spectrum-stripping, photopeaks are sequentially identified (in order of decreasing energy), integrated and their calculated low energy component stripped from the remaining spectrum (Heath and Schroeder, 1957). Peak-shaping involves processing a photopeak until an idealised shape is reached, thus, hopefully, removing all background contributions. In its simplest form this procedure involves taking only a segment of the photopeak which reproducibly corresponds to a set percentage of the total peak area (Covell, 1959; Yule, 1968; Wasson, 1968; Sterlinski, 1968; 1970; Quittner, 1969; Baedecker, 1971), while more complex approaches involve extraction of a Gaussian peak form from the complex peak shape by Fourier analysis or multiple differentiation (Yule, 1971). Both of these procedures, however, require direct computer spectral analysis to be applied to a large number of samples, a facility unfortunately not available in this project due to lack of a suitable interfacing medium. In this work, however, spectral analysis is considerably

FIGURE 2.4 Cs-137 CALIBRATION SPECTRA

i)NaI(Tl)

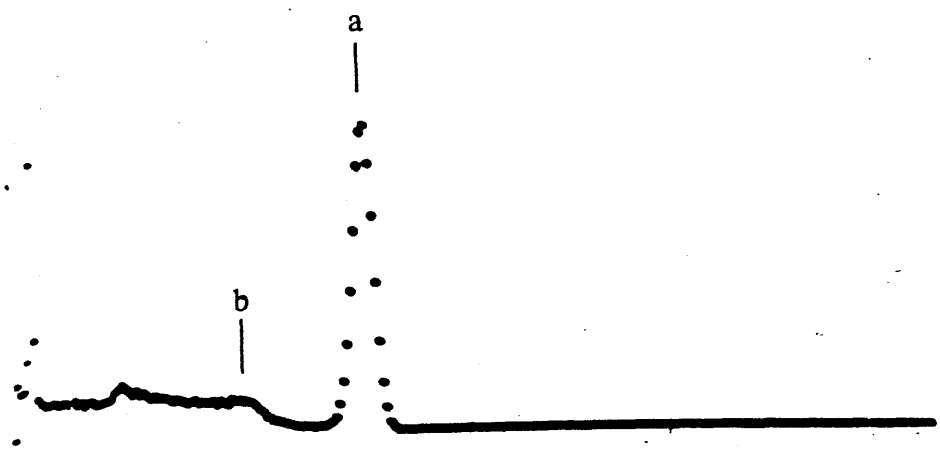

ii)Ge(Li)

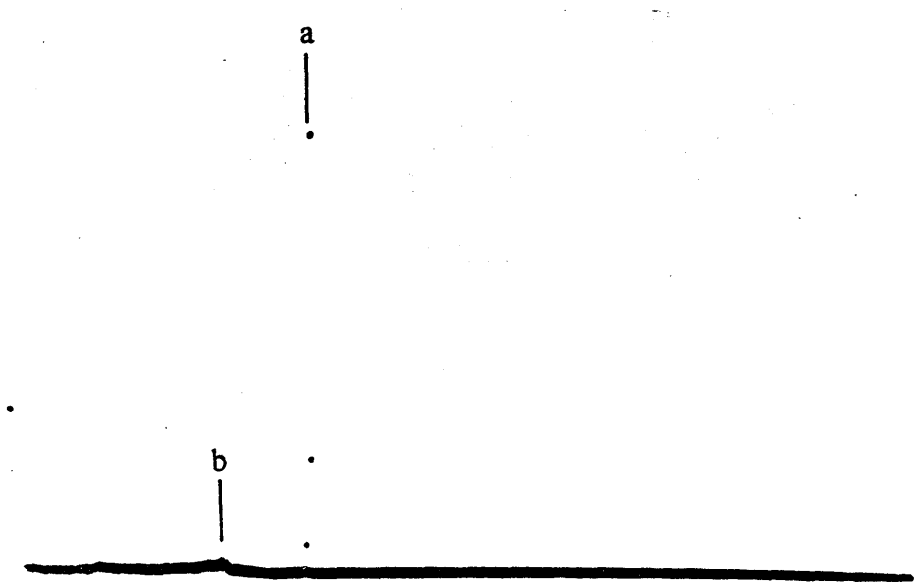

a — Photopeak
b — Compton edge

aided by the relative constancy of the radionuclide contents of samples.

Because of its lack of resolution, the NaI (Tl) detector is used only in conjunction with ion-exchange (KCFC) extraction of radiocaesium. From analyses of ion-exchange cartridges on the high resolution Ge (Li) system (Fig 2.5, Table 2.2) the only significant peaks in the blank KCFC cartridge background between 0.5 and 2.0 MeV are due to the nuclides ^{40}K, ^{208}Tl, ^{214}Bi and ^{228}Ac (apart from annihilation radiation) from natural radionuclide contamination in the ion-exchanger, detector, and shielding materials. The only additional or significantly increased peaks in the spectrum from a real sample are those due to the radiocaesium nuclides and thus the contaminant radionuclides represent an effectively constant background component (within $\pm$ 2σ replicate error). Comparison of these Ge (Li) spectra with equivalent NaI (Tl) spectra (Fig 2.3) shows, in the latter, incomplete resolution of the 605 and 662 keV photopeaks of ^{134}Cs and ^{137}Cs respectively. The extent of this overlap can, however, be rigorously defined. Thus an empirical factor relating the ^{134}Cs component within the ^{137}Cs window to the 797/803 keV ^{134}Cs photopeak can be calculated from the spectra of pure standard sources, during which process peak windows are also optimised to minimise overlap.

Spectra from the Ge (Li) are much simpler in that all peaks of interest between 0.5 and 2.0 MeV are well resolved. The samples counted on the Ge (Li) generally show, however, a much greater variation in radionuclide content. In deciding the best method of background subtraction from the

FIGURE 2.5 Ge(Li) SPECTRA OF "KCFC"

Peak	Nuclide
a	"e^+"
b	Cs-134
c	Tl-208
d	Cs-134/Bi-214
e	Cs-137
f	Cs-134
g	Ac-228
h	K-40
i	Bi-214

a)"USED KCFC"

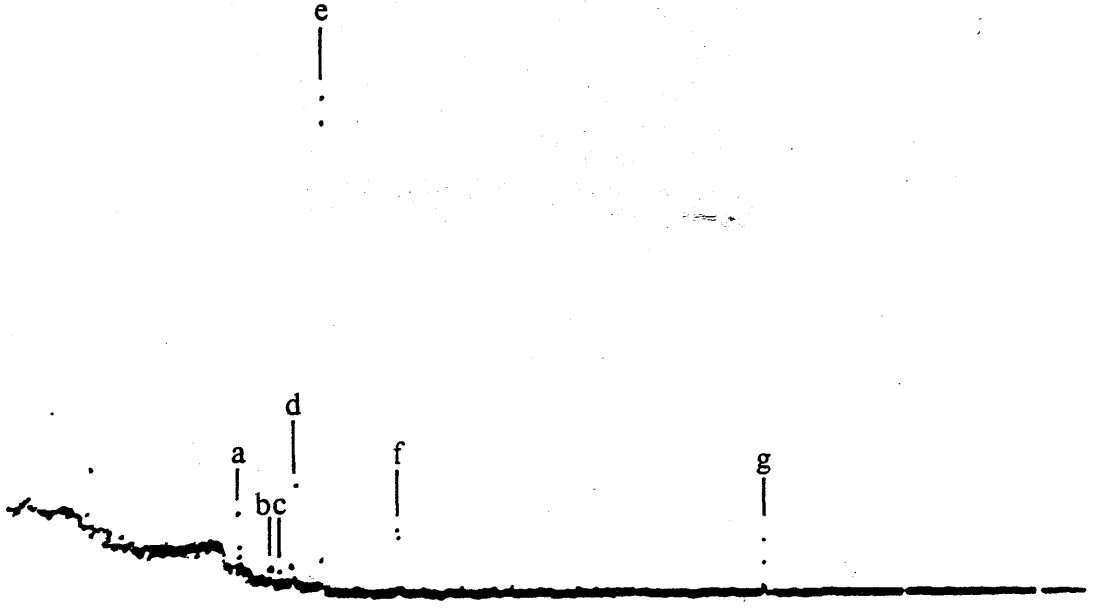

b)"BLANK KCFC"

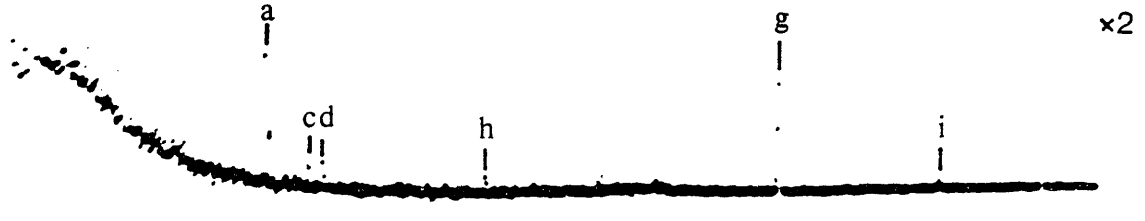

TABLE 2.2

PEAKS in KCFC (BACKGROUND SUBTRACTED)

ENERGY (KEV)		(/800m) COUNTS (BLANK)	(/800m) COUNTS (SAMPLE)
511	e^+	625	548
564	^{134}Cs	-	97
570	^{134}Cs	-	230
584	^{208}Tl	65	104
607	^{134}Cs	-	1800
610	^{214}Bi	71	
662	^{137}Cs	14	13765
799	^{134}Cs	-	1409
913	^{228}Ac	78	44
1460	^{40}K	933	984
1762	^{214}Bi	57	22

radiocaesium photopeaks, a series of homogeneous sediment replicates was analysed (Table 2.3). Linear regressions of peak integrals against sediment weights for the 662 keV ^{137}Cs and 797/803 keV ^{134}Cs photopeaks derived by a) total peak integration and b) Covell background subtraction (Covell, 1959) were compared. Slightly larger correlation coefficients were found for total peak integration in both cases (0.9934 and 0.8427 as opposed to 0.9913 and 0.8372) implying that, in this case, a constant background subtraction method is more appropriate than a simple digital analysis treatment. This apparently anomalous finding is probably due to the effects of a) a fairly constant background, b) a much higher activity of radiocaesium than of any interfering nuclides and c) the increased variance resulting from the raised baseline in Covell's method (Baedecker, 1971).

While it has been shown that for direct counting of environmental samples, the higher resolution of the Ge (Li) is essential at the cost of longer count times, the necessity to optimise the use of counting facilities requires consideration of the choice of detectors and count time for measuring ion-exchange extracted radiocaesium from water.

For very low activity samples the major consideration is the limit of detection of the counters which, in turn, is dictated not only by the detector efficiency but also by counter resolution and background. For a count time of 800 minutes (the M.C.A. timer maximum) the ^{137}Cs detection limit (3σ of background) is 3.9 dpm for the Ge (Li) which

TABLE 2.3

SEDIMENT REPLICATES

CODE	137-Integral	137-Covell Bk.	134-Integral	134-Covell Bk.	Weight (g)
1	1705	1371	439	56	4.685
2	1700	1357	440	94	4.697
3	1707	1360	484	77	5.339
4	1536	1172	443	71	4.465
5	1523	1208	448	72	4.292
6	1262	963	424	51	3.138
7	932	601	379	46	1.975
8	797	494	438	57	1.331
9	764	487	367	14	1.315
10	519	249	353	-1	0.575

Regression |137| vs wt corr. coeft. = 0.9934

(137-Bk) vs wt " " = 0.9913

|134| vs wt corr. coeft. = 0.8427

(134-Bk) vs wt " " = 0.8372

is lower than that for the flat-top NaI (Tl) (6.9 dpm) although higher than that for the well detector (1.3 dpm) thus determining counter selection. It is straightforward to calculate the sample activity at which the flat-top NaI (Tl) detector becomes superior to the Ge (Li) (in terms of counting error) by merit of its higher activity as:-

$$S = \frac{(T(2B + ex))^{\frac{1}{2}}}{Tex} \cdot 100\% \qquad \ldots\ldots\ldots 2.1$$

where S = the percentage counting error

T = count time (mins)

x = sample activity (dpm)

B = background (cpm)

e = detector efficiency

Thus, as the counting error for these two detectors is equivalent for an 800 min count at a sample activity of $\sim$ 16 dpm, the Ge (Li) would be used for samples expected to have activities $<$164 dpm while the flat-top NaI would be best used for measuring higher activities.

For high activity water samples counted on the NaI(Tl) detectors, however, optimal use of counting time favours periods less than the 800 mins timer limit. For convenience of scheduling sample changes, a short count of 400 minutes is generally employed. The desired counting error (1%) on ^{137}Cs can be obtained on a 400 minute count of samples with activities $>$729 or $>$164 dpm for the flat-top and well NaI(Tl) detectors respectively (eqn. 2.1). For real water samples, however, count times are generally determined by the ^{134}Cs content, as this species is present at levels $\sim$ 10 - 15% of those of ^{137}Cs. As the ^{134}Cs concentration

is routinely expressed as a $^{134}Cs/^{137}Cs$ activity ratio, which has less effective contribution from replicate errors, a higher counting error limit (2%) for this species can usually be tolerated. A 2% counting error criterion requires minimum ^{134}Cs activities of 280 and 106 dpm for 400 minute counts on the flat-top and well NaI(Tl) detectors respectively. To put the above numbers into perspective, a 10 litre water sample from the Clyde Sea Area (^{137}Cs ~ 140 dpm l^{-1}, ratio ~ 0.13) would require an 800 minute count on the flat-top NaI(Tl) but could be counted on the well detector in 400 mins. Similarly a North Channel sample (^{137}Cs ~ 180 dpm l^{-1}, ratio ~ 0.17) would require a count of only 400 mins on the flat-top while an Atlantic sample (^{137}Cs ~ 60 dpm l^{-1}, ratio ~ 0.11) would require an 800 minute count on the well detector.

2.3 Water Samples

The water sampling programme for this project involved a) regular monthly sampling of vertical profiles in Lochs Long and Goil b) sampling surveys throughout the Clyde Sea Area (C.S.A.) c) two annual sampling cruises in the Hebridean Sea Area (H.S.A.) off the west coast of Scotland and d) additional miscellaneous sample collections (Table 2.4).

Regular sampling from Loch Long/Loch Goil was performed in collaboration with the Clyde River Purification Board (C.R.P.B.) from their survey ship 'Endrick II'. This sampling schedule overlapped with that of MacKenzie (1977). Sampling from the C.S.A. was performed principally during cruise 16/77 of the National Environment Research Council (NERC) research ship 'John Murray' with additional samples

TABLE 2.4 WATER SAMPLING PROGRAMME

	a	b	c	d
SITE	L.Long/ L.Goil	Clyde Sea Area	H.S.A.	Gareloch L.Fyne N.Channel Shore Samples
SAMPLING FREQUENCY	monthly	one only	annual	various
No. OF TRIPS	25	1	2	-
No. of SAMPLES/ TRIP	~ 16	53	1)49 2)78	—
TOTAL No. OF SAMPLES	~400	53	127	50
SAMPLING MODE	Shipboard pump/NIO Bottles	Shipboard pump/NIO Bottles	Shipboard pump	various
BOATS UTILISED	Endrick II	John Murray Endrick II	Challenger	Endrick II Leander

TOTAL NUMBER OF SAMPLES ~630

collected from 'Endrick II'. Sampling from the H.S.A. was performed during cruises 8/76 and 7/77 of the NERC research ship 'Challenger' in collaboration with the Scottish Marine Biological Association (SMBA) laboratories. Miscellaneous samples were collected from Gareloch and Loch Fyne from 'Endrick II', from the North Channel in conjunction with the University Marine Station, Millport using the research ship 'Leander', while shore samples were occasionally collected from Lochs Lomond, Long, Goil and Fyne.

Sampling procedures are variable according to location and shipboard facilities and include direct bucket sampling of surface waters, sub-surface sampling via shipboard 'clean salt water' systems, and depth profiling by both pump connected to polythene hose and National Institute of Oceanography (NIO) messenger-closed sampling bottles on a hydrographic wire. Errors arising from sampling procedures must occur mainly in the collection of depth profiles where depth is specified only by the length of hydrographic wire released. Obviously the wire may in fact fall at an angle in locations with strong currents. Because of the inavailability of alternative methods, however, 'hydro-wire depths' are considered acceptable after the research vessel is stationed to minimise visible deviation of the wire from vertical. As the wire is generally less than 20^{o} from vertical, the error introduced in depth assignment should involve overestimation by less than 6%. An additional error when pumping from depth could arise if tube leakage occurs, resulting in sample contamination by shallower water. A procedure has thus been adopted in which a surface sample is taken first and the integrity of the hose confirmed by checking the absence of air bubbles leaking into

the transparent hose. In all cases pumped samples are collected only after the system has been thoroughly flushed out with water from the sampling location.

On collection all water samples are stored in polythene bottles previously washed with 2M nitric acid. After collection, samples are generally acidified to pH 2 with conc. nitric acid and stored in a cool location till analysis, storage time ranging from one week to several months. Acidification of samples to prevent loss of dissolved caesium either by sorption onto bottle walls or particulates or by biological removal (IAEA, 1970) would ideally be preceded by a filtration step to prevent solution of particulate-bound caesium by the acidification process. Unfortunately immediate filtration was not feasible in practice, so that the error due to the acidification process was evaluated by filtering a series of both acidified and non-acidified water samples through a 0.22 μm membrane filter (Millipore G.S.) and comparing the activities of the resulting filtrates. The results (Table 2.5) show that the amount of radiocaesium on filterable particulates is so small (<0.03 dpm ^{137}Cs/litre) that the error involved in acidification can generally be regarded as completely negligible.

In view of the large number of water samples to be examined, optimal use of counting equipment involves radiochemical extraction of radiocaesium, generally followed by measurement on a NaI(Tl) system. Of the wide range of radiochemical separation techniques available, amongst the simplest and most specific is ion-exchange onto transition

TABLE 2.5 EFFECTS OF FILTRATION

NUCLIDE	TOTAL COUNTS FOR 16 FILTERS(NON-ACIDIFIED)	13 FILTERS (ACIDIFIED)	BACKGROUND
Cs-137	357 ± 19	379 ± 19	356 ± 16
Cs-134	336 ± 18	348 ± 19	378 ± 21
K-40	679 ± 26	732 ± 26	807 ± 58

TABLE 2.6 COMPARISON OF ION-EXCHANGERS

	KCFC	ZrFC	CuFC
^{137}Cs efficiency+	28.02%	26.39%	19.96%
^{134}Cs efficiency+	12.26%	12.30%	9.92%
^{137}Cs Background×	1943	1573	1797
^{134}Cs Background×	1471	1140	1287

+ total counting and extraction efficiency

× counts per 800 mins in photopeak window

Work performed with A.G.Ballantyne.

metal and mixed metal ferrocyanides, (Prout et al, 1965; Boni, 1966; Folsom and Sreekumaran, 1970; Kawamura et al, 1971). The particular ion-exchanger utilised here is potassium hexacyanocobalt (II) ferrate (II) (KCFC) which has been widely used for this purpose despite its relatively high ^{40}K background from the potassium included in the crystal structure (Folsom and Sreekumaran, 1970). Comparison of KCFC with other ion-exchangers (Table 2.6) shows that, despite the higher ^{40}K-derived background in the radiocaesium windows (which is, in any case, effectively constant), its higher net efficiency (combining both chemical and counting efficiencies) for radiocaesium determination renders it a good choice of ion-exchanger. In addition KCFC shows relatively high selectivity, chemical and mechanical stability and effective insensitivity to flow rates (McKinley, 1975; MacKenzie, 1977; Ballantyne, 1978).

Additional practical advantages of KCFC are that it is comparatively inexpensive to buy (~£100/kg, Westo Industrial Products Ltd., 1976) or can be synthesised quite easily and cheaply (Prout et al, 1965; MacKenzie, 1977). Apart from its ^{40}K background, however, a disadvantage of KCFC is its lack of complete specificity, as other radionuclides , eg ^{60}Co, may be removed to a significant extent (Ballantyne, 1978). Because of the inherently low resolution of the NaI(Tl) systems, this uptake could produce significant overlap of the ^{60}Co compton edges with the radiocaesium photopeaks, in addition to raising the general compton continuum background. Evaluation of this potential error, by counting a series of KCFC-extracted samples from

different locations on the Ge(Li) detector, failed to indicate the presence of any interfering radionuclides with gammas in the range 0.5 - 2 MeV. This possibility was, however, borne in mind, especially when examining new regions of interest, by regularly counting randomly selected KCFC samples on the Ge(Li) system.

The experimental apparatus for radiocaesium extraction (Fig 2.6a) consists of an upper water reservoir, a membrane filter unit (Millipore, 0.22 μm), a KCFC ion-exchange unit and a lower reservoir - the entire system operating by gravity flow. This configuration was designed to minimise experimental difficulties and to render the extraction process as reproducible as possible. The purpose of the filter is to remove suspended particulates which, although shown not to contain radiocaesium to any significant extent, would be expected to raise the background of radioactive contaminants (and thus decrease the apparent experimental selectivity) if trapped in the KCFC column. After passage of each sample through the filter unit, the membrane filter is itself labelled and retained for possible counting later.

The KCFC column is prepared in 1 cm (outside diameter) polythene tubing, as illustrated (Fig 2.6b), and is a standard length of 4 cm. KCFC, sieved to 30-80 mesh, is washed free of fines with distilled water and slurried into the tubing, taking care to avoid the formation of air pockets in the column. Examination of the absorbed radiocaesium distribution within the column over a range of flow rates

FIGURE 2.6 CAESIUM EXTRACTION APPARATUS

a) EXTRACTION RIG

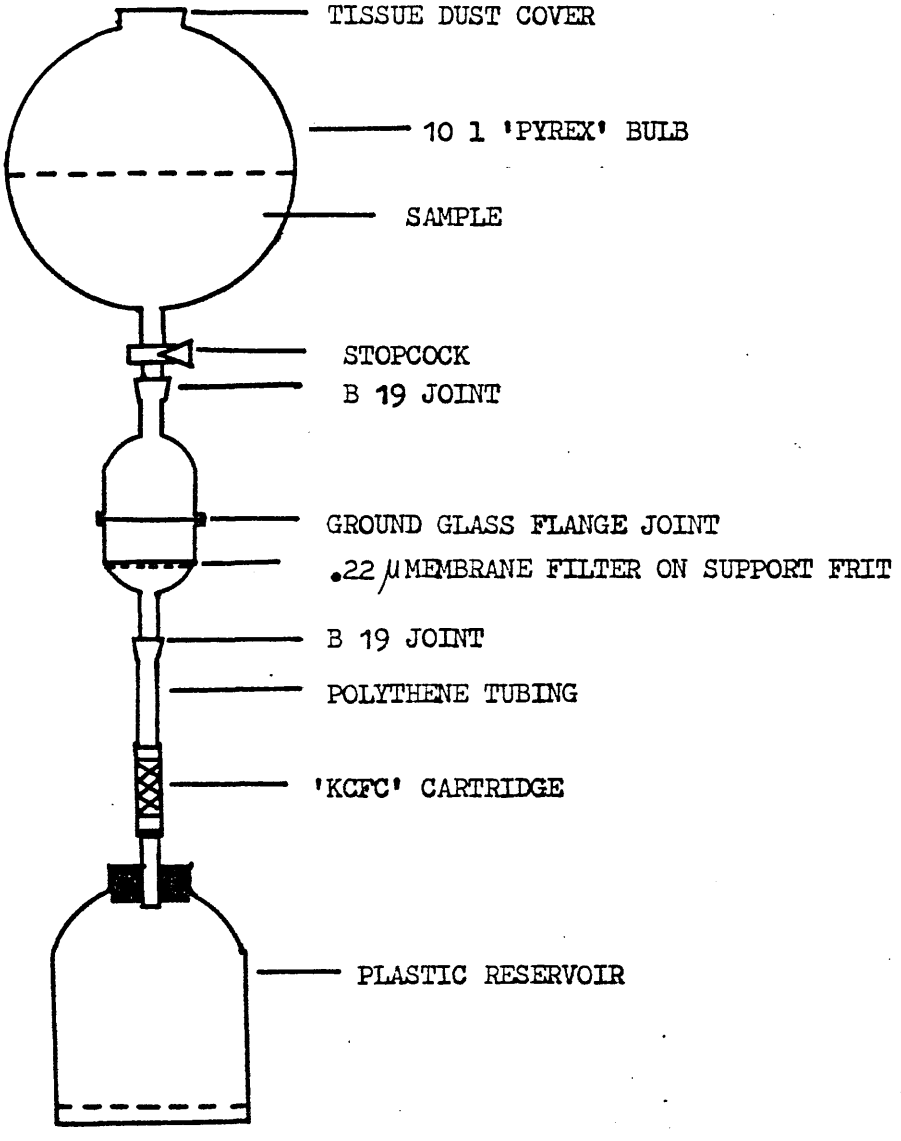

b) 'KCFC' CARTRIDGE

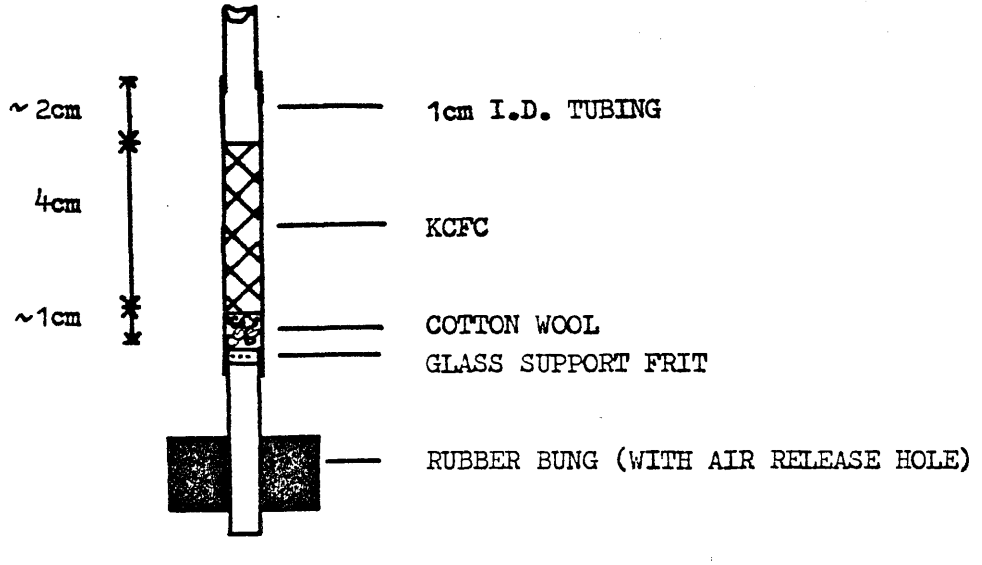

indicates effectively complete removal of radiocaesium into the first 1 cm of exchanger (Table 2.7). A 4 cm long column was, however, regarded as ideal for ensuring complete caesium removal, ease of handling and low ^{40}K background. The efficiency of the extraction process was additionally checked both by running eluted samples from the first pass through a second KCFC column and by comparing observed activities of spiked KCFC cartridges with theoretical activities from knowledge of the radiocaesium distribution and the counter efficiency (Table 2.8). Calculated efficiencies of 99.7% and 97% respectively for ^{137}Cs indicate that chemical removal is essentially complete. The possibility of an influence of salinity and pH on the extraction efficiency was also investigated, in collaboration with Ballantyne (1978), and the net effect shown to be negligible in both cases.

Flow rates through the extraction rig are dependent on the sample size (usually 1,5 or 10l) and on the extent of particulate clogging of the membrane filter. Flow times range from $\sim$2 hours to $\sim$ 2 days with average flow rates typically $\sim$ 0.5 l hr^{-1}.

After passage of the sample through KCFC, the ion-exchange unit is removed completely and dried in a filtered air stream. This method of drying was shown to be superior to oven-drying as the latter involves incorporation of salt from residual sea water (up to 6 ml) in the column and cotton wool plug, thus increasing the ^{40}K background (n.b. ^{40}K content of seawater $\sim$ 0.75 dpm ml^{-1}). If the airstream used is filtered to remove dust, the contamination involved in this drying method falls below the limit of detection even

TABLE 2.7 DISTRIBUTION OF Cs-137 IN KCFC.

COLUMN SEGMENT	137 INTEGRAL (cp800m)	134 INTEGRAL (cp800m)
0-1cm	67762	11993
1-2	10780	6220
2-3	10446	6054
3-4	10665	6329
4-5	10725	6238
Background (Empty Counter)	10694 ± 201	6155 ± 83
Background (KCFC column)	11023 ± 141	6479 ± 150
Background (1cm KCFC)	10760 ± 141	6220 ± 150
Implied efficiency	100%	100%

TABLE 2.8 CALCULATION OF KCFC CHEMICAL EFFICIENCY

	CODE	137^{+} ACTIVITY	134^{+} ACTIVITY
First Pass	γ138	70884 ± 266	13090 ± 114
2nd. Pass	γ140	11220 ± 106	6654 ± 82
Background		11023 ± 141	6479 ± 150
Implied Chemical efficiency		(99.7 ± 0.2)%	(97.3 ± 2.6)%

TABLE 2.8 (CONTINUED)

Absolute efficiency for 137	×15.0% (1x1cm source at12 cm)
peak/total ratio	×0.531
137 absolute intensity	×0.848
∴ theoretical counting efficiency	6.75%
observed total efficiency	6.54%
∴ chemical efficiency	97%

× CROUTHAMEL ET AL,1970

TABLE 2.9 DRYING METHODS FOR KCFC CARTRIDGE

	137+	134+
a) KCFC Blank dried in Air	10992 ± 105	6403 ± 80
b)+(Nat. Series Contamination)	11637 ± 108	6606 ± 81
c) Blank (oven dried/ aged)	11023 ± 105	6479 ± 80
a→b increase	6%	3%

+ Counts/800mins in photopeak window.

after exposure for 3 days (~70 times longer than normal drying period). It must be noted that increases in background of ~6% in the ^{137}Cs window and ~3% in the ^{134}Cs window have been observed in areas of high natural series background (Table 2.9) through incorporation of radon daughter products into the column (MacKenzie, 1977).

After drying, the KCFC cartridge is removed from the glass-frit support unit and, still contained in the polythene tubing, is plugged at its upper end by a 5 mm long, tight-fitting wooden plug and at its lower end by a plasticine seal. Excess tubing is then trimmed off and the cartridge is labelled and further sealed in a layer of adhesive tape.

For counting on either the flat-top NaI (Tl) or Ge (Li) detectors, the KCFC cartridge is placed in a perspex holder which reproducibly positions it over a diagonal of the crystal face with a point 1 cm below the top of the KCFC column directly above the crystal centre. For counting on the NaI (Tl) well detector, the KCFC cartridge is fitted snuggly, top down, into a plastic well-liner where the defined length of the wooden plug results in uniforn penetration into the well. In both these cases the procedure is defined to maximise counting efficiencies and reproducibility.

In addition to radiocaesium analysis, most water samples are also analysed for salinity, temperature and dissolved oxygen concentration - usually by measuring these parameters on a duplicate sample collected from the same location. Salinity is measured by the C.R.P.B. either directly by an in-situ conductimetric probe or by more accurate conductivity measurement on return to the laboratory. Temperature is

measured by reversing thermometers on NIO hydrographic sample bottles or by direct measurement via hand-held thermometer. Dissolved oxygen is determined by the Winkler method (Riley, 1975) or by a membrane D.O. meter. On occassions water transparency, nutrient and chlorophyll concentrations and pH were also measured by the C.R.P.B. (Leatherland, 1977).

2.4 Sediment and Biological Samples

A variety of methods have been used for collection of sediment samples. The most direct and primitive (but useful for rough evaluation) involves manual collection of muds exposed by low tide either by scooping surface sediment into a polythene bag or by slowly pushing rigid perspex tubing into the sediment, capping with a rubber bung and digging the tube out to obtain a rough core profile. The main disadvantage of these methods is the atypical nature of the deposits relative to deeper sediments.

Some deeper samples were in fact obtained by scuba divers using procedures analogous to those for tidally exposed muds, but limitations are the shallow maximum depth practical for scuba work (~30m), restrictions on the length of core obtainable and difficulties in ensuring that cores remain undisturbed during transport to the surface.

Deep water sediments, however, are most frequently and reliably obtained by Craib and gravity corers operated from a research ship. The Craib corer (Craib, 1965) is a small, damped piston-corer (Fig 2.7) which soft lands on the sediment surface and retrieves cores up to 30 cm long with

Figure 2.7

Craib Corer

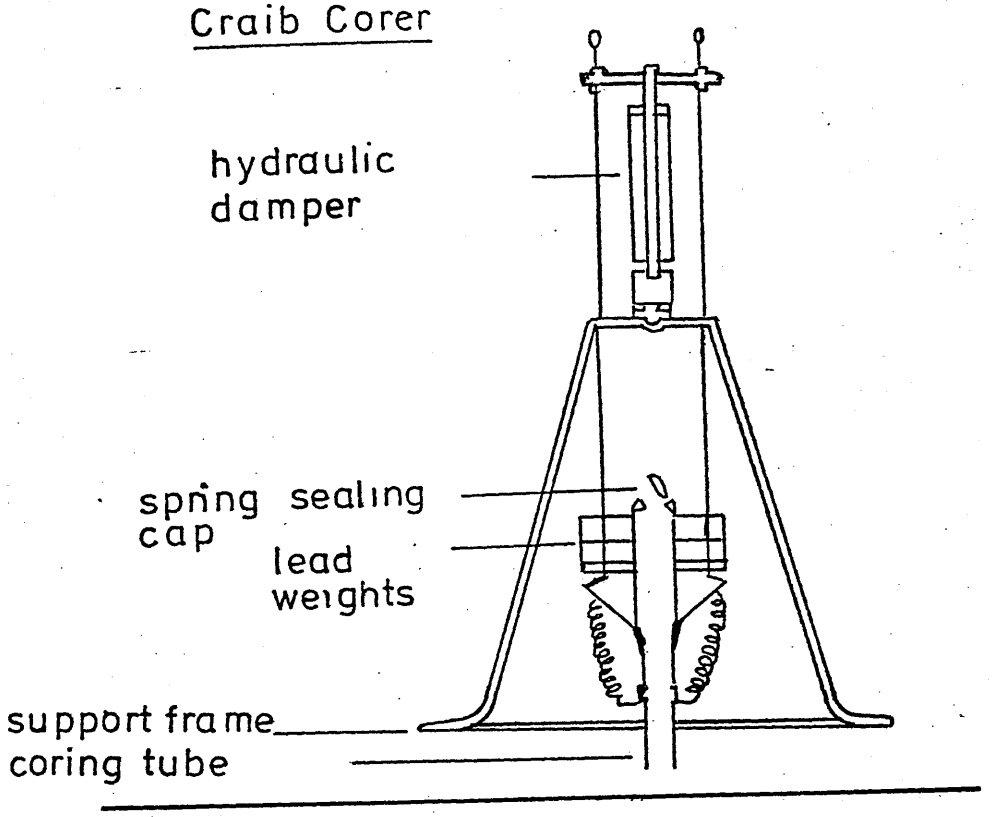

Figure 2.8

Gravity Corer

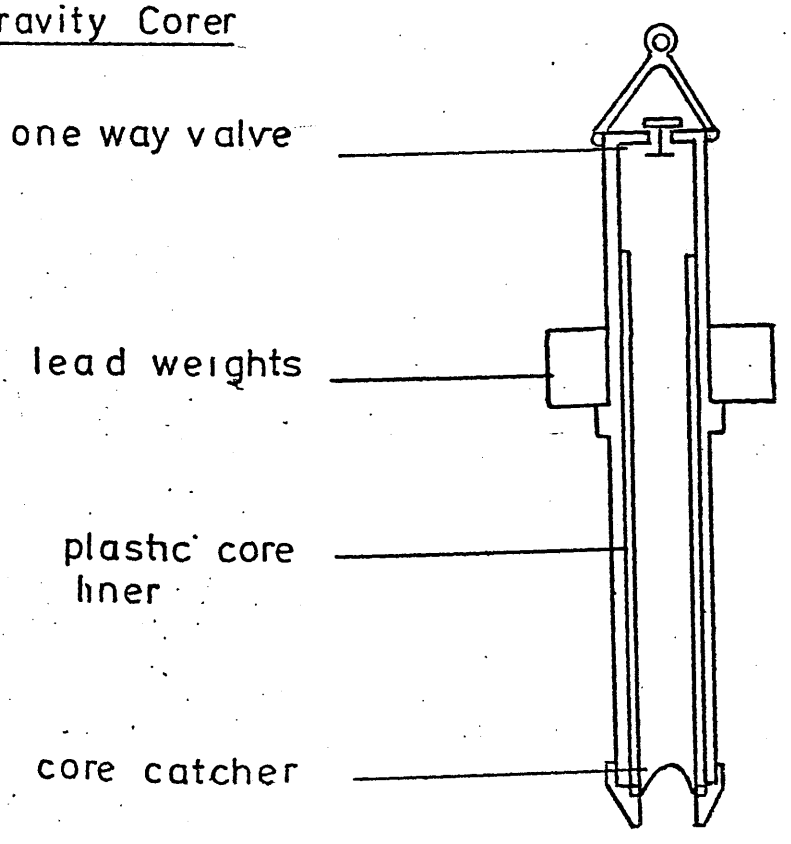

little disturbance of sediment by the coring process. Thus Craib cores generally exhibit a well-defined water/sediment interface and show minimal suspended material in supernatent waters. The perspex core-liner tube may be readily removed from this corer with negligible disturbance of the core and may be easily handled thereafter.

The gravity corer used (UMEL screw barrel, 6 cm diameter) consists of a steel coring tube either 3' or 6' in length, driven by an upper assembly of lead weights. A perspex core-liner and a brass core-catching mechanism are incorporated (Fig 2.8). This device is used to obtain longer sediment cores and generally shows little evidence of surface sediment retention. Handling of cores longer than 1 metre generally necessitates tilting on retrieval, a process which could cause some mixing of soft, upper sediments.

On collection of a sediment core, supernatant water is generally siphoned off and either retained for analysis or discarded. To prevent loss of core structure during transport, cores are generally either frozen or sectioned immediately after collection. Freezing is either slow, in a purpose-built freezer/transporter unit containing dry ice ($CO_{2(s)}$) or in a shipboard deep-freeze, or is rapid, by immersion in liquid nitrogen. Slow freezing often results in formation of long ice crystals detectable both visually and by X-radiography. These are not apparent in quick-frozen cores (Fig 2.9). These long crystals are undesirable as they could cause redistribution of both dissolved and particulate-bound species but the quick freezing process is hazardous as it occasionally causes core-liner fracture

FIGURE 2.9 X-RADIOGRAPHY OF FROZEN SEDIMENT

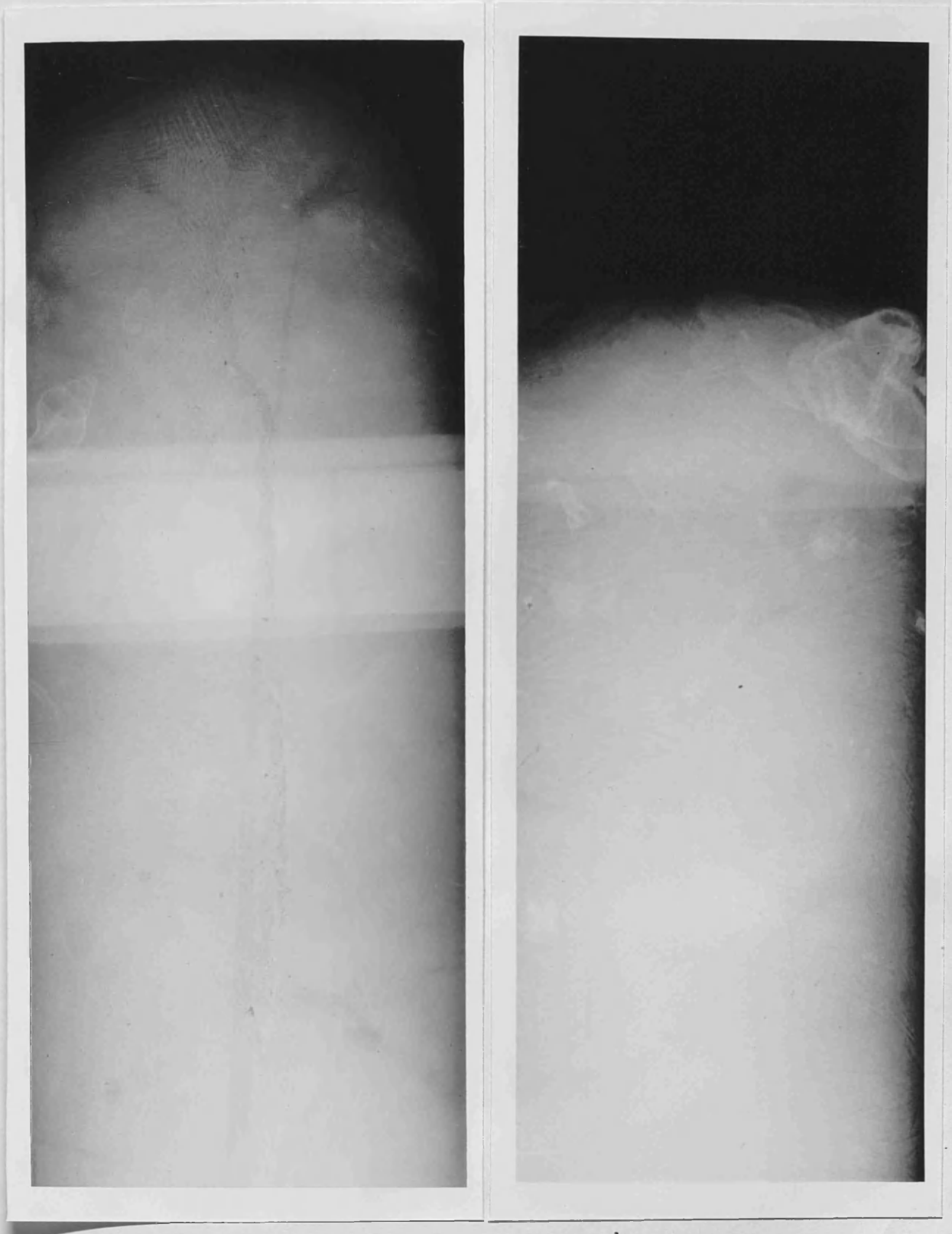

a b

a) Quick frozen core - ice crystals evident at core centre only

b) Slow frozen core - ice crystals throughout width of core

and subsequent core loss.

As an alternative to freezing, cores can be sectioned either by piston extrusion of Craib cores followed by sub-sampling with a plastic spatula or by splitting gravity core-liners with a circular saw prior to sectioning with a spatula. After sectioning, core segments are placed in labelled polythene bags for transport to the laboratory. Sediment is generally stored in refrigerators prior to analysis to minimise chemical and biological action during this period.

In the laboratory, frozen cores are X-rayed to indicate any structural characteristics and are then sectioned, while frozen, by band-saw, this in the case of Craib cores being preceded by piston extrusion from the reusuable core-liners.

In all cases, sediment samples are initially weighed, dried in an oven at $\sim 100^{\circ}C$ to constant weight and then re-weighed. Weighed samples of dried sediment are packed into standard counting vials which are counted in a plastic holder which positions the samples over the centre of the Ge(Li) crystal.

A series of other techniques routinely applied to sediment samples includes microanalysis for carbon, nitrogen and oxygen, trace metal analysis by atomic absorption or neutron activation methods, ^{210}Pb, ^{226}Ra and ^{228}Ra radio-chemical analyses, mineral and particle size studies and palynological and palaeomagnetic measurements. These techniques are performed by other workers, details of procedures being described elsewhere (MacKenzie, 1977; Lennie, 1978; Swan, 1978).

Marine organisms have been collected by removal from tidal beaches, collection by scuba diver or by trawling. Samples are returned to the laboratory in labelled polythene bags either frozen or at ambient temperature and stored till analysis under refrigeration. The samples are then dissected if necessary, weighed, dried in an oven at $\sim 100^{o}C$ to constant weight and reweighed. In some cases samples are concentrated by reaction with H_2O_2 and HNO_3 and evaporation to dryness. Dried samples are then powdered and homogenised, either with mortar and pestle or via ball-mill rock crusher, and counted directly in an identical way to sediments.

For both sediment and organic samples the presence of other γ-emitting radionuclides is normally detected. These radionuclides can be identified by γ-energy analysis and roughly quantified from detection efficiencies obtained from an extrapolated sediment energy/efficiency graph (Fig 2.10).

2.5 Errors, Reproducibility and Sample Calculations

A consideration of errors is central to the evaluation of any measurement system. These can be classified as either random or systematic, where random errors are those caused by unbiased fluctuations of a measuring system or property and which determine how closely repeated measurements of a single parameter tend to cluster round a specific value (i.e. precision); systematic errors, on the other hand, are caused by measurement bias and determine how closely mean experimental values correspond with the 'true value' (i.e. accuracy). Random errors are generally evaluated by repeated

FIGURE 2.10 Ge(Li) ENERGY/EFFICIENCY CURVE

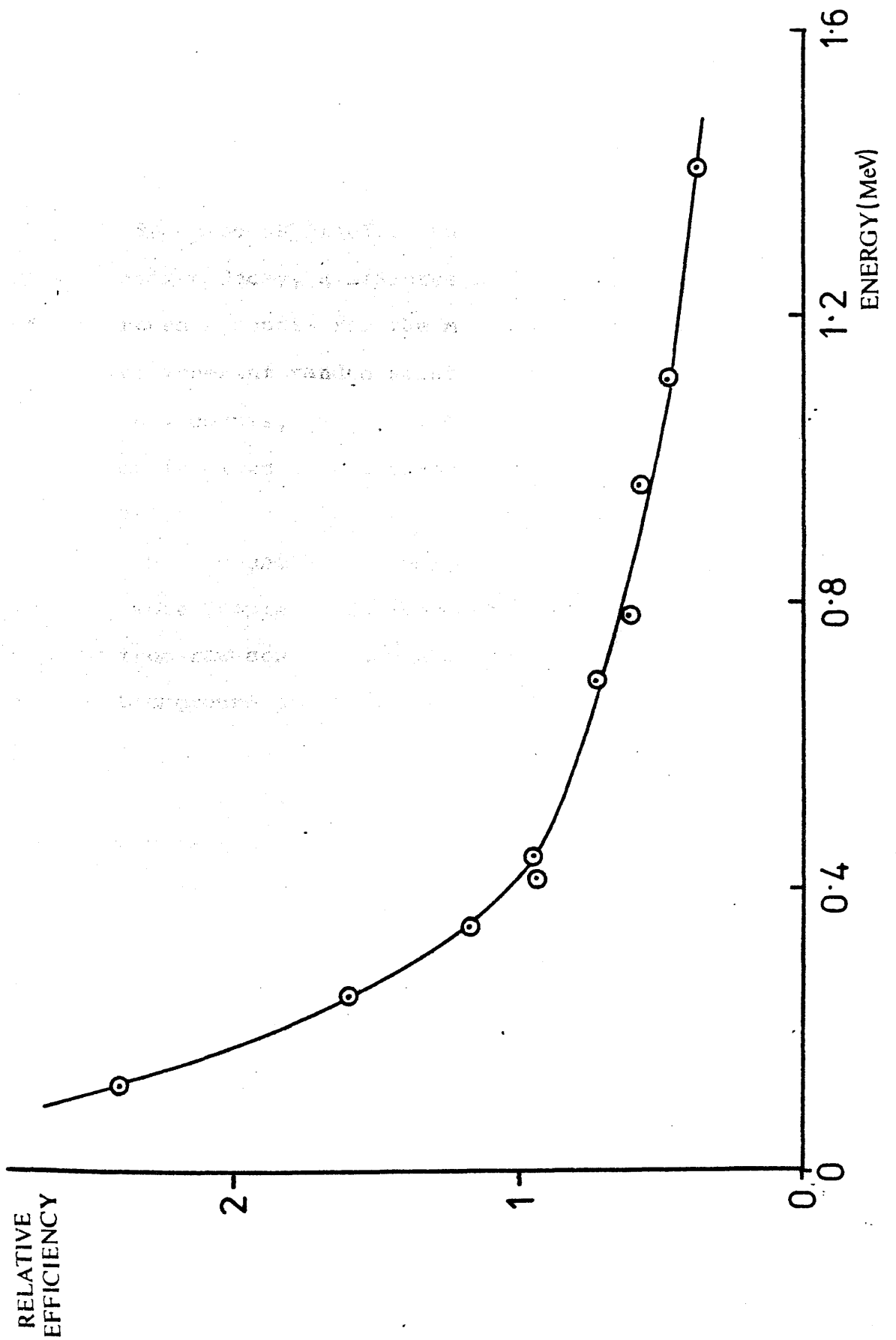

measurements of effectively identical samples (replicates) while systematic errors may be evaluated by measurement of a known sample (standard) or, when no such absolute standard exists, by inter-laboratory or inter-system calibration.

The most basic errors involved are those arising from the counting process itself. Due to the statistical nature of radioactive decay, a measurement of N counts on a system of background B counts for the measurement period has an associated inherent random error (standard deviation) on the residual counts, (N-B), of $\sqrt{N+B}$. (Full details of statistics involved in Friedlander et al, 1964; Meyer, 1972; Till, 1974).

For real counting systems, however, the position is slightly more complex. The background which must be subtracted from raw count rates has components both from the counter background and from the sample containers - the KCFC cartridge for water samples and counting vial for sediment and biological samples. The resultant variation in effective background is often greater than that expected from counting considerations alone, and may be assessed by counting a series of blank KCFC cartridges or empty sediment containers. The resultant backgrounds, in the ^{137}Cs and ^{134}Cs windows respectively, for KCFC cartridges are thus (13.8 ± 0.2) and (8.1 ± 0.2) cpm for the flat top NaI(Tl), (6.3 ± 0.2) and (7.1 ± 0.2) cpm for the well NaI(Tl) and (0.49 ± 0.02) and (0.53 ± 0.05) cpm for the Ge(Li) system. As these backgrounds show correlation with count rates in the ^{40}K window, they presumably reflect the effects of slightly varying column lengths and extent of physical compaction.

This variability is smaller for blanks of commercial KCFC than for ion-exchanger synthesised in the laboratory, presumably because of greater batch homogeneity in the commercial material. The latter was therefore used for all samples analysed after July 1976. The empty sediment container backgrounds on the Ge(Li) system are (0.44 ± 0.03) and (0.48 ± 0.02) cpm in the ^{137}Cs and ^{134}Cs windows respectively these showing only a very slight increase in variability over the 'counting-only' variance and thus reflecting the effective uniformity of the sample vials.

The overall reproducibility of the KCFC extraction and counting system was determined by splitting a 100l homogeneous sea water sample into 20 x 5l subsamples which were then assayed individually amongst routine analyses of other samples, half of the subsamples being extracted by another worker on a separate system (MacKenzie, 1977). The results (Table 2.10) give both a measure of the reproducibility (precision) of such system and an assessment of the level of agreement between extraction and counting systems (an internal assessment of accuracy). For 800 minute counts the residual error on both ^{137}Cs and ^{134}Cs count rates increased from the well NaI(Tl) (0.5 and 1.1% respectively) to the flat-top (2.4 and 1.2% respectively) to the Ge(li) detector (3.2 and 4.2% respectively). This marked trend was analysed further by counting two KCFC cartridges prepared from highly spiked water samples ($\sim 10^4$ dpm ^{137}Cs) and by subsequent comparison of their count rates a) without replacement and b) with replacement in the counter assembly (Table 2.11). Without replacement, only the expected counting derived variance in count rate was observed ($\sim 0.7\%$) but a

TABLE 2.10

REPLICATE ANALYSIS RESULTS.

	1	2	3	4	5
Mean ^{137}Cs activity dpml^{-1}	90	87	92	89	88
observed(%)	2.4	4.0	3.2	1.7	0.5
COUNT CALCULATED(%)	0.2	0.3	0.3	0.1	0.01
∴ RESIDUAL(%)	2.4	4.0	3.2	1.7	0.5
Mean ^{134}Cs activity dpml^{-1}	12	12	11	12	11
observed(%)	1.5	4.1	4.5	3.2	1.4
COUNT CALCULATED(%)	0.9	1.4	1.1	0.8	0.9
∴ RESIDUAL(%)	1.2	3.9	4.4	3.1	1.1

1.	Flat top NaI(Tl)	System 1 (ABM)	800 mins.
2.	"	System 2(IMcK)	"
3.	Ge(Li)	System 1	"
4.	Well NaI(Tl)	System 1	400 mins.
5.	"	System 2	800 mins.

TABLE 2.11 DEMONSTRATION OF GEOMETRIC EFFECTS

SAMPLE	COUNT NUMBER	GROSS COUNT	
		Without replacement	With replacement
HAR1	1	23 631	24 680
	2	23 945	23 245
	3	23 638	24 956
HAR2	1	25 209	25 756
	2	25 485	22 418
	3	25 351	23 598

large apparent difference existed between sample means (~7%) On replacement, the count rate variability for each sample increased (~5.4%) but the sample mean difference decreased (~1.5%). From these observations the residual errors on replicate samples can be explained in terms of a geometric effect - in normal circumstances the distribution of radiocaesium is non-symmetric and variable giving rise to a varying effective counting efficiency. The observed trend in the magnitude of this residual error with detector type is thus explained by a similar trend in detector sensitivity to source geometry.

Comparison of the mean ^{137}Cs and ^{134}Cs activities derived from the replicates (Table 2.10) show close agreement between extraction systems and counters (i.e. within 1.5% for ^{137}Cs evaluation). The apparently significant variation in implied ^{134}Cs activity (4.7%) is an artifact caused by decay correction, as the counting dates on the different detectors varied by up to 2 years.

The random errors involved in radiocaesium measurement by KCFC extraction are summarised in Table 2.12. As the counting and geometric errors are completely dominant, the total random error, to a good approximation, can be considered as resulting solely from these two sources.

The geometric error is proportional to the number of counts in the photopeak, while the counting error is proportional to the square-root of this parameter. Thus the total error tends to be dominated by the counting error component at low sample activities ($<\sim 50$ dpm) while the geometric error predominates at higher activities (>100 dpm) (Fig 2.11). As the geometric error may be equated with the

TABLE 2.12

ERRORS IN RADIOCAESIUM MEASUREMENT (Cs-137)

[10-2000dpm in 10 litres]

1) Volume measurement	0.05%
2) Extraction onto filter	0.05%
3) Varying KCFC efficiency	0.1%
4) Counting Errors	0.01-10%
5) Geometric Error	0.5-4%

TABLE 2.13

REPLICATE 1-1 SYSTEM (WELL)

	Mean	σ_{CT}	σ_{RES}	σ_{TOT}
Cs-137	71936cp800m	0.1%	1.7%	1.7%
Cs-134	3945cp800m	0.8%	3.1%	3.2%
⇒ RATIO	0.0548	0.8%	3.5%	3.6% calculated

σ_{TOT} observed = 3.0%

$\therefore \sigma_{RES}$ = 2.9%

residual error, derived from the replicates, a total error can be calculated simply for each sample.

In calculation of the error on the $^{134}Cs/^{137}Cs$ ratio, the effect of the correlated variation of both the ^{134}Cs and ^{137}Cs peaks due to geometric effects must be considered. For any set of replicates (e.g. Table 2.11) the resultant error on the peak ratio (3.0%) is for this reason less than that calculated by simple addition of errors on individual peaks (3.6%). The error on the ratio can thus be calculated from the counting errors on the ^{137}Cs and ^{134}Cs peaks added (in a reduced squares sense) to an empirically derived additional geometric error (in this case 2.9%).

The errors examined so far have been random, but a systematic error arises from calibration of the counting system. All systems were calibrated by extracting onto KCFC the radiocaesium from a series of sea water samples spiked with measured aliquots of ^{137}Cs and ^{134}Cs standard solutions (Radiochemical Centre, Amersham). The overall efficiency of extraction and counting can thus be calculated by linear regression of the observed count rate versus spike activity. The random error associated with sample spiking is small (the main error of ~0.1% being in spike measurement). The original standard solutions are however, only specified, on an absolute scale, to $\pm$1%. This systematic error of $\pm$1% is important only in specification of absolute values and, as samples are internally self-consistent, is not manifest in internal comparisons.

The systematic error for the entire sampling, extraction and counting systems was examined by comparing Glasgow results for a set of Hebridean Sea samples with those

obtained on equivalent samples (Table 2.14) by the Ministry of Agriculture, Fisheries and Food, Fisheries Radiobiological Laboratory (MAFF, FRL), Lowestoft (Jefferies, 1978). Although full errors for the MAFF data are not quoted, a maximum systematic error of -6.4% in efficiency and +0.27 dpm in system blank are implied for ^{137}Cs quantification. Comparison of derived ^{134}Cs concentrations is more difficult as the activities at this location are very low (below detection limit for 4 out 10 samples), but while the general trend in derived ^{134}Cs concentrations between samples is similar, the $^{134}Cs/^{137}Cs$ ratios obtained at Glasgow seem systematically lower than those derived by MAFF. The significance of MAFF intercalibration will be discussed further in later chapters.

Errors involved in the sediment preparation and counting procedures were examined by counting a series of subsamples of homogeneous sediment. A maximum replicate error of 6.6% for both ^{137}Cs and ^{134}Cs was determined. Counting efficiency was evaluated by spiking previously counted sediment with small volumes (0.1 ml) of standard ^{134}Cs, ^{137}Cs and ^{60}Co solutions (Radiochemical Centre, Amersham). The systematic error associated with this calibration method is effectively determined by the uncertainty in the standard absolute activity ($\pm$1%). All errors in the sediment analysis procedure, summarised in Table 2.15 are probably small relative to the less easily quantified errors arising during the coring process as further discussed in Chapter 6.

Details of the calculation of radiocaesium activities and associated errors are now presented. The ^{137}Cs activity

TABLE 2.14 G.U./M.A.F.F. INTERCALIBRATION

SAMPLE	G.U. RESULTS					M.A.F.F. RESULTS				
	(137)	σ_{tot}	(134)	σ_{tot}	RATIO	(137)	σ_{ct}	(134)	σ_{ct}	RATIO
2C	30.8	3.6	3.4	10.2	0.11	32.3	2.7	5.2	1.7	0.16
3C	13.8	4.2	1.7	18.6	0.12	16.9	0.5	2.6	3.3	0.15
4C	12.2	5.3	1.9	28.3	0.16	11.2	1.0	0.8	5.6	0.07
5C	4.1	19.8	***	****	****	7.0	0.8	0.9	6.3	0.13
6C	5.5	5.9	0.8	38.2	0.15	4.6	1.2	0.8	6.3	0.17
7C	11.8	4.3	1.6	19.3	0.14	10.8	0.5	1.5	3.6	0.14
8C	9.4	4.6	1.5	20.2	0.16	8.1	0.7	1.3	4.2	0.16
8AC	2.1	70.9	***	****	****	1.5	2.9	0.2	25	0.13
9AC	0.5	37.6	***	****	****	0.6	6.9	0.04	125	0.07
10C	0.1	292	***	****	****	0.6	6.9	0.04	125	0.07

Cs-137: G.U. vs M.A.F.F.

Correlation coefficient - 0.986
Slope - 0.936
Intercept - 0.266

Deviation - -6.4%
Zero error - +0.27 dpm/l

All activities in dpm/l Total (σ_{tot}) and counting (σ_{ct}) errors in %

**** - value indistinguishable from background

TABLE 2.15 ERRORS IN SEDIMENTARY RADIOCAESIUM EVALUATION (5-650 pCi)

1)	Weighing error	0.1%
2)	Counting error	1-20%
3)	Residual error	6.6%
4)	Systematic error on standards	1%

of a KCFC-extracted sample counted on a NaI(Tl) detector (D dpm) is given by

$$D = \frac{(C - (B \times T) - f_1(C' - (B' \times T))}{(1 - f_1 f_2)} \times \frac{\exp(\lambda \tau)}{e \times T} \quad \ldots(2.2)$$

where C is the count integral in ^{137}Cs window

C' is the count integral in ^{134}Cs window

B is the ^{137}Cs window background (cpm)

B' is the ^{134}Cs window background (cpm)

T is the count time (mins)

e is the detector efficiency for ^{137}Cs

f_1 is the fractional overlap of ^{134}Cs in ^{137}Cs photopeak

f_2 is the fractional overlap of ^{137}Cs in ^{134}Cs photopeak

λ is the decay constant for ^{137}Cs = 0.0000628 days^{-1}

τ is the delay between sampling and counting (days)

Similarly the ^{134}Cs (D' dpm) activity is given by

$$D' = [(C' - (B' \times T)) - f_2 A] \times \frac{\exp(\lambda' \tau)}{e' \times T} \quad \ldots.(2.3)$$

where λ' is the decay constant for ^{134}Cs = 0.0009254 days^{-1}

e' is the detector efficiency for ^{134}Cs

and $$A = \frac{(C - (B \times T) - f_1 (C' - (B' \times T))}{(1 - f_1 f_2)}$$

The random error associated with ^{137}Cs determination (S dpm) is thus given by

$$S = [(C+(E_1^2 x T^2) + f_1^2(C'+(E_2^2 x T^2)) + R_1^2 A^2]^{\frac{1}{2}} \times \frac{\exp(\lambda\tau)}{(1-f_1 f_2) x e x T}$$

....(2.4)

where E_1 is the random error on the background in the ^{137}Cs window (cpm)

E_2 is the random error on the background in the ^{134}Cs window (cpm)

R_1 is the residual error in the ^{137}Cs window derived from replicates

while the error on ^{134}Cs (S' dpm) is

$$S' = [(C' + E_2^2 \times T^2)) + \frac{f_2^2}{(1-f_1 f_2)^2} (C + (E_1^2 \times T^2)) +$$

$$f_1^2(C' + (E^2_2 \times T^2)) + R^2_2 B] \times \frac{\exp(\lambda' \tau)}{e' \times T} \quad ...(2.5)$$

where R_2 is the residual error in the ^{134}Cs window

$$B = [(C' - (B' \times T)) - f_2 A]$$

The errors associated with radiocaesium determination via the Ge(Li) detector are simpler as there is effectively no peak overlap. From any photopeak the radionuclide activity (D dpm) may be calculated as

$$D = (C - (B \times T)) \times \frac{\exp(\lambda\tau)}{e \times T} \quad ..... (2.6)$$

with an associated random error (S dpm) of

$$S = [(C+(B^2 x T^2)) + R^2(C-(B x T))^2]^{\frac{1}{2}} \frac{\exp(\lambda\tau)}{e \times T} \quad ...(2.7)$$

The system constants required for these calculations are summarised on Table 2.16 while a suite of computer programs to perform them are listed in Appendix II.

TABLE 2.16

SUMMARY OF SYSTEM CONSTANTS.

	KCFC			SEDIMENT
	Flat top	Well	Ge(Li)	Ge(Li)
B(cpm)	13.8	6.3	0.49	0.44
B'(cpm)	8.1	7.1	0.53	0.48
e	0.0572	0.2078	0.0189	0.0193
e'	0.0488	0.1237	0.0176	0.0158
f_1	1.353	0.299		
f_2	0.00198	0.00147		
E_1 (cpm)	0.2	0.2	0.02	0.03
E_2 (cpm)	0.2	0.2	0.05	0.02
R_1	0.024	0.017	0.032	0.066
R_2	0.012	0.031	0.044	0.066

Symbols defined in text.

Chapter 3

The Clyde Sea Area

3.1 Introduction

Previous work on water transport processes within the Clyde Sea Area (C.S.A.), as assessed by radiocaesium concentration (MacKenzie, 1977), was based on two main hypotheses, namely:-

1) that the C.S.A. can be regarded as a simple system with incursing Irish Sea - and Atlantic - derived salt water causing displacement of residual water with no resultant mixing or, conversely, with complete mixing, on the timescale of water exchange processes (several months) and

2) that peaks in the output level of ^{137}Cs from Windscale can be correlated with observed maxima in the ^{137}Cs concentration of C.S.A. waters.

In this chapter it is intended to examine these hypotheses and, on the basis of the investigations herein, to develop a more rigorous mathematical model of the C.S.A. system. This should lead to a more realistic treatment than the simple conservation of properties model proposed by MacKenzie (1977) and based completely on simple peak-matching.

Two extensive series of samples were obtained. The first set were collected from a wide range of locations in the C.S.A. in December 1977 (Fig 3.1) to examine the spatial distribution of radiocaesium in the area. The second set were taken, from a selected site in the north of the C.S.A.

FIGURE 3.1 STATION LOCATIONS IN THE CLYDE SEA AREA

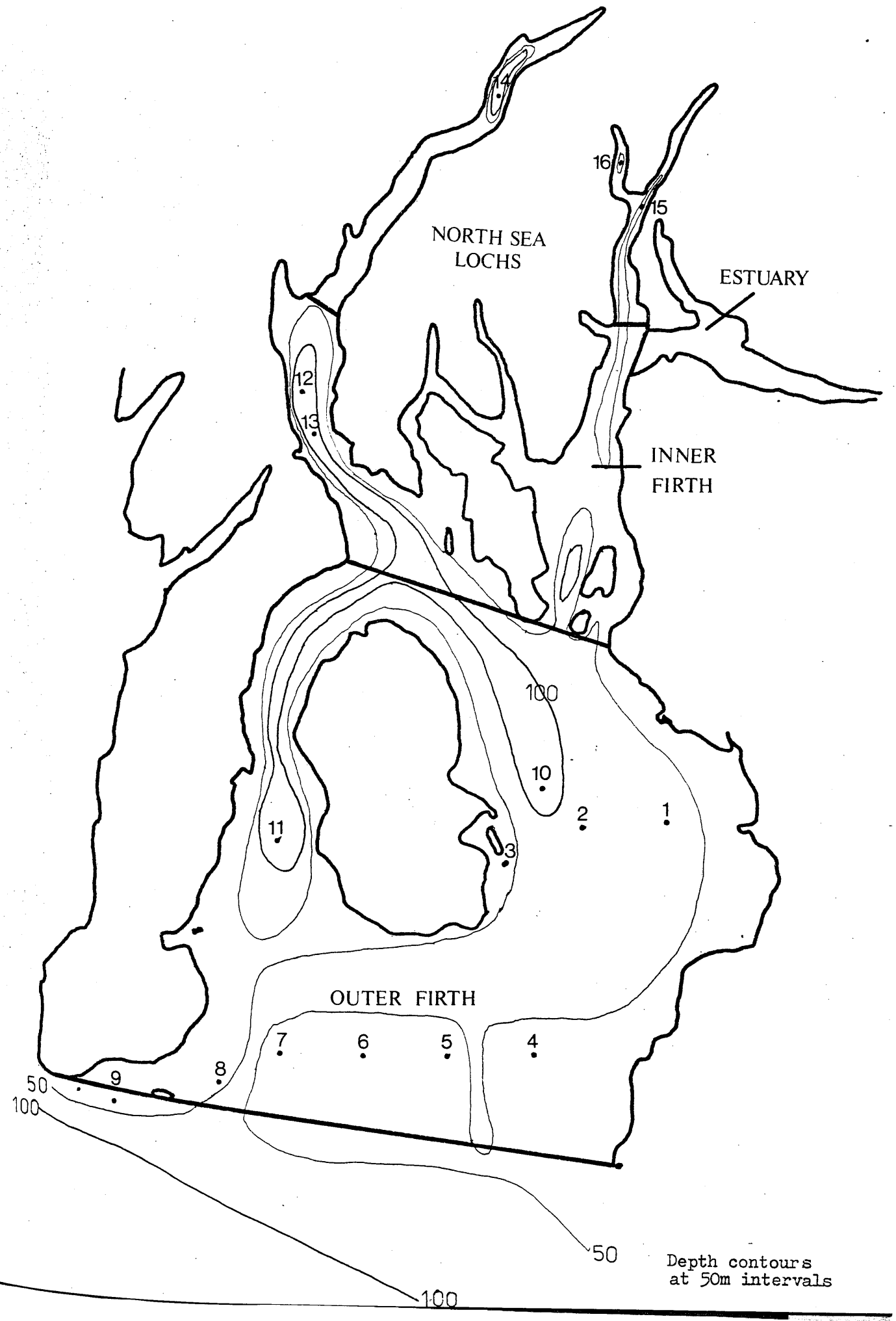

(L. Goil), at regular time intervals to extend the temporal data obtained by MacKenzie (1977) and to examine the validity of a simple peak-matching process.

The majority of samples for the areal study of December 1977 were collected during cruise JM/16/77 of the N.E.R.C. research ship 'John Murray'. Additional samples from Lochs Fyne, Long and Goil were collected on cruises of the C.R.P.B. research vessel 'Endrick II', as were the regular samples from Loch Goil.

All results of the spatial homogeneity study are tabulated in Appendix I.1 where the positions corresponding to the sample codes are given in Table 3.1 and plotted in Fig. 3.1. The large volume of data available is reduced by presentation of surface values of salinity-corrected ^{137}Cs concentrations throughout the area in Fig 3.2, while vertical profiles of ^{137}Cs, salinity-corrected ^{137}Cs and $^{134}Cs/^{137}Cs$ activity ratio are presented in Fig 3.3.

Temporal variations in radiocaesium in the C.S.A. are based on L. Goil depth profiles as tabulated in Appendix I.2 and are presented in Fig 3.4. These values have been selected from a depth of 10 m for reasons considered in Chapter 4.

3.2 Spatial Distribution of Radiocaesium in the C.S.A.

When corrected for salinity variations, surface ^{137}Cs concentrations in the Clyde Sea Area are seen to be fairly homogeneous (Fig 3.2). Thus the standard deviation of all sample data is <4% which is only slightly larger than that expected from the measurement process alone ($\sim$2%). The

TABLE 3.1 STATION POSITIONS FOR AREAL STUDY.

CODE	STN. NO.	DECCA RED	DECCA PURPLE	N LAT	W LONG	WATER DEPTH(m)
JM1,2	1	D 8.58	I 58.30	55 32.5	4 49.0	32
JM3,4,5	2	D 15.88	H 78.50	" 31.3	" 55.8	73
JM6	3	E 0.33	H 70.65	" 30.0	5 3.5	42
JM7	4	D 17.95	G 55.4	" 18.9	" 0.3	55
JM8	5	E 5.41	G 52.95	" 19.0	" 9.0	51
JM9	6	E 16.03	G 52.26	" 19.1	" 13.9	49
JM10,11,12	7	F 2.43	G 52.30	" 19.1	" 23.2	46
JM 13	8	F 12.7	G 50.3	" 18.6	" 30.2	51
JM 14	9	G 6.48	G 74.69	" 17.4	" 39.1	22
JM 15-21	10	D 20.88	I 61.69	" 34.4	4 59.4	113
JM 22-26	11	F 3.79	H 65.37	" 31.0	5 26.3	86
JM 27-32	12	E 23.3	A 60.2	" 55.0	" 23.6	146
SLF	13			" 52.64	" 22.55	170
NLF	14			56 12.1	" 4.9	135
LL 1	15			" 5.55	4 51.88	98
LG 1	16			" 8.39	" 53.49	86

FIGURE 3.2 DISTRIBUTION OF RADIOCAESIUM IN THE C.S.A.

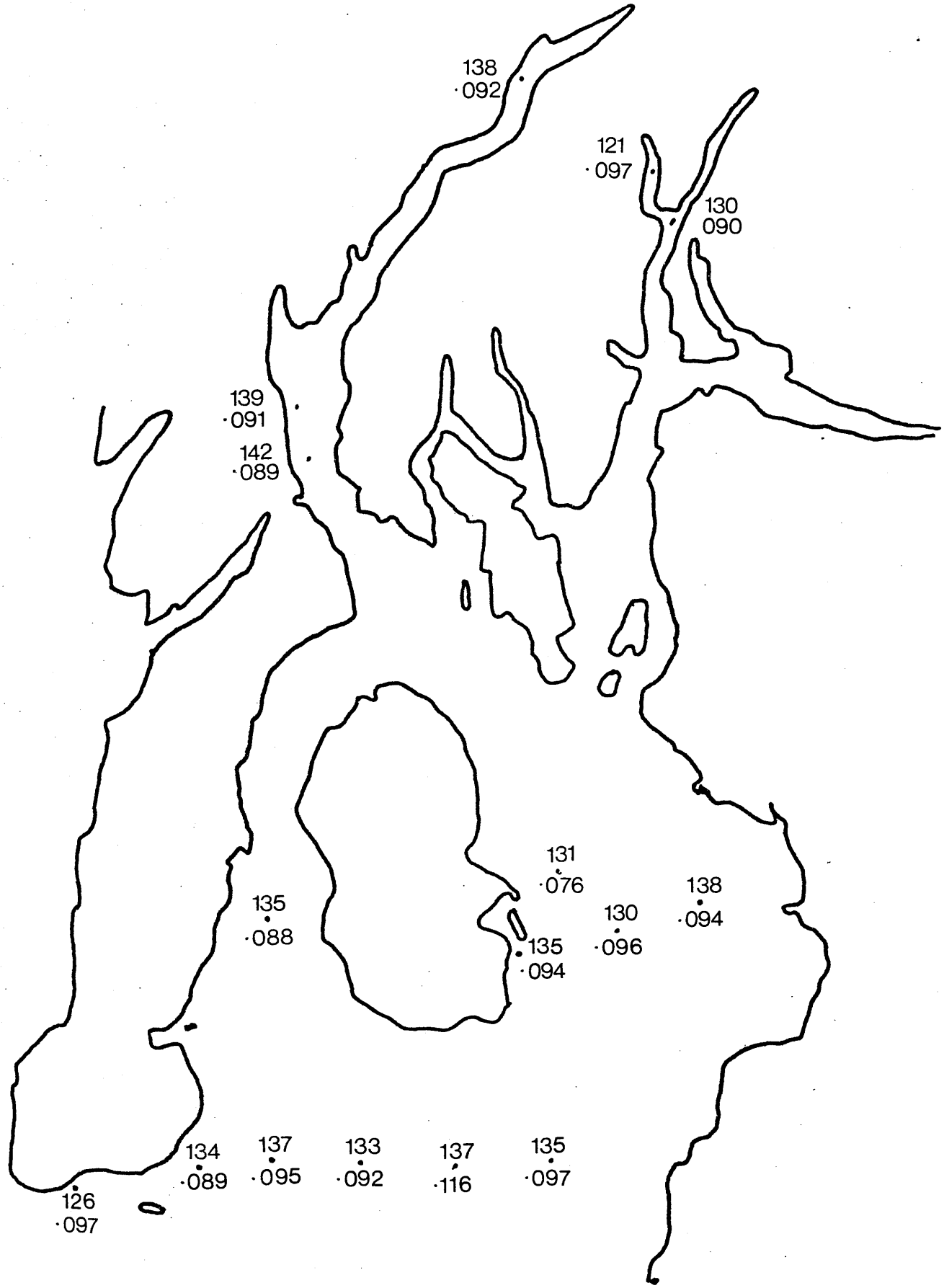

FIGURE 3.3 VERTICAL PROFILES FROM STATIONS IN THE C.S.A.

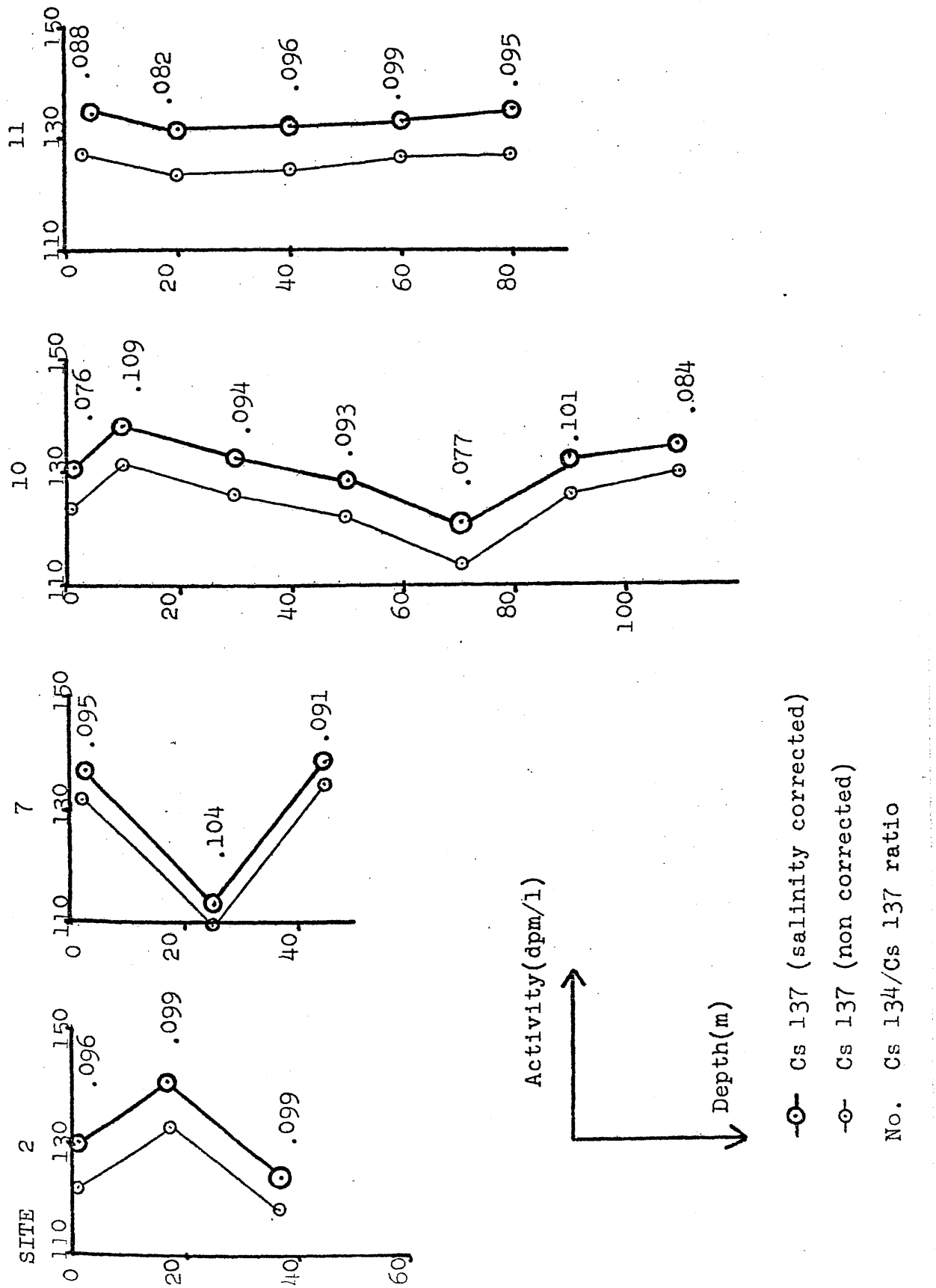

FIGURE 3.3 (CONTINUED)

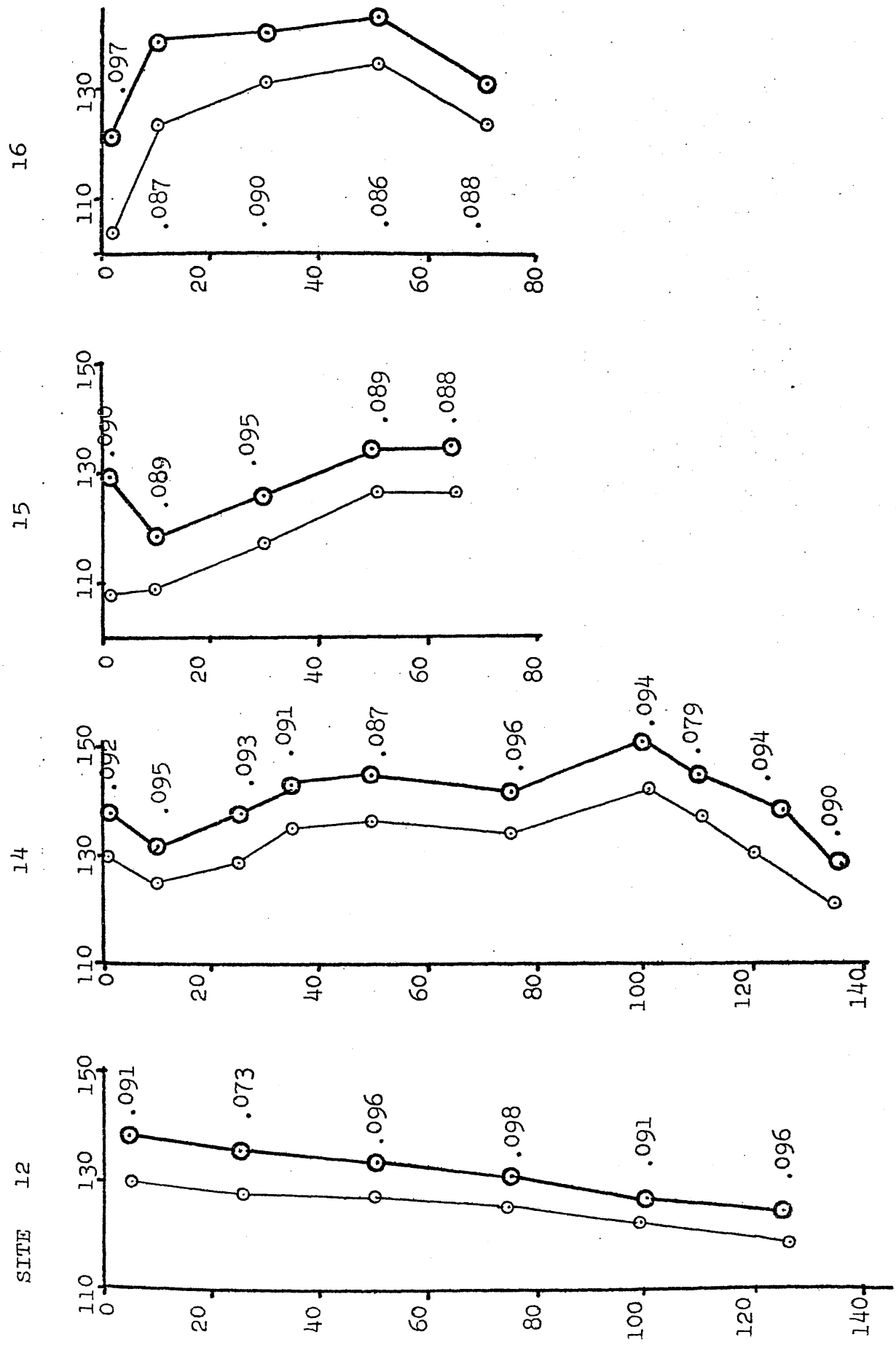

FIGURE 3.4 TEMPORAL VARIATION OF RADIOCAESIUM IN THE C.S.A.

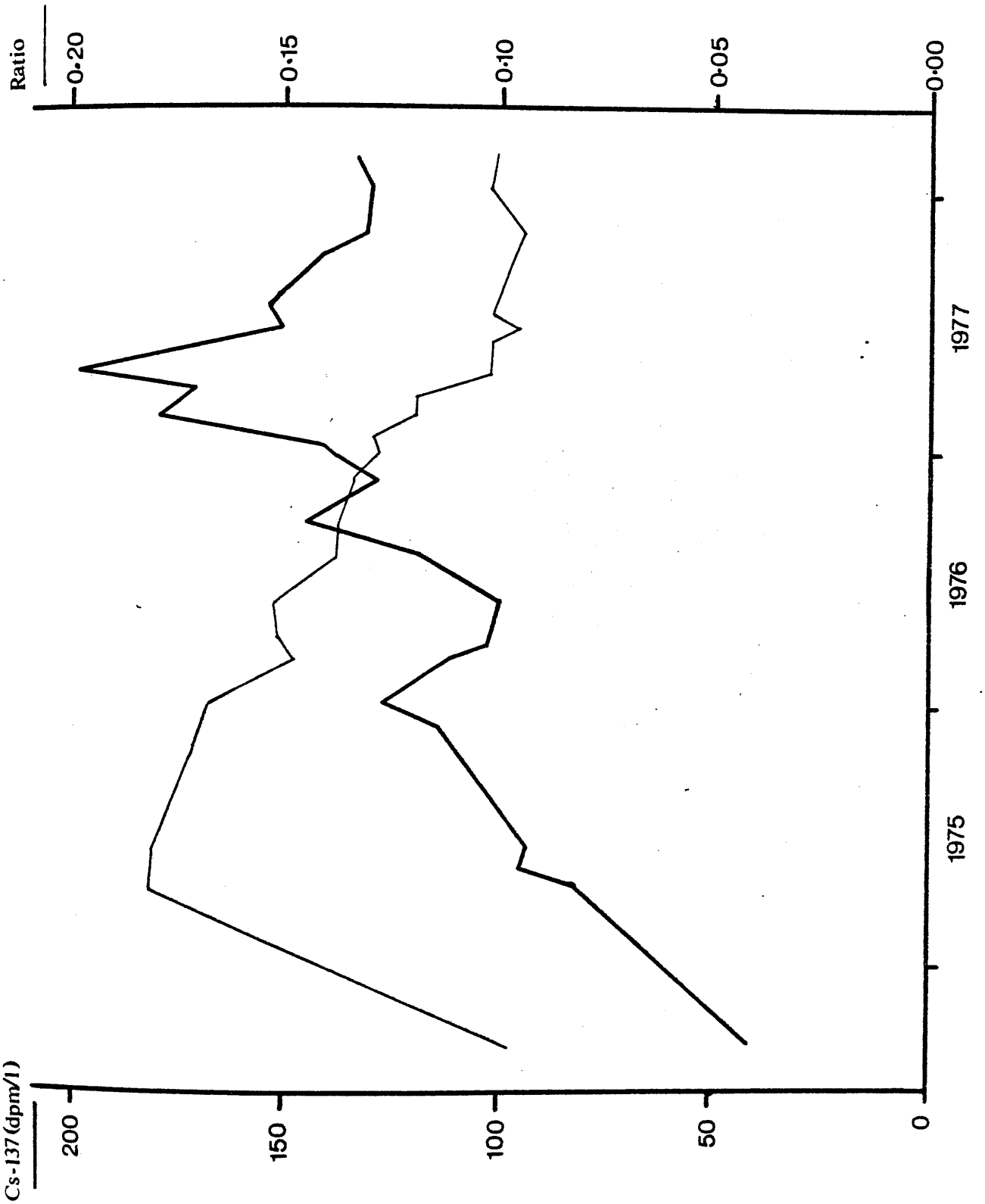

mechanism producing this surface homogeneity is almost certainly fast wind- and tide- driven surface water (0 - 10m) mixing and transport, the importance of wind-driven currents in the area having been described previously (Barnes and Goodley, 1961). Since the temporal variation in ^{137}Cs concentration during the months preceeding this survey (Fig 3.4) showed a generally decreasing trend ($\sim$ -7%/month) and as the survey shows no corresponding spatial variation in ^{137}Cs concentration, it is evident that surface mixing must occur on a timescale of $\lesssim$ 1 month. Surface $^{134}Cs/^{137}Cs$ ratios in the area average 0.093 with a standard deviation of $\sim$ 8.5% but no obvious spatial trends. The observed ratio variability is considerably larger than that expected from the measurement process itself ($\sim$ 4%), possibly due to short term fluctuations ($\sim$ weeks) in the ratio of incursing waters. In the months preceding the survey, random fluctuations of $\sim \pm$5%/month were observed (Fig 3.4) in the C.S.A. ratio. Interpolation of a regular ratio trend is therefore impossible, so that sizeable fluctuations in ratio input could have occurred on a timescale less than the sampling frequency (1/month).

More distinct ^{137}Cs concentration variations exist, however, in the vertical radiocaesium profiles (Fig 3.3). The four profiles from the Outer Firth (stations 2, 7, 10 and 11) show depth variations which are larger and more regular than any expected analytical error. Stations 2 and 10, to the east of Arran, show an increase in ^{137}Cs concentration from surface to $\sim$ 15 m followed by a decrease

to depth, this trend being more marked at the shallower, southerly site. The data for the deeper station also pass through a minimum at ~70 m. The western profiles (stations 7 and 11) exhibit an opposite trend, with a decrease in ^{137}Cs from surface to ~20 m followed by an increase towards the bottom. Again this profile is more marked at the shallower, more southerly site. There is very little marked trend within the variations of $^{134}Cs/^{137}Cs$ ratio, as would be expected in view of the highly irregular temporal changes in this parameter over the time period of the study.

Although interpretation of these radiocaesium profiles is difficult without comparison to others from additional times of year, a tentative explanation may be proposed. The region of the Outer Firth consists of an area of deep water (>50m) separated from the deeper water (>100m) of the North Channel (N.C.) by a broad plateau of average depth ~40m (Fig 3.1). Within this area extensive deep trenches (>100m) - extensions of the L. Fyne fjord - extend round the north coast of Arran (c.f. Chapter 1.4). Water transport in the Outer Firth can thus be regarded as due to freshwater input, mainly from the estuary, and exchange with the waters of the North Channel with additional fast mixing and transport of surface waters as previously discussed.

As the radiocaesium concentration of North Channel water is regularly monitored (Dutton, 1978; Jefferies, 1978) it is known that, at the time of the Clyde Survey, incursing N.C. water had a lower ^{137}Cs concentration than residual C.S.A. waters. Thus the waters at 40m at station 2 and 70m at station 10 are more typical of the North Channel (^{137}Cs ~ 110 dpm l^{-1})

FIGURE 3.5 RADIOCAESIUM DATA FOR THE NORTH CHANNEL

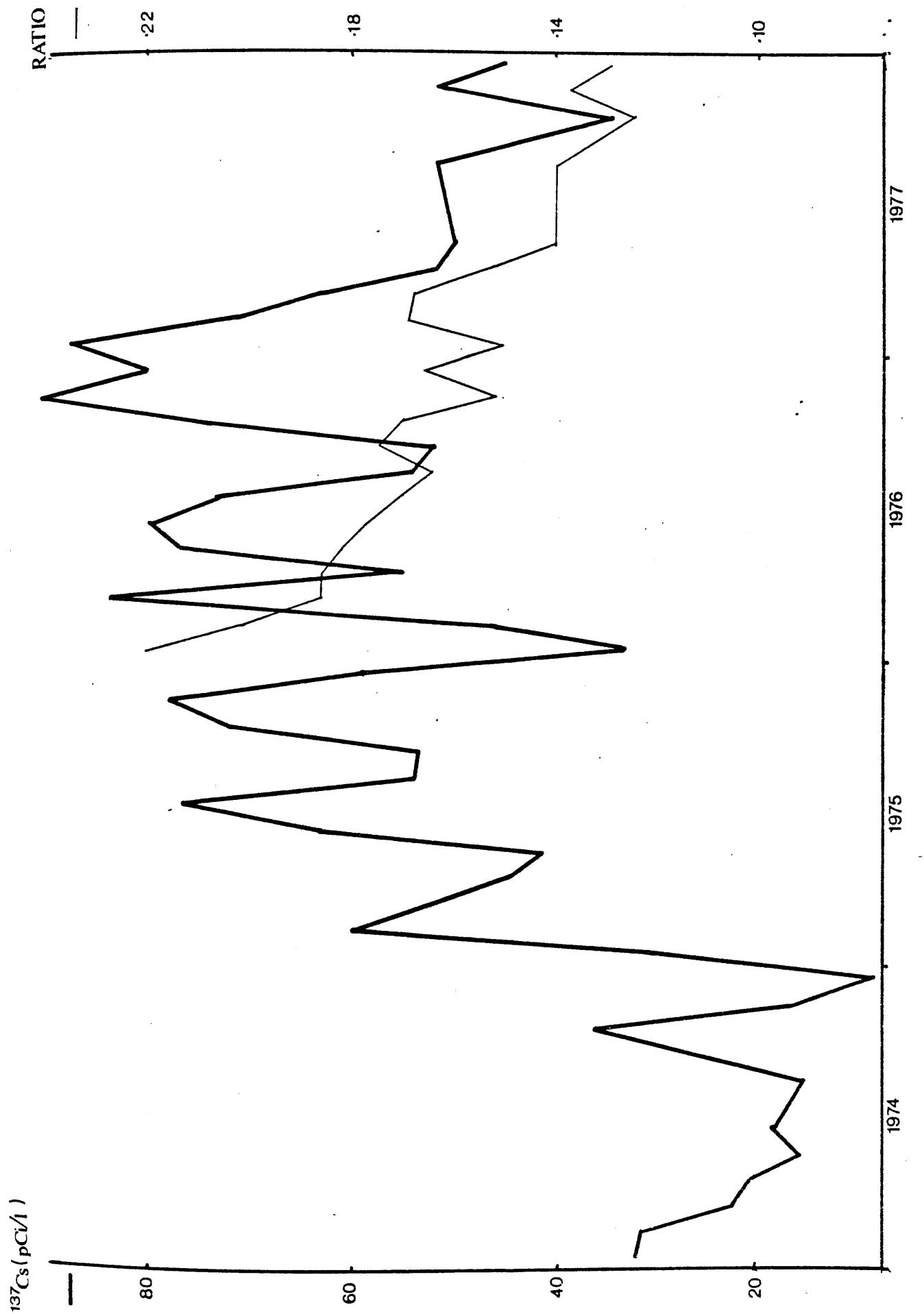

rather than of residual Clyde Sea water ($^{137}Cs \sim 135$ dpm l^{-1}). To the west of Arran, incursion occurs at shallower depth ($\sim$25m) and, although incoming water is quite distinct at site 7, station 11 presents a well-mixed profile with ^{137}Cs $\sim$125 dpm l^{-1}, midway between C.S.A. and N.C. values. This profile shows a slight minimum at $\sim$25m which could indicate a current at this depth flowing northwards along the west coast of Arran, gradually losing identity through vertical mixing. The maxima in the ^{137}Cs profiles at $\sim$15m at stations 2 and 10 and at $\sim$40m at station 7 may indicate return flows out of the Clyde Sea at these depths.

The profile from the continuation of the north west trench system into south L. Fyne (station 12) shows a slight but regular increase in ^{137}Cs from bottom to surface (Fig 3.3) indicating a fairly well-mixed system with newer water being introduced at depth followed by upwards mixing. By comparison, the north basin of L. Fyne (station 14) has a distinctive profile with a radiocaesium maximum at 100m, 23% higher than the depth average for the Outer Firth. This maximum is almost certainly due to entrainment of deep water over a timescale of months (c.f. Chapter 4). As this deep basin is separated from the southern trench system by a 10-mile stretch of loch of average depth $\sim$40m, only water from depths $\lesssim$40m would be expected to spill into the north basin. As the salinity at $\sim$40m in the south basin matches that of the deepest (>120m) low ^{137}Cs concentration water in the north basin, the data may reflect flow over the sill from the south basin displacing the bottom waters of the north basin, thus giving rise to the

observed profile. If the maximum activity of north basin waters is matched against the temporal variation of radiocaesium in the Clyde Sea (Fig 3.4), an ambiguous correlation, both in terms of ^{137}Cs activity and $^{134}Cs/^{137}Cs$ ratio, is obtained, the water having an apparent residence time of either $\sim$ 4 months or $\sim$ 1 year. This ambiguity arises from the maximum in ^{137}Cs concentration and the decreasing trend in the $^{134}Cs/^{137}Cs$ ratio in the C.S.A. in the preceding year and prevents more precise residence time determination on the basis of this single profile.

The radiocaesium profile in L. Long (station 15) indicates surface lowering of ^{137}Cs concentrations followed by an increase to relative constancy at depths below $\sim$ 50m. A mechanism of surface transport of low activity waters followed by vertical mixing to depth is suggested. Sill-protected L. Goil (station 16) shows a profile similar to that of north L. Fyne in that lowering of ^{137}Cs concentrations is evident towards both surface and depth, implying a similar mechanism of water renewal both by surface transport and mixing and deep water displacement (c.f. Chapter 4).

A simple representation of the derived deep water flows for the area (Fig 3.6) shows a main flow northwards along the east coast of Arran to the south basin of L. Fyne, with some continuation over the sill into the north basin. A less well-defined flow northwards occurs along the west coast of Arran, with return transport along both coasts although most return flow probably occurs in surface waters. It must, however, be strongly emphasised that the derivation of these flows is

FIGURE 3.6 PROPOSED DEEP CURRENTS IN THE C.S.A.

tenuous. In addition, because of the limited temporal baseline of this study, no indication of the permanence of the proposed transport pattern can be obtained. Indeed flow characteristics within the area may be variable on a timescale of days or weeks.

At a more realistic and quantitative level, the average (salinity-corrected) surface ^{137}Cs concentration in the Outer Firth is 134.1 $\pm$ 3.6 dpm l^{-1} compared to the average for all depths of 132.5 $\pm$ 6.1 dpm l^{-1}. This comparison shows clearly that, despite the obvious water structure in the area, the volume-average radiocaesium activity lies close to that for surface waters. To be more rigorous, a weighting factor must be applied to radiocaesium concentrations at different depths to account for changes in water columns for the various bathymetric regions (Table 3.2). Using this weighting process, the average ^{137}Cs concentration for Outer Firth waters is 130.4 dpm l^{-1} which differs from the surface average for the entire Clyde Sea Area by only 2.6%, well within the derived 1σ error.

The conclusion from this study is thus that, although definite vertical structure exists within the Clyde Sea Area, the average ^{137}Cs content of the Outer Firth is closely matched by surface concentrations which are effectively homogeneous throughout the entire C.S.A., in agreement with other studies (Jefferies et al, 1973; Steele et al, 1974; MacKenzie, 1977). The situation in the sill-protected northern sea lochs is more complex, however, as significant entrainment of water occurs in deep basins as considered further in the next chapter.

TABLE 3.2

DEPTH WEIGHTING OF ^{137}Cs CONCENTRATION IN C.S.A.

a) DEPTH BAND(m)	RELATIVE AREA	CUMULATIVE TOTAL	WEIGHTING FACTOR
0-20	546	3547	1
20-60	2246	3001	1.692
60-100	1440	1755	0.990
100-160	276	315	0.262
160	39		0.022

b) DEPTH	^{137}Cs MEAN	S.C. ^{137}Cs MEAN	WEIGHTED ^{137}Cs MEAN	WEIGHTED S.C. ^{137}Cs MEAN
0-20	127.9 ± 3.5	135.7 ± 3.1	128	136
20-60	122.9 ± 7.6	128.8 ± 8.0	208	218
60-100	123.3 ± 6.2	130 ± 6.4	122	128
100-160	129.9	135.3	34	35
PROFILE MEAN	126	133	125	131

All activities in $dpml^{-1}$

S.C.-Salinity corrected

Although not specifically investigated in this study, there is no evidence of a 'Hunterston effect' due to radiocaesium release from this nuclear power station. The total activity of effluent released from this reactor (excluding ^{3}H) is only ~115 Ci/year (1975) compared with ~1.2×10^{5} Ci of ^{137}Cs alone from Windscale in that same year (Mitchell, 1977). At the time of the areal study the total Clyde Sea content of ^{137}Cs was ~ 9.8×10^{3} Ci ie about two orders of magnitude greater than the entire Hunterston annual release. Any Hunterston effect must therefore by highly localised and is insignificant in calculations involving the entire C.S.A.

3.3 Temporal Variations in the Radiocaesium Content of the C.S.A.

As indicated in the previous section, even though regional variations in ^{137}Cs concentrations may exist, surface ^{137}Cs activity is effectively constant throughout the area and may be regarded as approximately equivalent to the average ^{137}Cs concentration for the entire C.S.A. For analysis of temporal variations in radiocaesium content of the Clyde Sea a necessary assumption is that the situation as it existed in winter 1977 may be regarded as generally typical on a year round basis. Support for this assumption comes from the known dependance of surface water transport, and its implied resultant water mixing, on wind direction and speed (Barnes and Goodley, 1961; Dooley and Steele, 1969), parameters which, on a monthly average, are relatively constant in this region at all times of the year. Exceptions to this generalisation occur in the months of March and May,

when the prevailing wind direction is from the north east rather than from the south west but, as the net change is not great, the general assumption of reasonably fast mixing ($\sim$1 month) and a water mass approximating to homogeneity throughout the year may be tentatively accepted.

The temporal variation of salinity-corrected ^{137}Cs concentration in the Clyde Sea Area (Fig 3.4) shows a generally increasing trend to a maximum of $\sim$200 dpm l^{-1} in April 1977 followed by a decrease from that date. $^{134}Cs/^{137}Cs$ ratios during the corresponding time showed an increase to a maximum of 0.18 in April 1975 followed by a fairly regular decrease of $\sim$15%/year. The most interesting general point from this curve is the occasional rapid change in ^{137}Cs activity indicative of relatively short water residence in the area.

At a simple level, and with some experimental justification, the C.S.A. can be regarded as a single water mass which is completely mixed on a timescale of $\sim$1 month. This 'mixing box' is characterised by volume (V) and average water residence half-time ($\tau_{\frac{1}{2}}$) with respect to exchange with North Channel water. Freshwater flow may be considered negligible to a first approximation (Craig, 1958). The concentration of any conservative dissolved species originally present in this system, but absent in incoming 'new' water, will decrease such that:-

$$C_t = C_o e^{-\left(\frac{0.693 \times t}{\tau_{\frac{1}{2}}}\right)} \qquad \ldots.3.1$$

where C_o and C_t are the concentrations of the species at time zero and t months respectively.

From this equation it is apparent that the residence half-time can be specified in terms of the input (or output) water flow (f):-

$$\tau_{\frac{1}{2}} = \frac{0.693 \times V}{f} \qquad \ldots.3.2$$

From the data of Craig (1958), $f = \frac{3V}{2}$/year, and thus $\tau_{\frac{1}{2}} = 0.46y \equiv 5.54$ months. The average water residence time thus implied (~8 months) may thus be directly compared to a value of ~9 months quoted without derivation by Heath (1974).

From April - June 1977, the ^{137}Cs content of the Clyde Sea Area decreased by ~15% (Fig 3.4). As ^{137}Cs decay is insignificant over this time period, the decrease must be the result of exchange process within the C.S.A. If, as an extreme case, incoming water was assumed to be 'Atlantic-derived' and thus was effectively free from radiocaesium, applying equation 3.1 for C_o = 198 dpm l^{-1}, Ct = 168 dpm l^{-1} and t = 1.6 months gives $\tau_{\frac{1}{2}}$ = 6.7 months which is a maximum possible value. This completely 'Atlantic-derived' flushing model is, however, immediately disproved by MAFF measurements of radiocaesium in the North Channel (Stranraer-Larne) and and Islay-Malin channel over this period (Jefferies, 1978). More reasonably, an approximate concentration of ^{137}Cs in the incoming water may be obtained from the MAFF measurements of radiocaesium in the North Channel (Fig 3.5) bearing in mind the G.U./MAFF intercalibration constant (Chapter 2.5).

Although MAFF measurements of radiocaesium in the N.C. are restricted to surface waters, the water column in this area has been shown to be effectively homogeneous with depth (Bowden, 1950; Proudman, 1948; 1953; Preston, 1973; Officer, 1978) and thus surface values may be regarded as representative of the entire water mass. Taking a minimum value from the North Channel concentration curve at this time (114 dpm l^{-1}), an input concentration of 110 dpm l^{-1} can be derived by considering intercalibration and correction to salinity of 35% from a typical North Channel salinity of 34% (Bowden, 1950). Taking the C.S.A. values previously considered, the proportion of 'residual' water after three months (x) is given by

$$198x + 110(1-x) = 168 \qquad \ldots.3.3$$

$$\Rightarrow \quad x = 0.66$$

and thus, from equation 3.1, $\tau_{\frac{1}{2}}$ = 2.7 months. This figure indicates that the exchange rate during the summer is faster than the annual averages quoted by Craig (1958) and Heath (1974) but is in agreement with a 'best estimate' residence time of 3.9 months derived from radiocaesium analysis by MacKenzie (1977). Since winter water renewal is theoretically expected to be more rapid than in summer (eg due to increased vertical mixing through breakdown of the summer thermocline) it is also implied that fast mixing occurs generally throughout the year. Short residence times have in fact been quoted for the C.S.A. (renewal time $\sim$4 weeks corresponding to $\tau_{\frac{1}{2}}$ = 2.8 weeks (Steele et al, 1974)) but, for the time period considered, these very short residence times seem incompatible with the radiocaesium data.

If the approximate validity of the calculation above is accepted, it can be used as the basis of an indirect intercalibration of calculated ^{134}Cs concentrations with MAFF data as this was not practical by direct methods (cf Chapter 2.5). To improve the accuracy of this calculation a more realistic value of 147 dpm l^{-1} is taken as the ^{137}Cs concentration of incoming water, this figure being obtained by averaging the February and March concentrations in the North Channel (corrected for salinity and intercalibration) as opposed to the minimum value considered earlier. Using this ^{137}Cs concentration, the proportion of residual water is calculated as 0.41 corresponding to a residence half-time of 1,2 months. Taking the initial and final ^{134}Cs concentrations in the C.S.A. as 17.8 and 17.6 dpm l^{-1} respectively, and the concentration in incoming water as 24.8 dpm l^{-1} (obtained in similar manner to the ^{137}Cs input concentration), the following equality is obtained:-

$$\delta(17.8 \times 0.96 \times 0.41) + (24.8 \times 0.96 \times 0.59) = 17.6\,\delta$$

where δ is the intercalibration constant and the factor 0.96 accounts for decay over the time considered. This calculation yields a value for δ of 1.33; thus MAFF measurements of ^{134}Cs are systematically 33% higher than Glasgow values which, bearing in mind the intercalibration constant of 1.07 for ^{137}Cs, implies a G.U./MAFF intercalibration constant of 1.24 for measured $^{134}Cs/^{137}Cs$ ratios. Alternatively, deriving ^{137}Cs and ratio inputs to the area from N.C. values for March and April, the value of δ obtained is 1.28 giving a ratio intercalibration constant of 1.20. The relative consistency

of the values obtained by the two calculations above indicates an insensitivity of the results to small variations in the input parameters chosen and thus averaged intercalibration constants of 1.30 and 1.22 for ^{134}Cs and ratio determination respectively may be accepted as reasonable estimates.

While it would be possible to calculate a series of implied residence half-times throughout the year by the method above, this is not generally practicable because of difficulties in specifying exact transit times from the MAFF North Channel station to the Clyde Sea Area and thus in assessing a reasonable average value for the radiocaesium concentration of incoming water, as the latter varies considerably on a monthly basis (Fig 3.5).

In the previous radiocaesium study of the C.S.A., MacKenzie (1977) matched observed radiocaesium variations from 8/74 - 3/76 (Fig 3.4) with the Windscale output curve (Fig 3.7). As a result of the low sampling frequency, only a tentative match could be obtained - a point emphasised by comparison of the Windscale output curve (Fig 3.7) and the observed variation in radiocaesium concentration in the North Channel (Fig 3.5). Not only is unambiguous peak matching impossible in this simpler system, but the general trend in peak heights differs - output maxima between 1974 and 1977 showing a decreasing trend while concentration maxima in the N.C. show a general increase. The difference between these curves may be explained in terms of internal mixing within the northern Irish Sea (Bowden, 1950; 1955; Proudman, 1948; 1953; Preston et al, 1972; Preston 1973; Officer, 1978) so that it is unrealistic to consider transport from Windscale to the North Channel as simple advective flow.

FIGURE 3.7 RADIOCAESIUM OUTPUT FROM WINDSCALE

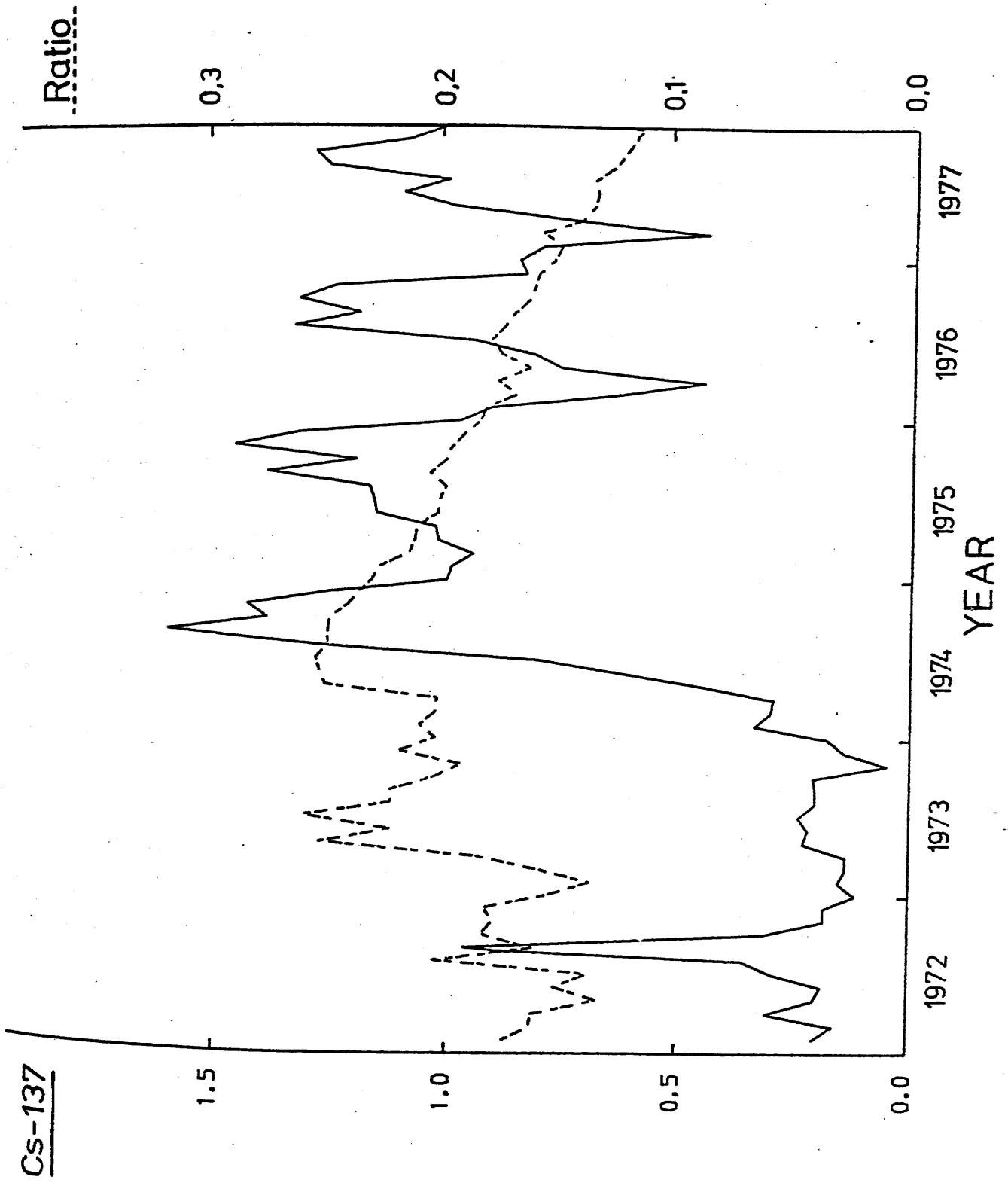

The effect of internal mixing may be examined by considering the north Irish Sea as a single mixing box with a characterisitc average residence half-time, a single source of radiocaesium at Windscale, a diluting input of radiocaesium - free, north-flowing, Atlantic-derived water and a single output through the North Channel. The effect of variation of this residence half-time on the derived output curve can be readily illustrated using an electronic analogue circuit (Fig 3.8) in which an input waveform. which mirrors radiocaesium output from Windscale, is produced by a signal generator and is integrated by an operational amplifier. Negative feedback of the integrated output is controlled by a variable resistor which is, in effect, representative of the residence half-time and the resultant output curve, on electronic differentiation, represents the derived North Channel output (Hardy, 1969).

While the applicability of this model was initially determined using the electronic circuit above, calibration and enlargement of the circuit to mimic a second mixing box was hindered by a lack of necessary electronic assistance. Thus the model was transferred to a digital computer. Although digital programs lack the continous variability of parameters and, in this case, also the interactive nature of analogue circuitry, practical consideration of the required development times determined the choice for this analysis (Appendix 2.2).

Thus, from digital simulation of a one-box mixing model, a series of output curves may be derived from the Windscale input curve corresponding to different values of the box residence half-time (Fig 3.9). The observed North Channel curve (Fig 3.5) has a marked peakedness (kurtosis) in comparison

FIGURE 3.8 1 BOX MODEL ANALOGUE CIRCUIT

a) INTEGRATOR WITH VARIABLE NEGATIVE FEEDBACK

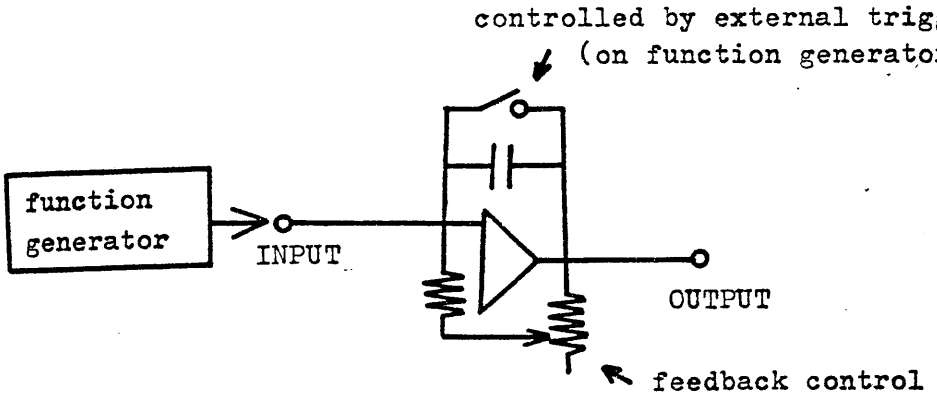

b) DIFFERENTIATOR

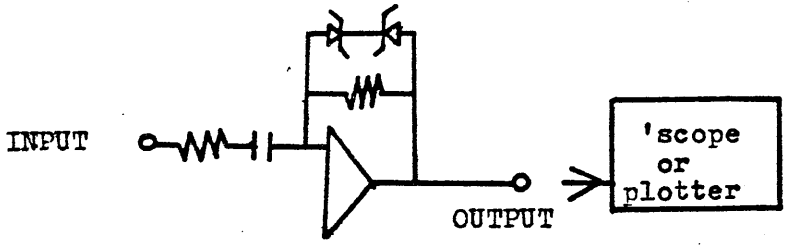

FIGURE 3.9 ANALOGUE 1 BOX MODEL OUTPUT - WINDSCALE Cs-137

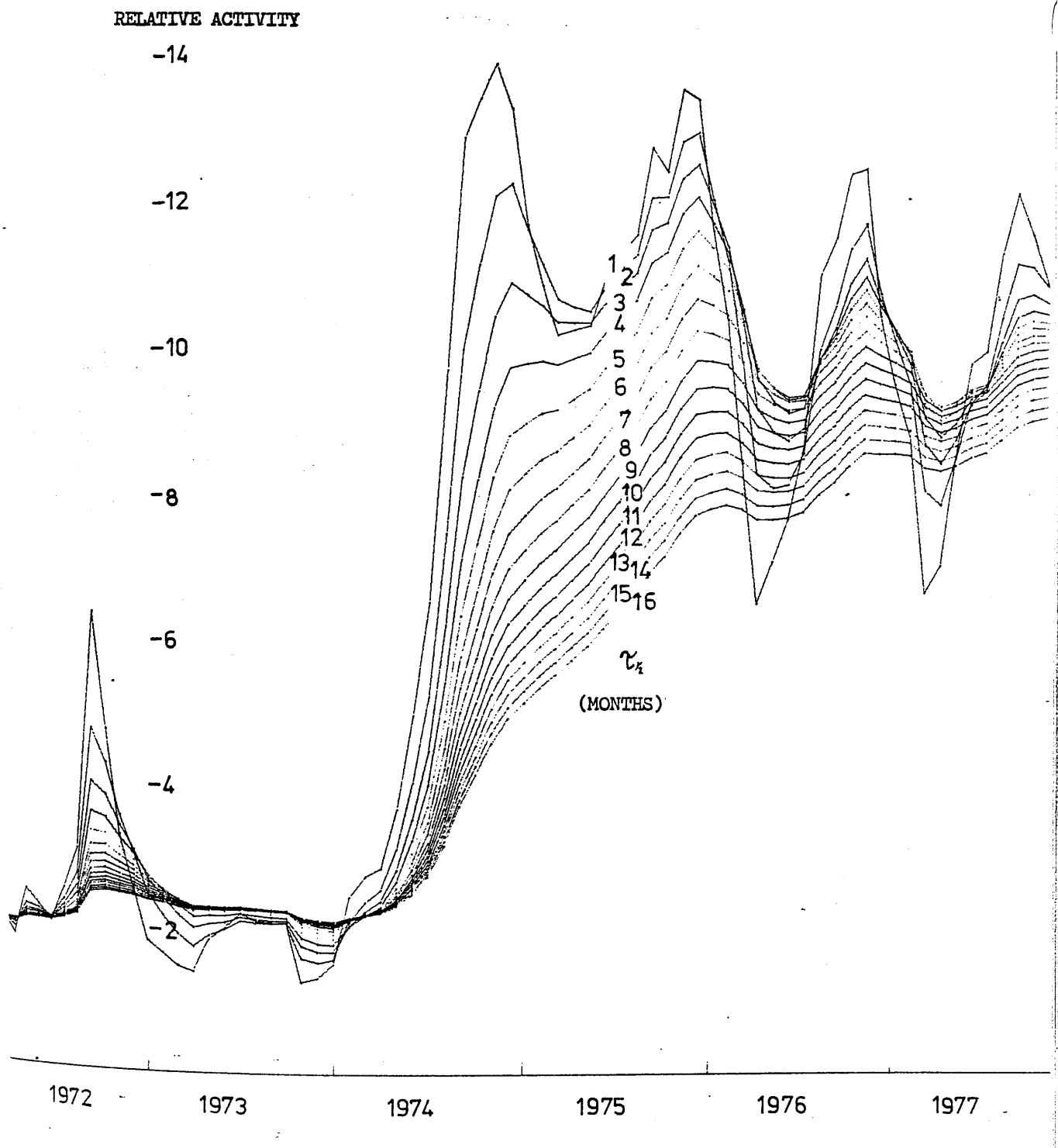

to the smooth box-model output curves, a feature which may be due to short term (monthly) variations in the degree of Atlantic incursion in the North Channel and hence in the extent of dilution of Windscale-derived water or may, to some extent, be an artifact caused by sampling. The MAFF samples are obtained in an undisclosed manner from the Stranraer-Larne ferry and thus the depth of the 'surface' sample may not be well defined. As very marked radiocaesium profiles in the upper few meters may be caused by rainwater and coastal runoff dilution, slight variations in the depth from which the sample is obtained and the weather over the week preceding sampling may critically affect the observed radiocaesium concentration. As salinity data for the MAFF station are not available, it is not possible to define the cause of the observed short term variations. Therefore, to allow comparison of yearly trends in the N.C. with box-model curves, the effect was minimised by considering a three month running mean of MAFF radiocaesium values (Fig 3.10). When this curve is compared with box-model output curves (Fig 3.9) a reasonable match in overall trends over the period 1973-1976 is observed with curves corresponding to residence half-times in the range 10-14 months. The match obtained may be illustrated by comparing the fit between predicted and observed ^{137}Cs curves with a box residence half-time of 12 months with that obtained from a shorter residence box ($\tau_{\frac{1}{2}}$ = 2 months) when a lag-time is introduced based on the 'marker' of the rapid output increase of early 1974 (Fig 3.11). Significant monthly variations exist between the observed and predicted curves but, up till 1977, the model with $\tau_{\frac{1}{2}} \sim 12$ m. provides a good match in terms of both the ratio of average ^{137}Cs

FIGURE 3.10 RADIOCAESIUM DATA FOR THE NORTH CHANNEL

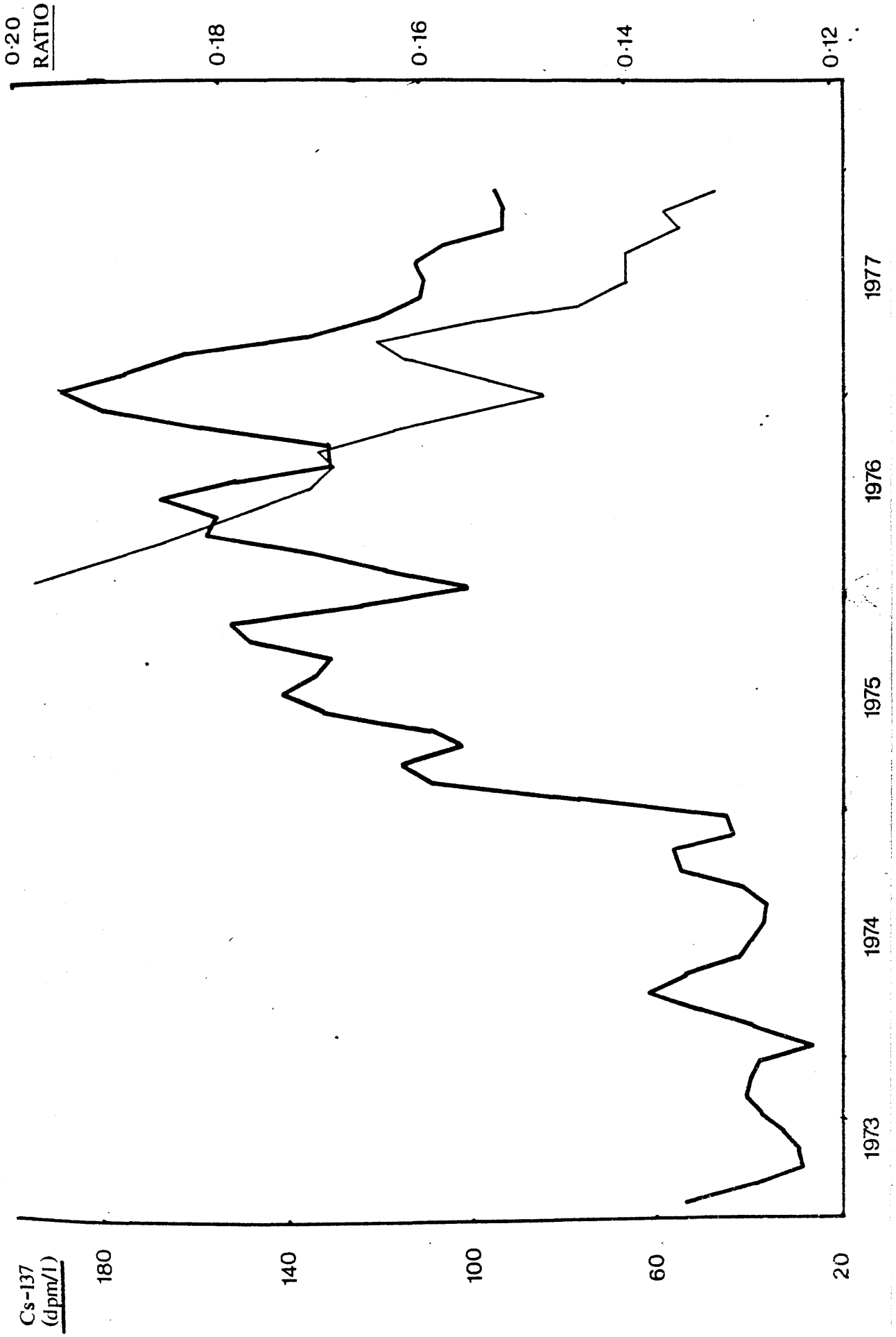

FIGURE 3.11 COMPARISON OF OBSERVED AND MODELLED CURVES - NORTH CHANNEL Cs-137

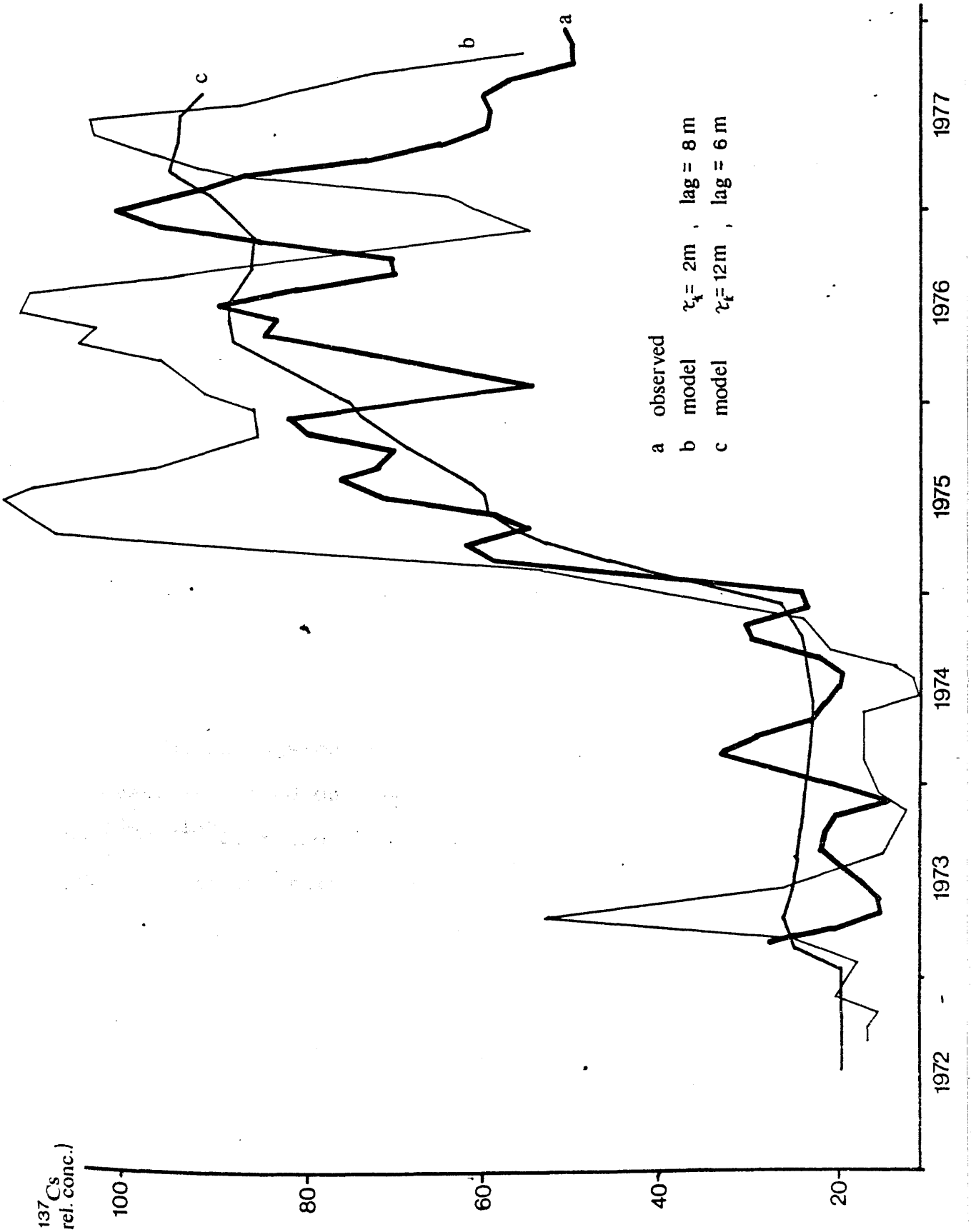

content before and after the input increase event and the total integral under the curve. The observed deviations are thus explained in terms of seasonal changes in the extent of dilution, during transport,by either fresh or Atlantic-derived waters. As previously considered, in the absence of salinity data it is impossible to distinguish between these diluting processes.

In the match proposed above, a lag time of ~6 months was introduced - based mainly on correlation of the rise predicted by the model for mid-1974 with that observed in early 1975 - implying an additional delay of ~6 months in transport to the North Channel station (mid Stranraer-Larne). The entire process may thus be regarded as a combination of mixing with characteristic $\gamma_{\frac{1}{2}} \sim 12$ months (probably in the N.E. Irish Sea) and advective flow with a transit time of 6 months. These derived values are similar in magnitude to, but shorter than, the Windscale to North Channel transit times of 1.1 - 1.8 years quoted by Jefferies et al (1973) and ~ 1.8 years derived by Livingstone and Bowen (1977). These estimates, however, are based on a model of simple advective flow and on $^{134}Cs/^{137}Cs$ ratio changes in transit. It is clear from this work that internal mixing within the Irish Sea is an essential consideration and one which significantly modifies values for apparent transit times. The estimates of the other workers are therefore erroneously high.

The internal consistency of the model presented thus far may be checked by comparing the observed North Channel $^{134}Cs/^{137}Cs$ ratio data (Fig 3.10) with the theoretical ratio curve (Fig 3.12) calculated from Windscale output values and using a residence half-time of 12 months decreased by 6 months:

FIGURE 3.12 ANALOGUE 1 BOX MODEL OUTPUT - WINDSCALE RATIO

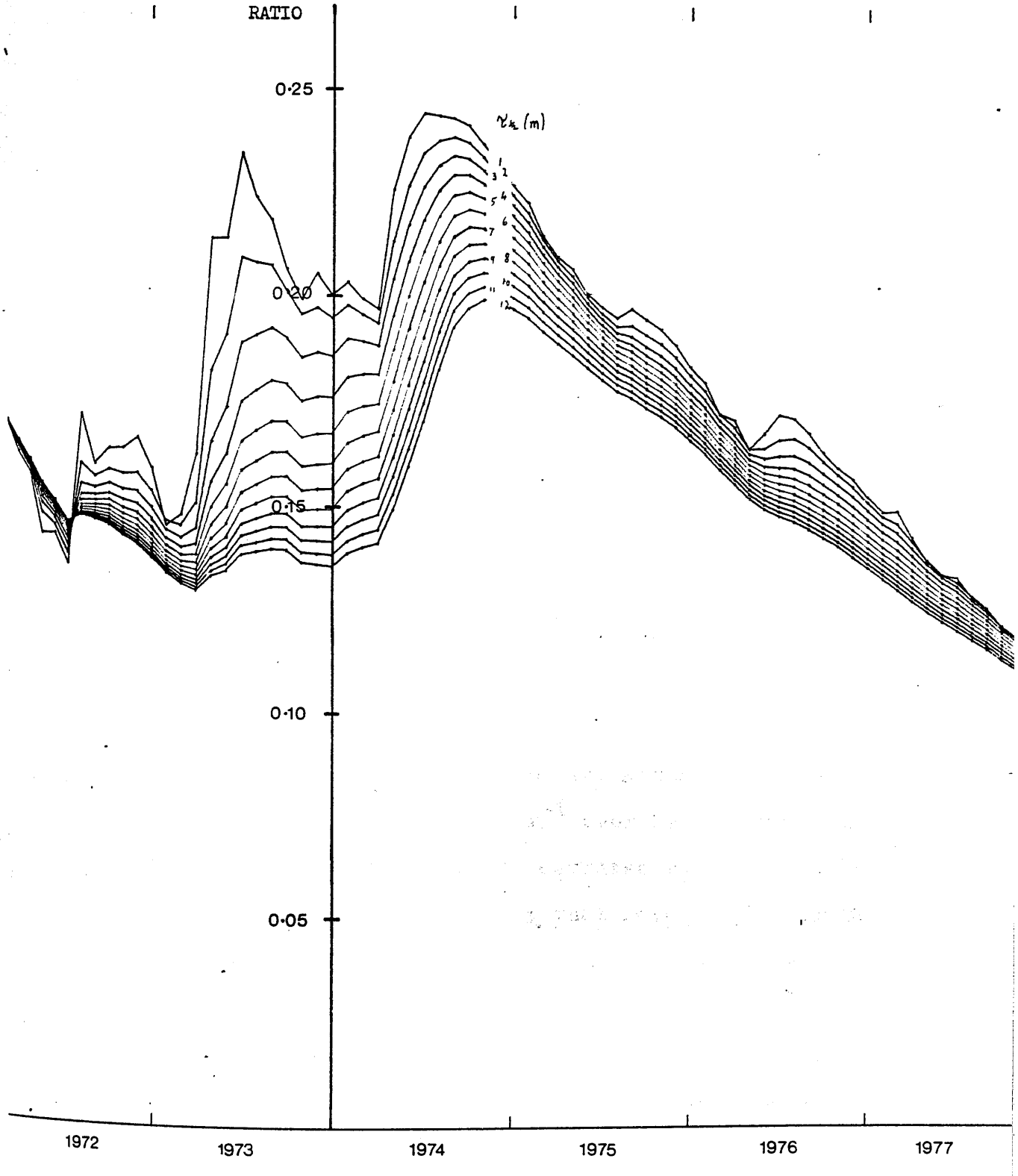

decay. The predicted ratio in the North Channel seems, however, to be markedly lower than predicted values, e.g. 0.154 for January 1976 relative to the observed value of 0.198. It was previously noted that MAFF data for North Channel ratios tended to be $\sim 22\%$ higher than Glasgow University (G.U.) derived values and thus, when this correction is taken into account, the observed value becomes 0.162, in fair agreement with the theoretical model (within 5%). If this modelling process is justified, therefore, indirect intercalibration indicates reasonable agreement in determined $^{134}Cs/^{137}Cs$ ratios between Windscale and G.U. with MAFF-derived values being systematically high by $\sim 23\%$. A deviation in ratio measurement between Windscale and MAFF is, indeed, implied by simple comparison of the Windscale release (Fig 3.7) and North Channel raw data (Fig 3.5). For example, even a simple advection model cannot explain the high ratio observed in January 1976 (water with ratio $\gtrsim 0.22$ being released only before 1975 and is thus decreased by decay to ~ 0.17). More generally, the MAFF ratio curve for the North Channel shows a regular decrease of ~ -0.044 year^{-1} over 1976 which is more negative than the Windscale ratio decrease rate of ~ -0.041 year^{-1} since 1974 despite the fact that both mixing and decay during transport would increase this gradient (i.e. make it more negative).

From the Windscale/N.C. curve match, an Environmental Appearance of ^{137}Cs in the North Channel may be calculated (after Dutton (1978)). The Environmental Appearance (E_A) of any waste radionuclide may be defined as the resultant water activity of that species (pCi l^{-1}) at a particular site per unit discharge (Ci day^{-1}). This parameter is more useful

than a dilution factor as it does not require data on the radionuclide concentration of the release stream. It does, however, require phase matching of measured and output values for exact calculation in any non-steady-state system. For the N.C. site an E_A for Windscale ^{137}Cs of ~ 0.25 pCi l^{-1}/ Ci day^{-1} is readily determined by comparison of modelled release and observed concentrations (Fig 3.11). This value may be compared with an E_A for ^{137}Cs of 5 pCi l^{-1}/Ci day^{-1} in the vicinity of the Windscale discharge pipe (Dutton, 1978), implying a dilution of $\sim$ x 20 during transport.

Taking both the systematic error between Windscale and MAFF values and radioactive decay during transport into account, there is agreement between the predicted and observed ratio curves over the entire period considered (Jan 1976 - Dec 1977), and between ^{137}Cs curves over the period Jan 1973 - Dec 1976. A very marked difference, however, exists in the ^{137}Cs curves over 1977 (Fig 3.11). The observed large decrease in ^{137}Cs activity in the N.C. in 1977 cannot be explained by any concommitant change in Windscale output and thus must be due to increased dilution of North Channel radiocaesium by 'uncontaminated' water. Rapid dilution of ^{137}Cs concentration by influx of Atlantic-derived water would explain the lack of perturbation of the ratio curve as this parameter is independent of dilution. From the data presented so far it is impossible to determine if this Atlantic incursion is from south through the St. George's Channel or from the north through the North Channel but measurements of radiocaesium in the Hebridean Sea Area prove the former to be the case (cf Chapter 5).

So far investigation of mixing in the north Irish Sea has been restricted to consideration of a single mixing box model but the digital computer program used may readily be expanded to a two-box model (or any higher level system) by simply nesting 'do-loops' (Appendix II.2). The families of curves obtained for predicted ^{137}Cs and $^{134}Cs/^{137}Cs$ ratio (e.g. Fig 3.13) show the same general trend as one-box curves but are extensively smoothed allowing systems involving long residence times in both boxes ($\gtrsim$ 6 months) to be completely discarded. As it is difficult to compare, in a quantitative sense, the curve match of one- and two-box models with the observed curves, due to varying curve smoothness, and, as no quantitatively better fit is observed with the two-box model, by Occam's Razor a one-box model is considered sufficient in this case.

Having considered, therefore, the origin of the variations in radiocaesium concentration at the North Channel site, these latter values may be compared with the observed temporal variation of radiocaesium in the Clyde Sea Area. As might be expected, the N.C. radiocaesium curves (Fig 3.5) show more similarity to the C.S.A. curves (Fig 3.4) than do the Windscale output curves (Fig 3.7), a similarity emphasised by consideration of the 3-month running mean smoothed N.C. curves (Fig 3.10). In the previous section it was considered reasonable to regard the Clyde Sea as a single well-mixed box and thus the process of North Channel water mixing into the C.S.A. may be reproduced by the analogue box-model discussed above. The predicted ^{137}Cs curves from this model show good agreement for residence half-times of 1 - 3 months. Longer times can be discarded both on the grounds of the excessive

FIGURE 3.13 ANALOGUE 2 BOX MODEL OUTPUT

a) WINDSCALE Cs-137

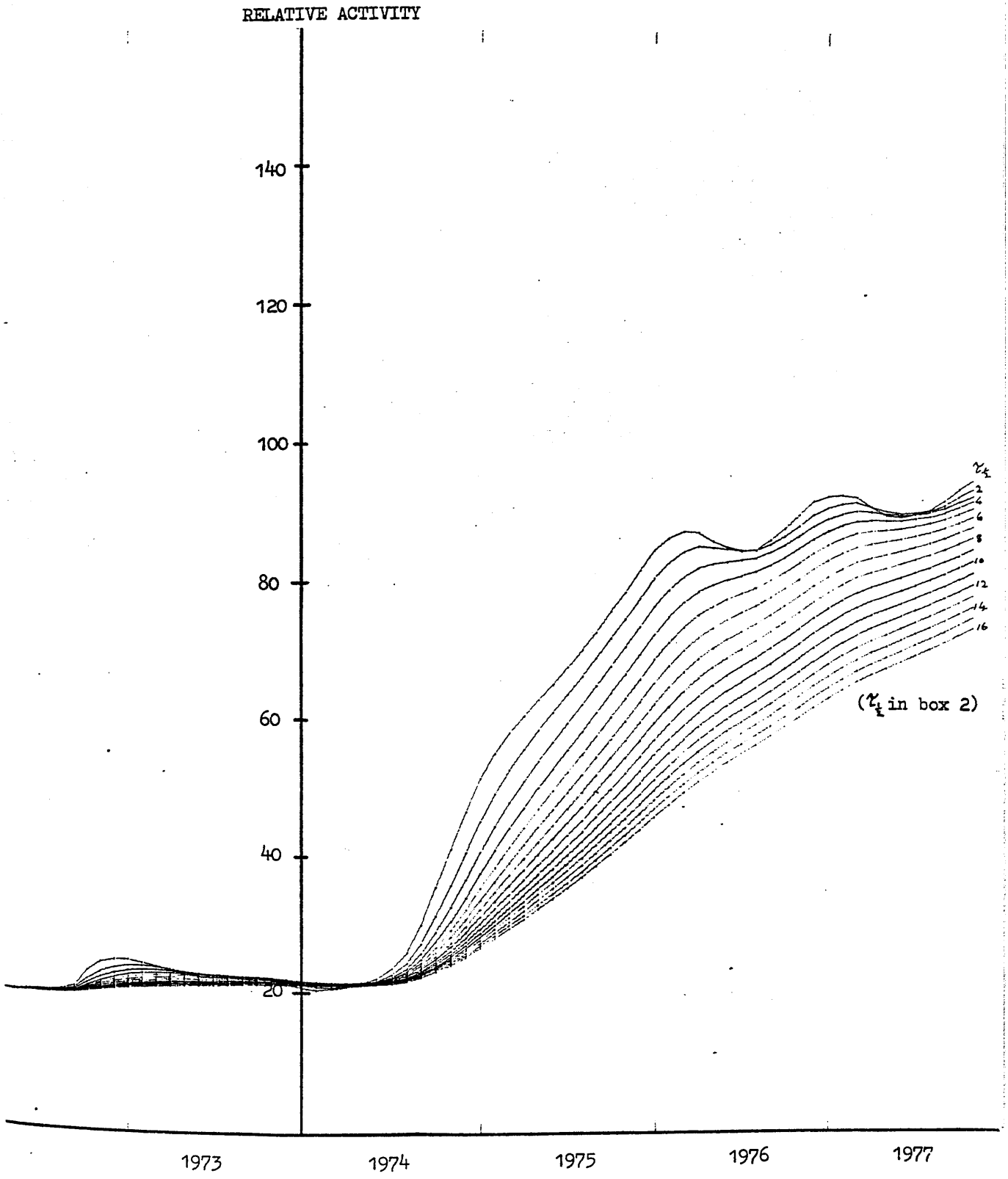

(Residence half-time in box 1 = 1 month)

FIGURE 3.13

b) WINDSCALE RATIO

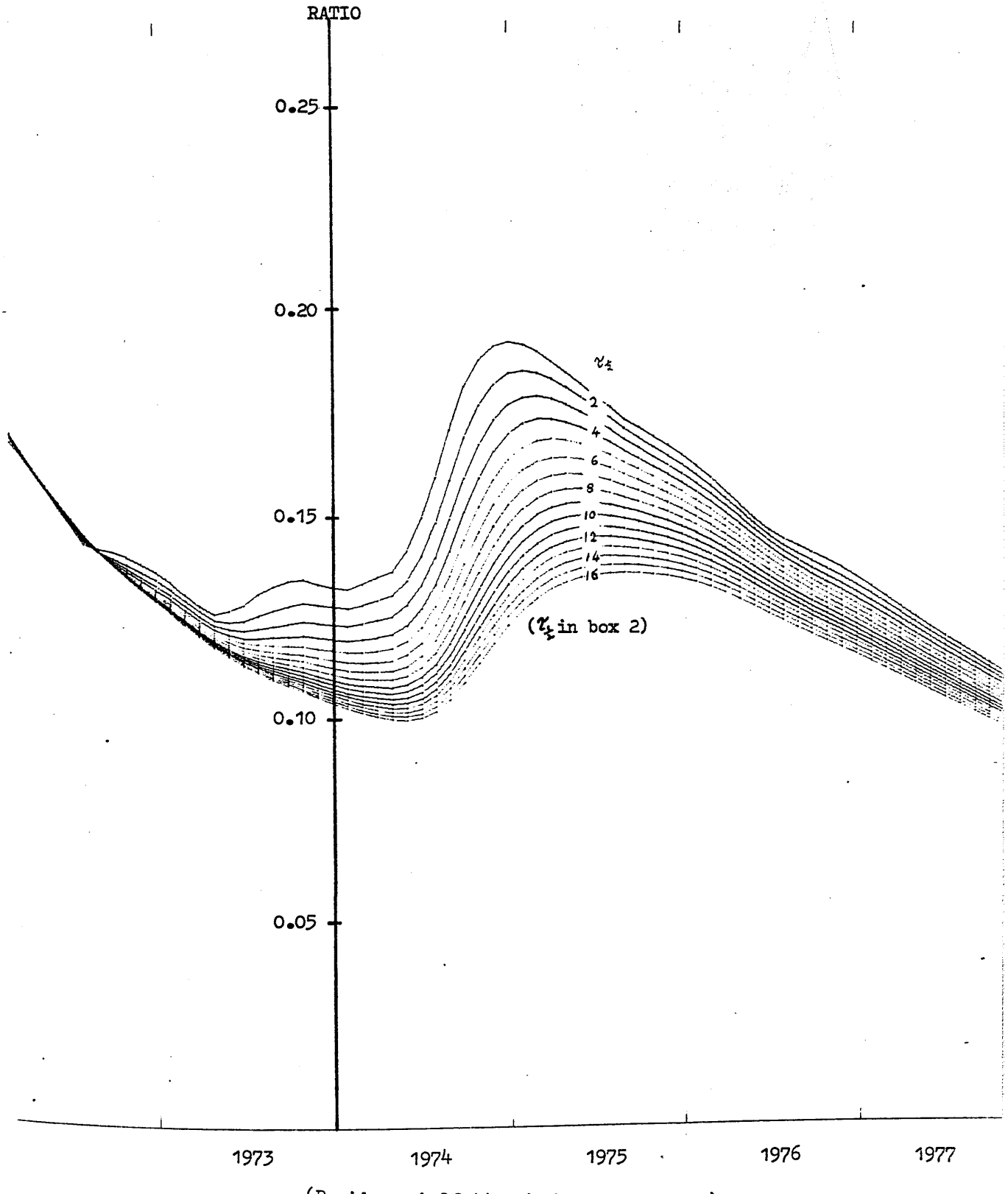

(Residence half-time in box 1 = 1 month)

FIGURE 3.14 ANALOGUE 1 BOX MODEL OUTPUT - N.C. Cs-137

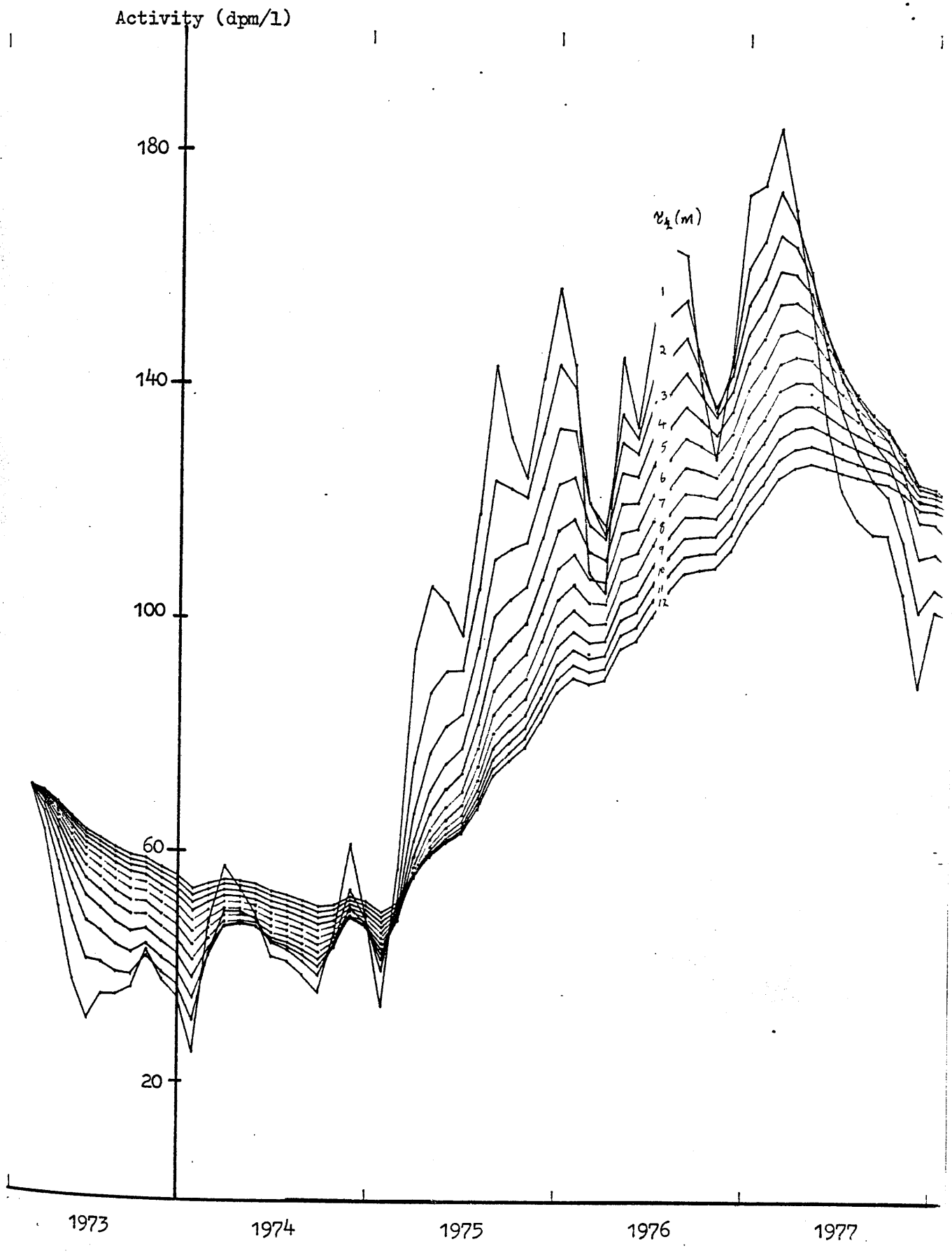

smoothing resulting from these values and from comparison of the magnitude of predicted and observed curve peaks when C.S.A. values are corrected to North Channel salinity (taken as 34%). The model may again be examined for internal consistency by using the mixing box to predict the $^{134}Cs/^{137}Cs$ ratio over the period which, for $\gamma_{\frac{1}{2}}$ = 1 - 3 months, shows remarkably good agreement with observed values when the inter-calibration constant is taken into account. Consideration of both ^{137}Cs and ratio results in a best match for $\gamma_{\frac{1}{2}}$ = 2 months (Fig 3.15) which shows excellent agreement between predicted and observed values, especially as peaks in these parameters in both the N.C. and C.S.A. tend to be very sharp and thus differences of a few weeks in the date of sample collection could considerably affect the observed value. This match is obtained by introducing a lag-time of 2 months between the North Channel and Clyde Sea Area which represents the transit-time between the two sites. Agreement between observed and predicted absolute concentrations of ^{137}Cs, especially between autumn 1976 and winter 1977, indicates very little dilution between the North Channel and the Clyde Sea and implies that any mixing between 'Irish Sea' and 'Atlantic' derived waters occurs in the North Channel itself. Thus there is no evidence of significant 'direct incursion' of Atlantic water into the C.S.A., any contribution of salt water from this source being $\ll$5%. The slightly poorer match during summer 1976 and early 1978 could be interpreted as the result of increased direct Atlantic incursion at these times but, equally well, these deviations could be caused by a slight ($\sim$1 month) increase in the residence half-time of the area. As temporary, small changes in residence time in the

FIGURE 3.15 COMPARISON OF OBSERVED AND MODELLED CURVES

- CLYDE SEA AREA

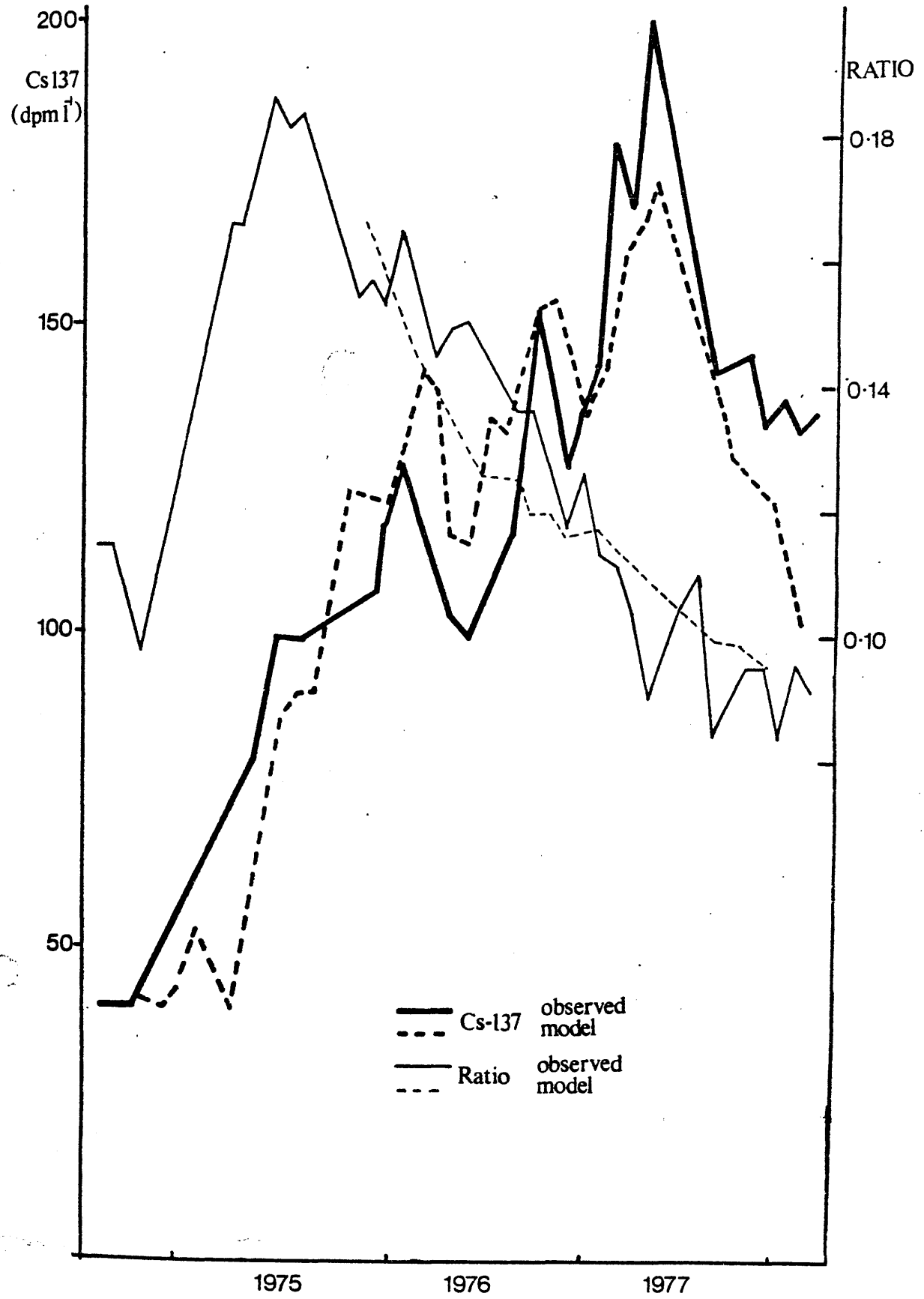

C.S.A. are not detectable because of the inherent lack of resolution caused by the sampling frequency, it is impossible to distinguish between these alternatives. This low temporal resolution also precludes examination of the coupling of N.C. flow to C.S.A. exchange as any change caused by the very large increase in N.C. flow between 1976 and 1977 is below the limit of detection in this study.

As dilution is insignificant between the North Channel and the Clyde Sea Area, the E_A of ^{137}Cs is again $\sim$ 0.25 pCi l^{-1}/ Ci day^{-1} in this region. Taking the volume of the C.S.A. as 1.65×10^{14} l (Cambray et al, 1975), the daily outflow from the area for $\tau_{\frac{1}{2}}$ = 3 months (as an upper estimate) is 1.27×10^{12} l day^{-1} and the net ^{137}Cs release from the area is thus 3.18×10^{11} pCi/Ci day^{-1}, i.e. $\sim$32% of the Windscale radiocaesium passes through the C.S.A. (as a minimum value). For a more likely $\tau_{\frac{1}{2}}$ = 2 months, the implied output passing through the C.S.A. is 47%. As a one month residence half-time requires 95% of Windscale radiocaesium to pass through the C.S.A., this value may be regarded as a lower limit of residence in the area.

3.4 Summary

The main results of this study of the Clyde Sea Area are:-

1) The C.S.A. approximates to a spatially homogeneous system, surface waters being very rapidly mixed throughout the area. The limited vertical structure observed is explicable in terms of short-term mixing processes. Significant entrainment of deep water seems to occur only in the Northern

Sea Lochs.

2) Consideration of the C.S.A. as a well-mixed reservoir enables the observed temporal variations in radiocaesium activity to be explained by input of North Channel water into a system with an average residence half-time of ~2 months (corresponding to an average water residence time of ~3 months), further implying that 30 - 50% of the total Windscale radiocaesium output passes through the C.S.A.

In addition, the observed N.C. radiocaesium variations may be explained by Windscale output mixing in the north Irish Sea with an average residence half-time of ~12 months and advection to the N.C. with a transport time of ~6 months over the period 1973-76 with a sudden, rapid flushing process occurring in 1977. Indirect intercalibration suggests agreement between $^{134}Cs/^{137}Cs$ ratio measurement at Windscale and Glasgow with MAFF values being systematically high by ~23%. These residence and transit times, evaluated by an analogue mixing model, represent average values over several years of study.

The data obtained by this treatment are obviously useful in many oceanographic and environmental studies. For example, a residence half-time of 2 months implies a salt-water input to the area of 1.92×10^{12} l day^{-1} which is vastly greater than the freshwater flow of 9.46×10^{6} l day^{-1} (MacKenzie, 1977). On a quantitative level, this fact together with the large percentage of Windscale output passing through the area emphasises the susceptibility of the C.S.A. to soluble pollutants introduced at distance into the Irish Sea, in agreement with the trace metal studies of Cambray et al

(1975). Further applications of the derived data and investigations of the radiological significance of the radiocaesium data will be considered in Chapter 7.

Chapter 4

The Northern Sea Lochs

4.1 Introduction

The northern sea lochs of the Clyde Sea Area occupy a series of trenches formed by glacial scouring during the Pleistocene age (Deegan, 1974). From west to east these comprise L. Fyne, L. Riddan/Kyles of Bute, L. Striven, Holy Loch, L. Long and Gareloch (Fig 4.1). Although a number of indentations in L. Fyne are named separately (East L. Tarbet, L. Gilp, Lochgair and L. Shira), these minor embayments will not be considered in this study. The bathymetrics of the lochs vary greatly; Gareloch, L. Goil, upper L. Fyne and, to a lesser extent, L. Long, are sill-protected, deep fjords, while lower L. Fyne is an extension of the N.E. Arran trench system (cf Chapter 3); Holy Loch is a simple extended embayment and the L. Riddan/L. Striven/Kyles of Bute system is a complex of glacial trenches extending to the deep waters of the Arran Basin (Mill, 1892; MacKenzie, 1977).

Major emphasis in this study has been on investigating water mixing processes within L. Goil and has involved regular monthly sampling of vertical water profiles in Lochs Goil and Long. The choice of L. Goil as the focus for this particular study resulted from 1) the ill-defined nature of water processes occurring within this loch with some preliminary evidence for water retention, 2) its importance with respect to naval, forestry, fisheries and recreational activity,

FIGURE 4.1 MAP OF THE NORTHERN SEA LOCHS

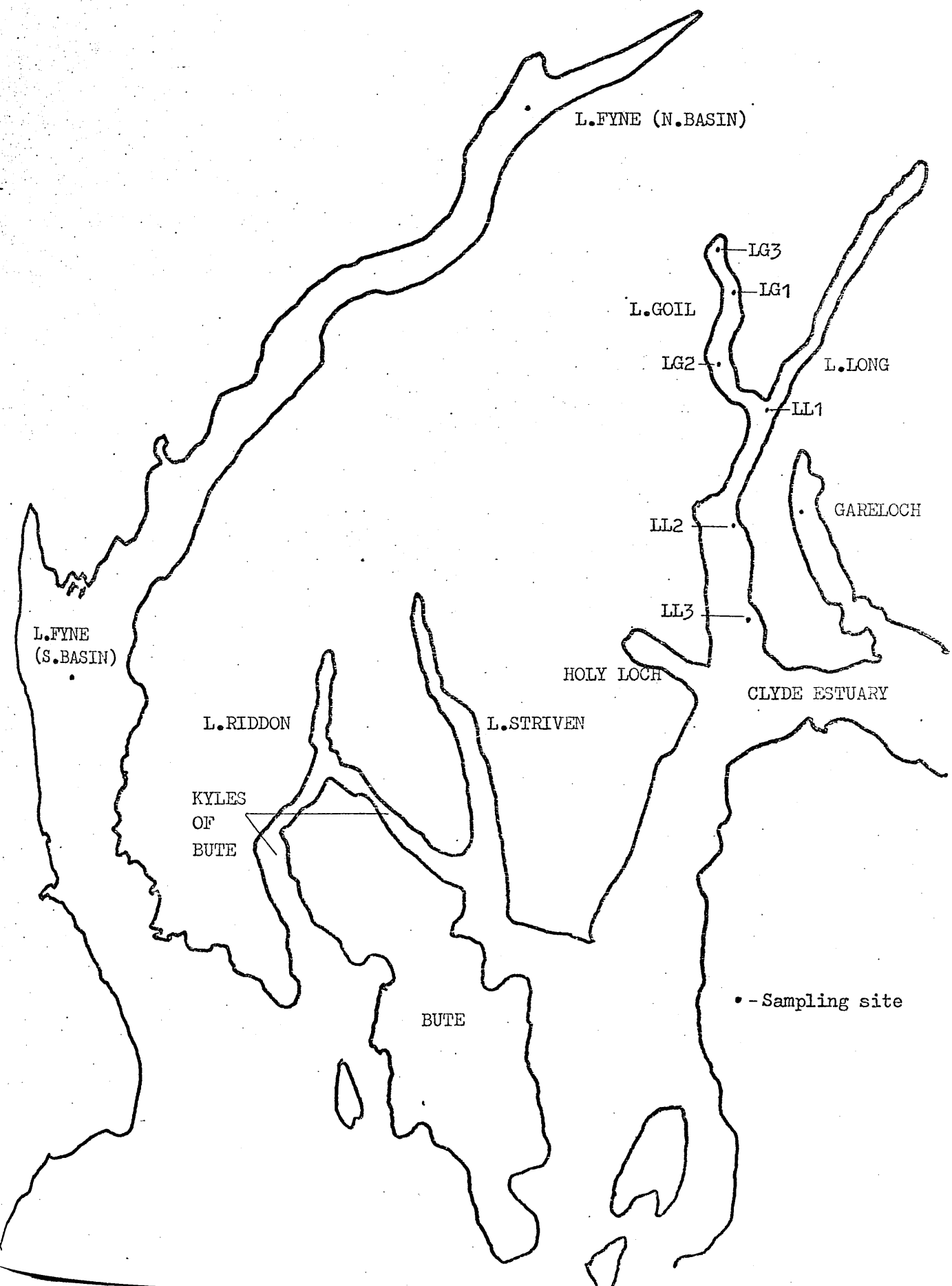

3) its environmental susceptibility to pollution from these sources, the Clydeside industrial conurbation and the nearby Finnart oil-terminal, 4) the general background of radionuclide data provided by recent studies of this area (e.g. MacKenzie, 1977; Swan, 1978) and 5) the general oceanographic interest in water renewal processes in fjords. The main sampling sites are in the middle of the deep basin in L. Goil (LG1) and in the deep 'hole' in L. Long opposite the mouth of L. Goil (LL1). Other sites within these lochs were occasionally sampled to examine the homogeneity of these water systems (Fig 4.1). In addition, some samples were obtained from stations in L. Fyne and Gareloch to allow their comparison with L. Goil.

The results of radiocaesium analysis of profiles from L. Goil together with relevant hydrographic data are listed in Appendix I.2, while data for all other sea lochs considered are listed in Appendix I.3 .

4.2 Qualitative description of mixing in L. Goil

At a qualitative level, water transport processes in L. Goil may be examined via monthly depth profiles of ^{137}Cs concentration at the L.G.1 site.

The extent to which profiles from the L. Goil deep site (LG1) are representative of the entire loch may be determined by comparing vertical profiles at 3 widely separated sites in the loch (Fig 4.2). Taking the errors associated with the measurement process into account, the 3 profiles may each be regarded as demonstrating effectively constant ^{137}Cs concentrations with depth ($\sim$ 103 dpm l^{-1}) when corrected for

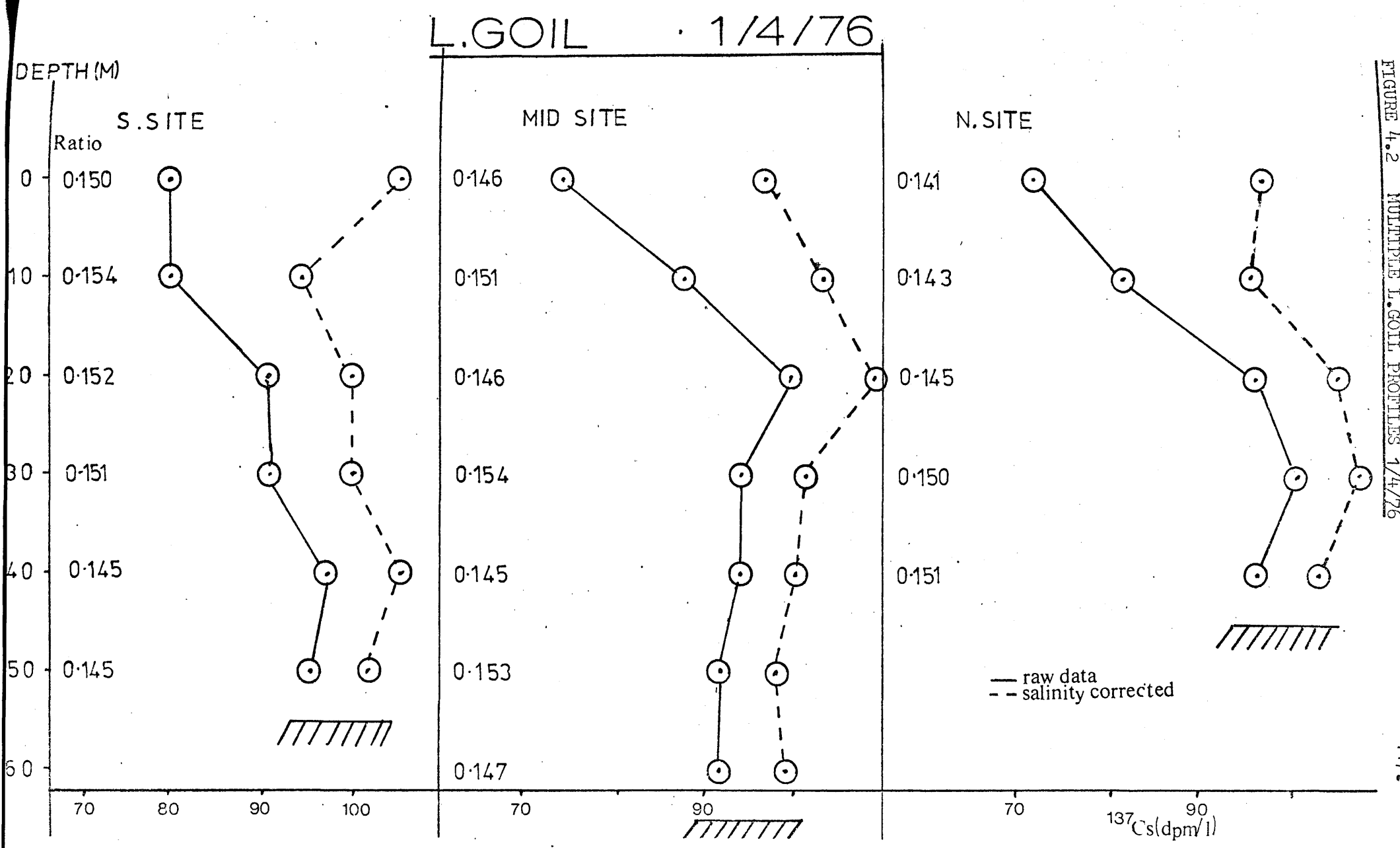

FIGURE 4.2 MULTIPLE L.GOIL PROFILES 1/4/76

fresh water dilution effects. While there is an apparent systematic variation in $^{134}Cs/^{137}Cs$ ratio along the loch, the ratio averages to 0.148 ± 0.004, ie shows a variation of 2.7% which is comparable to that expected from experimental error alone. The general validity of the above finding of horizontal homogeneity may be checked by comparing profiles obtained over a four month period at the LG1 site (Fig 4.3) with those obtained at the southerly LG2 site (Fig 4.4). Direct comparison both of profiles for particular dates and of trends between sampling dates shows remarkable similarity at these sites. The major difference between sites is in surface ($<10m$) ^{137}Cs values, which may be explained as follows. Surface ^{137}Cs concentrations have been shown to be fairly homogeneous throughout the entire C.S.A. through fast tide and wind-driven mixing (Chapter 3). Thus surface waters from the southern L. Goil site would be expected to exchange rapidly with those in L. Long. In times of high fresh water flow, however, as the major fresh input is at the head of the loch, pooling of this less-dense fresh water in the northern reaches of the loch may present a barrier to surface mixing. This process, coupled to the effects of estuary-type circulation, may cause the observed variations in surface ^{137}Cs concentrations. This explanation accounts for the observation that the main difference between sites is effectively restricted to surface waters, as fresh flow (averaging 6.7×10^8 l day^{-1}) is small relative to the total volume of the loch (3.1×10^{11} l) and is of more comparable magnitude tothe average tidal influx (3.4×10^{10} l low-high tide). Thus the total effect of the process on calculated inventories will probably be negligible.

FIGURE 4.3 WINTER 1975/76

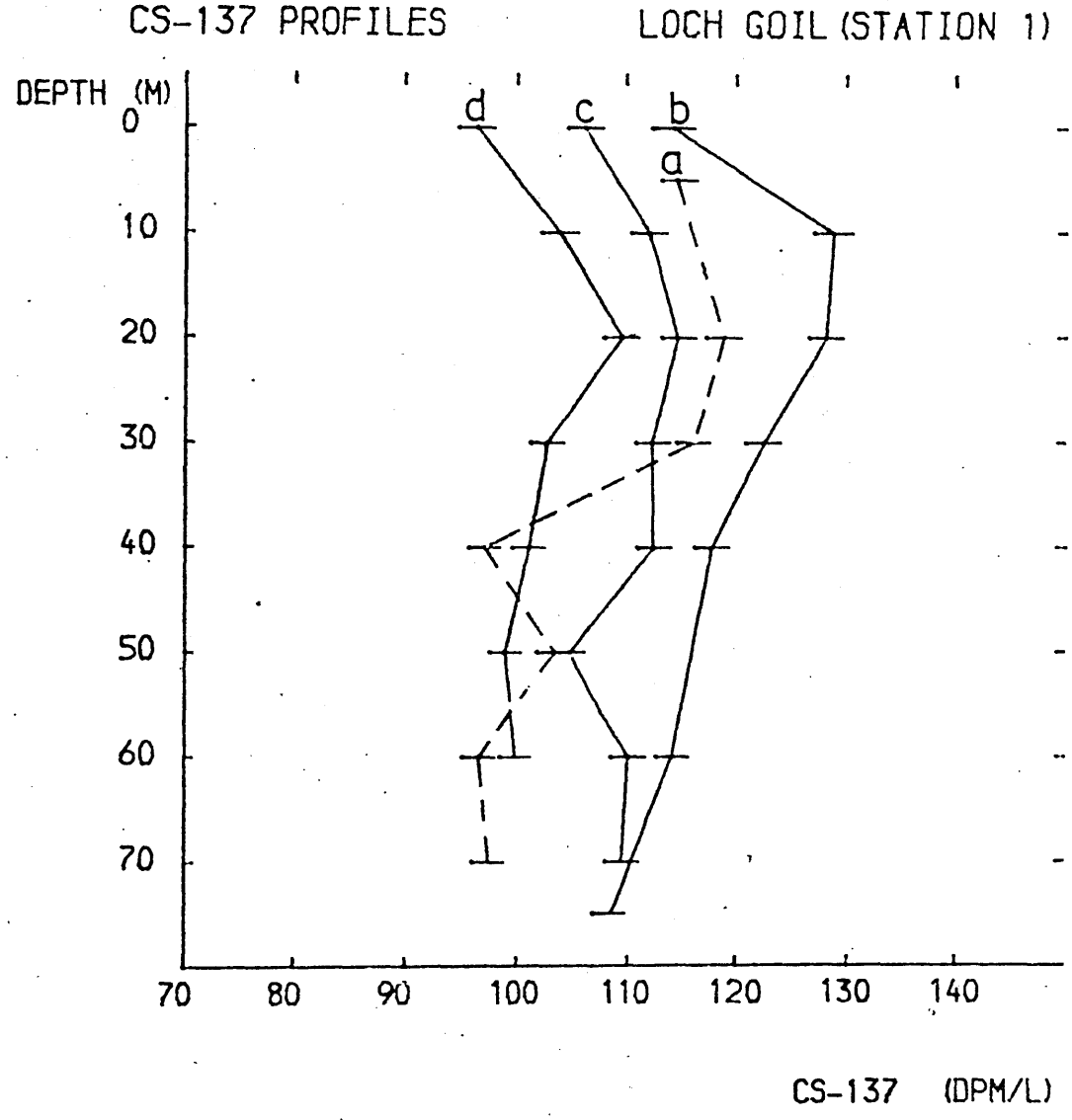

a 4/12/75
b 8/1/76
c 3/3/76
d 1/4/76

FIGURE 4.4 SALINITY CORRECTED Cs-137 PROFILES - LOCH GOIL STN.2

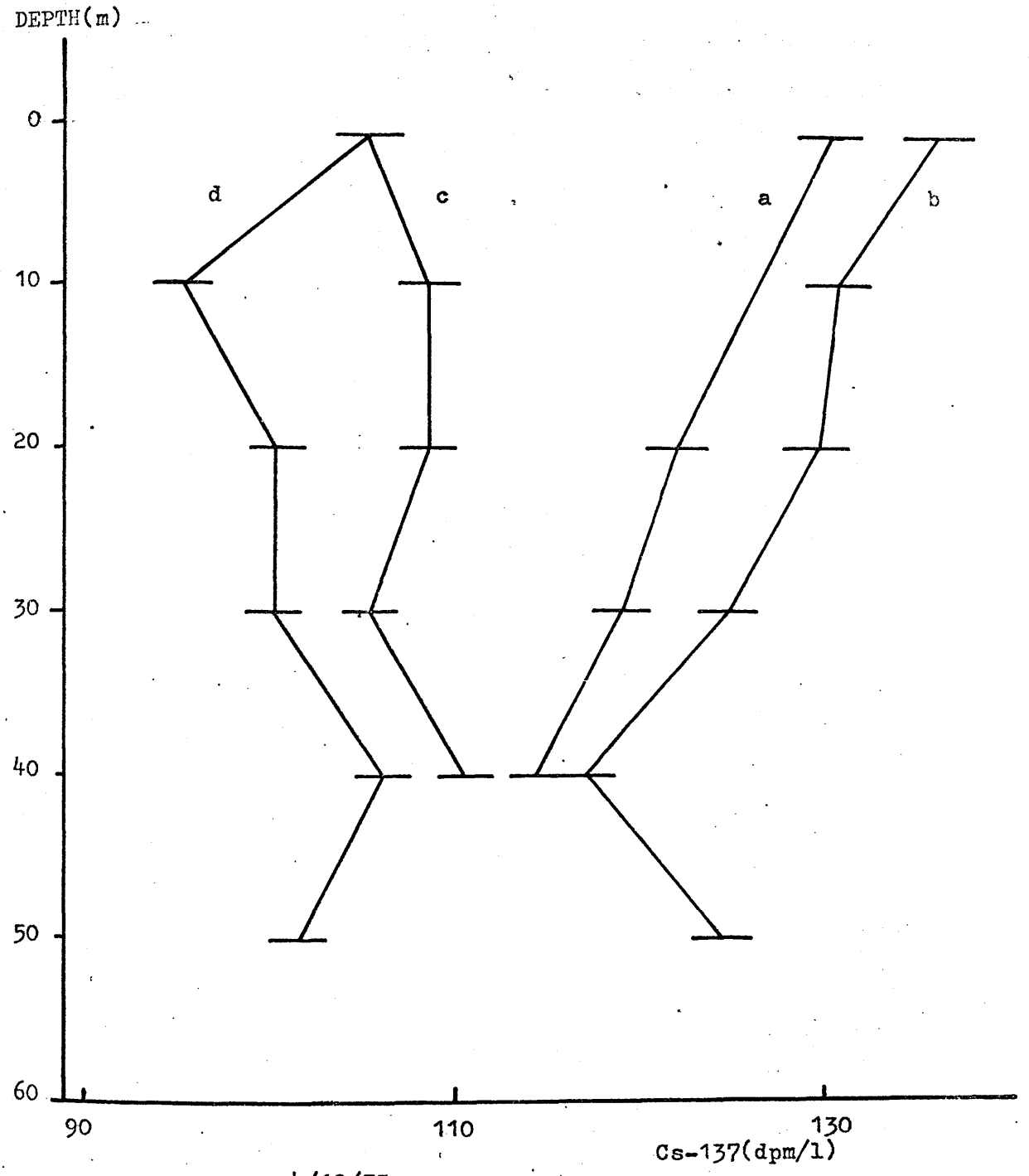

a - 4/12/75
b - 8/1/76
c - 3/3/76
d - 1/4/75

On this basis, study of monthly variations in the ^{137}Cs profiles in L. Goil caused by fluctuations in radiocaesium concentration in the Clyde Sea Area (cf Chapter 3) enables mixing within the loch to be followed through two annual cycles. Because of the excessive data involved and the need to minimise grammatical repetition of qualitative descriptions, the results are summarised using an abbreviated format as follows, with reference to Figures 4.3 and 4.5 - 4.10.

a) December 1975 - stratified profile with significant difference between surface ($\lesssim$30m) and deep ($\gtrsim$40m) water bodies.

b) January 1976 - less structured profile with total increase in integrated water activity of ~15% proving active 'external flushing' over this time period.

c) March 1976 - general decrease throughout water profile continuing through April indicating continuous fast flushing.

d) May 1976 - little change although slight indication of vertical differentiation of ^{137}Cs profile which intensifies over August and September due to marked increase in surface concentrations. General profile increases between May and September indicate dynamic water behaviour over this period of dissolved oxygen stratification (cf Chapter 1.4). By September, surface ($\lesssim$30m) ^{137}Cs concentrations are ~30% greater than those at depth.

e) December 1976 - vertical stratification intensifies and deepens till difference in ^{137}Cs concentration between 40m and 50m is $\sim$ 40%.

f) January 1977 - stratification completely destroyed by flushing event. Resultant profile exhibits general increase with depth possibly implicating a mixing process of deep

FIGURE 4.5 SUMMER 1976

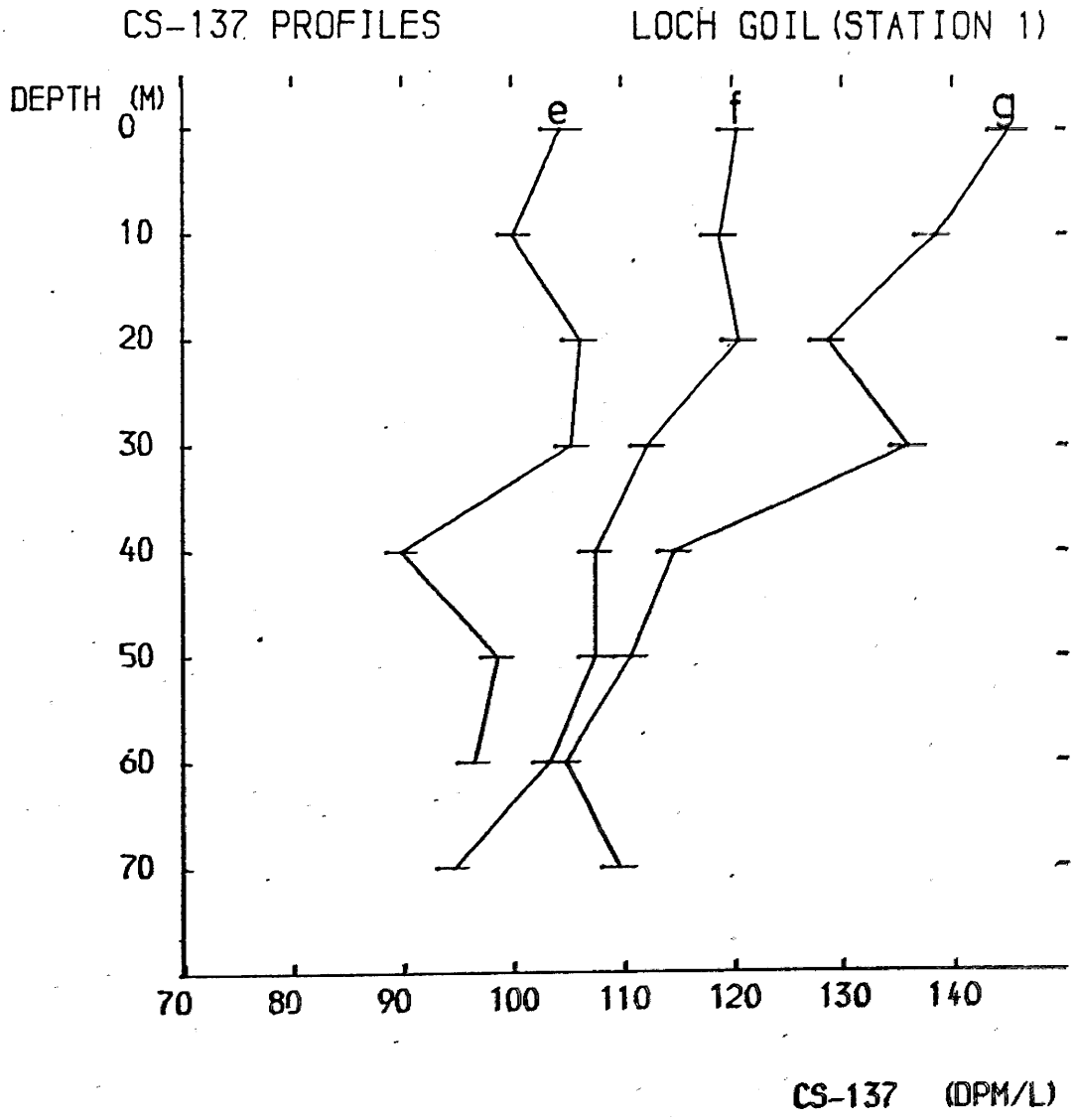

e 31/5/76
f 10/8/76
g 28/9/76

FIGURE 4.6 WINTER 1976/77

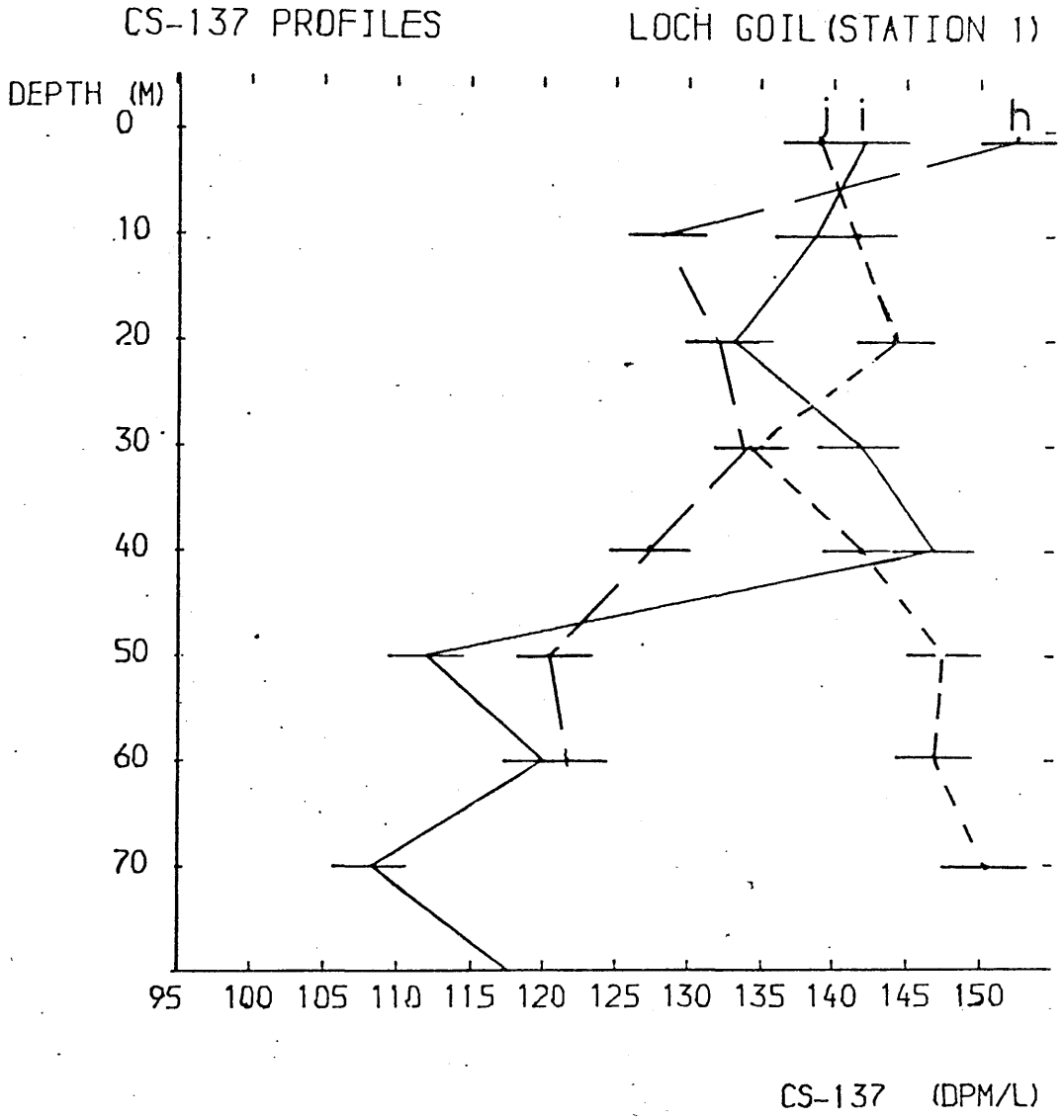

h 22/11/76
i 21/12/76
j 12/1/77

FIGURE 4.7 SPRING 1977

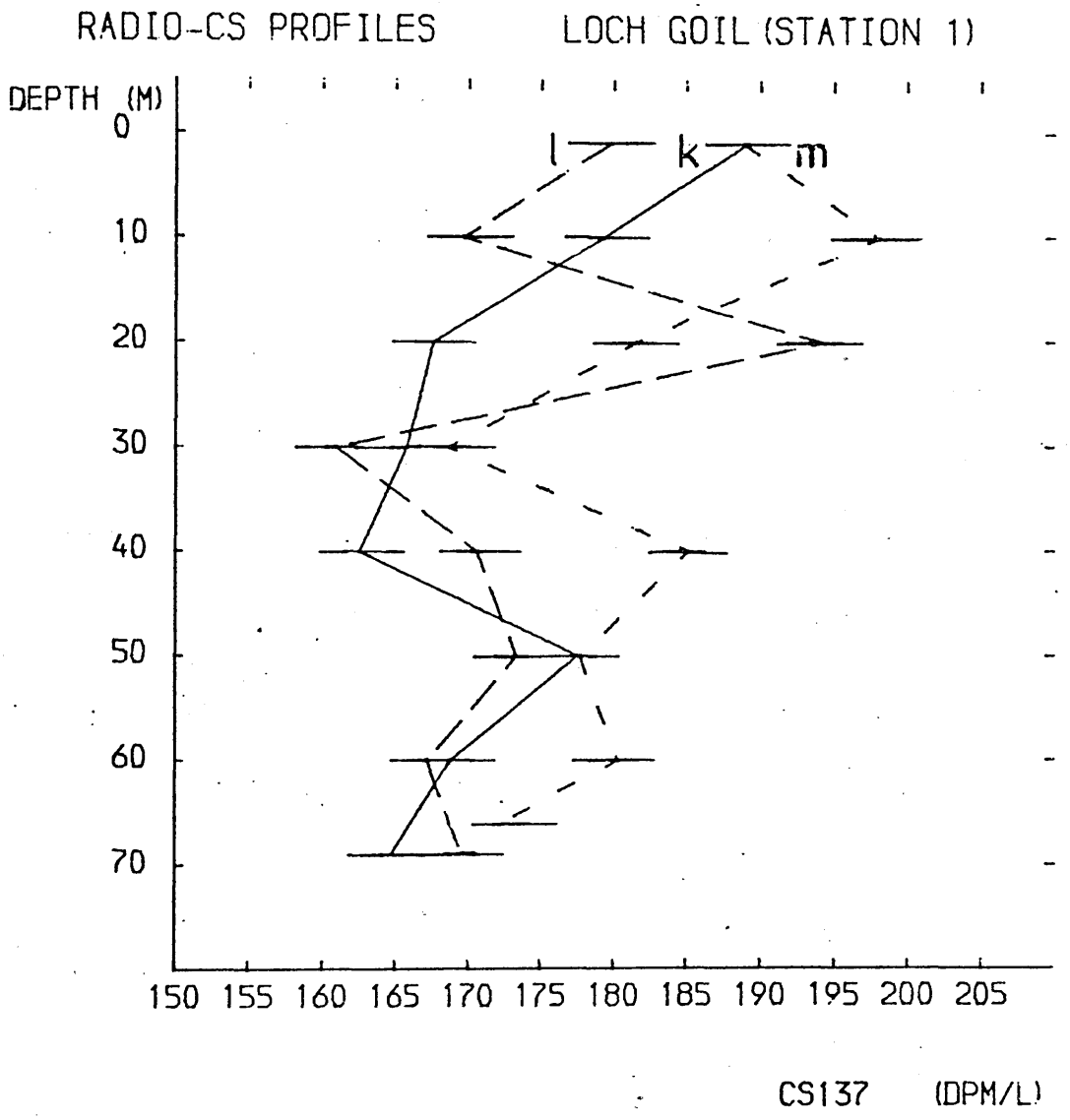

k 17/2/77
l 22/3/77
m 18/4/77

FIGURE 4.8 SUMMER 1977

Cs-137 PROFILES - L.GOIL(SEH.1)

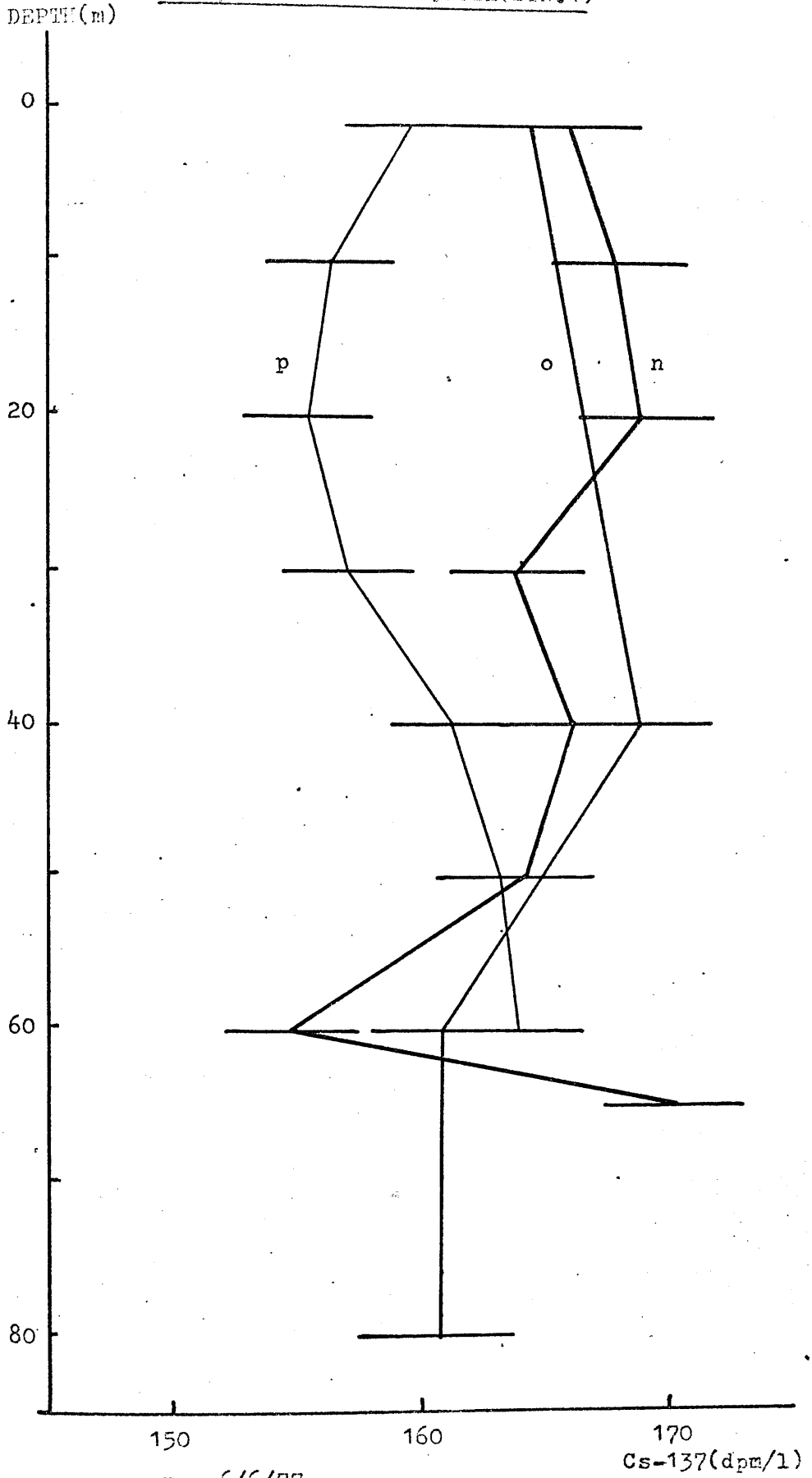

n - 6/6/77

o - 28/6/77

p - 19/7/77

FIGURE 4.9 AUTUMN 1977

Cs-137 PROFILES - L.GOIL(STN1)

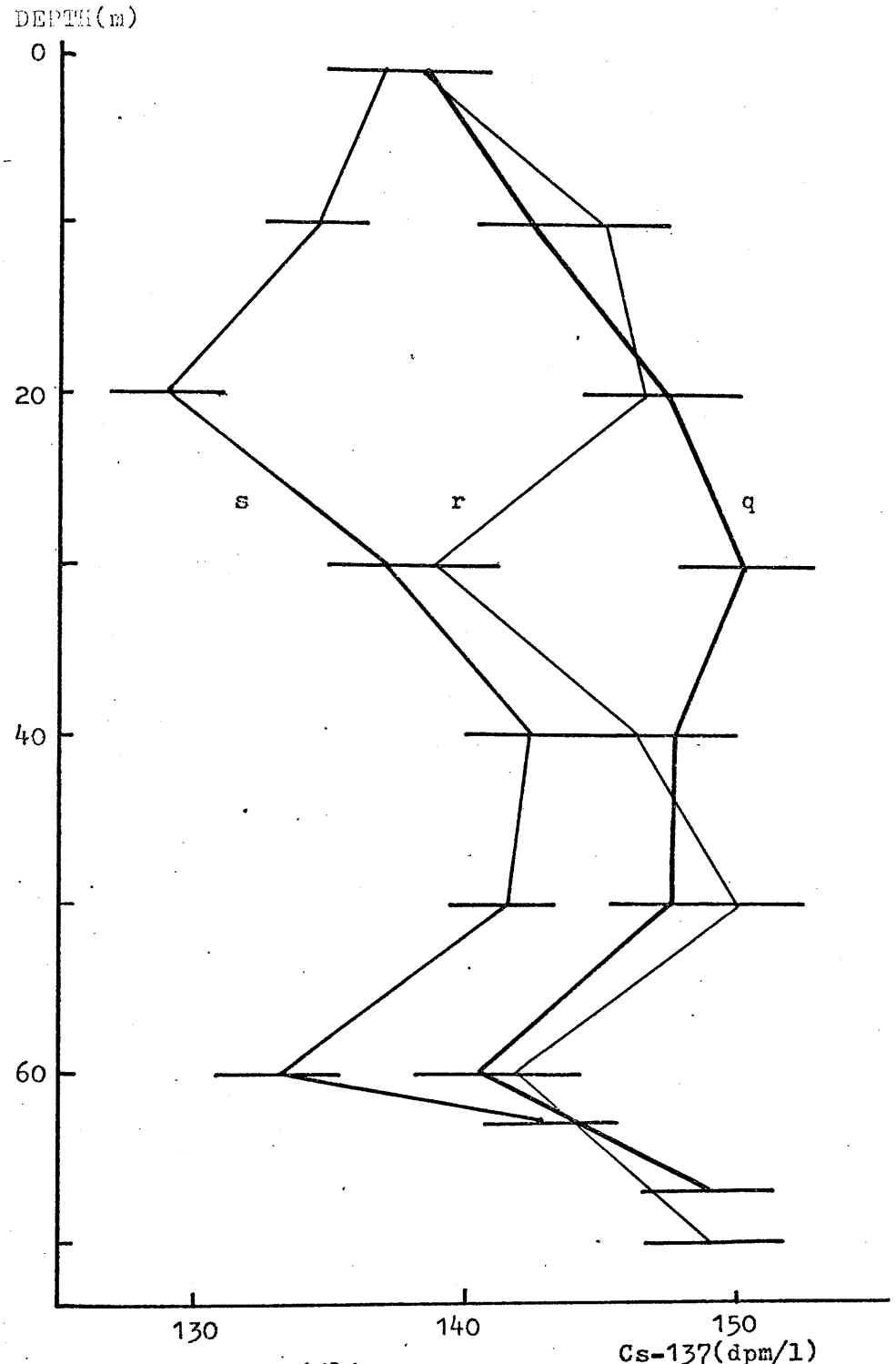

q - 16/8/77

r - 11/10/77

s - 15/11/77

FIGURE 4.10 WINTER 1977/78

Cs-137 PROFILES - L.SOIL(3.71)

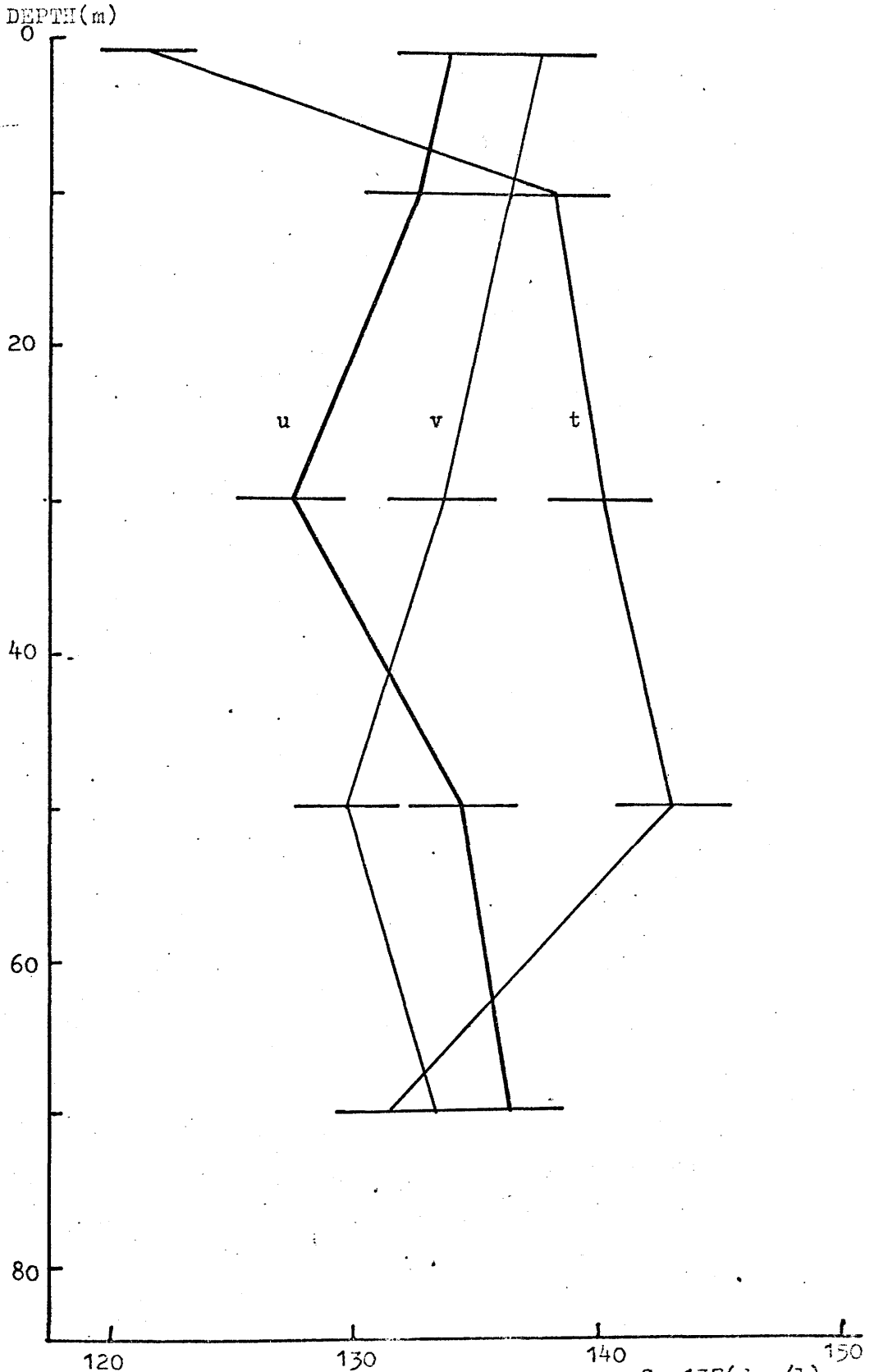

t - 28/12/77
u - 17/1/78
v - 21/2/78

water incursion followed by upwards mixing.

g) February 1977 - noticable increase in ^{137}Cs inventory of entire loch (by ~20%) due to rapid flushing with externally-derived water.

h) March 1977 - little change with the exception of development of a distinct maximum at ~20m - possibly reflecting incursion of higher activity water at this depth.

i) April 1977 - general increases throughout profile with maximum ^{137}Cs concentration now at ~20m - probably due to vertical mixing of the previously mentioned high activity influx.

j) June 1977 - both profiles obtained during this month show fairly homogeneous radiocaesium concentrations with values ~12% lower than the April maximum.

k) July 1977 - general decrease in ^{137}Cs concentration throughout profile with indication of decreased exchange at depths below 40m.

l) August 1977 - continued decrease of radiocaesium activity of the water column (by ~15%) demonstrating continuous dynamic behaviour over this period. Minima in ^{137}Cs concentration occur at the surface, as would be expected through fast surface exchange, but also at ~60m (as also observed on 6th June) suggesting possible incursion at this depth.

m) October 1977 - little change except for development of additional minimum at ~30m.

n) November 1977 - significant decrease throughout the entire water column due to external exchange (in comparison to the distinct deep water entrainment observed over this period of the previous year). Decrease is greatest at ~20m and ~60m implying external inflow at these depths followed by vertical

mixing.

o) December 1977 - little change in the total ^{137}Cs content of the loch but definite alteration in profile shape suggesting incursion of lower activity water to give minima at the surface and $\gtrsim$50m.

p) January 1978 - lower activity influx considered above appears to have mixed throughout the water column to give a fairly uniform ^{137}Cs distribution with depth which changes little over the next month.

In such a month by month interpretation of the L. Goil radiocaesium profiles it is difficult to identify the general pattern of mixing implied. To summarise, therefore, the depth variation of radiocaesium in L. Goil over the entire period is most effectively presented as ^{137}Cs isopleths on a depth-time plot (Fig 4.11). In this type of diagram vertical isopleths indicate fast external exchange coupled with thorough internal mixing while horizontal isopleths reflect restricted vertical mixing throughout the water column.

Over the two year period considered, the general behaviour of the loch is characterised by fast surface ($<$30m) exchange at all times with a limited barrier to vertical mixing developing in late spring (March - July), although slow exchange of deep water also occurs during this period. During winter and early spring (Dec - Mar) there is fast mixing and exchange at all depths possibly due to an external flushing mechanism. The main difference between the two years was in behaviour during autumn; in 1976, very extreme stratification was observed to build up over the period Aug - Dec with a marked barrier to mixing at $\sim$40m, while in 1977 fast vertical mixing was evident from July - Sept, followed

FIGURE 4.11 Cs-137 ISOPLETHS - L.GOIL

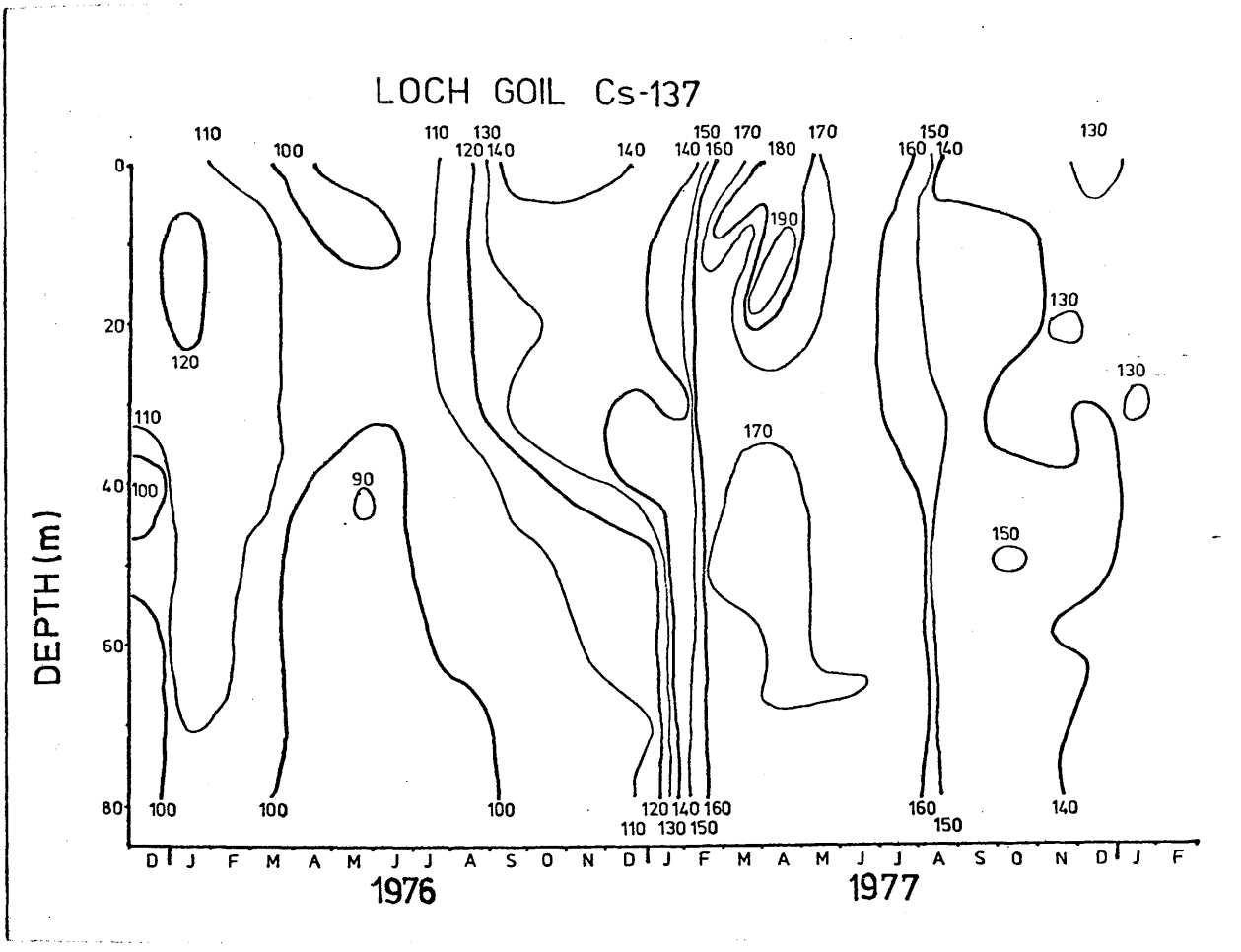

Cs-137 isopleths in dpm/l

by a much more limited degree of stratification. A more quantitative analysis of transport and mixing processes will be developed in the following section.

A previous semi-quantitative study of L. Goil mixing characteristics by MacKenzie (1977) was based almost entirely on radiocaesium (and radium) profiles within the loch itself, but more rigorous expansion of this analysis requires data on the L. Long source water. To allow reasonable consideration of L. Long data it is first necessary to consider the horizontal and vertical homogeneity of L. Long itself.

4.3 Water mixing and transport in L. Long

The spatial homogeneity of L. Long waters was first investigated by measuring radiocaesium concentration at several locations throughout the L. Long/L. Goil system on three successive months (Fig 4.12). From these measurements it is apparent that surface waters are fairly uniform in terms of both salinity-corrected ^{137}Cs concentration and $^{134}Cs/^{137}Cs$ ratio - being within 1σ (experimental) of the mean value at all sites. There are no marked trends across either the length or width of the loch, in agreement with the general fast surface transport found throughout the Clyde Sea Area (cf Chapter 3). At a depth of 25m, however, there appears to be a significant northwards decreasing trend in ^{137}Cs activity, particularly in the eastern half of the loch. This effect, however, may be an artifact caused by a particularly high value observed in Cove Bay, possibly reflecting some localised entrainment of water in this embayment. To examine this apparent horizontal differentiation of L. Long water, two

FIGURE 4.12 SURFACE RADIOCAESIUM IN LOCH LONG/LOCH GOIL

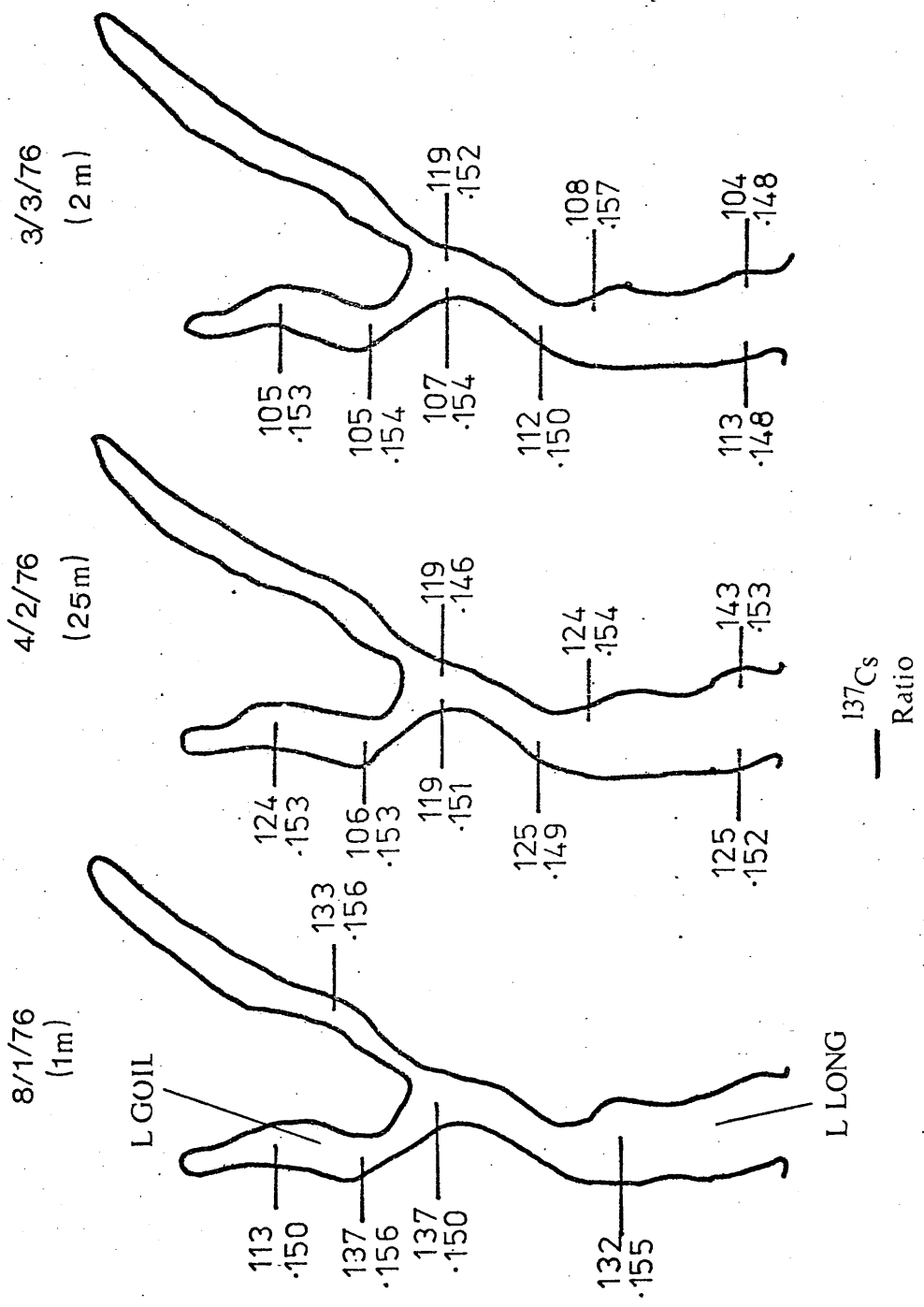

complete profiles from different areas were compared (Fig 4.13). It is immediately obvious that ^{137}Cs concentrations at all depths are greater at the more southerly site, although these differences are within 1σ (experimental) for surface and depths below 40m. The $^{134}Cs/^{137}Cs$ ratio shows very little variation at the north site, the standard deviation of the entire profile being 2.7%, which may be compared to the value of 1.4% expected from experimental errors on a series of 8 measurements. Although the southerly site has a depth average ratio within 0.1% of that at the northern site, these values show a much larger standard deviation of 5.1%. As the trend in both ^{137}Cs concentration and $^{134}Cs/^{137}Cs$ ratio over this time period was a general decrease with time, the observed differences between profiles may be explained by south-north advection of deep water (>30m) with significant upwelling in the northern reaches of the loch, followed by a surface (<30m) return flow. At the southerly station, the ideal profile of two distinct water bodies separated by a sharp discontinuity is disturbed by fast surface layer (<10m) mixing and transport as previously discussed. This model of loch circulation is confirmed by the salinity profiles at these sites (Fig 4.13b). At the north site salinity is almost constant with depth, implying a homogeneous water body, with the exception of a considerably diluted surface layer (<10m) as expected from fresh runoff. At the southerly site, however, low salinities are present to 20m indicating a more extensive but less diluted surface layer. If the major fresh water input occurs north of the L.L.1 site, the loch could be regarded as similar to a 'salt-wedge' estuary (ie type 'A' loch in the classification of Milne (1972)). Considering L. Long as a

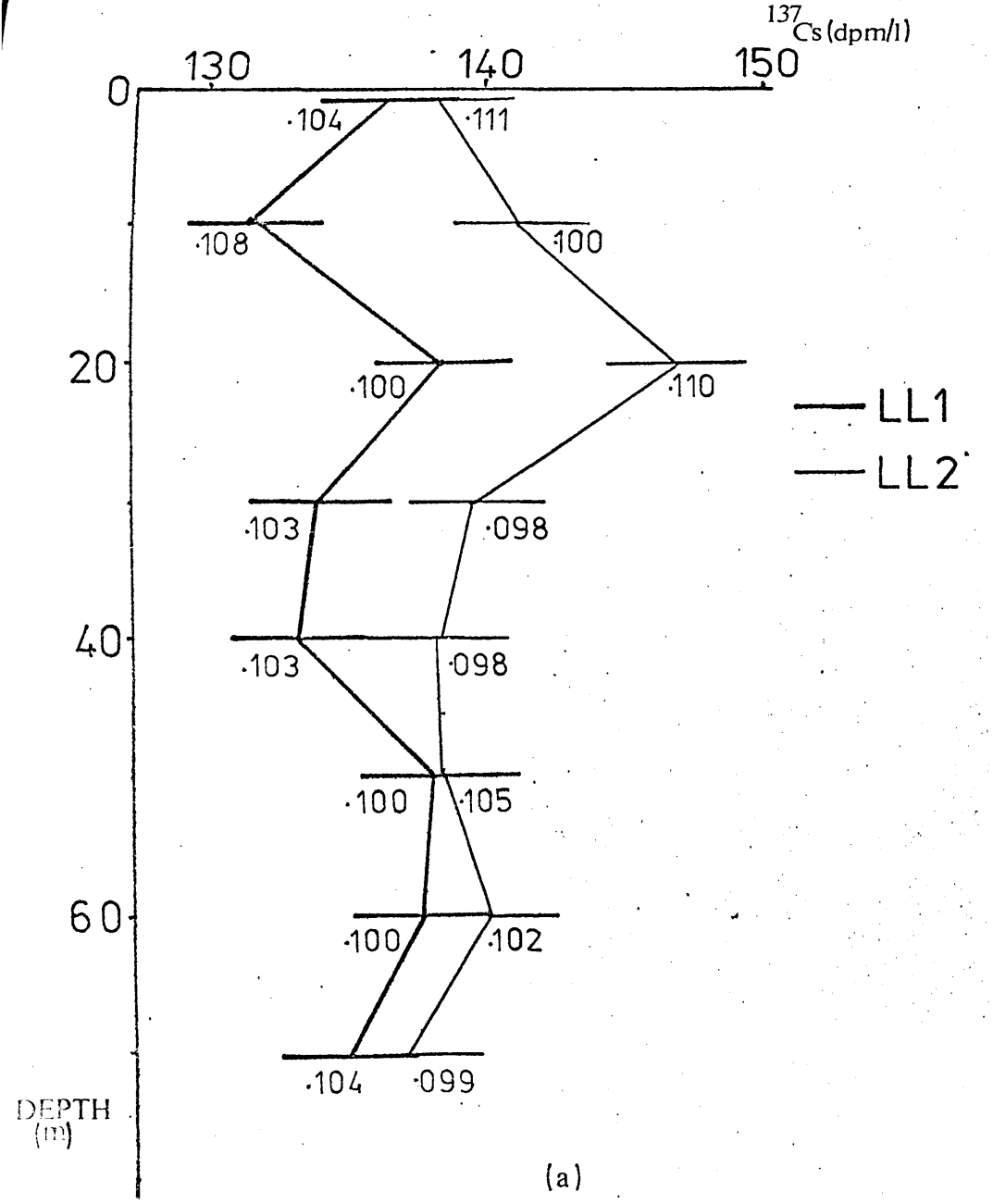

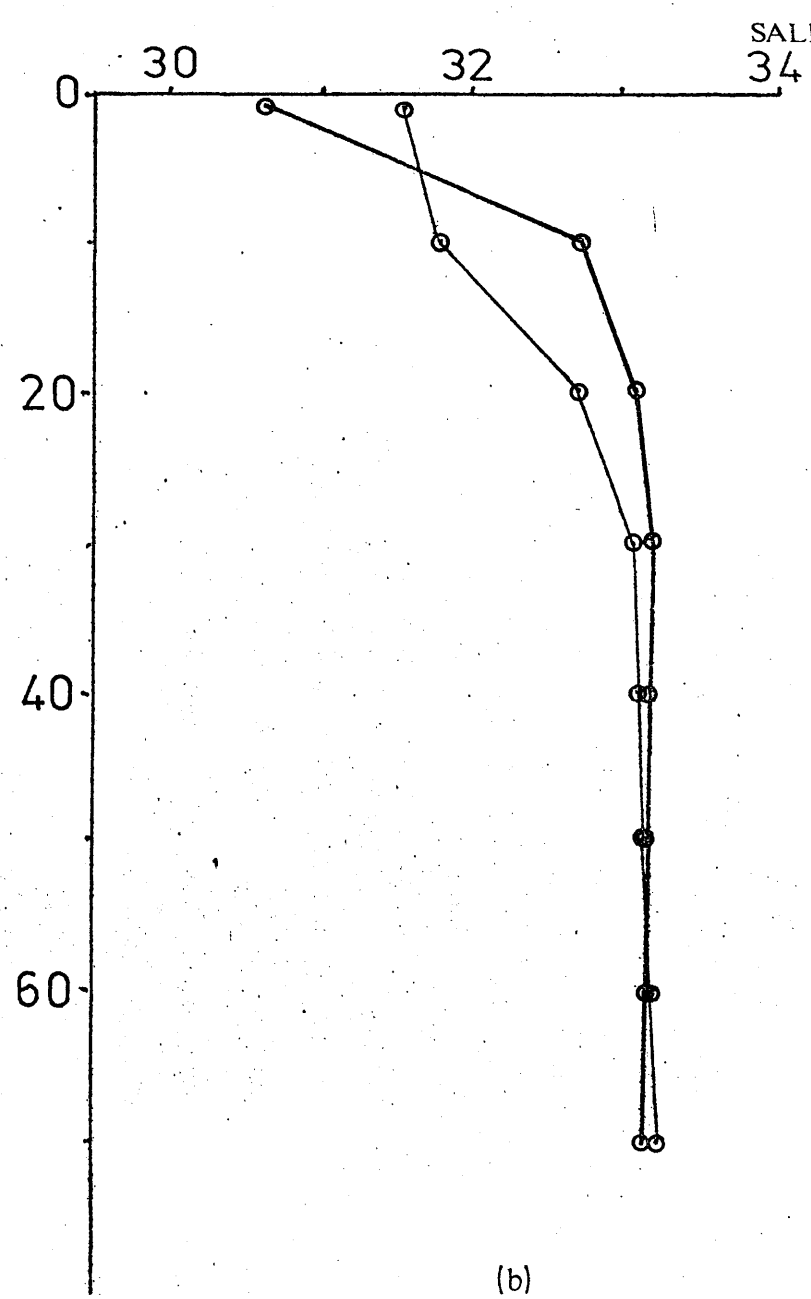

FIGURE 4.13 L.LONG PROFILES (27/9/77)

narrow estuary characterised by surface and bottom salinities (S_1 and S_2 respectively) and flows (F_1 and F_2), with a fresh-water inflow (F) into the head of the loch, the general treatments of Stommel (1953) and Craig (1958) can be applied thus:-

$$F_1 = F(\frac{S_2}{S_2 - S_1}) \quad , \quad F_2 = F(\frac{S_1}{S_2 - S_1}) \qquad \ldots.4.1$$

Taking S_1 = 31.7%, S_2 = 33.2% for the LL2 site, and the sum of the average fresh water flows into L. Long and L. Goil ($20.0 m^3 sec^{-1}$) as a good measure of F(Leatherland, 1976; MacKenzie, 1977), F_1 and F_2 values of 443 and $423 m^3 sec^{-1}$ are obtained respectively. Assuming an approximately rectangular cross-section for the loch, of width 2.2km and depth 70m, at this site, the rates of surface and return flows may be calculated as $\sim$0.58 and $\sim$0.42 km day^{-1} respectively. As the length of the loch is $\sim$25km, a simplistic estimate of the total flushing time of the loch, assuming constant flow rates, would be $\sim$50 days. This value is in reasonable agreement with the differences observed in radiocaesium profiles (Fig 4.13a) and monthly spatial radiocaesium distributions (Fig 4.12) in the light of the known temporal radiocaesium variations in the C.S.A. over the considered periods (Fig 3.4).

As significant horizontal differences exist in radiocaesium profiles throughout L. Long, it is important that a sampling site close to L. Goil is chosen to determine the radiocaesium concentration of source salt water for that loch. With this in mind, a series of radiocaesium profiles were examined during 1977 at the LL1 site opposite the mouth of L. Goil. The resultant variation in salinity-corrected ^{137}Cs concentration over this period is presented as a series of

^{137}Cs isopleths (Fig 4.14) in a manner similar to that previously discussed for L. Goil. The most marked feature in this presentation is the ^{137}Cs concentration maximum of March which is effectively restricted to water above 60m and is the most definite indicator of vertical stratification in L. Long over the period considered. As this maximum was very 'sharp', lasting $\lesssim$2 months, the temporal extent of stratification is difficult to determine in view of the low sampling frequency (monthly). During this period, however, a ^{137}Cs activity of 200.4 dpm l^{-1} was recorded which is the highest value observed in the Clyde Sea Area over a period extending from early 1974 to mid-1978 (cf also MacKenzie, 1977; Saad, 1978). Some further slight evidence of stratification occurred over winter 1977-78 but the low rate of change of ^{137}Cs concentration during this period makes this feature less obvious than that of March. At all other times the water column appears to be completely homogeneous.

4.4 Quantitative analysis of mixing in L. Goil

Water transport between Lochs Goil and Long is controlled by the sill at the mouth of L. Goil. This limits the depth at their junction to $\lesssim$20m (Fig 4.15). Comparison of the 1977 variations in ^{137}Cs concentration in L. Goil (Fig 4.11) with those in L. Long (Fig 4.14) shows plainly the complexity of the mixing process. Thus, though trends in surface ($<$20m) variations tend to be very similar, marked fluctuations at depth occur in L. Goil at various times of the year. During periods of low rates of change of source ^{137}Cs concentration, this effect can be demonstrated by considering the $^{134}Cs/^{137}Cs$ ratio (Fig 4.16). When comparing ratio variations,

FIGURE 4.14 Cs-137 ISOPLETHS - L.LONG vs L.GOIL

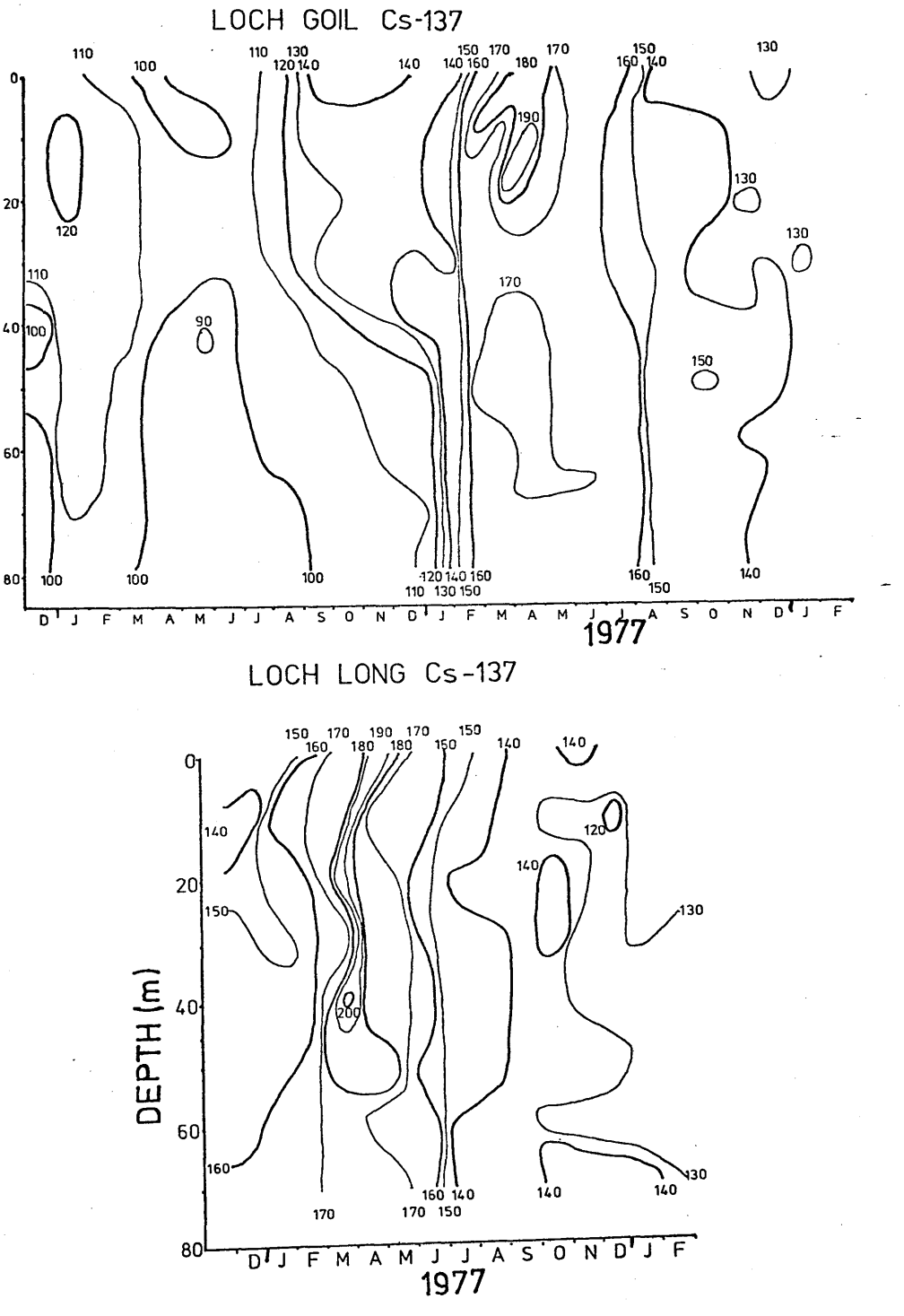

Cs-137 isopleths in dpm/l

FIGURE 4.15 L.GOIL BATHYMETRY

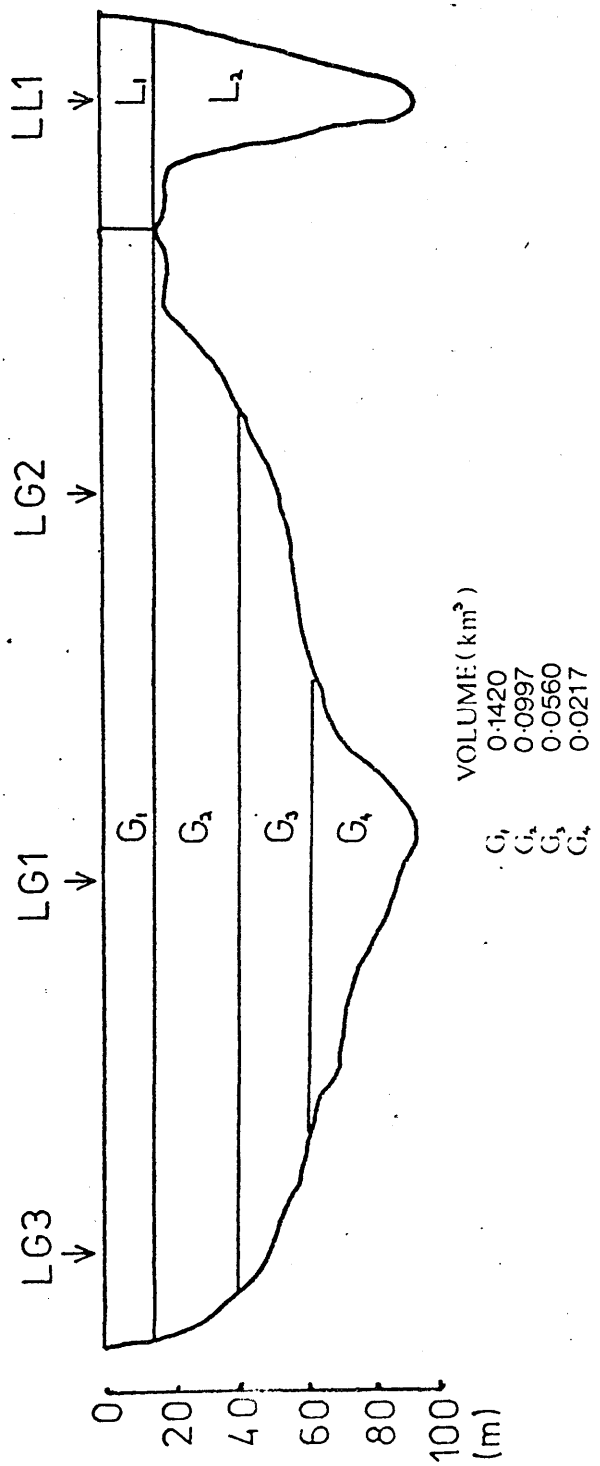

FIGURE 4.16 L.GOIL/L.LONG Cs 134/137 RATIO

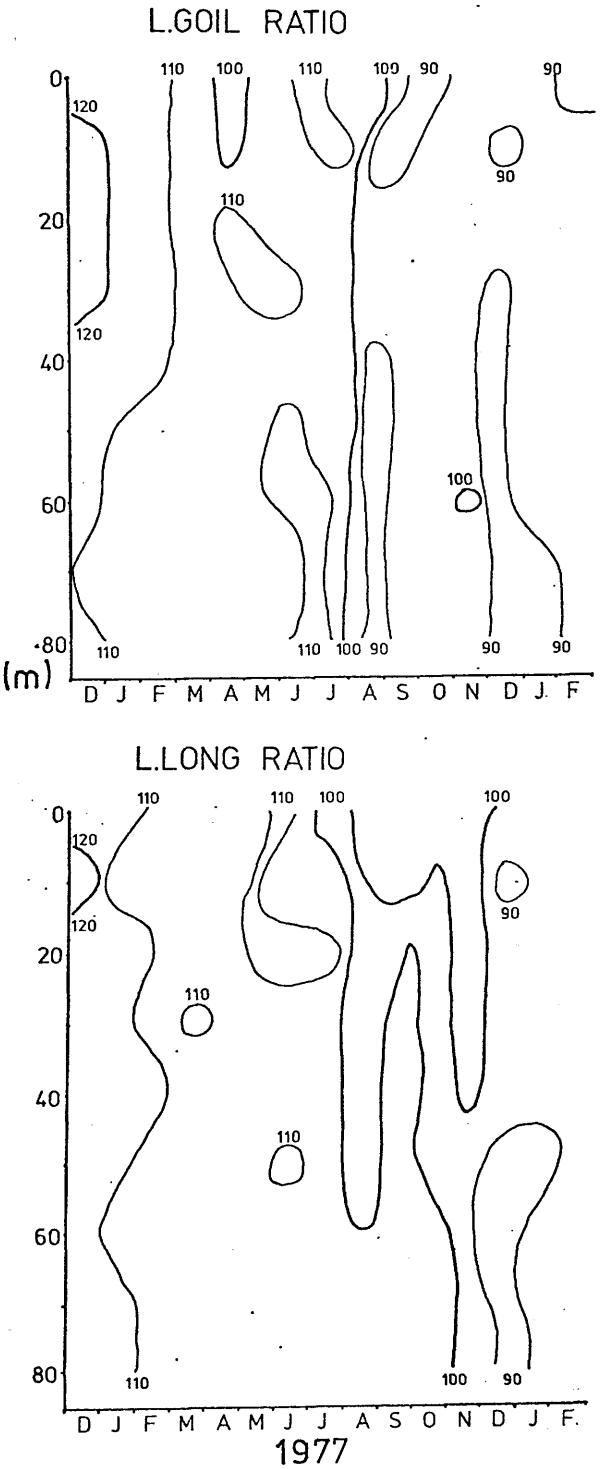

however, the effect of decay on a monthly timescale is significant and must be taken into account. For example, the high ratio (>0.11) deep water (>50m) in L. Goil over June/July 1977 may be unambiguously correlated with the high ratio surface water in both lochs, showing that considerable mixing of L. Goil bottom water occurred during this period. However, the low ratios observed in the deep water over Dec/Jan 1977/78 may be due either to exchange with surface waters or to entrainment coupled with radioactive decay (ratio decrease by decay $\sim 2.6\%$ per month).

A simple model may be postulated for water transport in L. Goil, involving fast exchange of surface ($\lesssim 20$m) waters with L. Long followed by vertical mixing to a variable extent, with deep waters. From monthly averages of surface and deep ^{137}Cs concentrations, the extent of deep mixing during each month may be estimated from a simple conservation of volume equation:-

$$D_t = \alpha D_o + (1-\alpha)\frac{(So+St)}{2} \qquad \ldots.4.2$$

where D and S are deep and surface ^{137}Cs concentrations at times o and t as denoted by the suffices and α is the remnant fraction of deep water. In this equation a mean value of the surface concentration is taken as representative of surface input concentration over the time considered. Solving equation (4.2) for α gives:-

$$\alpha = \frac{(2Dt - So - St)}{(2Do - So - St)} \qquad \ldots.4.3$$

which has been evaluated at approximately monthly intervals over 1977 (Table 4.1). The values obtained, however, often represent physically unreal situations (ie $\alpha < 0$) indicating that this model is an oversimplification of the real system.

TABLE 4.1 MONTHLY EXCHANGE OF L.GOIL DEEP WATER

MONTH	SURFACE Cs-137 (dpm/l)	DEEP Cs-137 (dpm/l)	FRACTION EXCHANGED (a)
D	136.1	122.8	
			-0.26
J	141.9	143.2	
			-0.41
F	169.1	160.6	
			0.49
M	180.9	168.0	
			0.51
A	188.9	176.3	
M			-4.25
J	166.1	163.7	
			0.24
J	157.0	161.4	
			-0.27
A	142.8	146.8	
S			0.55
O	143.2	145.1	
			0.17
N	133.3	139.4	
			0.86
D	129.7	138.3	
			0.19
J	133.3	132.8	

Factors unaccounted for in this simple model include 1) vertical structure within the regions considered as boxes, 2) non-linearity of trends and hence inapplicability of interpolation of average supply activity, 3) exchange rates faster than the sampling frequency (~1 month) and 4) direct incursion of L. Long water. All of these phenomena could cause failure of this derivation. With these reservations in mind, it may be implied that over periods when 'reasonable' exchange rates were observed (ie $0 \leqslant \alpha \leqslant 1$) the Loch Goil system may conform to the restrictions of this simple model. Thus, during the period Jan - March, surface exchange between Lochs Long and Goil may be fast with deep mixing more restricted - corresponding to ~50% per month, a value similar to that observed between August and October. An apparent increase in deep exchange is observed between October and November followed by highly restricted mixing during the period Nov-Dec. (~14%/month) and a further increase to ~81% per month over Dec-Jan. These periods for which the model seems to hold are significant as they correspond to periods showing reasonable stratification of the water profile as previously discussed. Negative ('unreal') values of α occur at times (Dec-Feb, April-June, July-Aug) when rapid changes in bottom ^{137}Cs concentrations were observed. It is therefore implied that at these times, the model breaks down due either to the effect of external incursion or to the rapidity of mixing processes. These causes cannot be distinguished by this simple treatment.

In the derivation of a more realistic model it is important to consider the physical processes occurring during mixing and transport. The basic description of mixing in a

sill-protected fjord has been theoretically derived (e.g. Sverdrup et al, 1942) and applied practically (e.g. Milne, 1972; Anderson and Devol, 1973; Edwards and Edelsten, 1976a; 1976b; 1977). This indicates that deep water renewal is determined by the density of external water at sill depth relative to that of the entrained water. From the salinity and temperature measurements during sample collection (Appendix I), the density profiles in Lochs Goil and Long may be determined by interpolation between curves obtained from tables (e.g. Millero and Lepple, 1973; tabulated in Riley and Skirrow, 1975) or by evaluation of a polynomial expansion. Although the cumbersome polynomial expansions are more accurate than either required in this application or justified by the quality of the hydrographic data, they have the advantage of being readily evaluated as part of a standard computer program. In this work, the expansion obtained by Cox et al (1970), was used to determine the specific gravity, i.e.

$$\sigma = \sum_i \sum_j a_{ij} T^i S^j \qquad 0 \leq i,j \leq 3 \qquad \ldots\ldots 4.4$$

with

i	j	a_{ij}
0	0	$8.00969062 \times 10^{-2}$
	1	$7.97018644 \times 10^{-1}$
	2	$1.31710842 \times 10^{-4}$
	3	$-6.11831499 \times 10^{-8}$
1	0	$5.88194023 \times 10^{-2}$
	1	$-3.25310441 \times 10^{-3}$
	2	$2.87971530 \times 10^{-6}$
2	0	$-8.11465413 \times 10^{-3}$
	1	$3.89187483 \times 10^{-5}$
3	0	$4.76600414 \times 10^{-5}$

T - temperature (^{o}C), S - salinity (‰)

(N.B. the exponent of 10 for a_{oo} is misquoted as 2 by Wilson (1975)). The resulting density variations over 1977 in Lochs Goil and Long are plotted in Fig 4.17. The most obvious features of the density plots in both lochs are the maxima in early summer and minima in late autumn. These features are produced by the annual variation in rainfall and temperature over the entire Clyde Sea Area (or coastal water catchment) as previously considered in more general studies (e.g. Mill, 1892; Barnes and Goodley, 1961). To simplify interpretation of the density data, the temporal variation in density at sill depth (20 m) in L. Long and at 40 m depth in L. Goil (a value chosen from the previous consideration of ^{137}Cs profiles) may be compared (Fig 4.18). It is immediately seen that favourable conditions for advective replacement of L. Goil deep water occur only for about a month in January and April, direct gravity-driven incursion being impossible at all other times. It is noticeable that the autumn rise in L. Long density occurs earlier and less rapidly in winter 1977/78 than in the previous year and that less density difference between L. Long surface and L. Goil deep waters develops. This undoubtedly explains the qualitative differences in extent of ^{137}Cs stratification between the two years as previously observed in section 2.

Bearing this in mind, a model for L. Goil mixing can be postulated such that the main residual flows are those of a surface layer ($\lesssim$10 m) out of the loch driven by runoff and a return flow (10 - 40 m) of salt water from L. Long (Fig 4.19). Deep water ($>$ 40 m) may be assumed to exchange with the overlying water body with occasional direct influxes from L. Long.

FIGURE 4.17 L.GOIL/L.LONG DENSITY

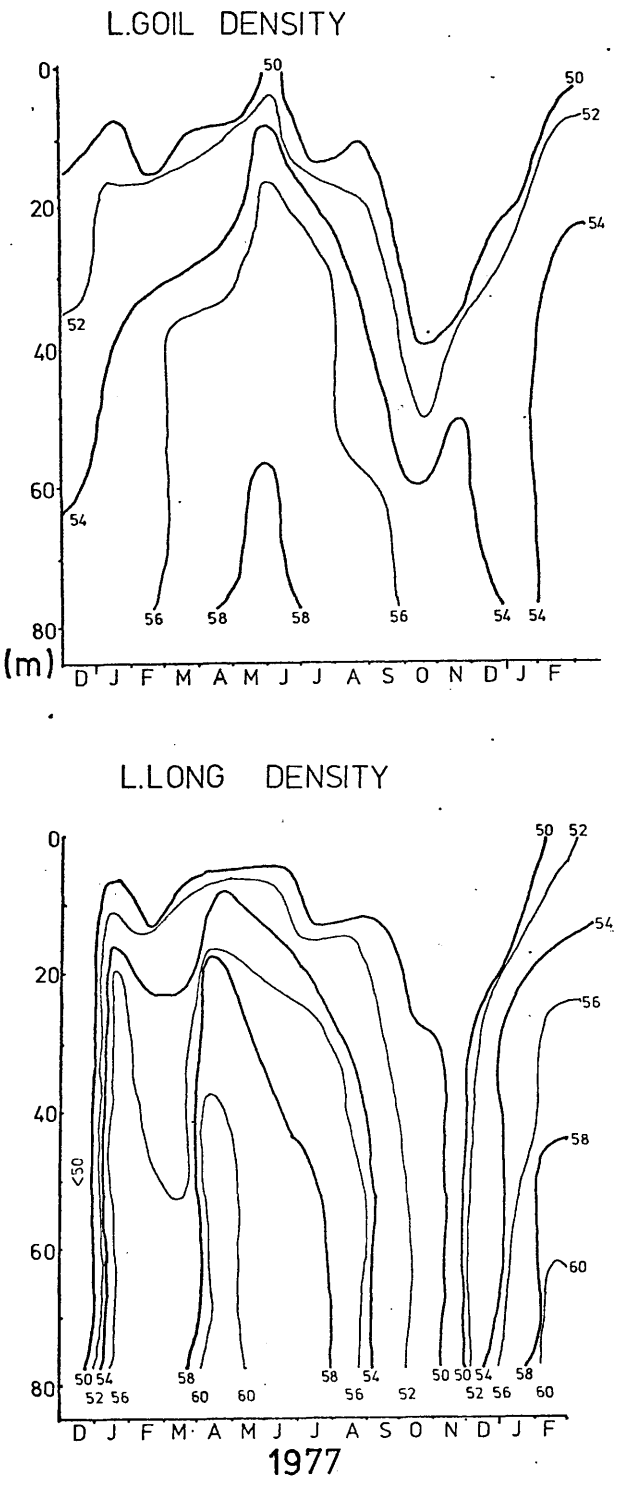

e=1·02

FIGURE 4.18 L.GOIL/L.LONG DENSITY COMPARISON

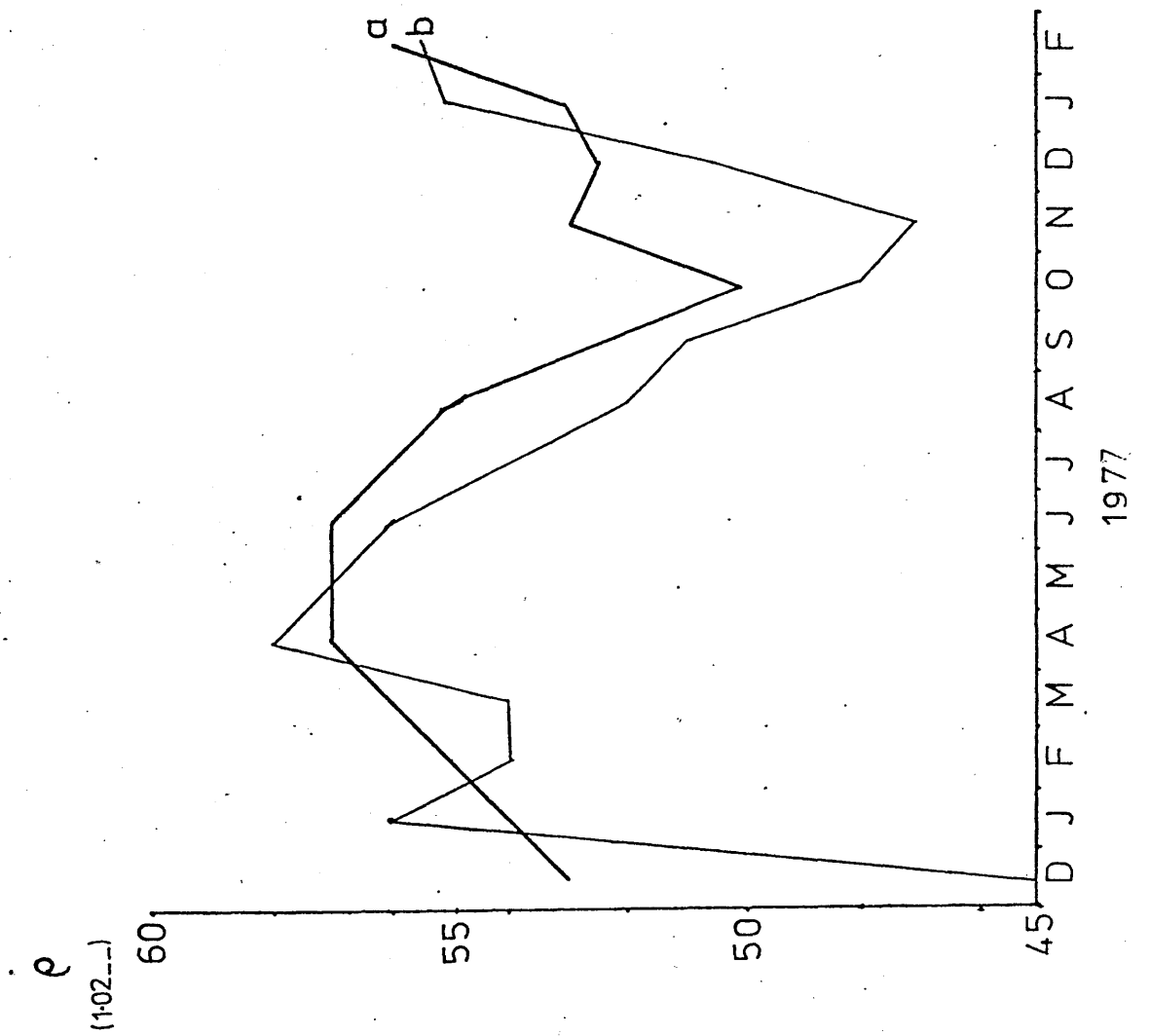

a - L.GOIL(40m)
b - L.LONG(20m)

FIGURE 4.19 L.GOIL MIXING MODEL

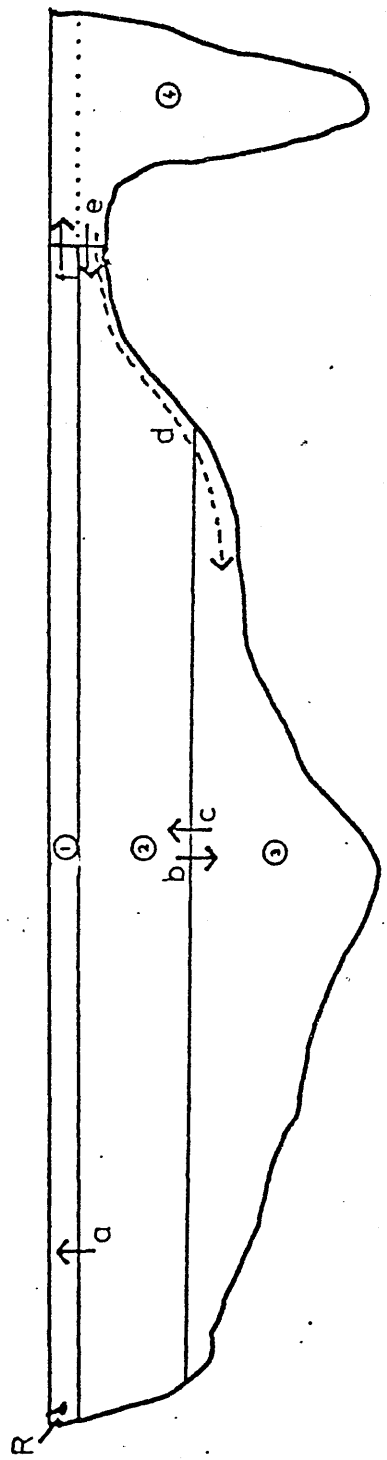

Labelling the flows between boxes as illustrated (Fig 4.16) a series of independent equalities can be derived immediately from conservation of water in each box (evaporation being accounted for in the runoff term, R):-

$$\left.\begin{array}{ll} (1) & a + R = f \\ (2) & e + d + R = f \\ (3) & d + b = c \end{array}\right\} \quad \ldots.4.5$$

(N.B. conservation equation a + b = e + c for box (2) may be derived from these equations and is thus not independent). As deep water replacement is expected to be the slowest process here, it is best suited to evaluation from low frequency sampling. For the deep box (3), to solve for three unknown flows, three independent equations are required:-

$$\left.\begin{array}{ll} \text{Conservation of water} & (1)\ c = d + b \\ \text{Conservation of } {}^{137}Cs & (2)\ |\Delta 7_3|_0^t = \int_0^t d\,7_4\,\partial t + \int_0^t b\,7_2\,\partial t - \int_0^t c\,7\,\partial t \\ \text{Conservation of salt} & (3)\ |\Delta S_3|_0^t = \int_0^t d\,S_4\,\partial t + \int_0^t b\,S_2\,\partial t - \int_0^t c\,S_3\,\partial t \end{array}\right\} \quad \ldots.4.6$$

where b, c and d are water fluxes as shown in Fig 4.16, 7_n, S_n are the concentration of ^{137}Cs and salinity respectively in box n and $|\Delta K_n|_0^t$ in the change in content of parameter K in box n over time $0 \rightarrow t$. Initial simplification may be performed by assuming (a) the fluxes to be independent of time and (b) the change of each parameter in a particular box to be linear with time, such that

$$\int_0^t r K_n\,\partial t = r\left(\frac{K_n^0 + K_n^t}{2} \cdot t\right)$$
$$= r\{K_n\}$$

Solution of the equations above gives:-

$$d = \frac{|\Delta S_3|_0^t - \left(\left(\{S_2\} - \{S_3\}\right) \cdot \left(\frac{|\Delta 7_3|_0^t}{\left(\{7_2\} - \{7_3\}\right)}\right)\right)}{\left(\{S_4\} - \{S_3\}\right) - \frac{\left(\{S_2\} - \{S_3\}\right) \cdot \left(\{7_4\} - \{7_3\}\right)}{\left(\{7_2\} - \{7_3\}\right)}}$$

$$b = \frac{|\Delta 7_3|_0^t - d\left(\{7_4\} - \{7_3\}\right)}{\left(\{7_2\} - \{7_3\}\right)}$$

$$c = d + b$$

....4.7

For the period December 1976 - January 1977, substitution of observed data in these equations yields values of 4.70×10^{11}, 4.79×10^{11} and 9.46×10^{9} l. month^{-1} for d, b and c respectively. As the volume of the deep box is only 7.77×10^{10} l, these values clearly indicate extremely rapid deep water replacement with an implied deep water residence time of ~5 days over this period. As this residence time estimate is much smaller than the sampling period, its reliability is questionable. However, complete flushing in less than one month is certainly implied in agreement with values obtained by MacKenzie, (1977). Fast flushing events of this type have been reported elsewhere (e.g. deep water renewal time of ~12 days for Saanich Inlet, Anderson and Devol, 1973) and thus the postulated renewal rate is not unreasonable. Exchange of the entire deep water body (7.77×10^{10} l.) in 1 month would involve an outwards flux (balanced by a return flow) of 30.0 m^3 sec^{-1} which is small compared to the tidal influx of 3.4×10^{11} l. (low - high) which corresponds to an inflow of 1.5×10^{3} m^3 sec^{-1}. Thus, even flushing of the deep basin in 5 days, requiring an inflow of 180 m^3 sec^{-1}, could be readily accomplished by tidal influx of dense L. Long water.

By contrast, it is evident from the density curves of Lochs Goil and Long (Figs 4.17, 4.18) that L. Goil deep water (>40 m) is considerably denser than L. Long sill waters over the months Aug - Nov and hence direct incursion cannot occur during this time. Changes in the L. Goil depth profiles of ^{137}Cs, ^{134}Cs and salinity during this period must thus be explained in terms of surface transport followed by internal vertical mixing processes. Over the period 16.8.77 - 15.11.77 there is little change (<0.1%) in the salinity of deep (>40 m) water, the main density change over this period being due to fluctuations in water temperature. The temperature profile gradually degrades from a difference of $>8^{o}C$ from 0 - 70 m in August to only $\sim 2^{o}C$ in November, mainly through surface cooling, while the low bottom D.O. values of August (3.7‰) decrease to virtually anoxic conditions (<0.7‰). In previous work oxygen depletion has been attributed to deep water stagnation through development of a strong pycnocline (C.R.P.B., 1974; MacKenzie, 1977), but the increase (by 13%) in $^{134}Cs/^{137}Cs$ ratio of bottom water over 16/8 - 11/10 shows definitively that this is not the case (during this period radioactive decay would be expected to produce a ratio decrease of 5%).

As no mechanism for vertical advection seems possible, the change in ^{134}Cs concentration over this time period may be attributed to diffusion. A barrier to mixing appears to exist at ~40 m as a marked gradient in ^{134}Cs concentration, temperature, density and dissolved oxygen exists between 30 and 40 m on 16/8 and 15/11 and, to a lesser extent on 11/10/77. Values of these parameters above and below this pycnocline are fairly constant and indicate relatively fast mixing of surface and

deep water bodies.

The simplest approach to the 30 to 40m mixing barrier is to average the ^{134}Cs concentration above and below it over the period 16/8 - 11/10, namely 13.0 and 12.5 dpm l^{-1} respectively so that, if mixing can be regarded as a steady state process, with diffusion balancing decay, a simple one-dimensional diffusion model may be used for its description (cf Chapter 1).

The steady state equation is:-

$$\frac{\partial}{\partial z}\left(K_z \frac{\partial c}{\partial z}\right) - \lambda c = 0 \qquad \ldots.4.8$$

which has the standard solution (cf, eg Chung, (1973), Baxter and McKinley (1978)) when appropriate boundary conditions are imposed of

$$C_z = C_o \exp\left(-z\left(\frac{\lambda}{K_z}\right)^{\frac{1}{2}}\right) \qquad \ldots.4.9$$

assuming K_z is independent of depth. Rearranging this equation gives

$$K_z = \frac{z^2 \lambda}{\left(\ln\left(\frac{C_z}{C_o}\right)\right)^2} \qquad \ldots.4.10$$

and thus, putting $\lambda = 0.028$ month^{-1}, $C_z = 12.5$ dpm l^{-1}, $C_o =$ 13.0 dpm l^{-1}, $z = 10$m; $K_z = 1.82 \times 10^3$ m^2 month^{-1}

$= 7.0$ cm^2 sec^{-1}.

This derivation, however, involves the standard assumption of $\frac{\partial c}{\partial t} = 0$, which is plainly not applicable in this case as deep ^{134}Cs concentrations actually increase over the period of interest. As, during 2 months, the deep ^{134}Cs concentration increases from 11.6 to 13.3 dpm l^{-1}, $\frac{\partial c}{\partial t} = 0.85$ dpm l^{-1} month^{-1}. Equation 4.8 thus becomes

$$K_z \frac{\partial^2 C}{\partial z^2} - \lambda c - 0.85 = 0 \qquad \ldots. 4.11$$

but in this case the concentration gradient is time-dependent and a general solution is:-

$$C(Z,t) = \frac{C_0}{2}\left[1 + \frac{2}{\sqrt{\pi}} \int_0^{\frac{z}{2\sqrt{K_z t}}} e^{-\beta^2} d\beta \right] \qquad \ldots.4.12$$

to which further terms must be added to account for decay (Daniels and Alberty, 1966; Duursma and Hoede, 1967). Because of the low spatial and temporal definition of the data in this project, however, rigorous solution of the above equation is not possible. An alternative method of compensating for diffusive increase at depth while retaining the simplicity of a mean concentration gradient is to introduce an additional 'in-situ' removal rate constant to balance the build up. In this way equation (4.8) becomes

$$\frac{K_z \partial^2 c}{\partial z^2} - (\lambda_1 + \lambda_2)c = 0 \qquad \ldots.4.13$$

with λ_1 the radioactive decay constant and λ_2 an in-situ removal rate constant balancing the increase rate (7.3% month^{-1}). The general solution for K_z is thus:-

$$K_z = z^2 \frac{(\lambda_1 + \lambda_2)}{\left(\frac{\ln(C_z)}{C_0}\right)^2} \qquad \ldots.4.14$$

which, using the values above (cf equation 4.10) and $\lambda_2 = 0.073$ month^{-1}, gives $K_z = 6.57 \times 10^3$ m^2 month^{-1}

$= 25.3$ cm^2 sec^{-1}

Although the calculations above are somewhat less than completely rigorous, it is perhaps reasonable to regard the vertical diffusion coefficient as falling within the range 7 - 25 cm^2 sec^{-1}, if the standard assumption of K_z being

independent of depth and time may be made. These values are, however, considerably larger than might be expected in view of the strong density gradient present (cf eg 1 - 1.5 cm^2 sec^{-1} for the main ocean thermocline (Broecker, 1966; 1974) and 3.9 cm^2 sec^{-1} in a basin (Santa Barbara) having a much less marked pycnocline (Chung, 1973)) and are more typical of values found in ocean bottom waters (2 - 200 cm^2 sec^{-1}, Broecker, 1974), ie in areas with negligible density gradient. If the high values are real - and are not simply produced by failure of model assumptions - they could be caused by turbulence through coupling with the surface, fresh water-driven flow. Indeed mixing through thermoclines has been postulated as due to the presence of internal waves (Bowden, 1975) which may possibly be generated by such turbulence. The reality of the fast diffusion rate is further implied by the large change in bottom density over the period considered - this resulting mainly from an increase in bottom temperature by $\sim$22%, indicative of considerable water exchange between deep and surface bodies. Perhaps the main difficulty associated with this fast diffusion rate would appear to lie in explaining the observed decrease in D.O. between August and September. This depletion may be assumed to be caused by rapid consumption of oxygen at depth, presumably by oxidation of organic debris, which may be largely residues of the summer plankton bloom (cf eg MacKenzie, 1977). This rain of organic debris may, however, be expected to perturb the earlier models if radiocaesium is associated with it and is transported to depth and released during organic decay. Taking an average Cs concentration factor of x 100 (cf Chapter 7) for plankton, the required organic flux to cause

the observed ^{134}Cs increase would be 28 kg m^{-2} $month^{-1}$. This particulate flux could not, however, cause major isotopic fractionation and hence would also involve transport of ^{137}Cs resulting in an increase of 17pCi l^{-1} over the time considered, as opposed to the observed increase of 0.6p Ci l^{-1}. On this basis, this transport mechanism may therefore be regarded as insignificant.

The absence of any marked depth variations in ^{134}Cs concentration within the deep body implies fast internal mixing - a difference of less than 5% over 40m implying $K_z \gtrsim 70$ cm^2 sec^{-1} (equation 4.10) as might be expected on the basis of the low density gradient in this region. From this minimum value of K_z in the deep water body an estimate of the rate of oxygen utilisation may be derived, assuming the removal rate to be first order. Further assuming a steady state gradient of D.O. in early November, with the bottom (70m) D.O. ~ 1.0‰ and the D.O. at 40m ~ 3.5‰, rearranging equation 4.10 gives

$$\lambda = \frac{K_z \left(\ln \frac{C_z}{C_o}\right)^2}{z^2} \qquad \ldots.4.15$$

yielding $\lambda = 1.2 \times 10^{-5}$ sec^{-1}. Thus, the maintenance of the observed profile would require a minimum consumption rate of ~1.5mg O_2 l^{-1} day^{-1} at 70m. It may, however, be more realistic to consider the oxygen removal rate (R_z) to be controlled by the organic particulate content (or some similar parameter) such that removal is effectively zero order with respect to D.O. Equation 4.8 thus becomes:-

$$\frac{\partial^2 C}{\partial z^2} = \frac{R_z}{K_z} \qquad \ldots.4.16$$

which, if R_z and K_z are independent of depth within the deep water zone, may be integrated twice to give:-

$$C_z = \frac{R_z z^2}{\alpha K_z} + \alpha z + \beta \qquad \ldots.4.17$$

where α and β are constants of integration. With the additional data that the D.O. at 55m is $\sim$ 1.8‰ in the steady state case considered above, three equations for C_z at depths 40, 55 and 70m may be solved simultaneously to give $R_z \simeq 1.9 \times 10^{-5}$‰ sec^{-1} ($\simeq$2.35 mg O_2 l^{-1} day^{-1}). While these oxygen removal rates may be atypical of the annual average for the loch, they lie at the low end of the range of Biochemical Oxygen Demand (0.2 - 38 mg l^{-1} day^{-1}) found within the Clyde and its tributaries (CRPB, 1976). Although B.O.D. values measured in the Clyde system may be correlated with inputs from rivers and sewage works (MacKay and Leatherhead, 1976), the oxygen demand in L. Goil will have additional significant components from the decay of plankton remains and possibly from reactions at the sediment/water interface (Steel, 1972). Without further data on the particulate flux in the area, however, it is not possible to comment further on these oxygen consumption estimates.

In general, therefore, water transport in L. Goil may be categorised as either rapid flushing with externally-derived water during which the residence time of even the deepest areas of the loch is $\lesssim$1 month, or fast surface exchange followed by mixing over a developing pycnocline which, even at maximum extent (in 1977) showed an average vertical eddy diffusion coefficient of 7 - 25 cm^2 sec^{-1}. The particular behaviour of the loch is determined by density gradients - flushing occurring when the density of L. Long water at sill

depth is greater than that of L. Goil deep water.

4.5 Gareloch and L. Fyne

In addition to the detailed studies of L. Goil and L. Long, occasional samples were obtained from Gareloch and L. Fyne.

Gareloch extends ~5 miles NNW from the Clyde Estuary and consists of a trench averaging ~40 m deep along its centre separated from the open estuary by a narrow sill ~20 m deep at Rhu. This loch is generally regarded as being greatly influenced by the estuary both in terms of water and sediment input (Mill, 1892; MacKenzie, 1977). Two samples taken from mid-depth (20 and 30 m) on 6.11.75 showed radiocaesium concentrations typical of the C.S.A. concentration at that time (cf also MacKenzie, 1977) and no significant difference was observed between the two depths. A complete profile was obtained however, on 3.8.76 (Fig 4.20) when a marked increase in ^{137}Cs concentration (salinity-correlated) was observed at 10-20 m relative to surface and deep values although no significant trend in ratio was noticeable. As the net trend in ^{137}Cs concentration in the C.S.A. over this period was a general increase (Fig 3.4), a water renewal mechanism may be postulated involving influx from the estuary at mid-depth (probably as a salt return flow). Older water is removed with the fresh surface flow and deep flushing/mixing is slow, on the timescale of months. In the absence of additional data, it may be suggested that, at this time of year Gareloch is similar to L. Goil, with fast runoff and tidally-driven surface exchange followed by more restricted mixing to depth although lower gradient of salinity, temperature and D.O. imply less restriction to vertical

FIGURE 4.20 GARELOCH PROFILE (3/8/76)

FIGURE 4.21 L.FYNE PROFILE (12/2/76)

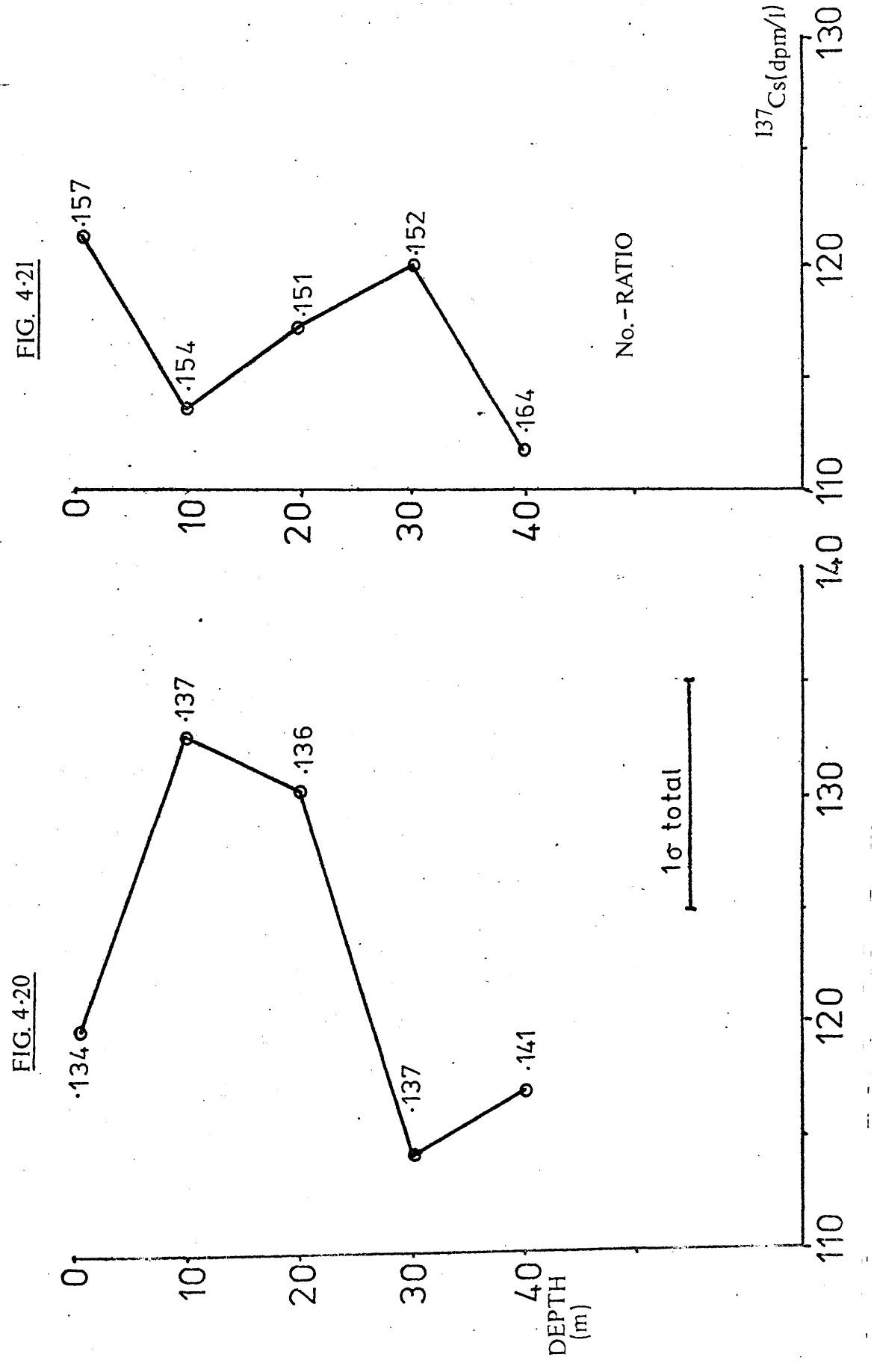

mixing in Gareloch.

Radiocaesium measurements previously considered (Chapter 3) indicate that L. Fyne may be regarded as comprising two distinctive regions - a southern basin, which is effectively a continuation of the N.W. trench system of the Clyde Sea basin, and a sill-protected northern basin. Initial measurements on 17.2.76 showed no systematic variation in radiocaesium concentration along the loch or in the surface layers (0-40m) of the north basin (Fig 4.21) and led MacKenzie (1977) to assume that the entire loch could be regarded as well-mixed. Surface and bottom sample pairs taken from the southern and northern basins on 24.11.76, however, indicated that the deepest water in the north basin was considerably different from that elsewhere, being ~30% lower in ^{137}Cs concentration and ~10% lower in $^{134}Cs/^{137}Cs$ ratio. As the C.S.A. in general is characterised by a salinity-correlated ^{137}Cs concentration of 130 dpm l^{-1} and $^{134}Cs/^{137}Cs$ ratio of ~0.117 (Fig 3.4), the entire south basin and surface waters in the northern reaches of the loch may be regarded as well-mixed while the north basin deep water is more typical of much 'older' water. Assuming complete entrainment of the deep water with negligible vertical exchange, a ^{137}Cs concentration of 100 dpm l^{-1} is similar to that found in the C.S.A. generally around May 1976 or April - November 1975. The ratio in May 1976 was ~0.15 which is reduced by decay to ~0.128 by November 1976 while that of April 1975 (0.17 - 0.15, MacKenzie (1977)) corresponds to 0.102 - 0.108 and November 1975 (0.158) to 0.115 by this date. It would thus seem that, if this deep water body can be regarded as isolated by a mixing

barrier, the entrained water has an 'age' of $\sim$ 1.6 years. It is not possible, in this case, to quantify the effects of vertical diffusion over this time but, in view of the trends in ^{137}Cs concentration and $^{134}Cs/^{137}Cs$ ratio over this time (Fig 3.4), the deep water residence time must be $\gtrsim$ 1 year.

The most detailed profile of the north basin was obtained on December 1977 (Fig 3.3) and, as previously discussed (Chapter 3), shows a distinct ^{137}Cs maximum at $\sim$100m. As a generally decreasing trend in ^{137}Cs concentration was prevalent in the Clyde Sea Area over this time, this maximum indicates significant entrainment of 'old' water in the basin. Decreased ^{137}Cs activities at surface and depth indicate that water transport to this basin is both by rapid surface mixing and deep water replacement by influx of high salinity water from the southern basin. From previous consideration of L. Goil mixing, it is probable that the deep water incursion process occurs only during the winter as observed in this case. Relative to the known variations in radiocaesium content of the Clyde Sea Area in the months preceding this study (Fig 3.4), the ^{137}Cs concentration and the $^{134}Cs/^{137}Cs$ ratio of the activity maximum in Loch Fyne indicate an 'age' of that water body of either $\sim$4 months or $\sim$ 1 year (assuming no diffusion). It is again impossible to define this deep water residence time because of the low sampling frequency. It seems, nevertheless that the north basin of L. Fyne probably experiences the longest periods of deep water entrainment of all the sea lochs studied and, as deep water residence times are $\gtrsim$1 year, the extent of annual renewal may well be greatly influenced by weather conditions.

Generally, therefore, the surface waters of the northern sea lochs examined exchange rapidly due to circulation induced by fresh water runoff with additional contribution from wind- and tidally-driven currents. Water exchange in sill-protected basins is either via vertical diffusion or by distinctive advective flushing processes when the external density at sill depth exceeds that of the deep water body.

4.6 General Overview

Examination of radiocaesium depth profiles in the L. Long - L. Goil system has allowed the water mixing processes in these lochs to be studied in some detail. L. Long may be regarded as a simple narrow estuary with circulation driven by fresh runoff and characterised by a total flushing time of $\sim$1 month. Little evidence of deep water entrainment is observed over an entire annual cycle. L. Goil, however, is characterised by rapid exchange of surface waters ($\lesssim$40m) at all times of year (residence time $\lesssim$1 month) but there is evidence of restricted deep water renewal during summer and autumn. During vertical stratification of this loch, a pycnocline develops between 30 - 40m which limits vertical mixing ($K_z \sim 7 - 25$ cm^2 sec^{-1}) while internal mixing in the deep water body is much faster ($K_z \gtrsim 70$ cm^2 sec^{-1}). When external density at sill depth (in L. Long) exceeds that of the L. Goil deeps, the bottom water renewal rate increases rapidly giving complete replacement in $\lesssim$ 1 month.

Preliminary measurements in Gareloch and upper L. Fyne show that, in contradiction to previous work, both these lochs display vertical structure which may be interpreted in terms of similar transport mechanisms to those invoked for L. Goil.

Chapter 5

The Hebridean Sea Area

5.1 Introduction

The Hebridean Sea Area may be considered as that region of the continental shelf between Malin Head in the south and the Butt of Lewis in the north (Fig 5.1). This area has been little studied in comparison to other coastal waters around the British Isles (Ellett, 1978a). In addition, any hydrographic studies of the region have concentrated on the shelf-edge, in particular in the vicinity of the Rockall Channel (Ellett, 1977a; 1978a). Water movement on the Hebridean Shelf may be regarded as a resultant of 3 water fluxes, derived from Atlantic and Irish Sea water bodies and from fresh-water runoff. Such flows have been studied via the salinity distribution (Craig, 1959), the salinity and temperature distribution (Ellett, 1977b; 1978a; 1978b), drift-bottle releases (Barnes and Goodley, 1961) and the distribution of Windscale-derived radiocaesium (Jefferies et al, 1973). From these investigations, the apparent general distribution of surface water currents has been derived for the summer months (April - October) (Ellett, 1978a). Even so, Ellett emphasised the sparsity of data for the area.

It is intended in this chapter to examine in some detail the flow of coastal, Irish Sea-derived water through the Hebridean Sea Area (H.S.A.) during the summer months and to determine the variability of this flow between successive

FIGURE 5.1 HEBRIDEAN SEA AREA STATIONS

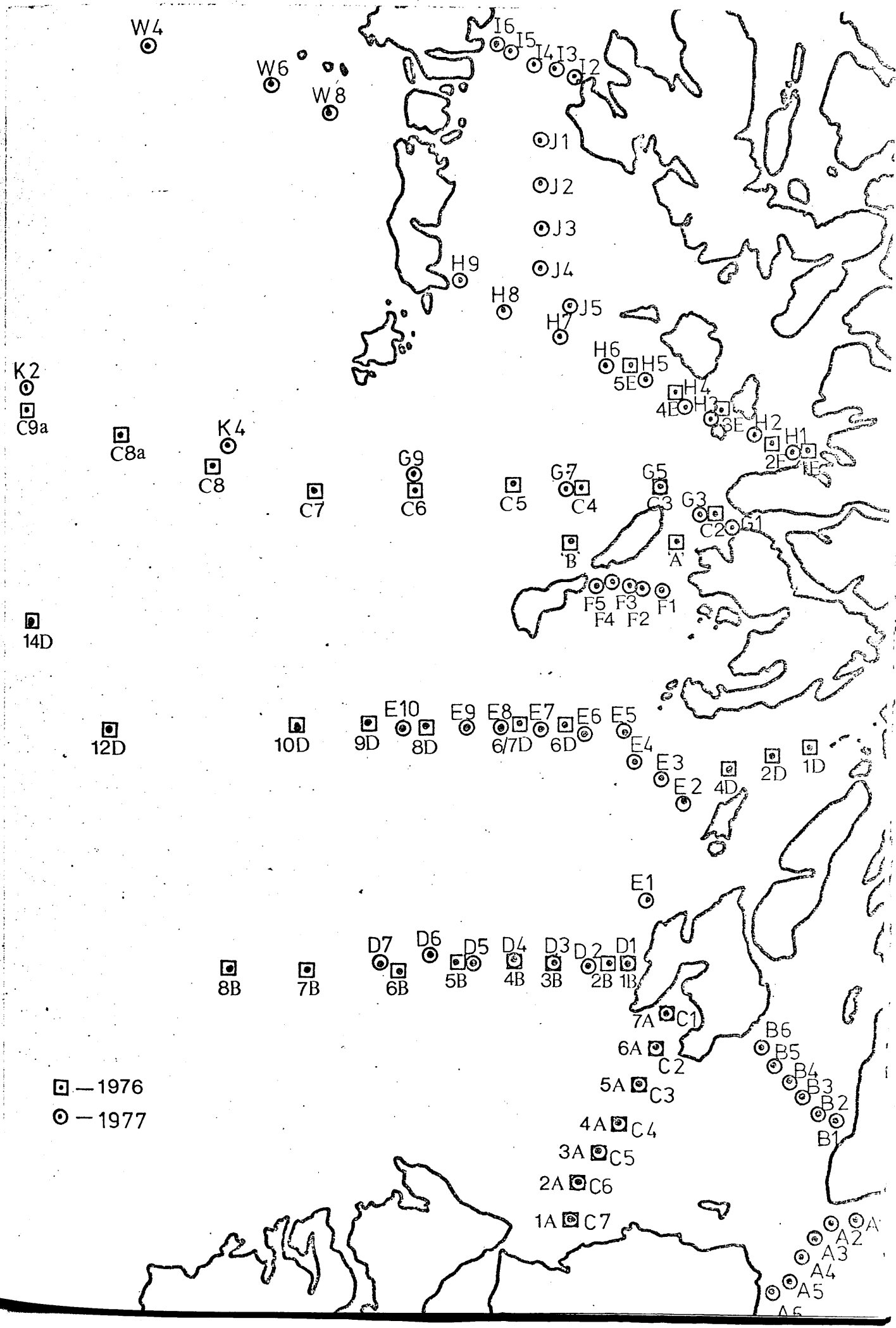

years. With this aim in mind, 43 samples in 1976 and 71 samples in 1977 were collected from a grid of stations in the H.S.A. by Ellett (of SMBA) during cruises 8/1976 and 10/1977 of the NERC research ship 'Challenger'. The results of radiocaesium analysis of these samples together with hydrographic data provided (Ellett, 1978c) are listed in Appendix 1.4. The positions and sample codes of stations used in both years are plotted in Fig 5.1.

5.2 Data for Summer 1976

The results of radiocaesium analysis of the samples obtained on 25-29 May 1976, when plotted on a map of the area (Fig 5.2), show a marked decreasing trend in ^{137}Cs concentration from south to north and east to west while trends in the $^{134}Cs/^{137}Cs$ ratio are less distinct. The distribution of ^{137}Cs in the area is more conveniently presented by drawing a set of '^{137}Cs-isopleths' which show the marked 'Cs-plume' of coastal water flow (Fig 5.3). As the only significant source of radiocaesium to the area is Windscale (Jefferies et al, 1973; Livingstone and Bowen, 1977), the dilution and dispersion of the Cs-plume may be regarded as representative of the processes occurring to the Irish Sea-derived coastal water body and its dissolved constituents.

Several points are immediately obvious from the radiocaesium distribution in the H.S.A.

1) There is a very marked horizontal stratification in the Islay-Malin Head Channel, with high ^{137}Cs activity Irish Sea-derived water flowing along the Scottish coast. This component is quite distinct from the low activity waters

FIGURE 5.2 RADIOCAESIUM DATA - SUMMER 1976

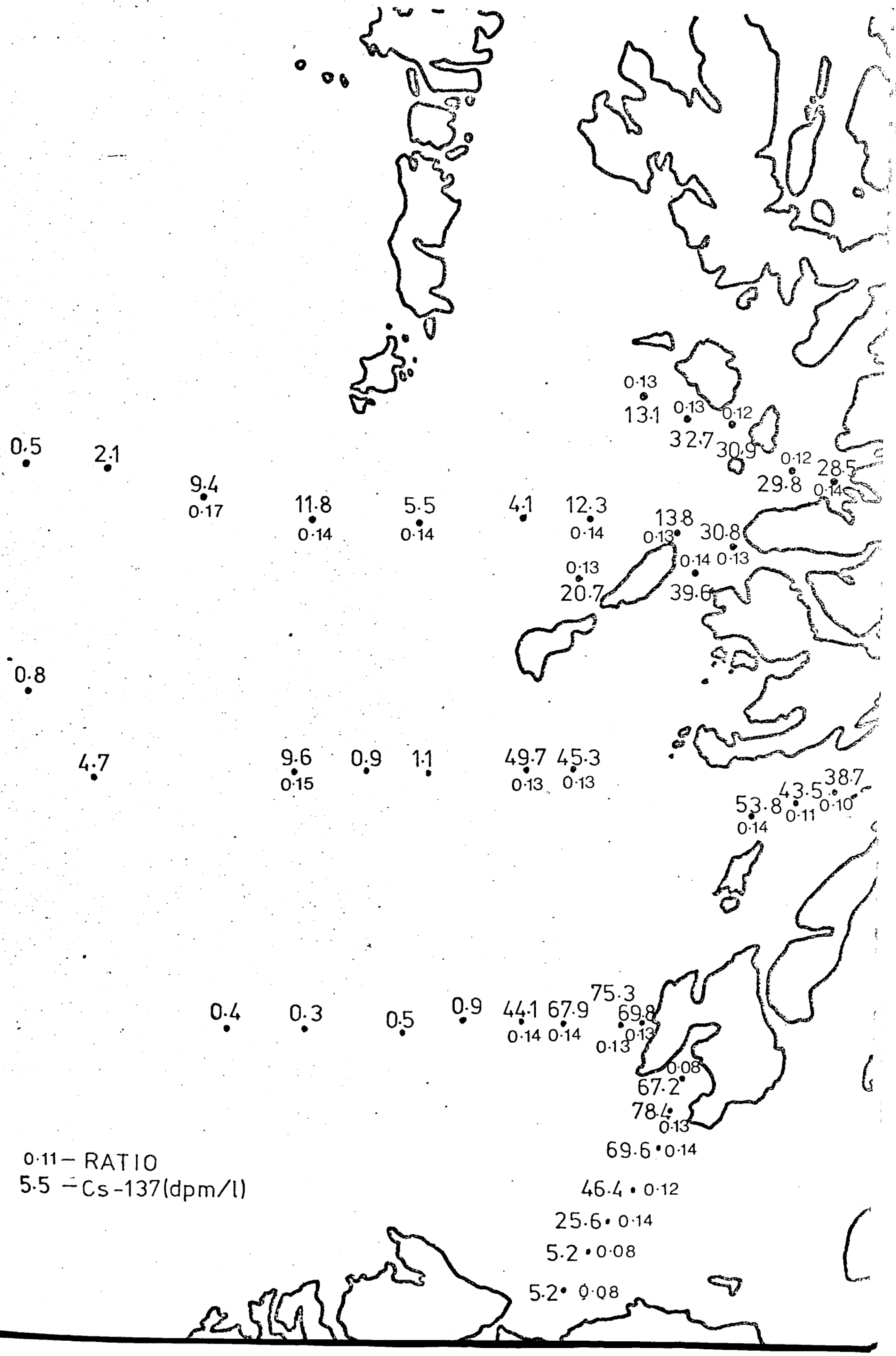

FIGURE 5.3 Cs-137 ISOPLETHS - SUMMER 1976

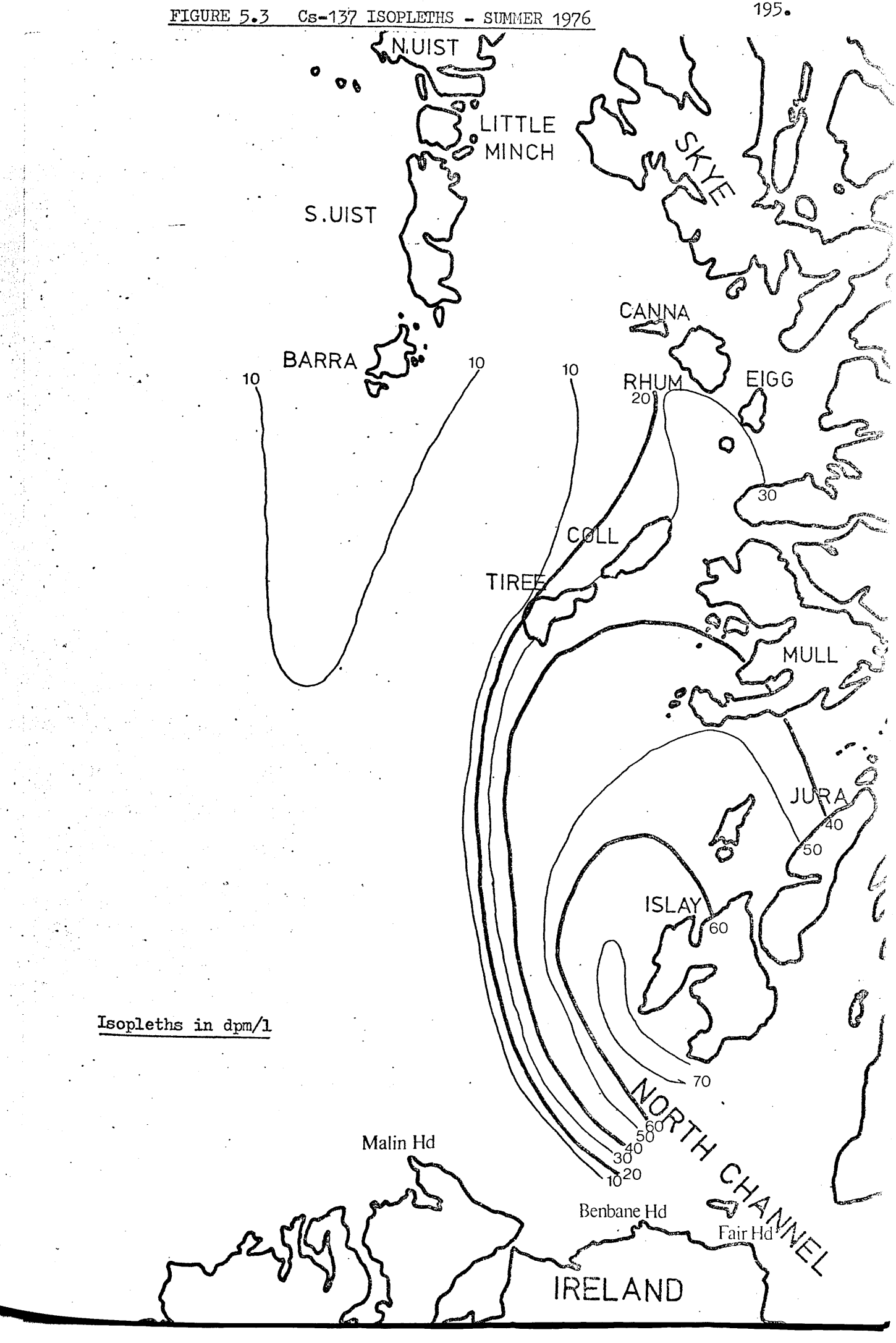

along the N. Irish coast, which probably reflect marked Atlantic incursion along the north of Ireland into the northern reaches of the North Channel. The steep ^{137}Cs gradient across this channel indicates little mixing of the Atlantic and Irish Sea-derived water bodies in this region. The $^{134}Cs/^{137}Cs$ ratio distribution across the channel shows little real variation - the low values observed at sites 1A and 2A (and 7A) have very large associated errors and thus are within $\pm 1\sigma$ experimental error of the average ratio for the area (3 - 6A).

2) There is a very marked front between Atlantic and coastal waters to the south of Tiree, running approximately along $7^{o}W$, indicating sharp differentiation of the two water bodies in this area. To the north of Tiree, however, the front is less well-defined, indicating substantially increased mixing and dilution of the coastal water flow. Such enhancement of mixing could be due to increased turbulence and complexity of the coastal flow through perturbing influence of the 'Small Islands', particularly caused by the channel restriction between Coll and Mull.

3) There is a marked tongue of high radiocaesium water extending to the south of Barra which may be due either to a sudden incursion of Atlantic water towards Skye, thus disrupting the coastal plume, or to a steady-state southwards flow from the Outer Hebrides. Indeed Craig (1956) has postulated a southwards flow along the east coast of S. Uist, round Barra Head and thence northwards to the Butt of Lewis, this caused by constriction of the northwards coastal flow

by the Little Minch. However, the occurence of high activity water ~50 km south of Barra may imply the presence of a weak counter-clockwise gyre in the area, possibly through coupling of the southwards flow at Barra with the eastwards Atlantic incursion and northwards coastal flow. The increased complexity of coastal transport caused by the Little Minch may also contribute to the breakdown of the well-defined front system observed above.

4) The concentration of ^{137}Cs in these coastal waters decreases by~x 3.5 from south to north of the area, implying considerable dilution of the Irish Sea-derived water with 'uncontaminated' Atlantic and runoff waters (c.f. the small extent of dilution observed between the MAFF North Channel site and the Clyde Sea Area - Chapter 3).

To examine these results more quantitatively, the temporal variation of radiocaesium concentration in the coastal water body must be known. Such an estimate may be derived from MAFF measurements of radiocaesium at either the North Channel (Fig 3.5) or the Islay-Malin Head stations (Fig 5.4). Although the ^{137}Cs maximum in early 1977 and the general decrease in ratio are comparable for these two sites, there is little similarity in overall curve shape. Nor is the match of these curves particularly improved by assuming mixing in the northern reaches of the North Channel or in the Clyde Sea Area and deriving resultant North Channel curves using the box-model discussed in Chapter 3 (Fig 3.13).

In this analysis the North Channel (Stranraer-Larne) radiocaesium curves will be taken as representative of the coastal source water radiocaesium variation with time, as the marked concentration gradient observed across the Islay-

FIGURE 5.4 RADIOCAESIUM DATA FOR THE ISLAY-MALIN CHANNEL

(after Jefferies, 1978)

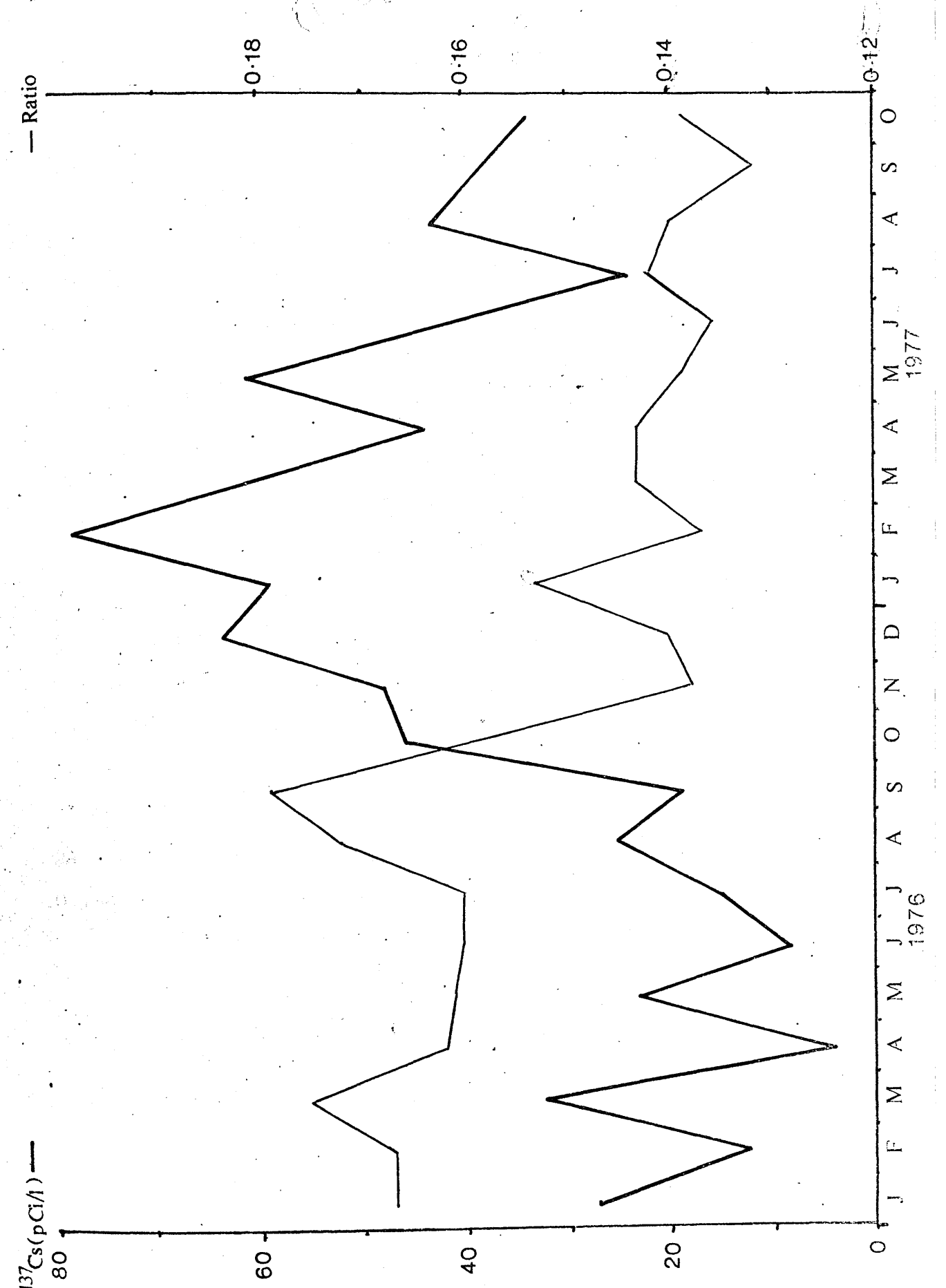

Malin Channel makes data obtained from a sampling station in this area highly susceptible to the effects of variations in 'Plume width', as will be emphasised in the next section.

As the ^{137}Cs concentration in the North Channel shows considerable fluctuation in the months preceding this survey, the dilution factor, as obtained previously, between south and north of the area must be regarded as a simplistic estimate of the true dilution. Accurate calculation of environmental appearance (E_A) values for ^{137}Cs in the area is therefore precluded (c.f. Chapter 3 for definition of the E_A units). The $^{134}Cs/^{137}Cs$ ratio in the North Channel does, however, show a much more regular trend over the preceding months and can be approximated via the linear function.

$$R_m = 0.221 - (0.008 \times m) \qquad \ldots\ldots.5.1$$

where R_m is the ratio at time m months after January 1976 (correlation coefficient 0.92). Bearing in mind the inter-calibration constant of 1.22 between MAFF and G.U. ratio data (Chapter 3) and radioactive decay, the transit time from the North Channel to Islay should be calculable from the 0.134 average ratio in the Islay-Malin Channel (Stations 2A - 6A). Thus, if transport is by simple advection,

$$0.134 = \frac{0.221-0.008(5-t)}{1.22} \times \exp(-0.02625xt) \qquad \ldots\ldots.5.2$$

where t is the transit time in months. This equation does not have a real solution nor is a solution obtained by considering the observed monthly ratio values for the North Channel reduced by the intercalibration correction and decay (Table 5.1a). Explanation of transport between the North Channel (Stranraer-Larne) and Islay in terms of simple

Table 5.1 Coastal source waters 1976.

Month	a)North Channel J	F	M	A	M	J	b)Clyde Sea Area J	F	M	A	M	J
Cs-137(dpm/l)	73	101	185	121	169	176	123	110	108	100	96	
Intercal. cor.	69	95	175	114	159	166						
Ratio	.221	.202	.187	.187	.182	.179	.165	.153	.144	.149	.150	
Intercal. cor.	.180	.164	.152	.152	.148	.144						
Decay cor.	.158	.148	.140	.144	.144	.144	.145	.137	.133	.141	.146	

Table 5.2 Coastal source waters 1977.

Month	a)North Channel O	N	D	J	F	M	A	M	J
Cs-137(dpm/l)	163	200	176	194	156	139	114	110	112
Intercal. cor.	154	189	166	183	147	131	108	104	106
Ratio	.170	.151	.166	.150	.169	.168	.152	.140	.140
Intercal. cor.	.138	.123	.135	.122	.137	.137	.124	.114	.114
Decay cor.	.112	.102	.115	.107	.123	.127	.118	.111	.114

Table 5.2 (continued).

b) Clyde Sea Area

Month	O	N	D	J	F	M	A	M	J
Cs-137(dpm/l)		127	137	143	178	169	198		168
Intercal. cor.									
Ratio		.117	.126	.113	.111	.104	.090		.105
Intercal. cor.									
Decay cor.		.097	.108	.099	.100	.096	.085		.105

Intercal. cor. — Corrected for intercalibration with MAFF.

Decay. cor. — Corrected for radioactive decay.

advection is therefore precluded. If, however, a similar calculation of the expected ratio at Islay is performed using as source data the ratio values observed in the Clyde Sea Area, a match is obtained for 'March' water from the C.S.A. (Table 5.1b). Comparison of ^{137}Cs concentrations between March C.S.A. water and observed Islay-Malin values shows that, if the above correlation is real, dilution by ~20% has occurred during transit between these sites through mixing with Atlantic or runoff-derived waters. A resultant value for the environmental appearance of ^{137}Cs at Islay of ~0.2 pCi l^{-1}/Ci day^{-1} is obtained.

This perhaps surprising match between calculated radiocaesium concentrations from C.S.A.-derived water and observed values in the H.S.A. may be due either to short residence of water in the C.S.A. and the implied large percentage of Irish Sea-derived water through the area (cf Chapter 3) or to the existence of a large area of mixing in the northern North Channel (including the C.S.A.) with an average residence half-time of 1-2 months. With a sampling frequency of 1/month it is impossible to distinguish between a model with the entire northern North Channel and C.S.A. acting as a single mixed box with residence $t_{\frac{1}{2}}$ ~2 months or an alternative with 2 linked mixing boxes, corresponding to the C.S.A. and the north reaches of the North Channel, each with residence $t_{\frac{1}{2}} \sim 1\frac{1}{2}$ months. Both models, however, imply that water transport from the MAFF North Channel site over this time period may be regarded as occurring via northwards advection with a transit time of ~1 month to an area of

mixing with residence $t_{\frac{1}{2}} \sim 2$ months around the Clyde followed be advection to Islay with transit time of ~ 2 months. At a more realistic level then, transport of radiocaesium through the North Channel may be considered to occur by a combination of mixing and advection processes, the former (residence $t_{\frac{1}{2}} \sim 2$ months) proceeding on a similar timescale to advection (transit time ~ 3 months corresponding to an average velocity of 1.6 km day^{-1}). Such a combination of mixing and advection is similar to the model previously invoked to explain radiocaesium transport in the northern Irish Sea and into the C.S.A., and probably reflects the superimposition of tidal and wind-driven mixing on residual advective flows. The derived values of ~20% dilution during transport through the North Channel and ~1.6 km day^{-1} average residual flow rate may be compared with values of 10% and 5 km day^{-1} respectively obtained by Craig (1959) from measurements of surface salinities.

The observed values of $^{134}Cs/^{137}Cs$ ratio are very similar throughout the area (Fig 5.2), values for even the most northerly area around Rhum being effectively within experimental error (1σ) of the average for the Islay-Malin Channel. As a result, the only match with calculated source-water values (Table 5.1) is again with that derived from March C.S.A. waters, implying fast transport throughout the region considered. As transport from Islay to Rhum is thus characterised by a transit time $\lesssim 1$ month the average flow rate through the area is at least ~5 km day^{-1} (in good agreement with the value obtained by Craig (1959)). Comparison of ^{137}Cs concentrations in the south and north of the

area is thus valid bearing in mind the rapid transit involved and the dilution of ~x 3.5 during transport results in an environmental appearance of ^{137}Cs at Rhum of ~0.06 pCi l^{-1}/ Ci day^{-1}. Comparison of water transport between Stranraer/ Larne - Islay and Islay - Barra therefore suggests that the very much greater transit velocity and dilution derived for the latter case may be linked, in that the Hebridean coastal flow may be driven to some extent by the diluting Atlantic and freshwater currents.

The validity of the calculations above may be very roughly checked by considering the flux of radiocaesium through the Islay-Malin Head Channel. Assuming a 90 m average depth for this channel, a plume width of 25 km, an average ^{137}Cs concentration of 30 pCi l^{-1} and a coastal water velocity of 5 km day^{-1}, the ^{137}Cs flux is estimated at ~450 Ci day^{-1}. This figure corresponds to a total annual flux of ~123,000 Ci $year^{-1}$, in reasonable agreement with the Windscale release rate (~ 141,500 Ci $year^{-1}$ for 1975). Indeed agreement is remarkable bearing in mind the crudeness of the calculation, the complexity of the transport process, the accumulation of ^{137}Cs in the Irish Sea and southwards removal from the Irish Sea through the St. George's Channel and possible seasonal fluctuations in the flow characteristics of the coastal currents.

5.3 Data for Summer 1977

The observed radiocaesium plume in the more extensive survey of the H.S.A. in summer 1977 (Fig 5.5) shows some

FIGURE 5.5 RADIOCAESIUM DATA - SUMMER 1977

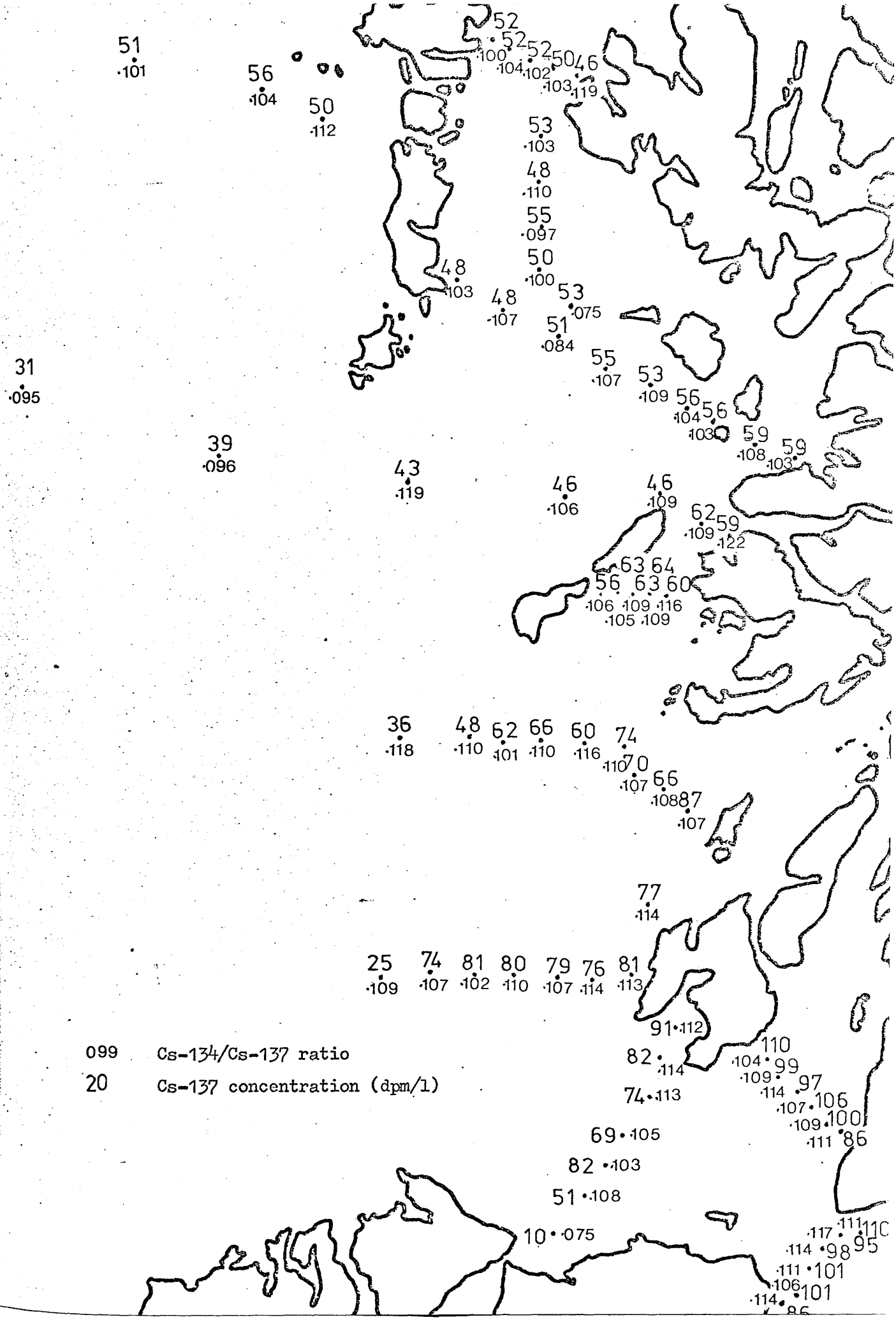

FIGURE 5.6 Cs-137 ISOPLETHS - SUMMER 1977

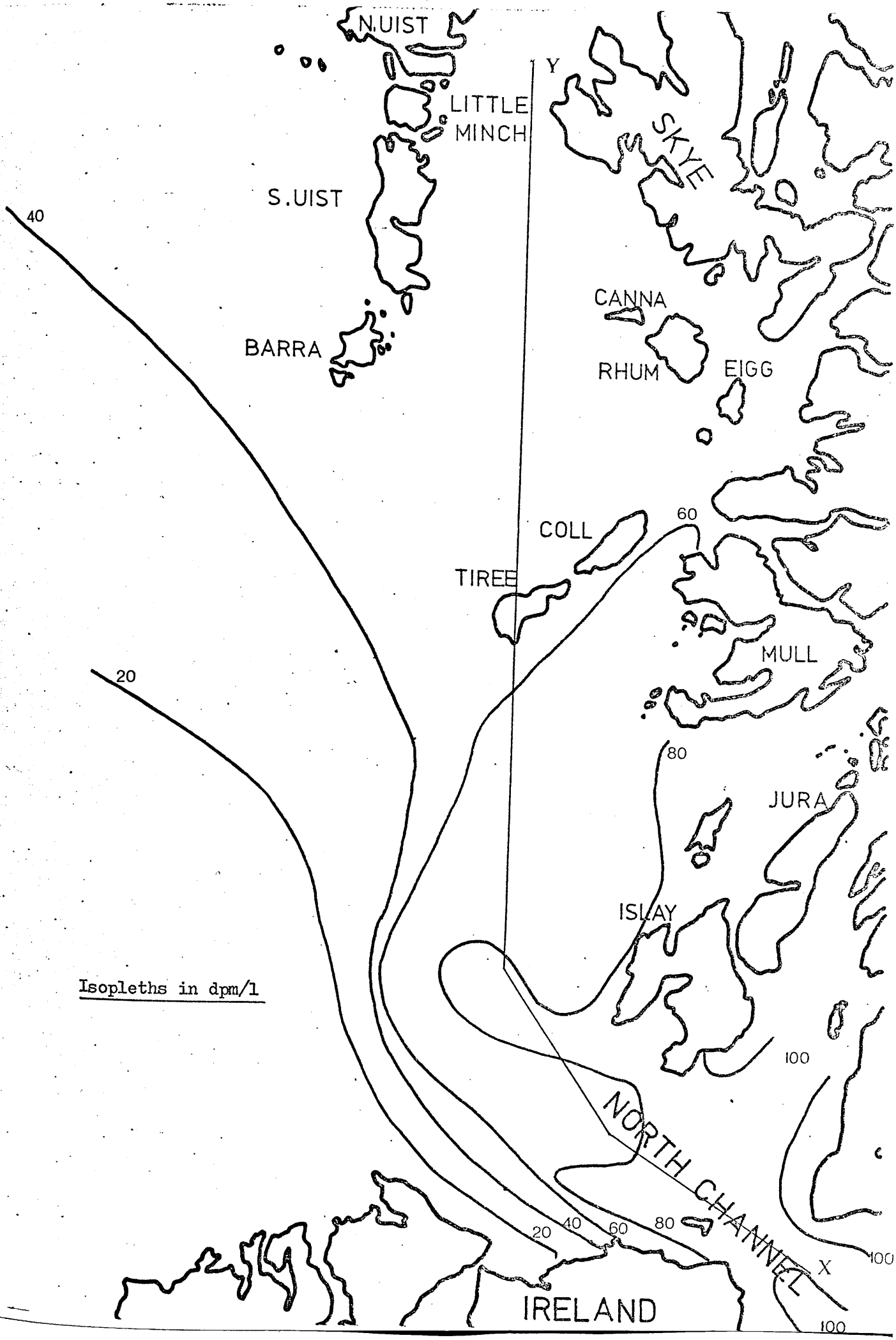

marked differences from the pattern of the previous year (Fig 5.2). These are emphasised by comparing ^{137}Cs isopleths for 1977 (Fig 5.6) with those for 1976 (Fig 5.3).

The main differences in radiocaesium distribution for the two years are:-

1) In 1977 both the physical extent of the plume and the average ^{137}Cs concentration within it are greater than in 1976. Although the sampling grid was insufficient to determine the east-west limits of the plume (as may be defined by the 1 dpm l^{-1} isopleth), the area enclosed for example, by the 30 dpm l^{-1} isopleth is $\sim$x3 greater in 1977. If the area is assumed to be of constant depth, the total ^{137}Cs inventory of the area under study may be calculated as >x2 the value for the previous year. By including the effects of increasing depths to the west of the area and of the unmeasured western extent of the plume, a more realistic estimate of the increase in ^{137}Cs content of $\sim$x3 is obtained.

2) Although once more there is a considerable horizontal gradient in radiocaesium concentration across the Islay-Malin Channel in 1977, there is no apparent Atlantic incursion into the North Channel. Indeed a steep ^{137}Cs gradient exists between Fair Head and Benbane Head on the North Irish coast. This represents a significant difference from the previous year, although it must be noted that the less extensive 1976 survey did not conclusively prove but, rather, strongly implied significant Atlantic incusion into the North Channel.

3) In contrast with the trends of 1976, there are quite significant variations in $^{134}Cs/^{137}Cs$ ratio throughout the area in 1977, a fact emphasised by the generally lower experimental errors on the more recent ratio determinations. The ratio shows a generally decreasing trend from south to north with an additional suggestion of systematic variations from east to west, particularly across the Outer Hebridean area. These ratio variations suggest significant internal transit times on the timescale of source-water radiocaesium fluctuations (i.e. in the order of months).

4) A strong front, as indicated by a steep ^{137}Cs gradient, extends from the North Irish Coast north east to approximately the latitude of northern Islay ($56^{o}N$), where it breaks down somewhat with marked widening of the plume. This observation may be compared with the strong front extending as far north as Tiree (56^{o} 30' N) in the previous year. This difference in circulation pattern could be due to the increased restrictive effect of the channels between the 'Small Islands' on the greater volume of coastal flow in 1977, causing more rapid disruption of simple northwards advection and increased lateral extension of the plume.

If the source of the coastal plume in the H.S.A. is assumed to be Clyde Sea Area/ North Channel waters, it is difficult to explain the observed differences between 1976 and 1977 ^{137}Cs plumes. Between spring 1976 and $\sim$ February 1977 there is a significant increase in the ^{137}Cs concentrations in both the N.C. and C.S.A. This increase, however, is not large enough to explain the $>100\%$ rise in ^{137}Cs content of the Hebridean Sea in 1977 on the assumption of similar water transport conditions to those derived for summer 1976. The

increase thus implied for coastal flow during summer 1977 is, however, in agreement with the large change in water transport through the N.C. around January 1977 as discussed in Chapter 3. There, it will be recalled, an extensive Atlantic influx into the Irish Sea was invoked with resultant increased water flow through the N.C. Consequent dilution of ^{137}Cs concentrations in the northern Irish Sea produced the observed relationship between N.C. and Windscale radiocaesium curves. On the basis of the data considered in Chapter 3, it was not possible to distinguish between mechanisms involving Atlantic incursion from the south through the St. George's Channel or from the north along the east Irish coast of the N.C. On the basis of the increased displacement of Irish Sea-derived water into the H.S.A. and the obvious absence of Atlantic incursion into the N.C., it may be concluded that the incursion event must, indeed, have occurred via St. George's Channel.

To facilitate analysis, the variation in average radiocaesium concentration with distance from the mouth of the North Channel, considered here as mid-way between the Mull of Kintyre and Garren Point, (along transect X - Y on Fig 5.6) may be plotted (Fig 5.7), postponing for the moment, consideration of sites west of the Outer Hebrides. From this curve it is noticed that a) over $\sim$300 km the ^{137}Cs concentration decreases by a factor of two, with major rates of dilution being 0 - 50 and 150 - 200 km from the N.C. mouth.

b) the $^{134}Cs/^{137}Cs$ is effectively constant at $\sim$0.110 over the range 0 - 200 km, after which it passes through a marked minimum of $\sim$0.097 at $\sim$260 km.

The ratio trend is particularly useful as it may be

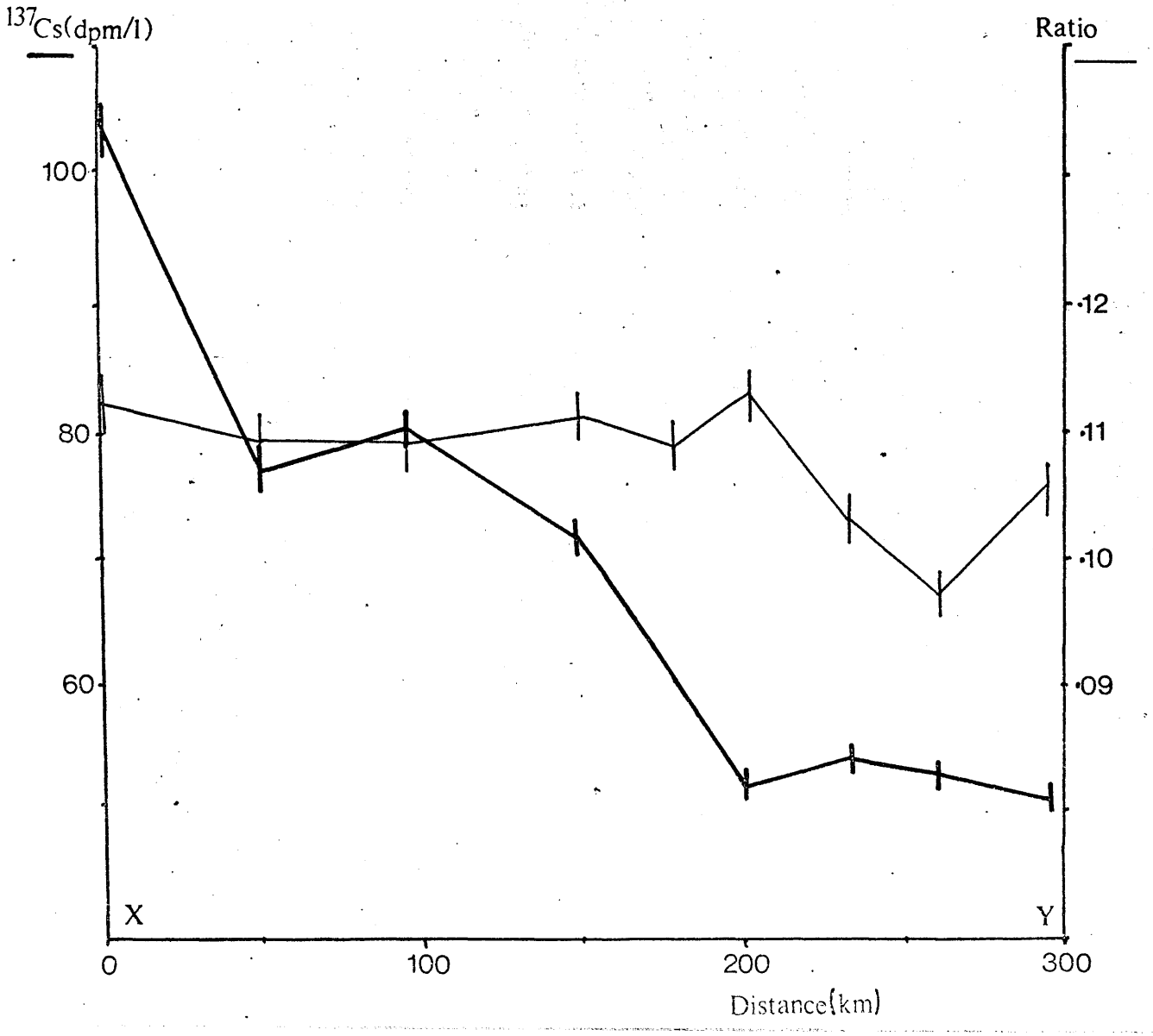
137Cs(dpm/l)
Ratio
100
80
60
·12
·11
·10
·09
X
Y
0
100
200
300
Distance(km)

(cf Fig. 5.6)

compared to curves of the temporal variation in coastal flow source water, displacement being directly related to time if the coastal advection rate is constant. To relate temporal ratio variation curves for the N.C. and C.S.A. to the observed ratio vs. distance plot, the effect of radioactive decay must be considered and, for the N.C. data, the inter-calibration constant must be invoked (Fig 5.8). No obvious relationship exists between the 'source water' curves (Fig 5.8) and the observed spatial variation, remembering that as distance is directly related to water age the x-axis of one of the figures must be inverted for direct comparison. In particular, as 'C.S.A.-type' water was considered representative of the coastal flow source, there is an absence of any feature in the June 1977 H.S.A. profile corresponding to the marked minimum in C.S.A. ratio of April while, equally, no feature matches the N.C. ratio maximum of March. A fairly constant source water curve may be generated, however, by 1:1 addition of C.S.A. and N.C. type waters with a 1 month lag of the former (which may correspond to the N.C. - C.S.A. transit time of 1 month derived in Chapter 3). This latter curve has an average ratio value of ~ 0.107 over the period January - June 1977, in reasonable agreement with the observed value of ~ 0.110 for the range 0-180 km from the N.C. mouth. The slightly lower value of the derived source average may be due to the actual percentage of 'N.C. type' water being greater than 50% (an average source ratio of 0.11 being produced by 66% N.C. plus 34% C.S.A. water types), while the lower variability of the spatial curve may reflect smoothing due to

a - North Channel (intercalibration corrected)

b - 50% N.C./C.S.A.(assumed lag 1 month N.C. site to C.S.A.)

c - Clyde Sea Area

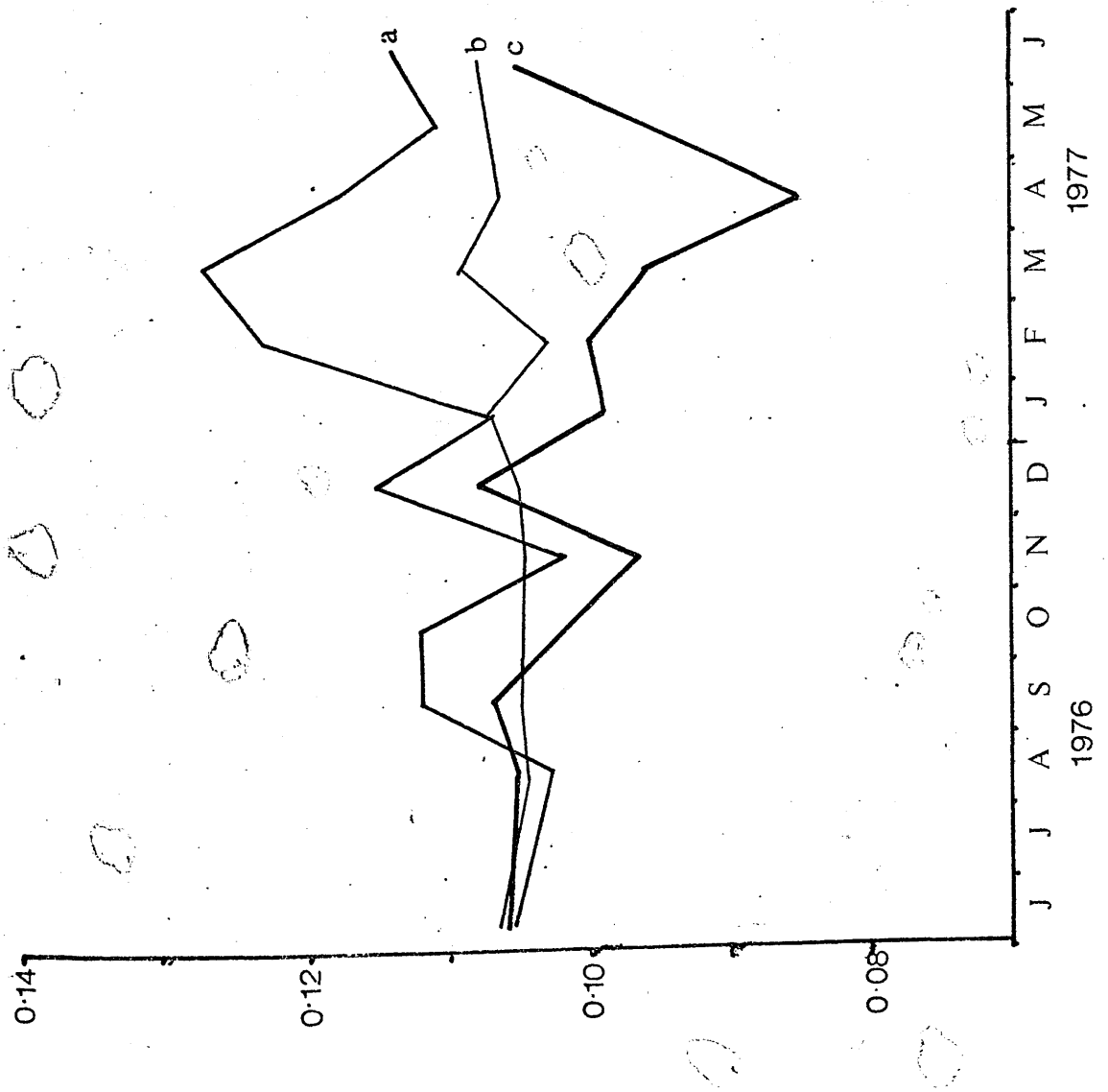

mixing in transit. Despite this initial agreement, however, there is no correlation between the derived ratio curve pre-January 1977 (very constant ratio ~ 0.105) and the observed minimum at 260 km from the N.C. It was previously noted, however, that, in January 1977, a marked change in the correlation between Windscale output and N.C. radiocaesium concentrations, occurred, implying a major alteration in the previously stable coastal flow characterisitcs (c.f. Chapter 3). If previous to January 1977, the coastal flow was as characterised for summer 1976, the source water at this time would be of 'C.S.A. type' and thus would show the ratio minimum (~ 0.097) of November 1976 corresponding to the spatial minimum of ~ 0.097. The higher ratio at ~ 300 km (0.106) may thus be matched with the C.S.A. - derived value for September 1976 (0.107). Although both the spatial and temporal sampling frequencies are low over the regions considered, from the match above an advective velocity of ~ 0.7 km day $^{-1}$ may be estimated for the southern approaches to the Little Minch. This figure, despite its very large associated errors, is much slower than any previously estimated velocities, possibly due to the complexity of the flow pattern caused by the funnelling effect of the Little Minch.

Correlating the ratio observed in the coastal water mass north of Coll with that originating from a C.S.A.-type mixing zone around November 1976 and taking the distance from this mixing box to the N.C. mouth (as defined) as ~ 50 km implies an average advective rate of 1.5 km day^{-1} through this region, markedly lower than that observed in the previous

year. (For direct comparison the 1976 transit time of 2 months from the mixing area to Islay-Malin and 1 month for Islay to Barra must be added to give an average advective rate for the entire transit of 3.4 km day^{-1}). This apparently contradictory decrease in coastal flow rate resulting from increased flow from the Irish Sea into the North Channel may, in fact, be a quite reasonable consequence of the associated marked widening of the coastal plume. Other possibly significant factors may be the absence of Atlantic incursion along the North Irish Coast into the Eastern N.C. and the decreased rate of dilution observed from south to north in the H.S.A. In the previous section it was noted that correlation between rate of dilution and advection rate implied 'driving' of the coastal current by Atlantic flow. Thus an absence of Atlantic incursion into the N.C. would preclude this driving effect and would therefore decrease the total change in advection expected from increased Irish Sea input to the North Channel. Widening of the plume would decrease the extent of Atlantic interaction with more easterly waters, as reflected in decreased dilution rates.

While this explanation of the observed distribution of ratio values in the H.S.A. is somewhat complex, additional support for the proposed model is to be found in the values obtained at sites to the west of the Outer Hebrides. Craig (1956) has shown that the constriction of the Little Minch causes a flow southwards along the east coast of Uist, round Barra Head, and northwards along the west coast of the Outer Hebrides. This transport phenomenon would explain the similarity in ratio between the sites to the south west of Uist and those in the southern approaches of the Little Minch, as

the water in these areas would be of similar 'age'. The more northerly sites to the west of Benbecula thus represent older water which has a ratio of ~ 0.108, in agreement with a predicted value from the model of ~ 0.107 assuming the rate of advection along the west coast of Uist is similar to that between the N.C. and Coll. The Barra Head - Benbecula transit time is therefore ~ 2 months.

5.4 General Conclusions

The radiocaesium distributions in the Hebridean Sea Area during the summers of 1976 and 1977 imply very marked differences in coastal flow through the region for these two years. For 1976, the 'coastal plume' can be explained by a flow from the mid-North Channel (Stranraer-Larne) to the southern region of the H.S.A., characterised by an advection velocity of ~ 1.6 km day^{-1} and a residence half time of ~ 2 months, followed by rapid northwards advection of a well-defined coastal water body at a velocity $\gtrsim 5$ km day^{-1}. In 1977 a more extensive plume resulted from effective flushing of Irish Sea water through the N.C. Thus, at the time of the survey, source 'coastal water' to the H.S.A. could be regarded as a composite of $\sim$66% directly advected mid-North Channel (Stranraer-Larne) water added (with a 1 month lag) to $\sim$34% water mixed with a residence time of ~ 2 months ('C.S.A. type'). In 1977 the N.C. - Barra advection rate has decreased by a factor of ~ 2 from the previous year to ~ 1.5 km day^{-1} while the northwards velocity in the southern approaches to the Little Minch was even lower at ~ 0.7 km day^{-1}.

In the above 'explanation' of observed variations in water flow within the H.S.A., only coastal phenomena have

been considered. A more direct explanation would involve consideration of the behaviour of Atlantic currents which, to a large extent, drive the coastal flow. This approach is, however, outwith the experimental limits of this project.

Because of the major differences in coastal flow pattern during the 2 years of study, it is difficult to present 'typical' values for hydrographic parameters within the Hebridean Sea Area. Records of long-term North Channel radiocaesium variations imply that 1977 was markedly different to preceding years (Chapter 3) but continued work in the area will be required both to prove this point and to determine the time required for the system to return to 'normal' after this flushing event.

Chapter 6

Sediments

6.1 Introduction

In previous chapters the effectively conservative nature of radiocaesium in the marine environment has been cited as a major advantage in its application as a water tracer. Loss to sediment has been considered negligible during water transport. In this chapter, however, the extent of radiocaesium removal into coastal marine sediments will be evaluated. Tracer applications in these deposits will also be considered.

As previously discussed (Chapter 1), there is considerable controversy with regard to the degree both of radiocaesium immobility (chemical) within the sediment column and of re-depositional mobilisation through physical and biological turbation processes. An additional restriction to the application of radiocaesium as a sediment tracer is the general requirement of retention of the sediment surface during coring (as its general use involves stratigraphic marking rather than establishment of a concentration gradient by decay). Thus a well-defined coring technique is essential. The importance of these limitations will be determined here in a general study of radiocaesium methodology as applied to coastal marine sediments. The radiocaesium data obtained will be compared with those from complementary natural series Geochemical studies (MacKenzie, 1977; Swan, 1978).

At this stage it is worth emphasising the importance of considering porosity variations when interpreting sediment data.

As the sediments of the C.S.A. have high surficial water contents ($\gtrsim 90\%$) decreasing with depth, it is difficult to define rigorously a sedimentation rate in cm y^{-1} (or alternative length-based unit) as no absolute datum line is available. Thus sedimentation rates quoted in this manner must be taken as the upwards velocity of the sediment/water interface relative to a reference position at depth in the sediment with defined porosity which is invariant with time (at least on the timescale considered). An alternative treatment circumvents the effects of porosity changes by defining depth in terms of g cm^{-2} - the cumulative mass of dry sediment per unit area profile (measured from the sediment/water interface) corrected for the weight of contained pore-water salt. This treatment also avoids some errors in sectioning as it does not require rigorous definition of sample thickness. Sedimentation rates may thus be defined as the rate of accumulation of sediment (in g cm^{-2}) above any distinctive feature at depth.

The radiocaesium profiles of all cores analysed in this study are listed in Appendix I.5, while positions corresponding to the sample codes are listed in Table 6.1 and plotted in Fig 6.1

6.2 Coring methodology

As discussed in Chapter 2, sediment cores have been obtained from the Clyde Sea Area using both a small diameter 'Umel' gravity corer and a soft-landing, hydraulically-damped, 'Craib' corer. Initial measurements by MacKenzie (1977) implied that the gravity corer tends to lose ~8 cm of surface sediment during coring, while the Craib corer recovers the sediment surface intact. This observation was examined further by

TABLE 6.1 CORE PROFILES ANALYSED.

SITE	DATE	CODE	CORE TYPE	TOTAL LENGTH
L.GOIL 1	4/2/76	LGG5	GRAVITY	45cm.
56 08' 20"N				
04 53' 21"W	10/8/76	LGC9	CRAIB	18cm.
	28/6/77	LGC11	CRAIB	13cm.
		LGC12		10cm.
L.GOIL 2	4/2/76	LGG7	GRAVITY	
56 06' 8"N				
04 53' 1"W	3/3/76	LGC4	CRAIB	18cm.
GAIRLOCH	14/1/74	GLG1	GRAVITY	
56 02' 42"N				
04 49' 36"W	6/11/75	GLC3	CRAIB	15cm.
HOLYLOCH	28/6/77	HLC1	CRAIB	10cm.
L.LOMOND	22/8/76	LLRPM1	MACKARETH	96cm.
56 03' N				
4 35'W				

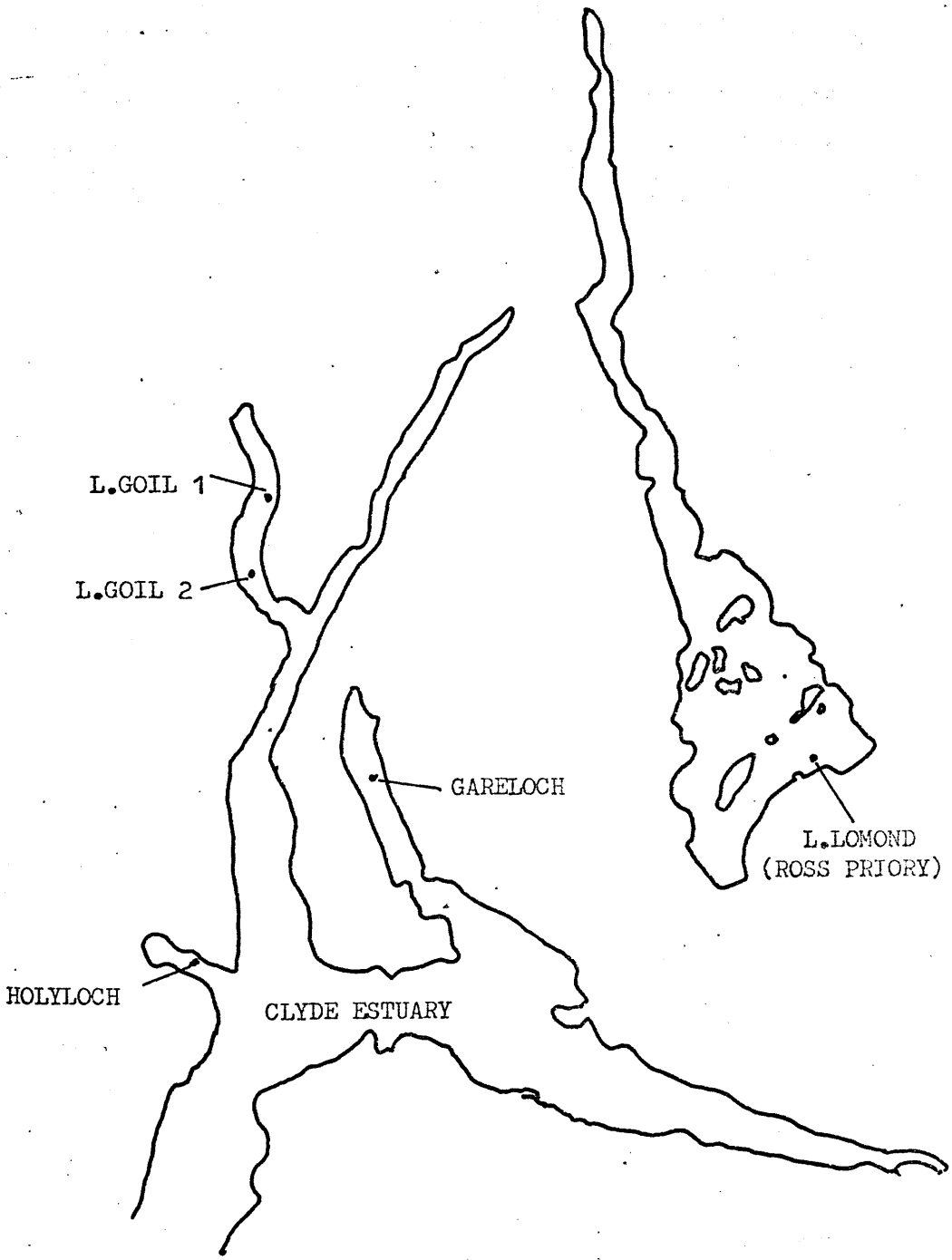
L.GOIL 1
L.GOIL 2
GARELOCH
L.LOMOND
(ROSS PRIORY)
HOLYLOCH
CLYDE ESTUARY

comparing radiocaesium profiles in gravity and Craib cores from three different sites (Fig 6.2 - 6.7).

At L. Goil site 1, comparison of LGG5 (Fig 6.2) with LGC9 (Fig 6.3) indicates considerable disturbance during gravity coring. As the ^{134}Cs concentration is within $\sim 1\sigma$ of background at the surface of LGG5, loss of $\sim$ 10 cm ($\sim$2.6 g cm^{-2}) is implied. The ^{137}Cs concentrations in the gravity core between 1 - 4 cm, however, correspond to concentrations found at ~8 - 9 cm in the Craib core. These observations are probably best explained by postulating that gravity coring has induced considerable mixing and loss of surface sediment. As the ^{137}Cs activity at 8 cm ($\sim$ 2.1 g cm^{-2}) in the gravity core is less than that at 17 cm ($\sim$4.9 g cm^{-2}) in the Craib core, a loss of $\gtrsim$10 cm length (or more rigorously $\sim$ 2.8 g cm^{-2}) of the sediment column is implied. At station 2 in L. Goil, a more distinct profile in the gravity core (LGG7 - Fig 6.4) is apparent, but comparison with a Craib core from the same site (LGC4 - Fig 6.5) indicates that 0 - 3 cm (0 - 0.5 g cm^{-2}) in the gravity core is the residue of a mixing/loss process during coring, while 3 - 5 cm (0.5 - 1.1 g cm^{-2}) may overlap with 15 - 17 cm (5.1 - 5.5 g cm^{-2}) in the Craib core. As the 6 - 7 cm (1.4 - 1.5 g cm^{-2}) section in the gravity core has a ^{137}Cs concentration less than that at 17 cm (5.5 g cm^{-2}) in the Craib core, a loss of at least 11 cm length ($\sim$ 4 g cm^{-2}) is implied. Cores taken from a different loch (Gareloch - cores GLG1, Fig 6.6 and GLC3, Fig 6.7) show exactly the same trends with a mixed residue present in the upper few centimeters ($\sim$0 - 0.5 g cm^{-2}) and a total column loss of $\gtrsim$13 cm ($\sim$4.1 g cm^{-2}).

FIGURE 6.2 L.G.G.5. RADIOCAESIUM PROFILE

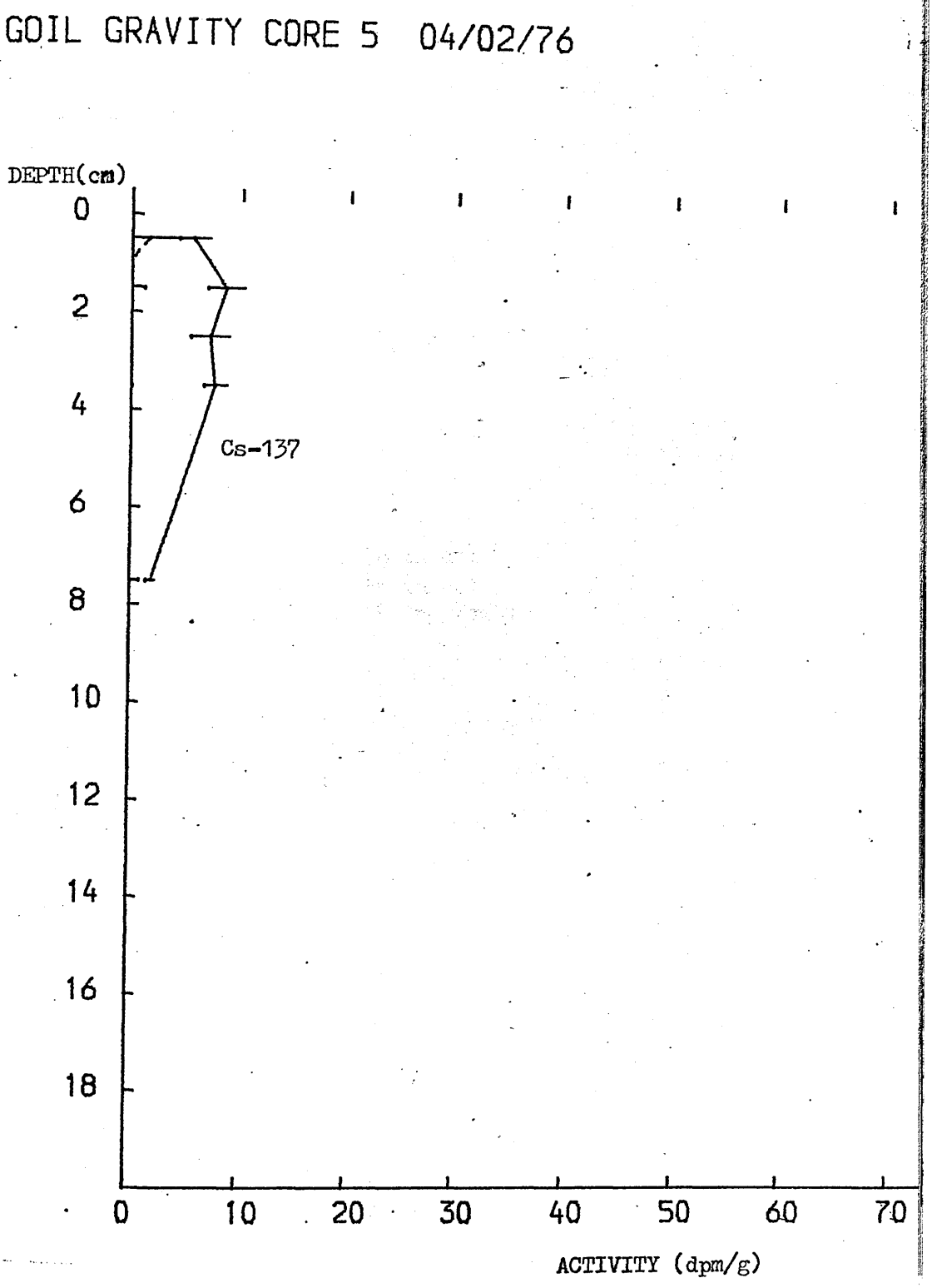

FIGURE 6.3 L.G.C.9. RADIOCAESIUM PROFILE

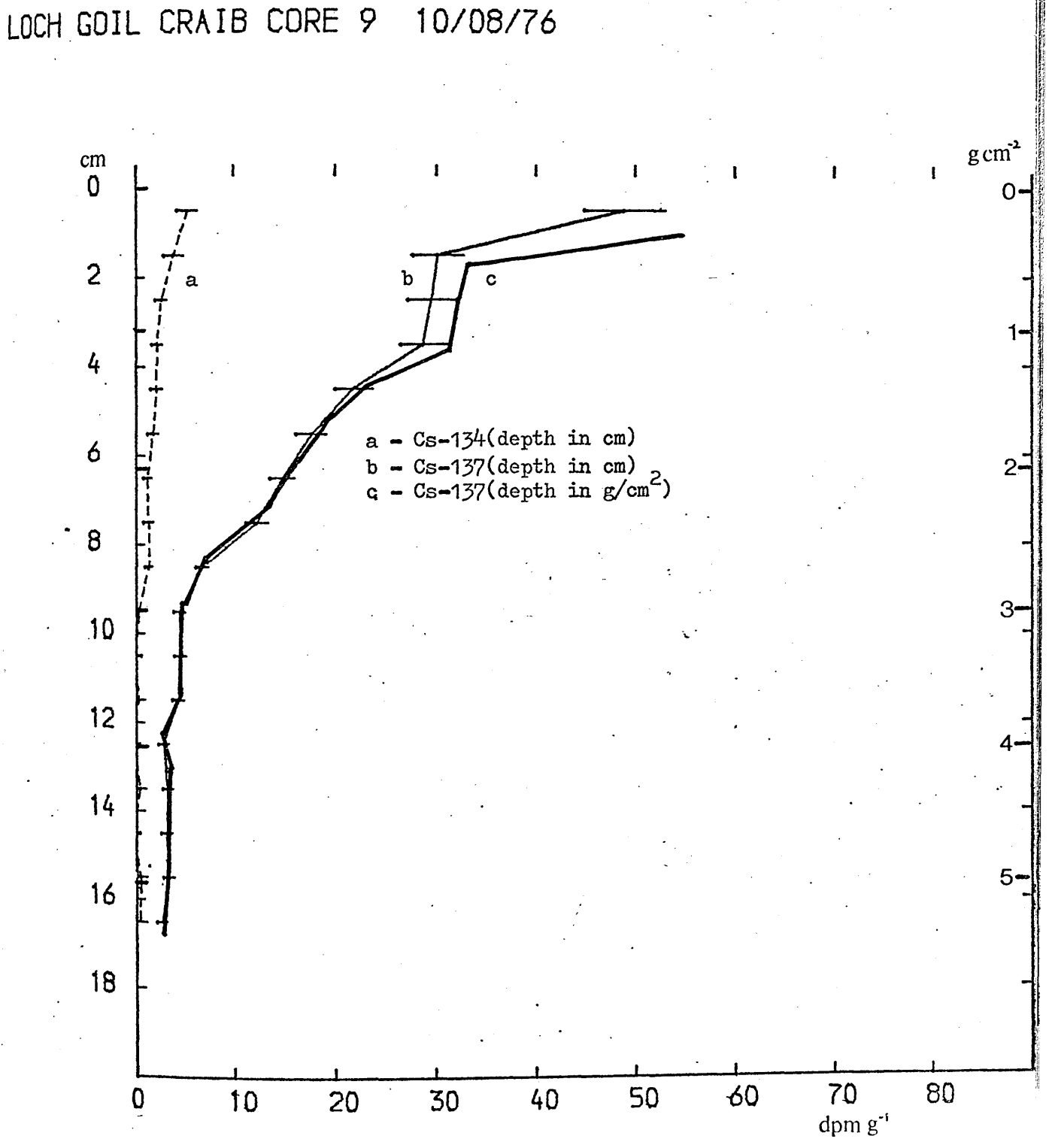

FIGURE 6.4 L.G.G.7. RADIOCAESIUM PROFILE

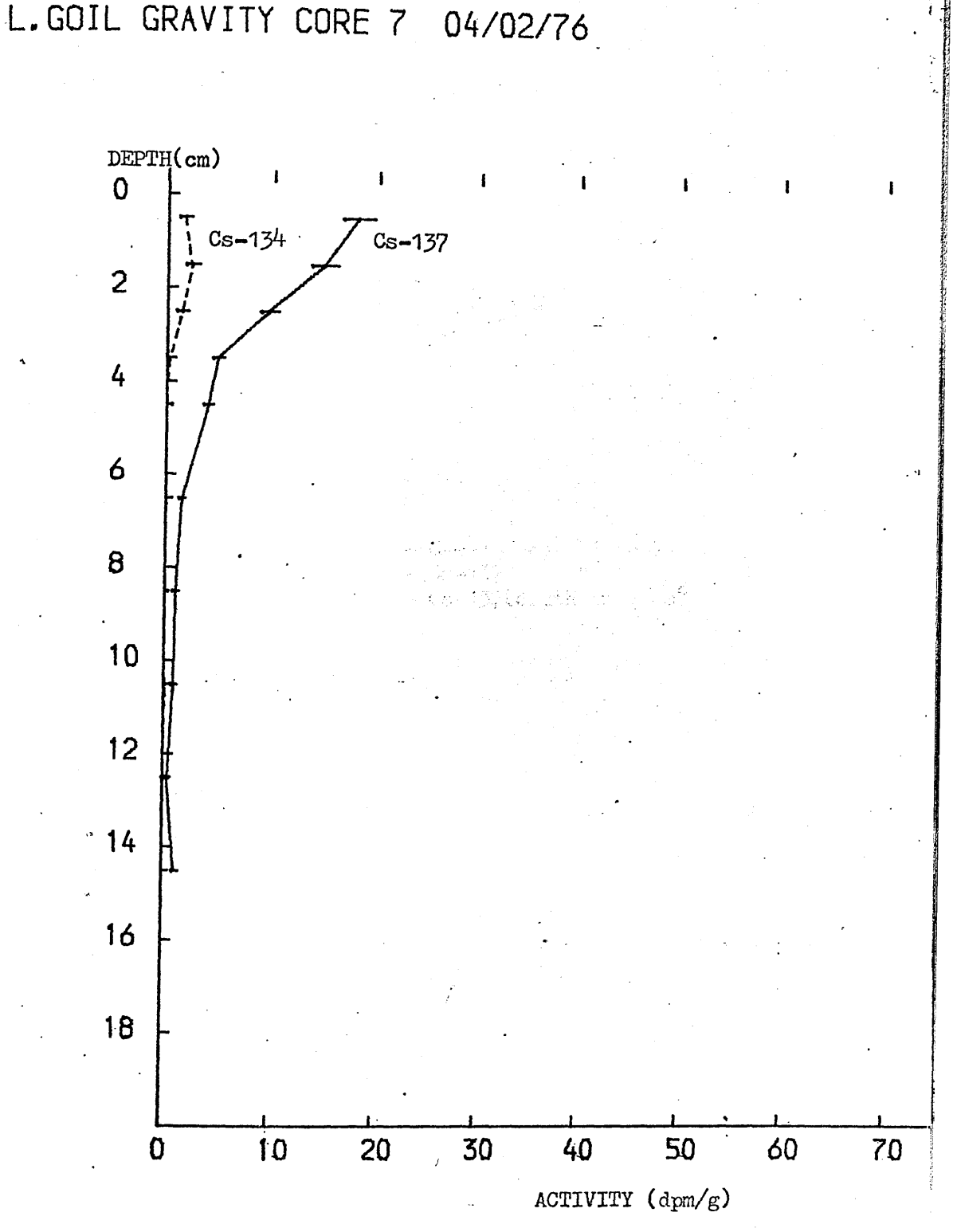

FIGURE 6.5 L.G.C./4. RADIOCAESIUM PROFILE

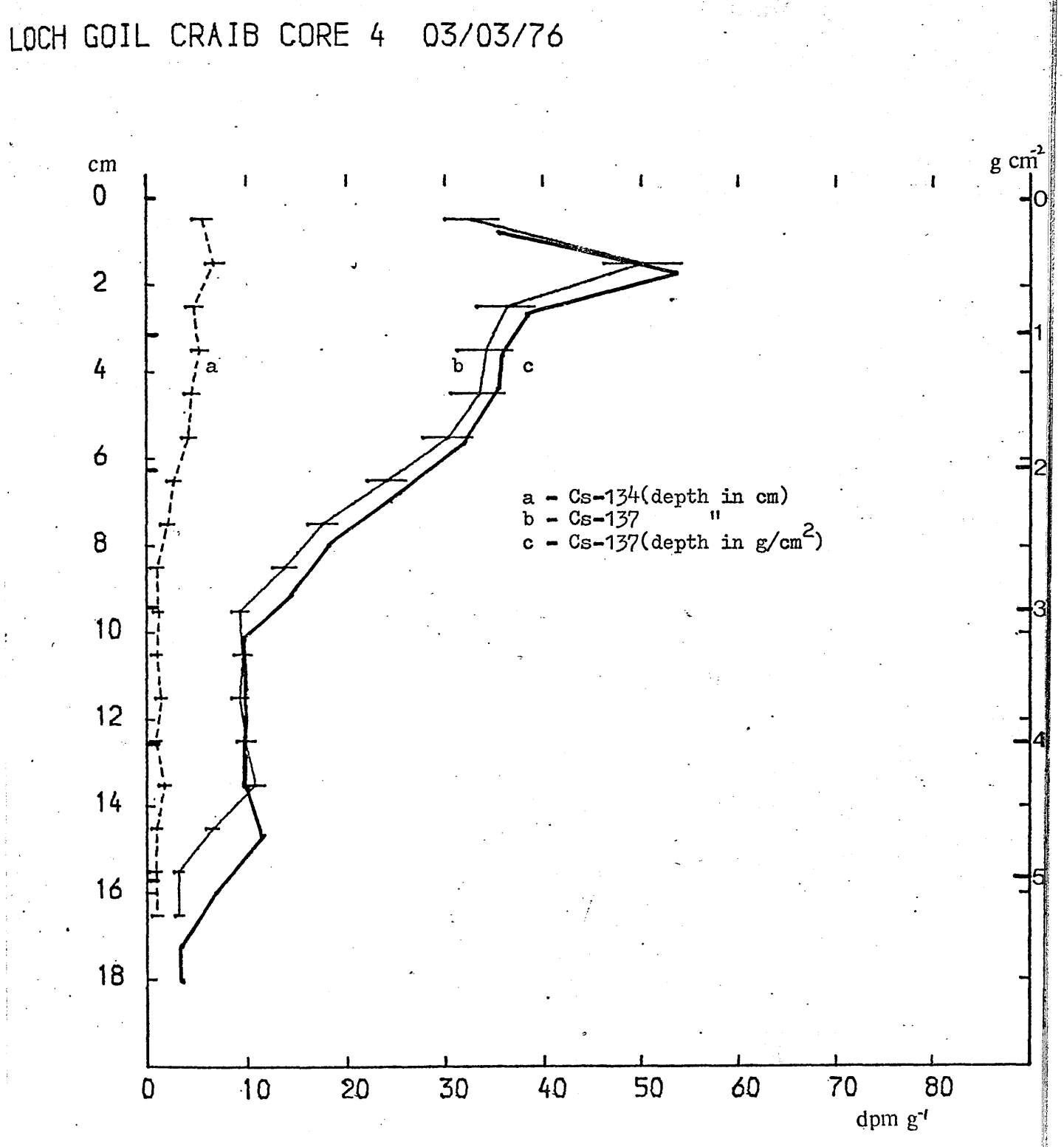

FIGURE 6.6 G.L.G.1. RADIOCAESIUM PROFILE

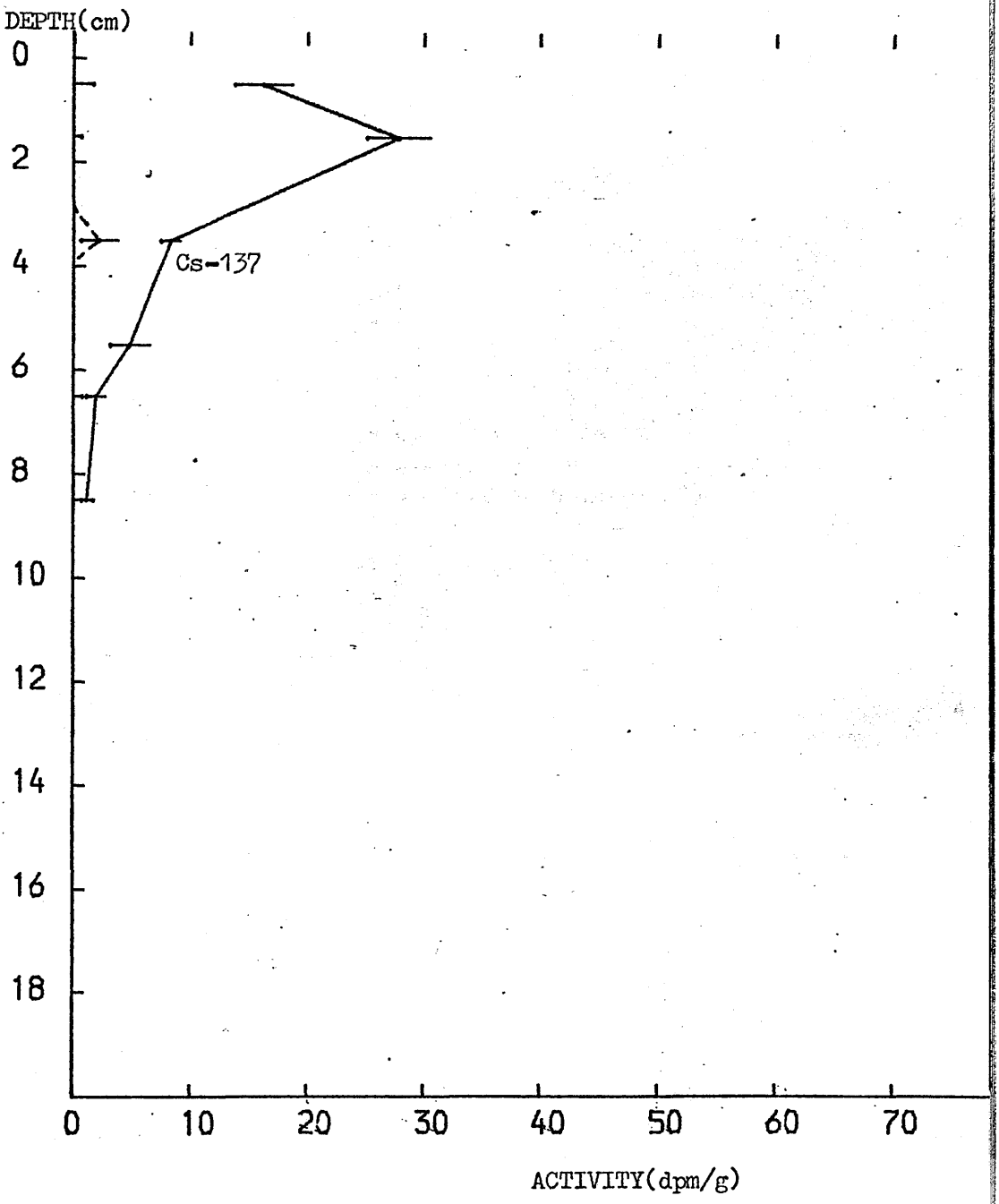

FIGURE 6.7 G.L.C.3. RADIOCAESIUM PROFILES

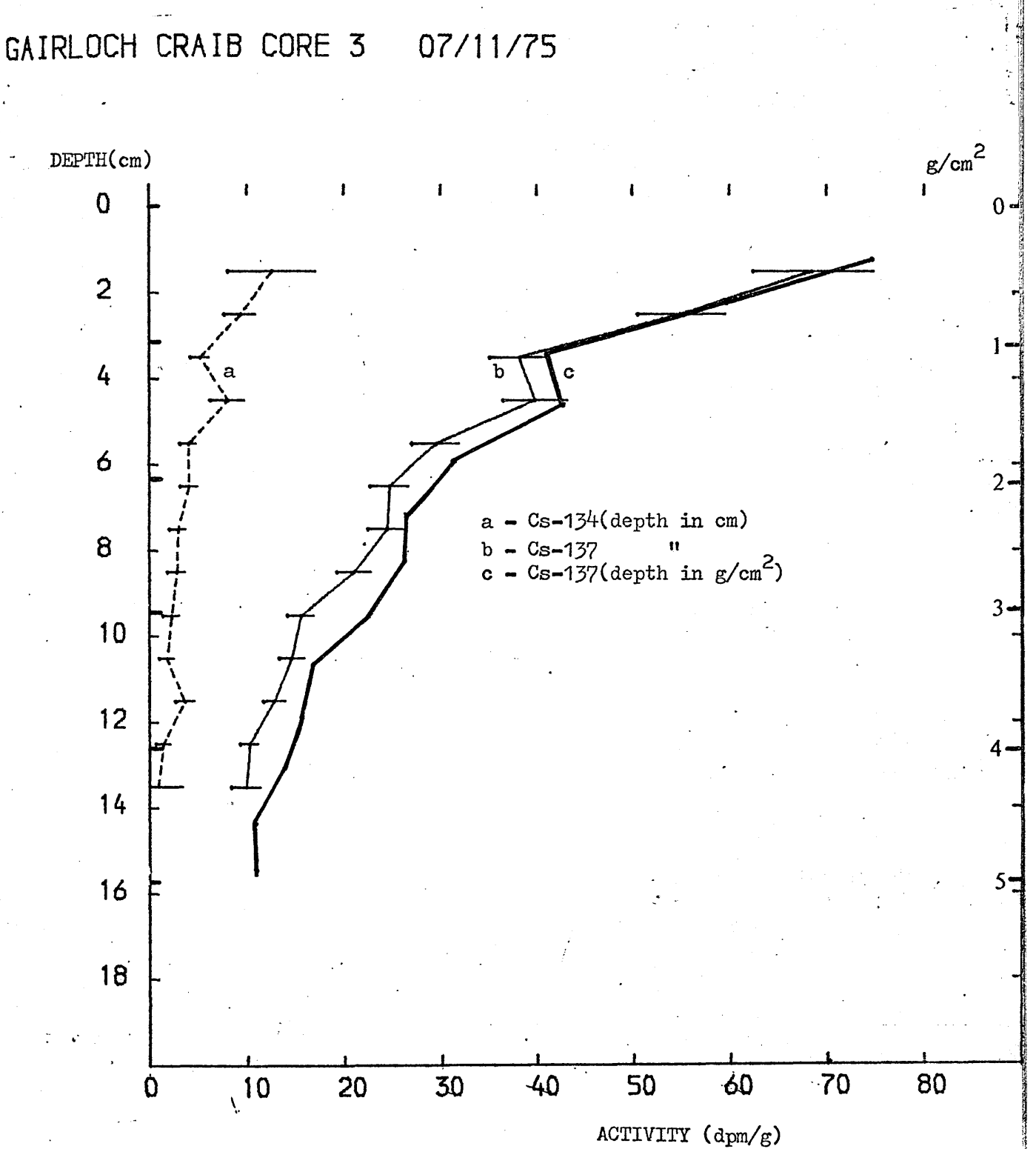

These observations agree well with conclusions from other radionuclide data in Clyde Sea Area sediments (MacKenzie, 1977; Swan, 1978) and prove that gravity coring of high porosity sediments has not retained surface ($\lesssim$15 cm or 4.5 g cm^{-2}) material. Furthermore, the apparent surface of such cores is actually a residue of mixed sediment from undefined depth. This loss appears, however, to be much less in sediments of lower porosity but may still be significant (Swan, 1977).

A major, but unproven, assumption of previous studies, however, is that the Craib corer reproducibly retains surface sediment, thus allowing evaluation of total ^{137}Cs or ^{210}Pb inventories (MacKenzie, 1977; Swan, 1978). This premise was investigated by comparing radiocaesium profiles of duplicate cores, LGC11 and LGC12 (Figs 6.8 and 6.9), taken at the same site on the same day. It must be noted however, that after collection, core LGC11 was immediately frozen and, after return to the laboratory, sectioned with a band-saw, while LGC12 was directly extruded with a piston, sectioned while wet and then frozen pending analysis.

At a simple level, comparison of these profiles indicates a very good match below 1 cm depth in both profiles - a match improved to near identity by downwards displacement of LGC11 by $\sim$0.5 cm. This would appear to imply the loss of most of the surface 1 - 1.5 cm in LGC11 during coring leaving only a high porosity suspension in its place. Integrating the total ^{137}Cs activity over the region 0 - 10 cm yields a value of 1482 dpm for LGC11 compared to 1697 dpm for LGC12 - a net difference of $\sim$13%. It is interesting to note that this 217 dpm inventory deficit of LGC11 is larger than the expected content

FIGURE 6.8 L.G.C.11. RADIOCAESIUM PROFILE

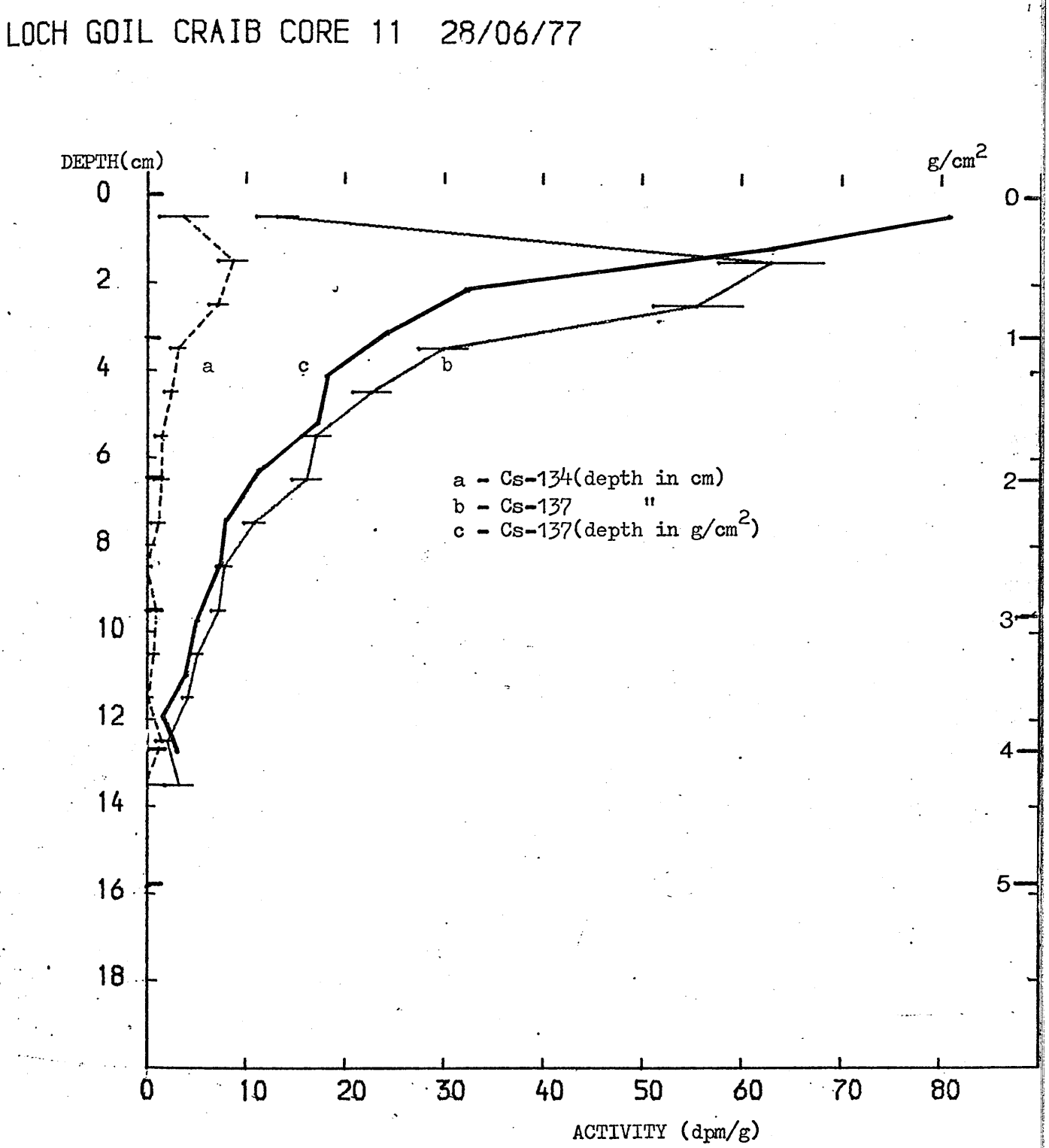

FIGURE 6.9 L.G.C.12. RADIOCAESIUM PROFILE

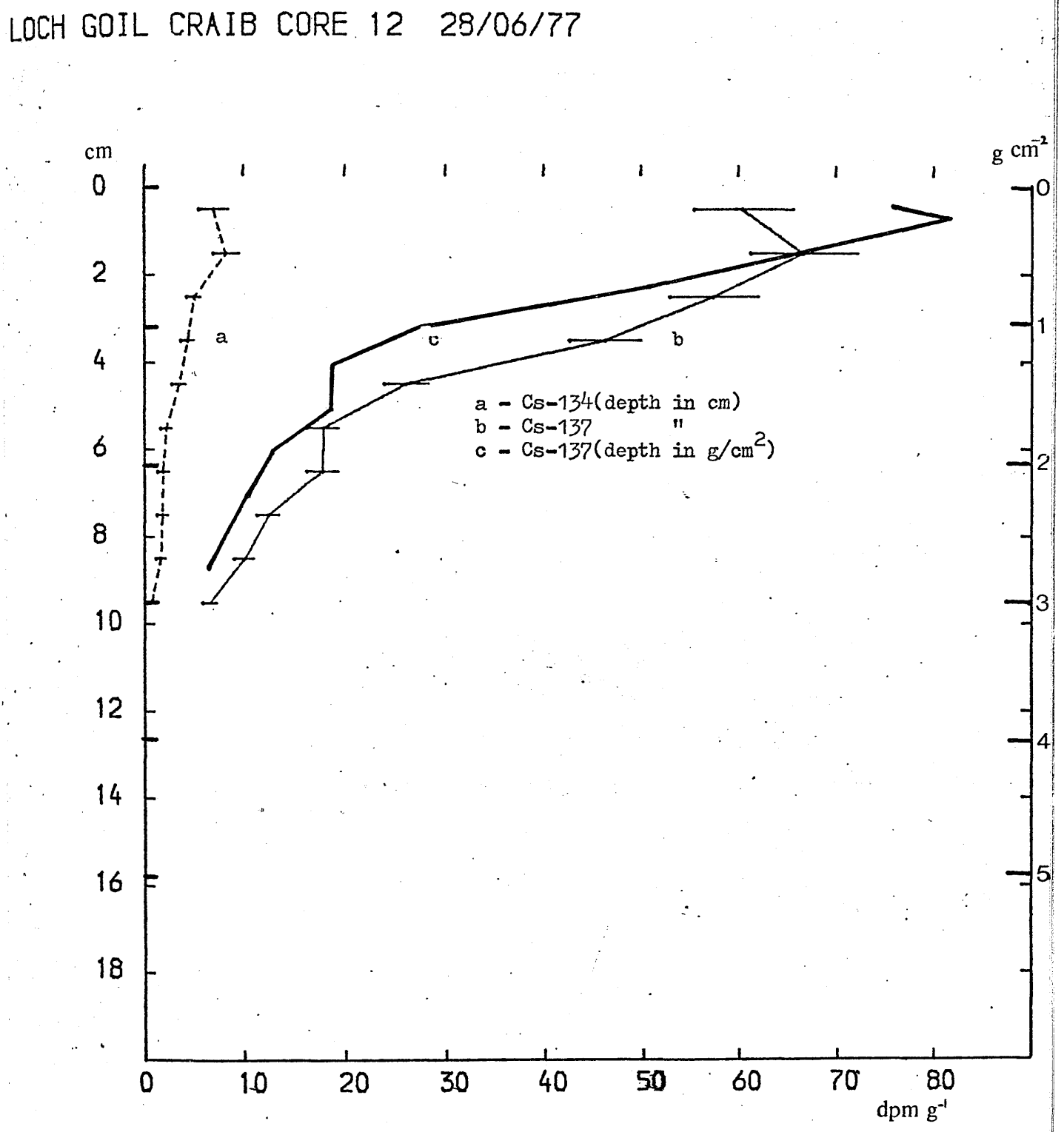

of the 'lost' 1.5 cm ($\sim$ 170 dpm). Similarly, comparison of the porosity-corrected profiles for LGC11 and LGC12 indicates a surface loss of $\sim$0.08 g cm^{-2} with an overall difference in integral from 0 - 2.3 g cm^{-2} of 8.72 dpm - equivalent to LGC11 being~11% less than LGC12 (the expected content of the surface 0.08 g being $\sim$6.5 dpm).

The deficit in LGC11 integral over that expected by surface loss may be explained by loss during sectioning. This may seem anomalous as LGC11 was directly extruded while wet on board ship and thus might be expected to have suffered more loss of material than LGC11 which was sectioned in the laboratory. Careful direct wet extrusion and sectioning, however, observably results in little material loss. Sub-sampling of frozen cores by band-saw, on the other hand, results in loss of an undefined portion of the core dependent on the effective cutting width of the blade. Such loss is difficult to quantify directly because of the effects of evaporation and spattering caused by frictional heating and high speed saw action and of water vapour condensation on the cold core. This explanation is further supported by the observed better match for non-porosity-corrected profiles than for the corrected data (if sub-sample width determination is accurate) and by the slightly decreased integral deficit between corrected profiles.

An additional duplicate pair of Craib core radiocaesium data is provided by GLC3 and GLC1 (analysed by MacKenzie (1977)), these cores being obtained on the same day from the Gareloch site. Although only counting errors associated with MacKenzie's determination are presented, there is, nevertheless, very good apparent agreement throughout the profiles (Fig 6.10)

FIGURE 1.10 CAESIUM PROFILES BY DEPTH

(analysed by MacKenzie, 1977)

GARELOCH CRAIB CORE 1 7/11/75

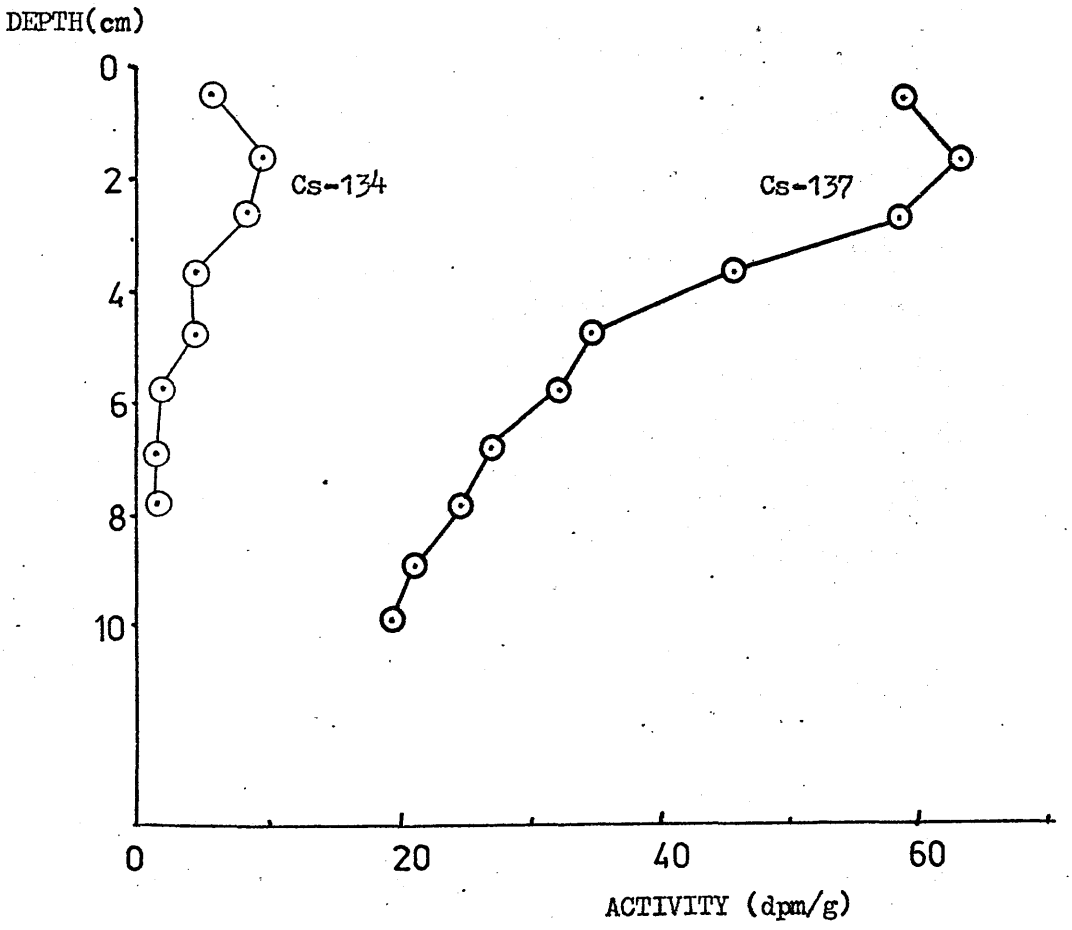

(noting that section 1 of GLC3 was unobtainable for radiocaesium analysis). This match indicates both reproducible sampling with surface retention by the Craib corer and good inter-calibration between the measurement system used in this project (direct counting on a Ge(Li)) and that of MacKenzie (total sediment dissolution, extraction onto KCFC and counting on a flat-top NaI(Tl) detector). The deeper penetration of ^{134}Cs observed in GLC3 relative to GLC1 is probably an artifact resulting from the lower detection limit of the Ge(Li) system because of the lower counter background, higher resolution and greater quantity of material used in the non-destructive analytical system (cf Chapter 2). Similarly, the generally lower ^{134}Cs values observed by MacKenzie indicate a systematic error in determination of this parameter, but this discrepancy may be exaggerated bythe proximity of nuclide levels to the detection limit (particularly in the case of the NaI(Tl) system).

It is thus concluded that the Craib corer is generally reliable but may lose $\sim 1 - 1.5$ cm (or, more rigorously, ~ 0.08 g cm^{-2}) of surface sediment. Such losses decrease the ^{137}Cs inventory to depth by $\sim 10\%$ while sectioning with a band-saw may introduce a further decrease of $\sim 3\%$. Direct wet extrusion and sectioning thus appears to be a preferable technique to cutting of frozen core because of the decreased extent of material loss in the sectioning process. It must be noted that the magnitude of these inventory losses will be dependant on the actual radiocaesium distribution and that they are underestimated by measuring depths in g cm^{-2}. In comparison of core profiles, therefore, expression of depth in g cm^{-2} to

avoid porosity changes may thus introduce alternative errors - particularly when comparing cores sectioned by different methods.

6.3 L. Goil - Site 1

In previous work on sediments from the Clyde Sea Area, MacKenzie (1977) considered that, while radiocaesium proved to be a good qualitative indicator of bioturbation of upper sections of sediment cores, it could not be used as a reliable geochronological tracer. As the extent of remobilisation of radiocaesium in marine sediments is, however, unresolved in the literature (cf eg Auffret et al, 1971; Duursma and Eisma, 1973; Hetherington and Jefferies, 1974; Hess et al, 1978; Patel et al, 1978) and is probably dependant, to some extent, on sediment type, it was intended to investigate this process further.

A preliminary estimate of the mobility of radiocaesium in C.S.A. sediment was derived from a simple desorption experiment in which 25g aliquots of a homogeneous bulk sediment sample from L. Goil, site 1 (previously dried by suction through a 0.22 μm Millipore filter) were shaken with a series of solvents. Each sample was vigorously shaken mechanically with 100 ml of each solvent, filtered dry and the process repeated a second time. The combined filtrates were evaporated to dryness and counted by direct γ-spectrometry in a standard counting vial (Table 6.2). Although this experiment is somewhat crude, it illustrates reasonably strong binding of the radiocaesium, with $<10\%$ being removed by agitation in artificial sea water (indeed this value is probably an overestimate of the

TABLE 6.2

SOLVENT EXTRACTION OF ^{137}Cs FROM BULK SEDIMENT.

SAMPLE CODE	SOLVENT	% REMOVAL
SE 1	$CHCl_3$	0
SE 2	C_2H_5OH	4.6%
SE 3	CCl_4	6.7%
SE 4	Sea Water (artificial)	7.9%
SE 5	0.1M HCl	48.4%
SE 6	1M HCl	100%

true extent of removal because of the probable contribution from salts dried during evaporation of pore waters). In addition, <50% is removed by 0.1M HCl. The low efficiency of elution by organic solvents suggests that radiocaesium in these sediments is associated mainly with the inorganic sedimentary phase. These findings are in good agreement with those of Heatherington and Jefferies (1974) for a similar estuarine sediment. The extent of caesium remobilisation will be considered further in the interpretation of observed vertical profiles of radiocaesium in L. Goil sediments.

Much quantitative information on sedimentation processes occurring in the Clyde Sea Area may be obtained from interpretation of data from cores from the L. Goil deep site (LG1) as three Craib cores have been obtained there at approximately yearly intervals - LGC2 (analysed by MacKenzie (1977) again by core dissolution and KCFC extraction of radiocaesium followed by counting on a flat-top NaI (Tl) detector (Fig 6.11)), LGC9 and LGC12. Comparison of the radiocaesium profile of the most recently obtained core, LGC12, (Fig 6.9) with the annual variation in Windscale output of ^{137}Cs and ^{134}Cs (corrected for decay to 1977) (Fig 6.12) suggests a simple relationship between the two curves. The apparent similarity is emphasised by expressing the depth axis in units of mg cm^{-2}. Direct correlation of the 1975 Windscale output peak to the maximum at $\sim$90 mg cm^{-2} and the beginning of the output plateau of 1970 to the feature of $\sim$1250 mg cm^{-2} yields an apparent sedimentation rate of $\sim$230 mg cm^{-2} y^{-1} (in good agreement with a sedimentation rate of 200 mg cm^{-2} obtained for this site by ^{210}Pb dating (Swan, 1977)). The inapplicability of this simple accumulation

FIGURE 6.11 L.G.C.2. RADIOCAESIUM PROFILE

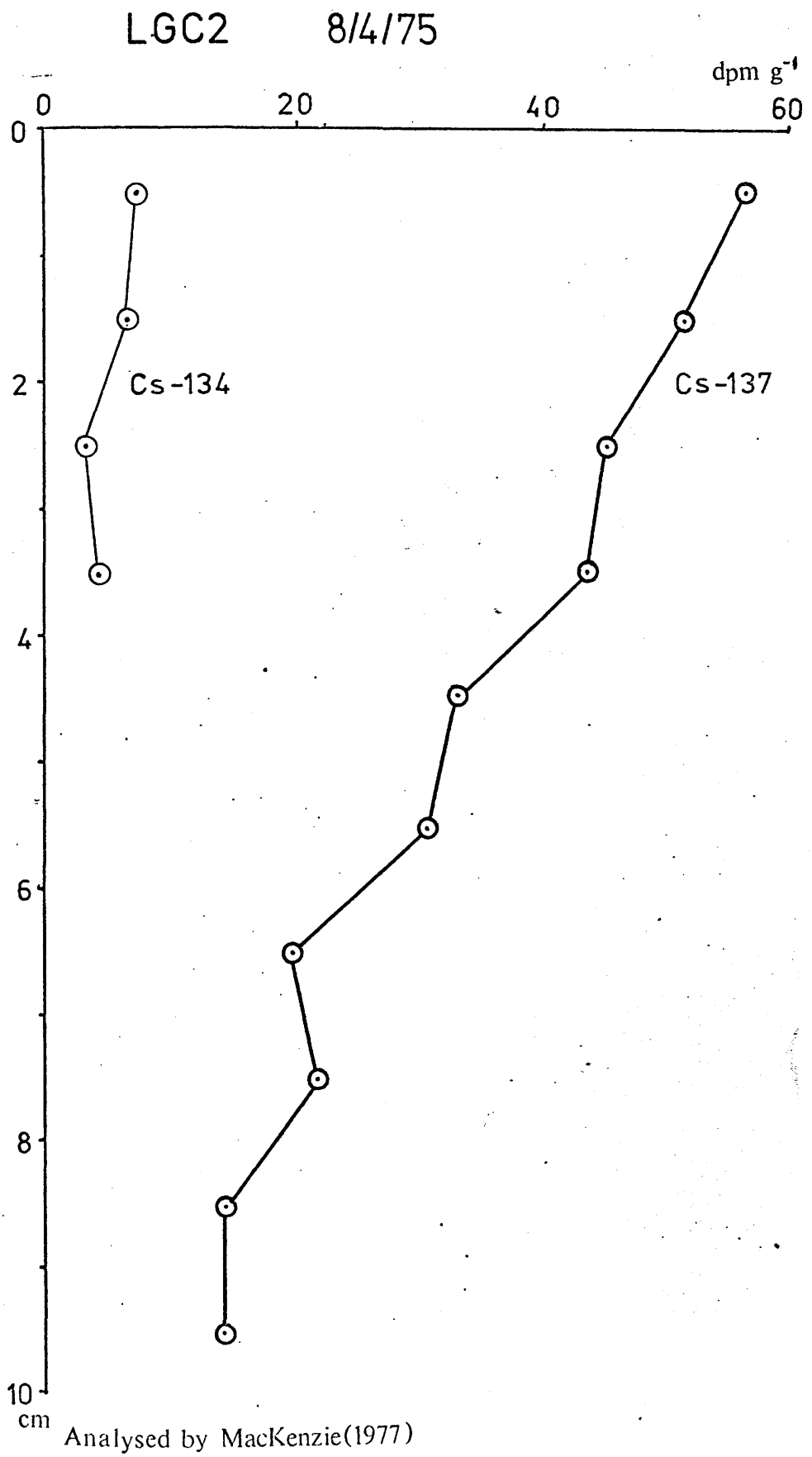

Analysed by MacKenzie(1977)

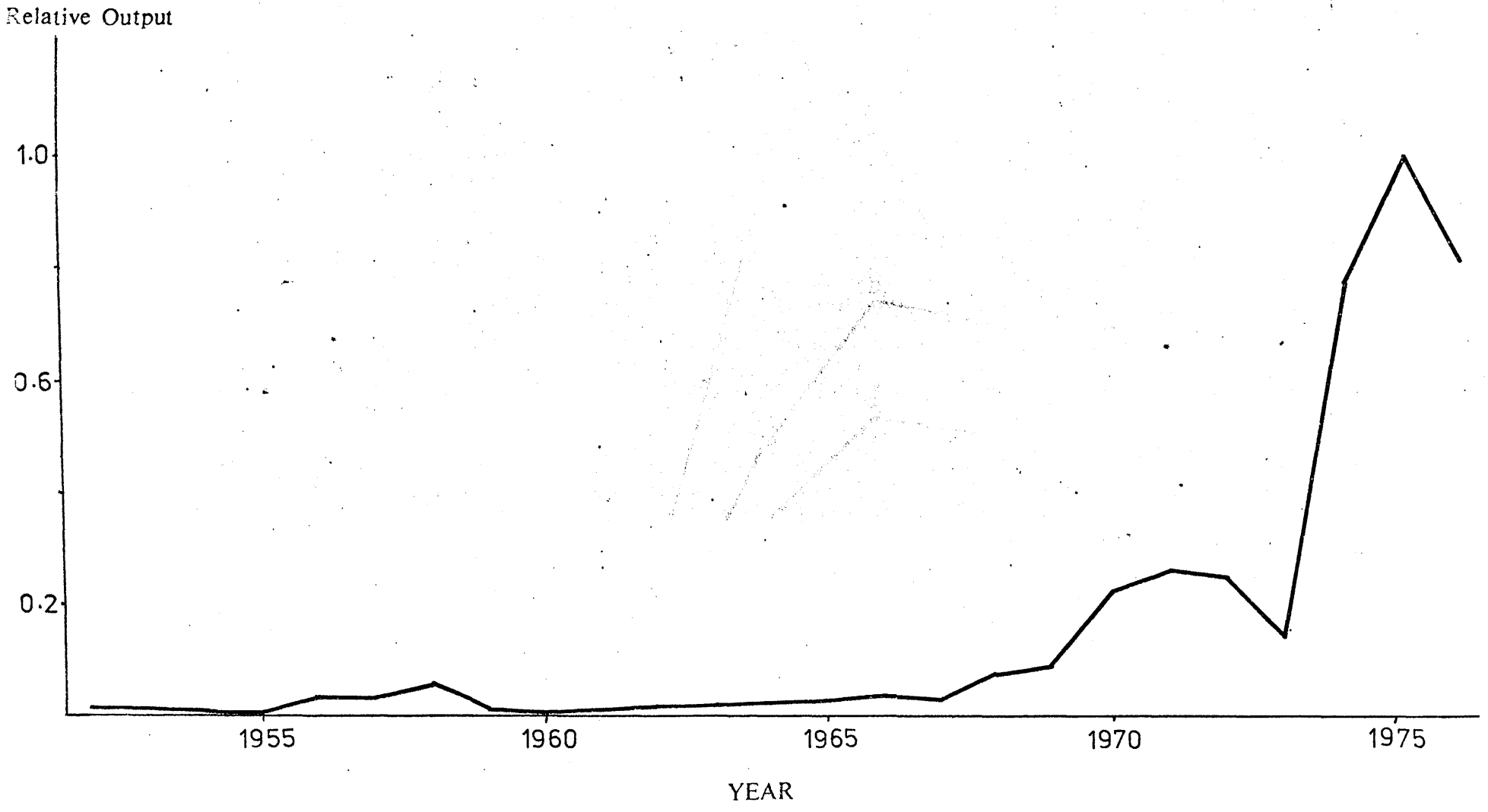

a)Cs-137(decay corrected to 1977)

b) Cs-134

a - Cs-134 output

b - Decay corrected to 1976

c - Decay corrected to 1977

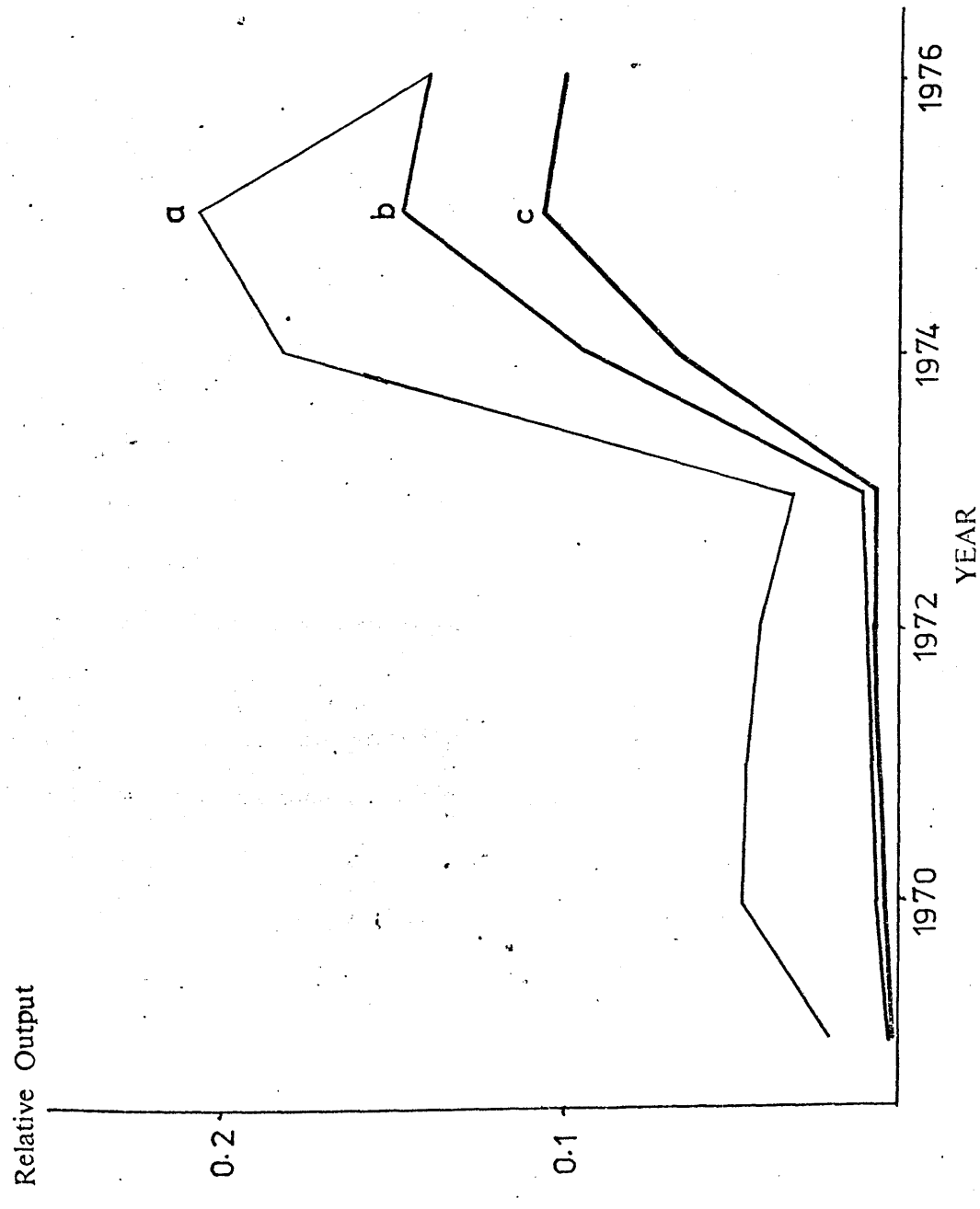

model is, however, demonstrated by considering the profile obtained 10 months earlier - LGC9 (Fig 6.3). Straightforward comparison of LGC9 and LGC12 shows distinctly that the latter cannot be derived from the former by a direct accumulation process. There is, nevertheless, a very good match between radiocaesium concentrations in the region 4 - 10 cm in both cores - a match which is improved to near identity by a downwards displacement of the LGC9 profile by $\sim$ 0.5 cm (Fig 6.13). This extremely close match strongly implies that

1) the Craib corer is obtaining undisturbed cores reproducibly, with little loss of surface material, and

2) the sedimentation rate at this site is $\sim$5 mm/10 months or $\sim$0.6 cm year^{-1} (defined as the upwards velocity of the sediment/water interface from a fixed datum-line in a region of effectively constant porosity $\simeq$ 0.3) - in very good agreement with the value of 6 mm y^{-1} obtained by Swan (1978) from ^{210}Pb analysis and

3) the extent of downwards diffusion of radiocaesium (including molecular diffusion, pore water diffusion or physical sediment mixing) is small below a depth of $\sim$ 4 cm over the timescale considered.

Bearing in mind the possibility of surface loss effects, the veracity of the above conclusions may be checked from the results obtained by MacKenzie (1977) for analysis of LGC2 (Fig 6.11). If the LGC2 profile is superimposed, after downwards displacement by 1.3 cm - corresponding to 26 months sedimentation at 6 mm year^{-1} (Fig 6.13) excellent correlation with the previous 2 cores is observed. Thus the conclusions above seem justified and, in addition, there appears to be

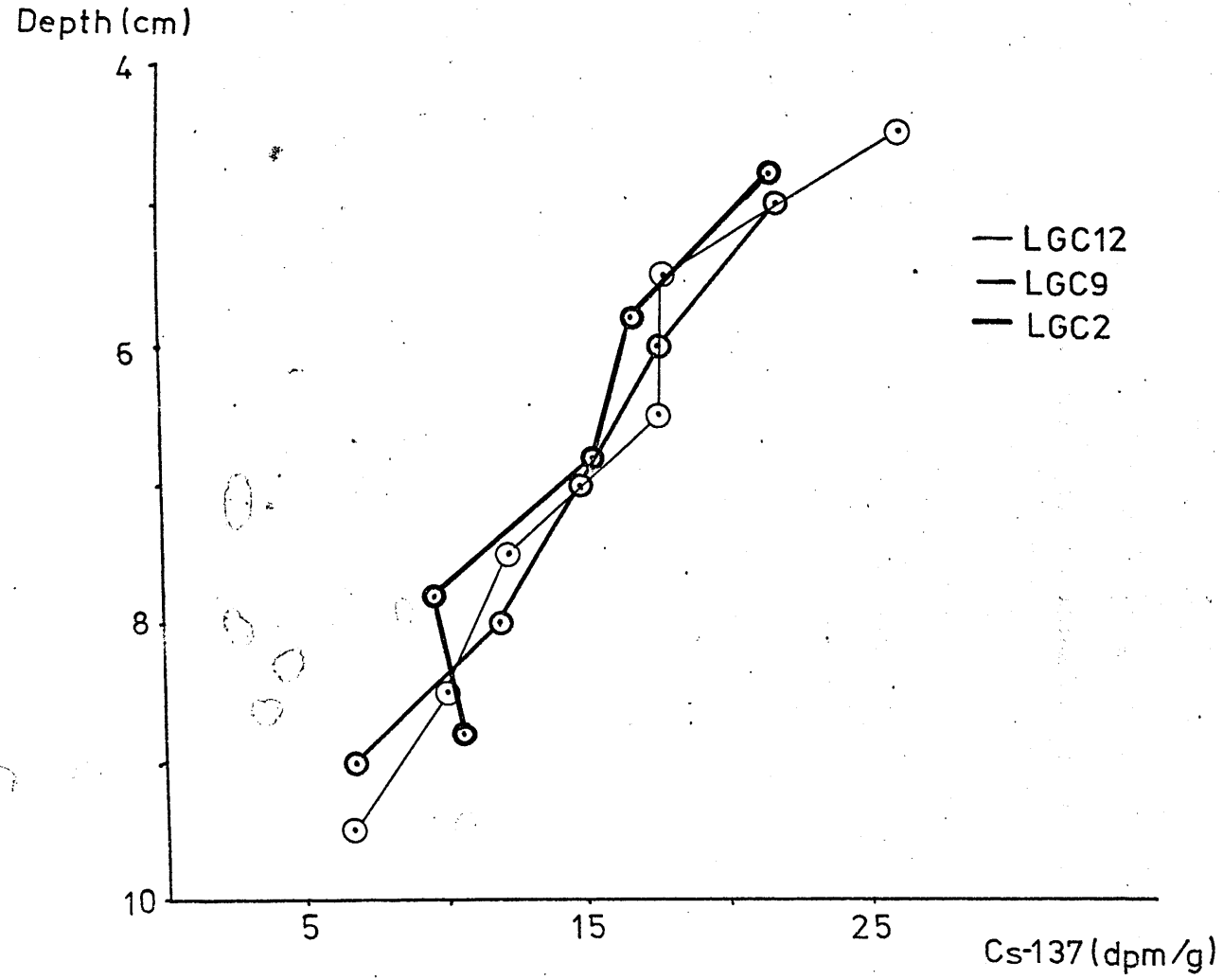
Depth (cm)
4
6
8
10
5
15
25
Cs-137 (dpm/g)
LGC12
LGC9
LGC2

excellent intercalibration agreement between the direct counting method used in this project and the solution and extraction method of MacKenzie (1977).

By integrating the radiocaesium content from surface to 8.7, 9.5 and 10 cm in cores LGC2, 9 and 12 respectively, the extent of ^{137}Cs removal to sediment may be calculated for the time periods between collecting these cores. No correction is attempted for sediment loss during sectioning of cores LGC2 and 9 (as previously discussed) since the extent of this loss, in terms of ^{137}Cs content, is probably dependant on the ^{137}Cs profile and its relationship to porosity variations. This uncertainty ($\sim$ 3%) may be considered an inherent error in the following treatment. The integrals for LGC2, 9 and 12 are 1083.8, 1507.9 and 1697.2 dpm respectively. The increase of this integral in the 10-month period between sampling LGC9 and 12 is thus 189.3 dpm corresponding to 7.41 dpm cm^{-2} or 3.37 pCi cm^{-2} (as the core cross-sectional area is 25.52 cm^2). Taking a 7-month transit time between Windscale and C.S.A. (cf Chapter 3), this increase may be attributed to an output of 9.8×10^4 Ci. An extraction coefficient may be defined for sediments (E_c) as the activity input to sediments (in pCi cm^{-2}) per unit Windscale release (Ci). The extraction coefficient over this period is thus calculated as 3.44×10^{-5} pCi cm^{-2}/Ci. An alternative unit, which will be termed the environmental appearance (E_A), by analogy to that defined for water (Chapter 3), has been utilised in sediment studies (Jefferies, 1968; Heatherington and Jefferies, 1974) and relates the concentration of a radionuclide in sediment (pCi g^{-1}) to the corresponding Windscale output rate (Ci $month^{-1}$). This unit is often more difficult

to evaluate directly if redistribution processes occur in the sediment but may be estimated from E_c if the sedimentation rate (in g month^{-1}) is known. Thus

$$E_A = E_C . f \qquad \ldots.6.1$$

where f is the reciprocal of the sedimentation rate. From ^{210}Pb studies, f = 60 g^{-1} month for this site (Swan, 1978) and thus a value of $E_A = 2.06 \times 10^{-3}$ pCi g^{-1}/Ci month^{-1} may be derived. To extend the temporal baseline, the difference between profile integrals for LGC2 and LGC12 (10.92 pCi cm^{-2}) together with the lag-corrected Windscale output (3.407×10^5 Ci) over this period may be used to yield $E_C = 3.21 \times 10^{-5}$ pCi cm^{-2}/Ci and $E_A = 1.94 \times 10^{-3}$ pCi g^{-1}/Ci month^{-1}. The very good internal agreement of these values again emphasises the reproducibility of the coring mechanism and justifies the basis of the calibration.

An apparent anomaly arises, however, if the ^{137}Cs integral to the depth of the longest core (LGC9), 31.2 pCi cm^{-2}, is compared to a theoretical value of 16.4 pCi cm^{-2} derived from (a) the total Windscale output to that time (lag-corrected) of 4.776×10^5 Ci and b) E_E value of 3.44 pCi cm^{-2}/Ci (this value being chosen as the Windscale lag-time is better defined over the period of its determination). This $\sim$100% difference between predicted and observed values may imply a large associated error in calculation - due, for example to variations in sedimentation rate, water transport from Windscale to the C.S.A., changes in the extent of radiocaesium removal, remobilisation, or a combination of these processes. Such an associated error seems strange in view of the good agreement of E_E values derived over a period of 2 years and, indeed, a

simpler explanation in terms of the effects of fallout ^{137}Cs may be more valid.

The use of fallout ^{137}Cs as a geochronological tracer in lacustrine systems is well documented (cf Chapter 1). Fallout over Britain was greatest over the period 1954 - 66 (Pennington et al, 1973), the total deposition up to 1975 being ~ 44 dpm cm^{-2} at L. Windermere. This value is in good agreement with an integrated activity of ~ 42 dpm cm^{-2} obtained during this project by measurement of ^{137}Cs in a MacKereth core from L. Lomond (LLRP1 - Fig 6.14) despite the undefined extent of removal of fallout ^{137}Cs from the water column, input from catchment area and variation in fallout relative to Windermere (through latitudinal and climatic factors).

In L. Goil, the difference between predicted and observed ^{137}Cs integrals could thus be explained in terms of a fallout contribution to the inventory of ~ 14.8 pCi cm^{-2}. While, from the low extent of Cs removal from salt water observed previously, only very limited removal of dissolved fallout ^{137}Cs would be expected, input from particulate-bound fallout (as considered in Chapter 1) or ^{137}Cs sorbed onto particulates from fresh-water in the catchment area may be significant. ^{210}Pb studies at this site have shown that the input flux of this species is ~ 2.5 dpm cm^{-2} y^{-1} compared to an atmospheric deposition of only 0.38 dpm cm^{-2} y^{-1} (Swan, 1978), a discrepancy explained in terms of a dominant contribution to this flux from particulate-bound ^{210}Pb. Thus, it is reasonable to expect a significant contribution to the ^{137}Cs flux from fallout sorbed onto particulates during the period 1954 - 1966. Such an input mechanism would necessarily tend to result in 'smearing' of the bomb-fallout profile because of lags between adsorption

FIGURE 6.14 L.L.R.P.M.1. RADIOCAESIUM PROFILE

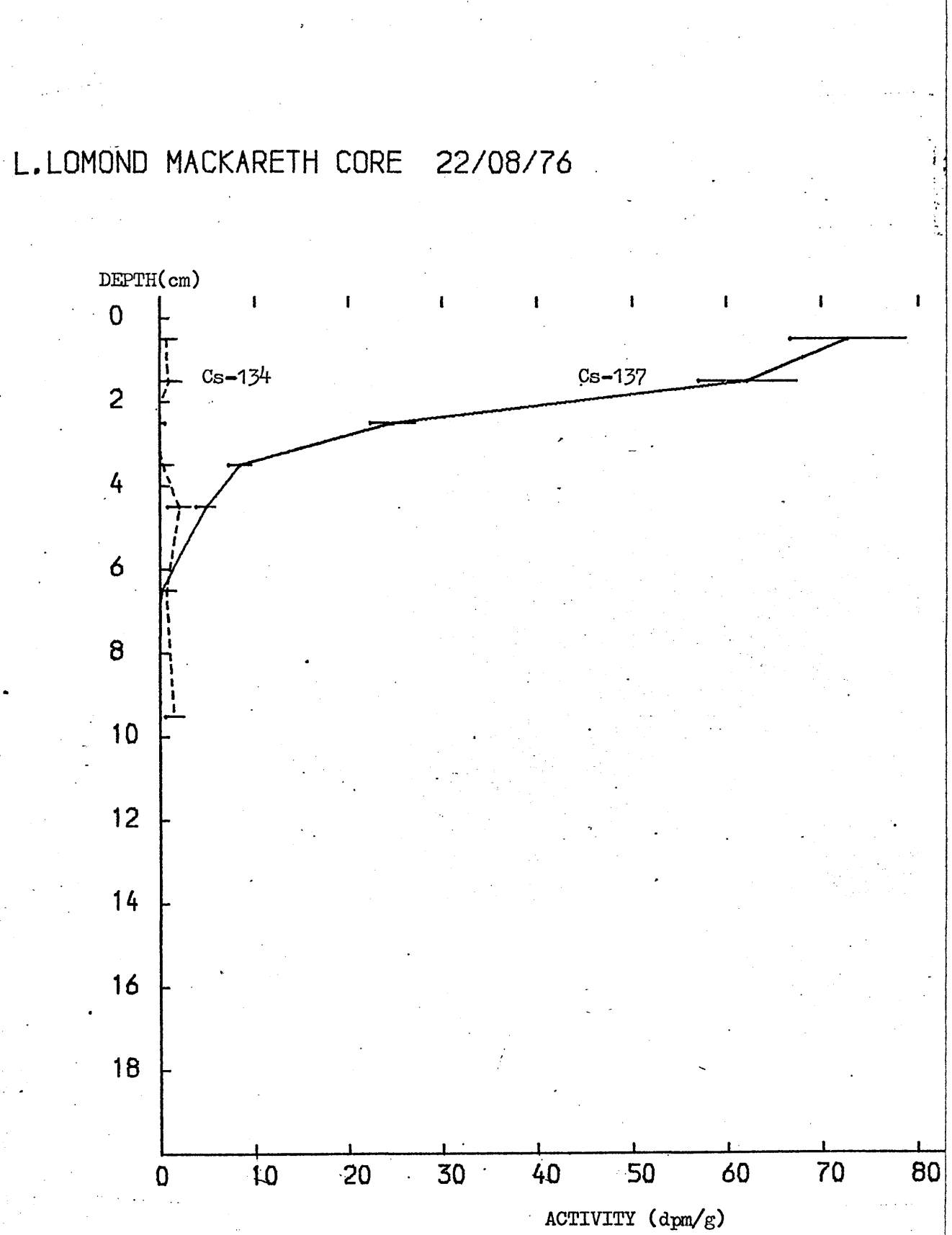

onto particulates in the catchment area and subsequent erosion, transport and incorporation into the sediment column. Maximum input, however, would be expected to occur before 1966 (Pennington et al, 1973), that is, at a time when Windscale output was still fairly small at $\sim$200 Ci month^{-1}. Assuming a steady state and an $E_A \sim 2 \times 10^{-3}$ pCi g^{-1}/Ci month^{-1}, a relatively constant region of concentration of $\sim$ 0.4 pCi g^{-1} ($\sim$0.9 dpm g^{-1}) would be expected from Windscale release at that time. In LGC9, however, from 12 - 17 cm (corresponding to sediment deposited before 1966) a fairly constant concentration of $\sim$ 2.5 dpm g^{-1} is observed, i.e. $\sim$1.6 dpm g^{-1} greater than expected from Windscale. This excess may be attributed to fallout. In the region above 12 cm it is difficult to distinguish sources of ^{137}Cs because of increases in Windscale output and the effects of surface mixing (as discussed later) but it is probably reasonable to consider fallout input negligible, relative to that from Windscale, after 1975 (as assumed in the E_A and E_C calculations above). A further check on the results above is the calculation of a ^{134}Cs inventory for the sediment column (LGC9) by decay-correcting Windscale ^{134}Cs output rates to 1976. Assuming a decay and transport lag-corrected ^{134}Cs output integral of 4.8 $\times$ 10^4 Ci and an E_C of 3.44 x 10^{-5} pCi cm^{-2}/Ci, a C.S.A. sediment inventory of 1.7 pCi cm^{-2} is derived, corresponding to 3.6 dpm cm^{-2}. This figure is in reasonable agreement with the observed value of 5.2 dpm cm^{-2}, particularly in view of the uncertainties in the calculation, namely 1) the relatively large errors associated with ^{137}Cs evaluation (25%) 2) errors associated with the decay correction process based on annual values (which may amount to 10%) and 3) the major dependence of the theoretical values on the value chosen for the Windscale-

- C.S.A. lag time, as a result of the large effects of decay - a decrease in lag time of 2 months prior to collection of the core increasing the calculated input by ~25%.

Thus far, little consideration has been paid to the radiocaesium profile in the upper 4 cm of the sediment core. On the basis of radiocaesium analysis of core LGC2, MacKenzie (1977) proposed fairly rapid mixing of the upper 4 cms of the sediment profile at this site, an observation later confirmed by ^{210}Pb analysis (Swan, 1978). The origin of this mixing process could lie in bottom turbidity, biological activity, gas evolution etc or could be induced by the coring process itself. Although observed reproducibility of sediment cores argues against mixing by the corer, X-radiographs of frozen cores show quite distinct burrow structures to ~4 cm (Swan, 1978) and marked deep-water flushing events are known to occur in this loch (Chapter 4) indicating probable contributions from these latter two processes. That surface radiocaesium redistribution of some type does occur is shown distinctly by comparing the profiles LGC9 and 12. These can be explained only by a mixing mechanism if the previous argument against ^{137}Cs diffusion is assumed to hold generally throughout the sediment column. The presence of distinct variations in ^{137}Cs concentrations in the 0 - 4 cm region (particularly the surface value of LGC9) and the marked ^{134}Cs profiles in both cores indicate that mixing is slow on the timescale of water variations (months). While the increase in ^{137}Cs content of C.S.A. waters during 1976 is reflected by an increase in activity at the surface of LGC9, the continued input from high water activity has mixed fairly well throughout the top 4 cms by mid-1977 (LGC12). Assuming homogeneity resulting from mixing

in a zone of depth x cm and sedimentation rate cm y^{-1}, a minimum value of the mixing coefficient (K) may be calculated as:-

$$K \gtrsim 10 \times (x) \times V \quad \ldots.6.2$$

(Berger and Heath, 1968; Guinasso and Schink, 1975; Schink and Guinasso, 1977).

Using the data above, assuming $x \sim 4$ cm and $V \sim 0.6$ cm y^{-1}, yields $K \gtrsim 24$ cm^2 y^{-1}. As mentioned, however, it is obvious that complete homogenity has not been achieved. As an alternative approach, the large increase in water concentrations of radiocaesium might be regarded as causing an ''impulse'' of high ^{137}Cs activity sediment (after the notation of Guinasso and Schink (1975)) occurring $\sim$8/76, this impulse being then subject to mixing and sedimentation until 6/77. By comparing the observed LGC12 profile to those generated by the time-dependant mixing model of Guinasso and Schink (1975) (for t* $\sim$0.14), a value for the mixing parameter (G) of $\sim$0.7 is estimated.

As $$G = \frac{K}{x.V} \quad \ldots.6.3$$

in the previous notation, a value of $K \sim 1.7$ cm^2 y^{-1} is suggested. As the impulse and complete homogeneity models would tend to generate, in the present case, low and high values of K respectively, limits on the value of the mixing coefficients may be taken as $2 \lesssim K \lesssim 24$ cm^2 y^{-1}. While these values for K are larger than deep sea data (.0005 - 0.4 cm^2 y^{-1}, Guinasso and Schink (1975)), they lie at the low end of the range generally observed in the coastal marine environment (1 - 10^3 cm^2 y^{-1}, Guinasso and Schink (1975)). While this low value may be an artifact caused by the assumptions inherent in the

calculations, it is probably realisitic as fast coastal mixing processes are generally attributed to bioturbation effects (Guinasso and Schink, 1975; Aller and Cochran, 1976; Schink and Guinasso, 1977; Swan, 1978) and the periodically low D.O. values experienced in the bottom waters of this site (Chapter 4) may well severely limit the benthic population.

6.4 L. Goil - Site 2 and Gareloch

Much less information may be obtained from the shallower site 2 (Fig 6.1) in L. Goil as only one Craib core, LGC4 (Fig 6.5), has been analysed. It is noticeable, however, that the integrated ^{137}Cs activity in this core to a depth of 17 cm (107.6 dpm cm^{-2}) is considerably greater than that for LGC9 from site 1 (72.8 dpm cm^{-2}) despite the fact that the latter was obtained 5 months after the former. This discrepancy indicates that there exists at the shallower site either more efficient removal of radiocaesium for a given particulate flux, a greater particulate flux or both. Assuming that the sediment type is similar at the two locations (which is not necessarily true, as considered later), the integrated activity at the shallow site may be compared with a derived value for the deep site at the same date (68.3 dpm cm^{-2}). This latter figure is obtained by subtracting 4.5 dpm cm^{-2} from the LGC9 integral, an amount calculated from the Windscale output over the appropriate five-month period (6.0×10^{6} Ci) multiplied by the Extraction coefficient (3.44×10^{-5} pCi cm^{-2}/Ci). If the sediment types are similar, the Environmental Appearance at both sites may be taken as 2.06×10^{-3} pCi g^{-1}/Ci month. By assuming that the ^{137}Cs profiles to a depth of 17 cm are directly proportional to the total depth integral, E_C at site 2 is given

as

$$\frac{107.6}{68.3} \times 3.44 \times 10^{-5} = 5.42 \times 10^{-5} \text{ pCi cm}^{-2}/\text{Ci}$$

and thus, from equation 6.1 f = 38.0, giving a sedimentation rate V = 316 mg cm^{-2} $year^{-1}$. As this calculation compares similar depths of profiles, the V value obtained is necessarily an underestimate as an increased V will result in a lower proportion of the total profile being contained in the 17 cm zone. If it is assumed, on the basis of the constancy of the ^{134}Cs profile, that relatively fast mixing occurs in the upper $\sim$6 cm of LGC4, by comparison with the output profile (Fig 6.12), the marked increase from 16 - 14 cm depth could be correlated with the Windscale output rise of 1968 - 70 thus suggesting a sedimentation rate of $\sim$ 550 mg cm^{-2} y^{-1}. This sedimentation rate may be checked by considering the ^{134}Cs profile - ^{134}Cs being observed at $\sim$ 17 cm in LGC4 as opposed to a cut-off at $\sim$ 9 cm in LGC9. Matching these ^{134}Cs cut-off points (taking into account the relative depths of mixed zones) implies a sedimentation rate of $\sim$513 mg cm^{-1} y^{-1}. These values are in good agreement in view of 1) the possibility that ^{134}Cs may extend below 17 cm in LGC4 and 2) the 1 cm sampling frequency in these cases which inherently limits the sensitivity of this type of treatment.

An alternative explanation of the observed profile in terms of either diffusion or mixing (possibly biological) causing homogenisation of the upper 6 cm of sediment and slower transport of radiocaesium to depths of $\sim$ 14 cm seems unlikely in view of the ^{137}Cs distribution - transport significant on the scale of the $t_{\frac{1}{2}}$ of ^{134}Cs being expected to cause equally efficient transport of ^{137}Cs to depth.

The above discussion, based on an assumption of similar E_A values at the two sites in L. Goil may, however, be unjustified. Indeed, taking the sedimentation rate of ~ 530 mg cm^{-2} y^{-1} obtained above and the calculated E_C (5.42 x 10^{-5} pCi cm^{-2}/Ci) yields an E_A of 1.23 x 10^{-3} pCi g^{-1}/Ci $month^{-1}$, which is approximately half that found at site 1. A study of superficial sediment deposits in the C.S.A. by Deegan (1974) indicates that sediment texture at the two sites is quite different - station 1 sedimentation being a mud while at station 2 the deposits are classified as a mixture of mud, sand and clay. This dissimilarity is emphasised by the preliminary particle size analysis of sediments from this area by Lennie (1977) and, further, by studies of porosity profiles by Swan (1978). Using the previously derived E_C value for this site (5.42 x 10^{-5} pCi cm^{-2}/Ci) and the sedimentation rate (123 mg cm^{-2} y^{-1}) obtained via ^{210}Pb analysis (Swan, 1978), an E_A value for this site of 5.29 x 10^{-3} pCi g^{-1}/Ci $month^{-1}$ may be calculated. This figure is $\gtrsim$ 100% greater than that for site 1. The implied higher efficiency of Cs removal may well reflect a higher clay content in the sediment of site 2, the affinity of Cs for clays, especially illite, being well documented (eg Pickering et al, 1966; Duursma and Bosch, 1966; Auffret et al, 1977). Nevertheless there does appear to be a discrepancy between the sedimentation rates obtained by considering the $^{137}Cs/^{134}Cs$ profiles (~530 mg cm^{-2}) and by ^{210}Pb analysis (123 mg cm^{-2}). This anomaly cannot be resolved by analysis of a single core.

Again, from just one core, only a crude estimate of the rate of mixing in the '6 cm mixed zone' may be obtained using

the total homogeneity assumption (Equation 6.2). The sedimentation rate derived from the radiocaesium profiles corresponds to ~ 1.54 cm y^{-1} at the porosity of the mixed zone thus giving $K \gtrsim 92$ cm^2 y^{-1} which is considerably larger than that calculated for site 1. The larger value of the mixing coefficient at site 2 might be expected to result from greater biological activity, due to the lesser water depth and greater average bottom D.O. concentration at this position. It is interesting to note, however, that on the basis of the ^{210}Pb sedimentation rates a value of $K \gtrsim 31$ cm^2 y^{-1} is calculated for both sites (Swan, 1978).

Although 2 Craib cores have been analysed from Gareloch, GLC1 and GLC3 (Fig 6.10), these cores are duplicates and thus the extent of radiocaesium interpretation possible is again limited. Simple comparison with L. Goil profiles shows much higher surface sediment concentrations (~ 75 dpm g^{-1}) in Gareloch than in L. Goil 4 months later (~ 40 dpm g^{-1}). Taking a mixed layer of 3 cm (from GLC1 - MacKenzie, 1977) and matching the first measurable ^{134}Cs to 1970 gives a sedimentation rate of ~ 640 mg cm^{-2} y^{-1} (~ 1.8 cm y^{-1}) which, bearing in mind the simplicity of the calculation, is in good agreement with a value of 543 ± 130 mg cm^{-2} y^{-1} calculated by Swan (1978) on the basis of ^{210}Pb measurements. The observed inventory of ^{134}Cs for the column (22.03 dpm cm^{-2}) relative to the decay-corrected output from Windscale yields a value for $E_C = 3.5 \times 10^{-4}$ pCi cm^{-2}/Ci which, with the above sedimentation rate, gives $E_A \simeq 6.5 \times 10^{-3}$ pCi g^{-1}/Ci $month^{-1}$. Although the errors associated with calculations involving ^{134}Cs are relatively large, the high E_C value is in agreement with the increased inventory of ^{137}Cs relative to the well-defined L. Goil site 1.

It is interesting to note that the $\sim$ x 10 increase in E_C relative to site 1 is due equally to a $\sim$ x 3 increase in sedimentation rate and $\sim$ x 3 increase in E_A.

Again an estimate of the mixing rate in the upper 3 cm may be calculated from equation 6.2, giving $K \gtrsim .45$ cm^2 y^{-1}. This value is greater than that for the L. Goil deep site for similar reasons to those outlined above for L. Goil site 2.

6.5 Holyloch

One Craib core was obtained from Holyloch, HLC1 (Fig 6.15) and the data for this may be compared with the results for L. Goil site 1 core LGC12 (Fig 6.9) taken on the same day. The ^{137}Cs profiles of these cores are similar in general shape but the rate of decrease of ^{137}Cs with depth is markedly less in Holyloch, implying a greater sedimentation rate at this site. An estimate of the sedimentation rate may be obtained by assuming a surface mixing zone of $\sim$ 4 cm and, by comparison with the Windscale output curve, correlating the ^{137}Cs activity at 9 - 10 cm with 1973 output. This procedure yields V$\sim$1.5 cm y^{-1} (which is considerably larger than the 0.5 cm y^{-1} value quoted by Best (1970), without derivation, from a personal communication).

Further analysis of HLC1, however, shows high ^{134}Cs concentrations at depth and, indeed, the ^{134}Cs/^{137}Cs ratio passes through a definite maximum at $\sim$ 8 cm (Fig 6.15). Although the errors associated with this determination are large, the general trend in ^{134}Cs/^{137}Cs ratio follows that of ^{60}Co which is also measureable in this core. ^{60}Co (easily identified by the 1.17 and 1.3 MeV γ's) is the only artificial

FIGURE 6.15 H.L.C.1. RADIOCAESIUM PROFILE

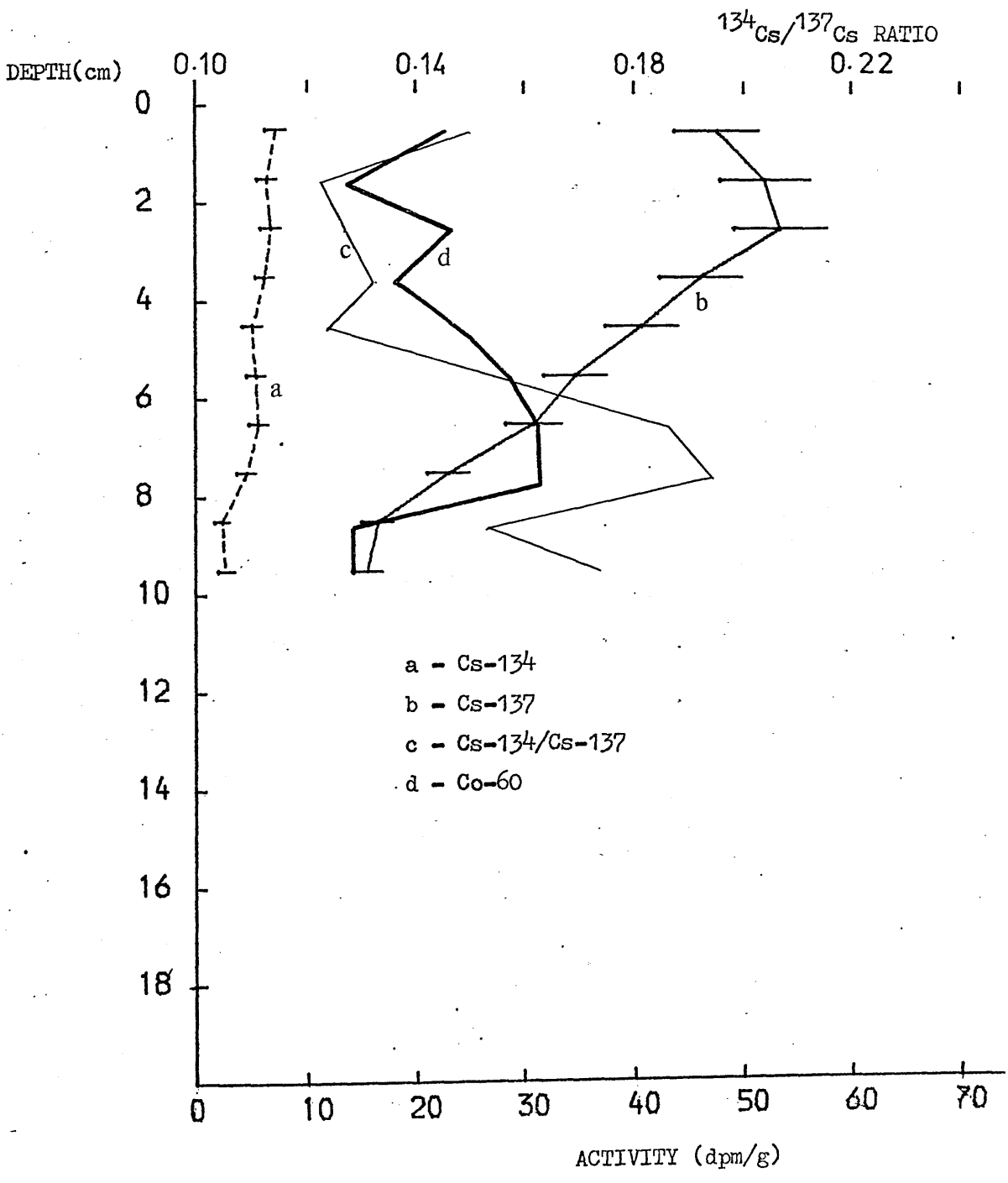

radionuclide, apart from radiocaesium, positively identified by high resolution γ-spectrometry in C.S.A. sediment and its presence is indicated only at this site.

The presence of ^{60}Co and the anomalous ^{134}Cs profile may be explained in terms of an additional radionuclide source in this loch from the American nuclear submarine depot-ship. During the shut-down and re-activation cycle of nuclear submarine reactors several hundred litres of primary coolant water are discharged into the loch (Best, 1970). While the total activity released is negligible relative to the C.S.A. inventory, (annual discharge limits for 1975 being less than 1 m Ci of long-lived γ emitters - primarily ^{60}Co, 1 m Ci of short-lived radionuclides, 1 m Ci of fission products and 10 m Ci of ^{3}H (Mitchell, 1977)), it has been shown to be significant in terms of the radionuclide concentration in the sediment (Dutton and Steele, 1966) and marine organisms (Goodair, 1967) in Holyloch. The effluent released has radio-active components associated with both the dissolved and particulate phases. The particulate phase (which he termed 'crud') has been studied by Best (1970) and contributions from the radionuclides ^{141}Hf, ^{51}Cr, ^{58}Co, ^{54}Mn and ^{60}Co to the total radioactivity were determined using direct γ-spectrometry (on a NaI(Tl) detector). With the exception of the very distinctive ^{60}Co doublet, however, these identifications must be regarded as suspect, this only partly due to insensitivity of the methodology. For example, ^{58}Co was identified by a peak at 0.45 MeV (possibly due to confusion with the positron emission at 0.48 MeV) while the most intense γ from this nuclide ($A_I \sim 98.5\%$) occurs at 0.81 MeV; on the other hand,

^{181}Hf, identified from a 0.11 MeV γ (lit ~ 0.13 MeV, $A_I \sim 50\%$), has a more intense γ ($A_I \sim 83\%$) at 0.48 MeV.

More detailed examination of the sediment itself revealed the presence of red and black crystalline particulates in the upper 3 cms of sediment, the amount of which distinctly decreased with depth over this range (Ballantyne, 1978). Direct γ-spectrometry of these particulates (After separation by hand) showed the associated activity to be effectively within 2σ error of background for ^{134}Cs, ^{137}Cs and ^{60}Co. This agrees with the main particulate forms identified by Best (1970) namely; a) black crystalline corrosion products formed during hot pressurised reactor operation and b) flocculent grey material containing reddish-brown particles typical of corrosion during cold or warm-up conditions. In effluent, however, 60 - 100% of the total activity was found to be associated with the particulate phase and, in addition, Best was able to separate effluent particulates on the basis of magnetic properties whereas neither sediment constituent was found to be magnetic.

The observed ^{60}Co profile may thus be explained in terms of input from submarine reactor effluent - mainly in the form ofparticulates which appear to break down quite readily in the sediment column (within the mixed zone) with associated rapid loss of contained radionuclides. The ^{60}Co maximum at ~8 cm may thus be produced either by a maximum input ~1970 (from the sedimentation rate derived from the ^{137}Cs profile) or by migration downwards following 'crud' particle degradation. The $^{134}Cs/^{137}Cs$ profile may be similarly explained as due to input of ^{134}Cs in the 'crud' particles, this nuclide being

present presumably due to activation of stable Cs (^{133}Cs - 100%). Only a small contribution from this source ($\sim$2 dpm g^{-1}) would be sufficient to yield the observed profile. These input pulse and remobilisation/migration models could be readily distinguished by correlating the observed ^{60}Co profile with annual release variations (if measured and unclassified) or by analysing a core obtained from this site at a later date.

As radiocaesium from this area cannot be unambiguously identified with Windscale output (although such an association is strongly suggested for ^{137}Cs), E_A and E_c values cannot be calculated and the estimated mixing coefficient, $K \gtrsim 60cm^2\ y^{-1}$, from the total mixing model, has an unquantified associated error. This area, however, is very unusual in receiving 3 independent radiocaesium inputs from bomb fallout (almost entirely ^{137}Cs), Windscale (^{137}Cs and ^{134}Cs) and submarine reactors (presumably mainly ^{134}Cs or with high $^{134}Cs/^{137}Cs$ ratio). Differences in the extent of association of radiocaesium from these sources with the various sediment components (if any) would be of considerable interest and might be worth further study.

6.6 Practical Applications and General Results

The use of radiocaesium as a tracer of sedimentation processes has been well defined in the study of the Loch Goil deep site. Comparison of a series of cores yields well defined sedimentation surface mixing depths and mixing rates which agree well with those obtained by natural series methods and have the additional advantage of defining these parameters over a specific period of time (between sampling dates). Less

rigorous estimates of these parameters may, however, be obtained from a single core, if certain assumptions are made:-

1) A mixing depth may be defined (e.g. by uniformity of ^{134}Cs concentration) in which mixing is fast and below which radiocaesium is immobile, this depth being invariant with time.

2) Sedimentation rate, sediment type and water transport conditions are constant over the time considered.

3) Coring method reproducibly retains the entire sediment column undisturbed.

If these assumptions hold, the sedimentation rate may be estimated by the depth between the bottom of the mixed layer and specific, datable features in the ^{137}Cs profile, e.g. the first significant input (both Windscale and fallout) $\sim$ 1952/3 and the marked rises in Windscale output in 1969/70 and 1973/4 (reflected in the C.S.A. water $\sim$ 1 year later). In cases when the core is insufficiently long to reach zero ^{137}Cs, large errors maybe associated with this method when the mixing depth is large relative to the annual sediment deposition (e.g. L. Goil site 2) as rises in Windscale output may be considerably 'smeared' by mixing and further complicated by variations in the fallout component. In the future, however, with the continued decrease in Windscale releases, an unambiguous marker will be provided by the 1975 output maximum thus expanding applicability of the method.

The well defined results from a rigorous study of a specific area may, however, be used to derive more generally useful data. By taking the best defined site (Loch Goil deep site) as typical of the entire C.S.A. (which is obviously a gross oversimplification), an E_c of 3.44×10^5 pCi cm^{-2}/Ci

would imply a ^{137}Cs inventory of 27.5 pCi cm^{-2} by the end of 1977 (Windscale - derived). Taking the sediment area of the C.S.A. as 2.5×10^{13} cm^2, a total sediment ^{137}Cs content of 688 Ci is derived, i.e. $\sim$0.01% of the total Windscale output. Assuming 40% of Windscale output passes through the Clyde Sea (cf Chapter 3), 0.025% of this water-borne radiocaesium inventory is removed into sediment during residence in the area. Because of the proximity of land to the L. Goil site, the particulate flux and hence caesium removal rate in this region is probably larger than generally found in the C.S.A. Thus the values above may be regarded as upper-estimates - justifying the description of ^{137}Cs as a conservative tracer. At a more quantitative level, the observed 0.025% removal in the C.S.A. may be combined with the mean water residence time of the area ($\sim$ 90 days) to yield a water residence half-time for ^{137}Cs of 2.4×10^5 days (660 years) - corresponding to an average residence time of about 950 years. This value is markedly less than previously discussed deep ocean measurements of this parameter (6.5×10^4 - 6.5×10^5 years, cf Chapter 1) and reflects the importance of near-shore effects - primarily the high particulate flux - in increasing sequestration into sediment as predicted by, for example, Noshkin and Bowen (1973) and Turekian (1977).

As the E_A for ^{137}Cs in water in the C.S.A. is $\sim$ 0.25 pCi l^{-1}/Ci day^{-1}, the observed sediment E_A of 2.02×10^{-3} pCi g^{-1}/Ci $month^{-1}$ represents a ^{137}Cs concentration factor (water - dry sediment) of x 240. The major advantage of this mode of calculation is that the value obtained is an environmental measurement based on averages over periods of $\gtrsim$2 years and,

as such, represents an average annual value of this parameter. Duursma and Eisma (1973) define a distribution coefficient (K) as the dimensionless ratio of the amount of radionuclide per ml sediment (dry basis) to that per ml of sea water. Taking an in-situ bulk density of 2.3 g cm^{-3} for C.S.A. sediment (Swan, 1978), yields K for ^{137}Cs of $\sim$ 560. Laboratory determinations of this parameter for various sediments range from 10^2 - 10^5 - but the value for a particular sediment may vary by almost 2 orders of magnitude depending on the method used (Duursma and Eisma, 1973). It is felt that these radiocaesium distribution data based on direct analyses of C.S.A. samples have many advantages over the results produced by artificial laboratory experiments (which have major problems of simulating marine conditions, of adsorption by surfaces etc) and by field studies in the Windscale area (which necessarily are complicated by large spatial and temporal concentration gradients and by direct sediment transport).

6.6 Summary

In this chapter the wide applicability of radiocaesium as a sediment tracer has been demonstrated. Comparison of profiles obtained from Craib and gravity cores from 3 different sites show that the latter lose a considerable depth of surface sediment ($\sim$10 cm) and that the surface profile observed in these cores results from mixed remnants of this loss process. This proves the inapplicability of the gravity corer to studies of surface ($\lesssim$20 cm) profiles of high porosity sediments. In addition, comparison of radiocaesium profiles from duplicate Craib cores indicates good reproducibility in this coring method with surface loss $\lesssim$1.5 cm ($\sim$0.08 g cm^{-2}) and implies that

further loss may result from the core-sectioning process - this latter effect being minimised by direct wet extrusion and sub-sampling.

From analysis of 3 radiocaesium profiles from Craib cores obtained at ~ yearly intervals from L. Goil site 1, it is shown that the extent of radiocaesium redistribution (by either diffusion or physical mixing) is low below ~ 4 cm and that the sedimentation rate is ~0.6 cm y^{-1} (~ 200 mg cm^{-2} y^{-1}). Defining an extraction coefficient (E_c) as the activity removed into sediment per unit Windscale release, comparison of these profiles yields $E_c = 3.44 \times 10^{-5}$ pCi cm^{-2}/Ci corresponding to an environmental appearance (E_A) = 2.06×10^{-3} pCi g^{-1}/Ci $month^{-1}$. From these parameters, the total ^{137}Cs inventory in the longest core from this site (31.2 pCi cm^{-2}) may be attributed to ~16.4 pCi cm^{-2} from Windscale releases and 14.8 pCi cm^{-2} from bomb fallout. Radiocaesium redistribution appears to occur rapidly in the upper 4 cm of the sediment column as a result of a physical mixing process (correlating with the observation of burrow structures to this depth) and a mixing coefficient may thus be calculated to lie in the range $2 \lesssim K \lesssim 24$ cm^2 g^{-1}. This low value is possibly generated by the limiting effects on benthic fauna of the occasional low D.O. concentrations observed in the bottom waters of this site.

Less data are available for L. Goil site 2 but a sedimentation rate of ~ 1.5 cm y^{-1} (~ 530 mg cm^{-2} y^{-1}) may be derived from the radiocaesium profiles. The ^{137}Cs inventory yields an $E_c = 5.42 \times 10^{-5}$ pCi cm^{-2}/Ci and $E_A = 1.23 \times 10^{-3}$ pCi g^{-1}/Ci $month^{-1}$. An estimate of the mixing coefficient in the upper 6 cm, $K \gtrsim 93$ cm^2 y^{-1}, is greater than that calculated for site 1,

probably reflecting greater biological activity in the shallower site.

Similarly, a sedimentation rate of $\sim$ 1.8 cm y^{-1} ($\sim$ 640 mg cm^{-2} y^{-1}) is obtained for Gareloch while, from the ^{134}Cs inventory, estimates of E_c = 3.5 x 10^{-4} pCi cm^{-2}/Ci, E_A = 6.5 x 10^{-3} pCi g^{-1}/Ci month and, in the upper 3 cm, $K \gtrsim 45$ cm^2 y^{-1} are obtained.

One Craib core from Holyloch showed a more complex radionuclide profile - containing ^{60}Co in addition to ^{134}Cs and ^{137}Cs. From the ^{137}Cs profile a sedimentation rate of $\sim$1.5 cm y^{-1} ($\sim$ 600 mg cm^{-2} y^{-1}) may be estimated. The ^{60}Co and excess ^{134}Cs observed may be attributed to releases from the nuclear submarines based in this loch. Although a major component of the activity released from this latter source is attributed to corrosion particulates, these appear to be quickly degraded within the top 3 cm of the sediment column with associated radionuclide release.

Generally it may be calculated (based on L. Goil site 1 data) that the C.S.A. sediments contain $\sim$690 Ci corresponding to $\sim$ 0.01% of total Windscale output. As this corresponds to removal of $\sim$ 0.025% of the C.S.A. water content of ^{137}Cs, a water residence half-time of 660 years may be calculated. From the sediment concentration factor of x 240 observed in the area a distribution coefficient for ^{137}Cs in C.S.A. sediment of $\sim$560 is obtained.

Chapter 7

Synthetic Overview

7.1 Introduction

This chapter presents a summary of the major results contained in previous sections and, from this base, investigates some interrelationships between coastal oceanographic processes on various spatial and temporal scales. In addition, a budget accounting for the ^{137}Cs released from Windscale will be derived. On the basis of these data, some practical applications to more specialised fields of interest will be discussed. Finally, some possible developments in radiocaesium tracer applications to the future study of the coastal marine environment will be proposed.

7.2 Summary of Results

In this project radiocaesium has hopefully been shown to be a versatile marine tracer and its associated methodology has been defined. From release at Windscale, transport of radiocaesium from the outfall area to the North Channel, for the period 1972 - 1976, is characterised by a residence time of $\sim$12 months compounded with a lag-time of $\sim$ 6 months. Variability within this coastal system is illustrated in 1977 by a greatly increased outflow of Irish Sea water through the North Channel as a result of Atlantic influx from the south through the St. George's Channel. Water transport northwards through the North Channel is accompanied by exchange with the waters of

the Clyde Sea Area which are, themselves, characterised by a residence time of ~3 months. A transit time of ~ 1 month between the North Channel sampling site (mid Stanraer-Larne) and the Clyde Sea Area is observed. In addition, it may be calculated that ~40% of the Irish Sea - derived water flux from the North Channel passes through the Clyde Sea Area. Generally, transport from the North Channel to the Minch is fast (advection rate ~ 5 km day^{-1}) because of the driving effects of Atlantic currents which, together with fresh runoff, cause a radiocaesium dilution of ~ x 3.5 over this region. In 1977, however, this 'coastal' water presence in the Hebridean Sea Area was much more extensive although a decreased northwards advection rate (~ 1.5 km day^{-1}) was observed.

The horizontal and vertical homogeneity of radiocaesium in the Clyde Sea Area allow its treatment as a 'single mixing-box'. Exceptions to this generality demonstrate the entrainment of deep water in Lochs Fyne and Goil. Detailed studies of vertical radiocaesium profiles in Lochs Long and Goil enable the monthly variation in mixing between these lochs to be evaluated. Thus renewal of L. Goil deep waters is shown to be controlled by the density of L. Long waters at sill depth. Fast deep water flushing in L. Goil (residence time < 1 month) is observed during late winter and spring. Renewal at other times is limited to diffusion through a pycnocline which, at maximum development, is characterised by a vertical eddy diffusion coefficient Kz, such that $7 \lesssim Kz \lesssim 25$ cm^2 sec^{-1}. More extensive deep water entrainment (residence time ~ 1 year) is apparent in the N. Basin of L. Fyne. Shorter deep water residence (~ months) is observed in Gareloch and, possibly, L. Long.

From radiocaesium analysis of sediment cores from the deep site in L. Goil, a sedimentation rate of ~ 200 mg cm^{-2} y^{-1} may be calculated. Redistribution of radiocaesium input in the upper 4 cm of these profiles allows evaluation of a sediment mixing rate constant (defined by analogy of the mixing process to diffusion) of $2 \lesssim K \lesssim 24$ cm^2 y^{-1}. This mixing of surface sediment may be attributed to bioturbation with a possible contribution from bottom water turbulence. The shallow site in L. Goil appears to have a higher sedimentation rate (~ 530 mg cm^{-2} y^{-1}) with faster mixing in the upper 6 cm ($K \gtrsim 92$ cm^2 y^{-1}) caused by enhanced biological activity. A similar sedimentation rate (~ 640 mg cm^{-2} y^{-1}) is calculated for Gareloch, with mixing of the upper 3 cm characterised by $K \gtrsim 45$ cm^2 y^{-1}.

While the ^{137}Cs profile in Holyloch sediment indicates an accumulation rate of ~ 600 mg cm^{-2} y^{-1} below an ~ 4 cm mixed zone, this material is anomalous in containing ^{60}Co and ^{134}Cs from effluent released by the nearby U.S.N. nuclear submarine base. Although this latter input is expected to be primarily in the form of active corrosion particulates, these appear to degrade quickly within the upper 3 cm of sediment.

Windscale derived radiocaesium is thus an ideal tracer of the coastal marine environment as its coastal residence time of ~ 950 years justifies its treatment as a conservative water tracer while a concentration factor of 240 onto sediment also allows applications in this phase. Temporal marking is provided both by output variation and decay of ^{134}Cs.

7.3 Geochemical Budget for Windscale - released ^{137}Cs

From the data presented thus far, it is possible to derive a budget accounting for all ^{137}Cs released from Windscale up to December 1977. By combining relative output rates measured at Windscale (Howells, 1978) with absolute values for particular years (Howells, 1966; Woodhead, 1973), the total activity of ^{137}Cs discharged into the Irish Sea from 1952 until the end of 1977 may be calculated as 6.89×10^5 Ci. Of this activity, 4.44×10^4 Ci (or 6.4%) would be lost through decay between release and 1977.

The presence of high ^{137}Cs concentrations in the vicinity of the Windscale outfall is well documented (eg Mauchline and Templeton, 1963; Templeton and Preston, 1966; Jefferies, 1968; Jefferies et al, 1973; Hetherington and Jefferies, 1974). The most recent data (Jefferies, 1976, Mitchell, 1977) for January, 1976, indicates that a highly contaminated area of ~ 500 km^2 may be fairly arbitrarily defined as having a mean ^{137}Cs activity of 1000 p Ci l^{-1}. Taking the mean depth of this coastal area as 25 m (Bowden, 1955), its ^{137}Cs inventory is 1.25×10^4 Ci (or 1.8% of total output).

The total ^{137}Cs content of the Irish Sea is further determined by first dividing the area into North, Central and South regions (after Bowden, 1955), with the Northern region sub-sectioned into 3 areas (Fig 7.1). On the basis of previously measured ^{137}Cs activities in this area (Jefferies et al, 1973, 1976; Mitchell, 1977), an average concentration for each region can be estimated relative to that in the North Channel (Table 7.1). Taking a North Channel ^{137}Cs concentration of 40 pCi l^{-1} for December 1977, the total ^{137}Cs content of the Irish Sea may

FIGURE 2.3 IRISH SEA REGIONS FOR TRITIUM CALCULATIONS

Shaded area - Windscale vicinity

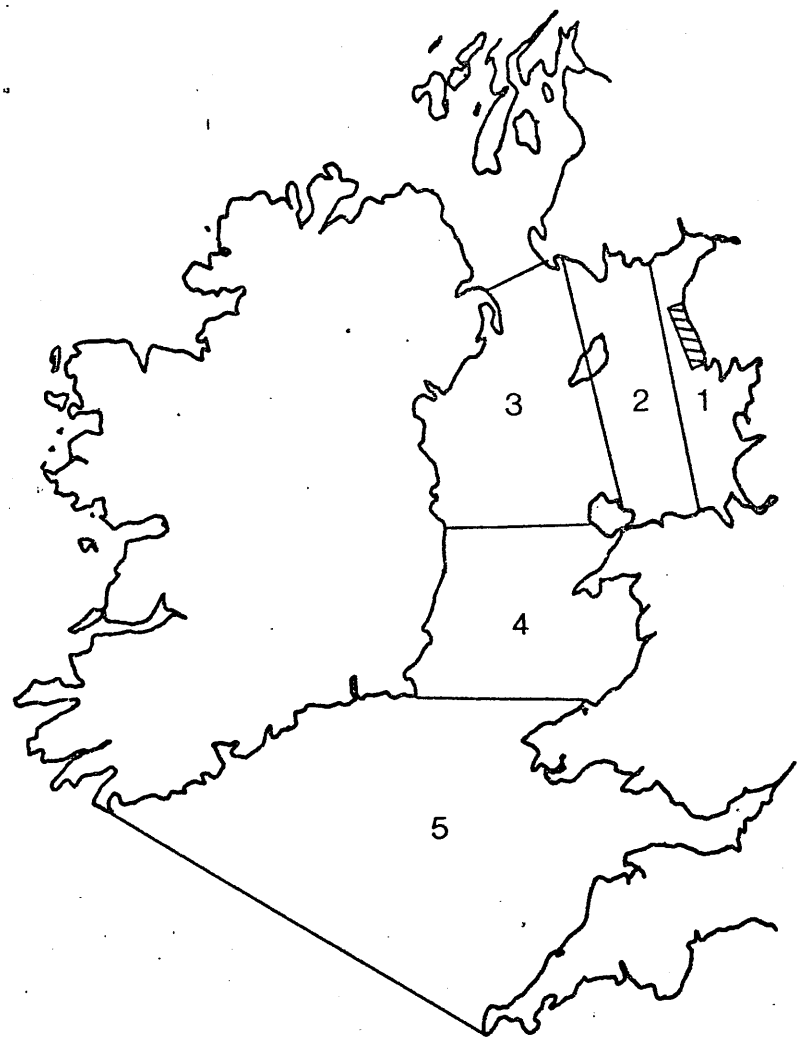

TABLE 7.1

CALCULATION OF ^{137}Cs INVENTORY IN IRISH SEA.

AREA	RELATIVE VOLUME	MEAN ^{137}Cs CONCENTRATION *	RELATIVE CONTENT	^{137}Cs CONTENT (Ci)
1	0.025	7.5	0.1875	3.75×10^{4}
2	0.047	4	0.1880	3.76×10^{4}
3	0.140	1	0.1400	2.80×10^{4}
4	0.165	0.3	0.0495	9.90×10^{3}
5	0.623	0.05	0.0312	6.23×10^{3}

N.C. concentration = $\frac{40 pCi\ l^{-1}}{}$ Total content= $\frac{1.19 \times 10^{5}}{}$

Irish Sea volume = $\frac{5 \times 10^{3}\ km^{3}}{}$

* concentration relative to that in the North Channel

be calculated as 1.19×10^5 Ci (or 17.3% of total output).

Estimating the volume of the North Channel at 180 km^3 (from Admiralty Charts), the ^{137}Cs content of this area may be calculated as 7.2×10^3 Ci and that of the Clyde Sea Area (volume 165 km^3) as 6.6×10^3 Ci. Thus the total standing crop in the combined North Channel/Clyde Sea Area at this time represents 2.0% of the total Windscale output.

Because of the distinctive annual variations in radiocaesium distribution observed in the Hebridean Sea Area, it is difficult to evaluate the ^{137}Cs content of this region. Nevertheless, by assuming that the situation in December 1977 was similar to that observed in the summer of that year, an approximate assessment may be made. Taking an average plume width of 105 km along the entire N.W. Scottish coast from the North Channel to Cape Wrath (390 km) and assuming an exponential decrease in concentration by a factor of 4 from south to north, the total ^{137}Cs inventory for this region is calculated as 8.86×10^4 Ci (or 12.8% of total output).

Mauchline (1978) has shown that a marked correlation exists between variations in measured ^{137}Cs concentration off the Aberdeen coast and annual release trends from Windscale if a 2 year lag-time is introduced. If, as implied by Mauchline, this relationship may be applied to the entire North Sea, radiocaesium contents of particular areas measured by Kautsky (1976) can be extrapolated to 1977 and a North Sea content of 1.36×10^5 Ci derived (19.7% of total output). In this treatment no account is taken of a ^{137}Cs component from Cap de la Hague - the correlation technique estimating only the Windscale-derived inventory. The total ^{137}Cs content of the North Sea

would thus be obtained by adding another term to account for this additional source.

In all calculations above the contribution to the measured activity from bomb fallout has been considered negligible. Kautsky (1976) has estimated the fallout - derived concentration in the North Sea as 0.15 - 0.2 pCi l^{-1} (1975) which is at least one order of magnitude lower than the Windscale component in all areas.

The extent of removal of radiocaesium into sediment has been calculated, for the Clyde Sea Area, as $\sim$ 0.01% of total output ($\sim$690 Ci). The environmental appearance of ^{137}Cs in sediment is considerably higher, however, in the vicinity of Windscale (E_A = 3.3 x 10^{-2} pCi g^{-1}/Ci $month^{-1}$ - $\sim$ x 16 that in the C.S.A. (Hetherington and Jefferies, 1974)), an area with a similarly higher E_A for ^{137}Cs in water ($\sim$ x 20 that in the C.S.A. in the vicinity of the outfall (Dutton, 1978)). Despite contributions from factors such as sediment type and particle size, as the basis of an estimation procedure, it is assumed that ^{137}Cs removal is directly proportional to the sediment area, water ^{137}Cs contribution and sedimentation rate of a particular region. In this manner estimates of ^{137}Cs content in the sediments of specific regions may be related to that calculated for the Clyde Sea Area if a relative sedimentation rate may be estimated .

Thus, relating the outfall vicinity to the Clyde Sea Area, assuming a similar sedimentation rate, an average water ^{137}Cs concentration (E_A) of x 20 and an area of x $\frac{1}{5}$ sediment content of 2760 Ci is estimated. Similarly, assuming that the average sedimentation rate throughout the Irish Sea, North Channel and

Hebridean Sea Area generally is ~ 0.5 that in the Clyde Sea Area, sediment contents of 8463, 360 and 1413 Ci respectively are calculated for these regions. If the sedimentation rate in the North Sea is assumed to be ~ 0.25 that in the Clyde Sea Area, a sediment radiocaesium inventory of 4209 Ci is derived for that area.

In the above treatment assumed sedimentation rates may be considerably overestimated and thus the sediment ^{137}Cs inventories obtained are maximum values. The sediment inventory of ^{137}Cs from the Minch calculated by Livingston and Bowen (1977) yields an $E_c = 6.9 \times 10^{-6}$ pCi cm^{-2}/Ci if 50% of this inventory is assumed to be fallout (as found in the C.S.A). This value is in fair agreement with an E_c of 8.6×10^{-6} pCi cm^{-2}/Ci derived from the previous calculations. Thus the assumed values for the various parameters may be reasonable. Even though probably an overestimate, the total coastal sediment inventory of 1.79×10^4 Ci corresponds to only 2.6% of the total Windscale output.

The ^{137}Cs content of coastal biota may be calculated from contribution at various trophic levels. ^{137}Cs concentrations in marine organisms have been measured in the Clyde Sea Area and related to ambient water activities. Apparent concentration factors (C_f) for this nuclide (Table 7.2) can therefore be calculated, where the C_f is defined as:-

$$C_f = \frac{^{137}Cs \text{ concentration in organism (pCi } g^{-1})}{^{137}Cs \text{ concentration in water (pCi } ml^{-1})}$$

(after Broom et al (1975))

This parameter is evaluated both in terms of observed wet and dry weights. Marked increase in concentration factor with increasing trophic level is observed (as also found by eg Bryan et al, 1966; Broom et al, 1975) although exact correlation is

TABLE 7.2 APPARENT ORGANIC ^{137}Cs CONCENTRATION FACTORS

	Concentration Factor (wet wt.)	Concentration Factor (dry wt.)
HERMIT CRAB (Eupagurus sp.)	10	40
SCALLOP (Chlamys Opercularis)	20	130
SCAMPI (Nethrops Norwegiens)	45	230
PLAICE (Pleuronectes Platessa)	45	220
COD (Gadus Morhua)	160	780

difficult due to fish mobility (which may be particularly important in the case of the cod samples measured). Thus migration could bias the apparent concentration factor as a result of recent movements through regions with markedly different ambient ^{137}Cs levels.

Assuming that the average phytoplankton standing crop for the North Sea (4 g dry m^{-2} - Drake et al (1978)) is typical of the entire coastal area and taking a typical dry concentration factor of 15 for these organisms (derived from Mauchline and Templeton, 1964; Drake et al, 1978), the ^{137}Cs content in this reservoir may be calculated for each region (Table 7.3). A total content of 0.53 Ci in phytoplankton is estimated. Similarly, taking the pelagic production rate of tertiary carnivores in the North Sea (2.5 g dry m^{-2} y^{-1}) as an estimate of the standing crop throughout the area and a typical dry concentration factor of 200; this contribution to the organic reservoir can be calculated as 4.42 Ci (Table 7.3). The effect of increased productivity in intertidal or shallow areas may also be important to this budget, but is difficult to assess quantitatively. An estimate of the size of this component may, however, be derived by assuming that seaweed collected by the alginate industry in the West Scottish Coast (3×10^{10}g $year^{-1}$ - Currie (1972)) corresponds to 1% of the standing crop and that a wet ^{137}Cs concentration factor for this material of 30 applies (Polikarpov, 1966). The ^{137}Cs component of this reservoir is then estimated as $\sim$1.8 Ci which represents a significant component of the total organic inventory. Finally, taking the total fisheries yield of the standing crop of fish as 8% (Drake et al, 1978) and assuming that all of this component is

TABLE 7.3 ORGANIC Cs-137 INVENTORY

REGION	PLANKTON CONTENT(Ci)	CARNIVORE CONTENT(Ci)
VICINITY	0.03	0.35
IRISH SEA	0.29	2.42
NORTH CHANNEL/C.S.A.	0.01	0.08
HEBRIDEAN SEA	0.05	0.42
NORTH SEA	0.15	1.25
TOTAL	0.53	4.42

used for human consumption, an annual input (maximum) to a human reservoir of 0.35 Ci y^{-1} may be calculated. As the biological half-time of ^{137}Cs is $\sim$140 days (Eisenbud, 1963), this would correspond to a human inventory of 0.19 Ci.

Even assuming an underestimation of up to x 10 in the above calculation of the total organic ^{137}Cs inventory, a content of $\lesssim$50 Ci (0.007% of total output) is implied. It is obvious that, in relation to the aqueous and sedimentary phases, the organic ^{137}Cs reservoir is negligibly small.

A total budget for Windscale ^{137}Cs output may thus be summarised (Table 7.4) in terms of contributions from decay (6.4%), coastal water inventory (53.7%) and sediment content (2.6%). The balance (2.57×10^5 Ci, 37.3%) corresponds to ^{137}Cs lost from the coastal water system into the north east Atlantic. From this budget the total environmental input of Windscale radiocaesium releases may be assessed while the general treatment may be applied to other, less well specified, soluble pollutants (as considered in the next section).

It must be emphasised that this budget is derived for December 1977 and will change with time. As $>$ 50% of Windscale output between 1952 - 1977 occurred in the 3 years prior to the budget date, the coastal water content is expectedly high and will decrease in the future - which may be emphasised by the current decreasing trend in ^{137}Cs output rate.

7.4 Practical Applications

The basic information on coastal marine processes summarised in previous sections has general applications as background data in a range of physical, biological, geochemical

TABLE 7.4

WINDSCALE ^{137}Cs BUDGET (TO END OF 1977)

Windscale output	6.99×10^{5} Ci
decay	4.44×10^{4} Ci

AREA	WATER*	SEDIMENT*	ORGANICS*
Vicinity	1.25×10^{4}	2760	
Irish Sea	1.19×10^{5}	8463	
North Channel	7.2×10^{3}	360	
Clyde Sea Area	6.3×10^{3}	690	
Hebridean Sea	8.86×10^{4}	1413	
North Sea	1.36×10^{5}	4209	
Total Coastal	3.70×10^{5}	1.79×10^{4}	5×10^{1}

Balance (North East Atlantic) 2.57×10^{5} Ci

*total activity in Ci.

and environmental oceanographic studies. In this section some specific environmental applications will be discussed.

One of the most obvious applications of the data lies in its use for assessing the radiological hazard associated with Windscale radiocaesium releases. The estimated 0.19 Ci ^{137}Cs inventory in the general population is probably an overestimate due to the effects of non-human or indirect fish consumption (eg of fish-meal) or of rejected components (eg head, bones, skin). It must be noted, however, that additional marine-derived contributions to diet have not been considered but would be expected to be small (for the previously mentioned alginates corresponding to 0.01 Ci in the unlikely case of total direct human consumption). Assuming that contaminated fish consumption is evenly distributed throughout the population of the United Kingdom ($\sim 5.6 \times 10^7$ people) (although a considerable proportion, especially of the North Sea catch, will be distributed throughout Europe), the average ^{137}Cs body burden per head of population is $\sim$3390 pCi. For an average man (weight 70 kg), this corresponds to a ^{137}Cs concentration of 48.4 pCi/kg. These values may be compared to the natural ^{40}K content of the average man of $\sim 0.1 \mu$ Ci ($\sim$1430 pCi/kg) or to a typical fallout-derived ^{137}Cs body burden (U.S.A., 1964) of $\sim$14000 pCi (200 pCi/kg) (National Research Council, 1973). Comparison of the derived quarterly intake of ^{137}Cs from fish (1560 pCi) with the NRPB oral intake limit (Morgan, 1974) of 30 μ Ci (total body) indicates that this input is only $\sim$0.005% of the permissible maximum. The average dose to the entire populationis, however, of limited practical value in calculating associated radiological (especially somatic) hazards as the concentration of radiocaesium in the

coastal environment is markedly heterogeneous, with highest levels in the vicinity of Windscale. Radioecological studies of the Windscalearea, and the Irish Sea in general, have been extensive (eg Bryan et al, 1966; Mitchell, 1975; 1977a; 1977b; Preston, 1975; Hetherington, 1976) and indicate that radiocaesium in fish is a major human exposure pathway (maximum exposure $\sim$ 44% of ICRP limit in 1976) while external dose from sediments is significant only in the immediate pipeline vicinity (Mitchell, 1977b). Little work has, however, been reported on calculated dose rates in other areas, the most significant of which is probably the North Channel/Clyde Sea Area region. From previously presented data, average concentrations of ^{137}Cs in fish and shellfish in the Clyde Sea Area can be calculated as 6.4 and 1.8 pCi g^{-1}. respectively (for December 1977) and thus a maximum consumption rate of 265 g/day (224 g/day fish, 41 g/day shellfish) would represent $\sim$9% of the ICRP limit (as estimated by Mitchell (1977b)). At this time, exposure to a critical group similar to that defined for the Windscale region would be $\sim$2% of the ICRP limit. During the period of maximum ^{137}Cs concentration in the Clyde Sea Area (April 1977) these exposures were $\sim$25% greater. It must be noted however that levels of this magnitude existed for a period of only $\sim$4 months and that the effective increase might be reduced by the influence of biological accumulation lag-time (cf eg Jefferies and Hewett, 1971). It is notable that, while the exposure to a critical group in the Clyde Sea Area is less than that to the general public consuming fish from the Irish Sea, a maximum consumer in the C.S.A. may receive a higher exposure,

more typical of that of a member of the Windscale area fish-eating community (Mitchell, 1977b).

While not, as yet, generally regarded as a pollution hazard, there is considerable interest in monitoring the low concentration of transuranic elements in the marine environment due to their generally high radiotoxicity, long half-life and complex chemistry (Noshkin, 1972). While the transuranics are generally fairly reactive and thus quickly removed into sediment from the marine water column, the presence of a 'soluble' Pu component has been reported and is of particular interest (eg Noshkin, 1972; Livingston and Bowen, 1977). ^{239} and ^{240}Pu (the sum of ^{239}Pu and ^{240}Pu components which cannot easily be determined individually due to the similarity of their α-energies) is released from Windscale and the activity ratio of soluble ^{239} and ^{240}Pu to ^{137}Cs has been reported as relatively constant over distances of 10 - 100 km from the Windscale outfall (Hetherington, 1976; Lovett and Nelson, 1978) implying that this soluble component may be regarded as conservative on timescale of coastal water transport processes. Although absolute release data are not available for ^{239} and ^{240}Pu, an estimate of the relative concentrations of soluble ^{239} and ^{240}Pu and ^{137}Cs in the Windscale vicinity may be derived from concentrations reported in fish from the area (high ^{239} and ^{240} Pu/^{137}Cs ratios in mussels in the vicinity of the outfall are not used, as a large proportion of the observed α-activity may be due to absorption of active particulates by these filter-feeding organisms). As quoted concentration factors for Pu in marine vertebrates (Noshkin, 1972) are similar to those previously calculated for ^{137}Cs it may be

assumed there is no significant fractionation of these nuclides during biological uptake. From measured concentrations of ^{239} and ^{240}Pu and ^{137}Cs in plaice from the Windscale area (0.0042 and 41 pCi g^{-1} (wet) respectively - Mitchell (1977b)). a relative water concentration of $\sim 1 \times 10^{-4}$ may be calculated which will be assumed to be fairly constant over 1975 - 1977 in the following treatment. If 'soluble' Pu is assumed to be effectively conservative, the E_A of ^{239} and ^{240}Pu in water will be similar to that of ^{137}Cs at particular locations and hence the Windscale-derived soluble ^{239} and ^{240}Pu concentration may be estimated (column A - Table 7.5) as ranging from $\sim$ 0.1 pCi l^{-1} in the outfall vicinity to $\sim$0.0005 pCi l^{-1} in the North Sea. If, however, as indicated by the measurements of Livingston and Bowen (1977), the E_A of ^{239} and ^{240}Pu in the Minch is $\sim$50% that of ^{137}Cs, it may be assumed that in addition to dilution during transport, removal of Pu into sediment is significant. If ^{239} and ^{240}Pu removal is assumed to be first order with respect to time, the E_A of this pair at any site will be given by:-

$$E_A^{Pu} = E_A^{Cs} e^{\frac{-0.693 \times t}{\gamma_{\frac{1}{2}}}} \qquad \ldots.7.1$$

where t is the transit time between outfall and a particular site and $\gamma_{\frac{1}{2}}$ is the water residence half-time of ^{239} and ^{240}Pu (which is known to be equal to the transit time from Windscale to the Minch from Livinston and Bowen (1977)). From the transit times previously derived for a 'typical year' (1976), the Windscale-derived soluble ^{239} and ^{240}Pu concentration may be calculated to range from $\sim$0.1 pCi l^{-1} in the outfall

TABLE 7.5 CALCULATED WINDSCALE DERIVED 'SOLUBLE' $^{239+240}Pu$ CONCENTRATION

REGION	E_A^{Cs}	$^{239+240}Pu$ CONCENTRATION(pCi/l)	
		A	B
VICINITY	5	0.1	0.1
IRISH SEA	0.5	0.01	0.0059
N.C./C.S.A.	0.25	0.005	0.0027
H.S.A.	0.1	0.002	0.001
NORTH SEA	0.025	0.0005	0.00013

A - 'soluble' Pu assumed conservative on a coastal timescale

B - 'soluble' Pu residence half-time in coastal water = 10 months

vicinity to $\sim$ 0.00013 pCi l^{-1} in the North Sea (Table 7.5, column B). These calculated values are within the range of values measured in British coastal waters (eg Murray and Kautsky, 1977; Murray et al, 1978) although these measurements include additional components from fallout and waste releases from Dounreay and Cap de la Hague.

The use of ^{137}Cs as a tracer of pollutant distribution, as considered above for Pu, can be applied to any other conservative or semi-conservative, stable or radioactive pollutant in the coastal marine environment. In addition, the physical oceanographic data provided from the radiocaesium study may be utilised in environmental studies.

Generally, for any conservative pollutant with a point source with characteristic output rate (F(t)) a function of time (t), from the measured water concentration at a distance with specific transit time (θ), a water environmental appearance ($E_A^{\ w}$) may be calculated as

$$E_A^{\ w} = \frac{c(t)}{F(t-\theta)} \qquad \ldots.7.2$$

(assuming transit by a simple advective process).
This $E_A^{\ w}$ value is, in effect, a measure of the dilution occurring during transport. If a specific, homogeneous region of known volume (v) and water residence half-time ($\tau_{\frac{1}{2}}$) is characterised by this E_A value, the fractional passage (P) of output through this area is

$$P = V.E_A^{\ w}.\frac{0.693}{\tau_{\frac{1}{2}}} \qquad \ldots.7.3$$

If the concentration of this species in sediment (c(s)) is a measurable function of depth (s), a similar sediment environmental appearance ($E_A^{\ s}$) may be calculated ie.

$$E_A^{\,s} = \frac{\int_0^{\infty} c(s)ds}{\int_0^{\infty} F(t)dt} \qquad \ldots.7.4$$

where the sediment concentration is integrated from surface to depth while the output rate is integrated from first output to a time before collection of the sediment sample. The concentration factor (C_F) of sediments of the area is thus

$$C_F = \frac{E_A^{\,s}}{E_A^{\,w}} \qquad \ldots.7.5$$

giving a fractional removal (R) of:-

$$R = \frac{E_A^{\,s} B.\gamma_{\frac{1}{2}}}{E_A^{\,w}.V.0.693} \qquad \ldots. 7.6$$

where B is the total sediment flux of the region. The residence half-time ($T_{\frac{1}{2}}$) for the pollutant in waters of this area is then given by

$$T_{\frac{1}{2}} = -\frac{\gamma_{\frac{1}{2}}}{\ln R} \qquad \ldots.7.7$$

As an example, the residence half-time of water in the Clyde Sea Area ($\gamma_{\frac{1}{2}} \simeq 2$ months) may be used, with the known input rate ($\sim 10^6$ m^3 day^{-1}) to calculate the standing crop of sewage in the region ($\sim 8.7 \times 10^7$ m^3). Thus the sewage dilution factor is 1:1900. In a more complex case, however, the average Ni concentration in the C.S.A. (0.53 μg l^{-1}) has been shown to be significantly higher than that (0.38 μ g l^{-1}) in the southern reaches of the North Channel (Preston, 1973). Assuming conservative behaviour of Ni, to maintain these levels it may be calculated from the above data that an input rate of 280 kg day^{-1} of dissolved Ni would be required within the C.S.A. As the dissolved Ni input from rain is $\sim$ 19 kg day^{-1} over the

area of the Clyde Sea (Cambray et al, 1975), it is evident that Ni input from the catchment (both natural and industrial) corresponds to ~ 260 kg day^{-1}. The dissolved Ni input to the C.S.A. waters are thus the North Channel (~ 6270 kg day^{-1}), the catchment area (~ 260 kg day^{-1}) and rain (~ 20 kg day^{-1}).

7.5 Further Developments

The variety of topics studied in this project hopefully demonstrate the versatility of tracer applications of radiocaesium in the coastal marine environment. It is anticipated that future research will see continued and expanding use of this radionuclide. From the experience gained here, suggestions for further development may be listed under various categories:-

1) Experimental a) more extensive intercalibration would be desirable - particularly with other research laboratories.

b) a corer capable of retrieving cores up to 50 cm long without disturbance or loss of surface is required for rigorous radiocaesium analysis of single cores from coastal areas.

2) The Clyde Sea Area a) repeated spatial sampling would determine the validity of assuming homogeneity.

b) continuation of regular monthly sampling would permit the box model treatment to be tested over a longer time period. The after- effects of the 'abnormal' conditions of 1977 on flow through the North Channel could also be assessed.

3) L. Goil - more intensive sampling over periods of rapid flushing or stratification may allow resolution of processes

on timescales $\lesssim$1 month while calculated diffusion rates through the pycnocline would be better defined.

4) The Hebridean Sea Area - a further sampling trip would enable assessment of the variability of coastal water flow in this region. Northwards extension of the sampling grid would also allow study of water flow through the Minch.

5) Sediment a) the decline of the Windscale radiocaesium output provides an ideal peak for future sediment work which could readily be utilised to study rates of sedimentation and surface mixing.

b) further investigation of the distribution of ^{137}Cs in the sedimentary column with respect to particle size, mineralogy etc. would be of particular interest - especially in view of the possibility of fallout and Windscale-derived ^{137}Cs being present on different sorption sites.

6) General - one of the main problems associated with this project was generated by the very success of the tracer technique and by its productionof an almost overwhelming amount of data ($\sim$1000 sets of data containing up to 15 parameters each). This great rate of data production mirrors that occurring generally as the capabilities of modern analytical equipment expand. Thus, by necessity, the computer has become an essential data-handling tool. Development of this facility, however, may not only assist in calculation and management of results, but may finally allow systems of the complexity of the marine environment to be modelled in a realistic manner and, ultimately, managed on a scientific basis.

REFERENCES CITED.

ALDRICH, C.T. & WETHERILL, G.W. , 1958.
Ann. Rev. Nucl. Sci. , 8 , 257-298.

ALLER, R.C. & COCHRAN, J.K. , 1976.
Earth Planet. Sci. Lett. , 29 , 37-50

ANDERSON, J.J. & DEVOL, A.H. , 1973.
Est. Coast. Mar. Sci. , 1 , 1-10.

ANDERSON, R.Y. , 1977. Limnol. Oceanog., 22 , 423-433.

AUFFRET, J.P., GERMAIN, P., GUEGUENIAT, P. & LEMOSQUET, Y., 1971.
Cahiers Oceanographique , 23 , 935-955.

BAEDECKER, P.A., 1971. proc. conf. Activation Analysis in Geochemistry and Cosmochemistry , Scandinavian University Books, Denmark.

BALLANTYNE, A.G. , 1978. B.Sc. Thesis, Glasgow University.

BARNES, C.A. & GROSS, M.G. , 1966. "Disposal of Radioactive Wastes into Seas, Oceans and Surface Waters ", pp 291-302. I.A.E.A. proceedings , STI/PUB/126 , Vienna.

BARNES , H. & GOODLEY, E.F.W. , 1961.
Bull. Mar. Ecol. , V (43), pp 112-150.

BAXTER, M.S. & HARKNESS, D.D. , 1975. proc. I.A.E.A. & F.A.E. conf."Isotope ratios as pollutant source and behaviour indicators." p.135.

BAXTER, M.S. & McKINLEY, I.G. , 1978.
Proc. Roy. Soc. Edin., 76B , 17-35.

BAXTER, M.S., McKINLEY, I.G., MACKENZIE, A.B. & JACK, W. , 1978.
Mar. Poll. Bull. In Press.

BEST, G.A. , 1970. Ph.D. Thesis , Liverpool University.

BHAT, S.G., KRISHNASWAMI, S., LAL, D., RAMA & MOORE, W.S. , 1969.
Earth Planet. Sci. Lett. , 5 , 483-491.

BIEN,G.S., RAKESTRAW,N.W. & SUESS,H.E. , 1965.
Limnol. Oceanog. , 10 , R 25-37.

BLAUER,H.M. , 1977. Ph.D. Thesis, Glasgow University.

BOLTER,E., TUREKIAN,K.K. & SHUTZ,D.F. , 1964.
Geochim. Cosmochim. Acta , 28 , 1459-1466.

BONI,A.L. , 1966. Anal. Chem. , 38 , 89-92.

BOWDEN,K.F., 1950. Month. Not. Roy. Astron. Soc. Geophys.
Supp., 6 , 63-87.

BOWDEN,K.F. , 1955. Fish. Invest. Lond. Ser.II, 18(8),1-69

BOWDEN,K.F. , 1975. "Chemical Oceanography" (Riley & Skirrow,
Eds.), 2nd. ed., Vol. 1,pp1-41. Academic Press,London.

BOWEN,H.J.M. , 1978. "The Chemical Environment." (Lenihan &
Fletcher, Eds.) pp 1-37. Blackie, Glasgow.

BOWEN,V.T. , 1971. "Radioactivity in the Marine Environment",
pp 68-69. N.A.S. , Washington D.C.

BOWEN,V.T., OLSEN,J.S., OSTERBERG,C.L. & RAVERA,J. , 1971.
"Radioactivity in the Marine Environment", pp 200-222.
N.A.S., Washington D.C.

BOWEN,V.T., NOSHKIN,V.E., VOLCHOK,H.L., LIVINGSTON,H.D. & WONG
K.M. , 1974.
Limnol. Oceanog., 19 , 670-681.

BRANNON,J.M., ROSE,J.R., ENGLER,R.M. & SMITH,I. , 1977.
"Chemistry of Marine Sediments" (Yen,ed.), pp 125-189.
Ann Arbor Science, Michigan.

BREWER,P.G. , 1975. "Chemical Oceanography" (Riley & Skirrow,
Eds.), 2nd. ed., Vol. 1 , pp 415-496.

BRINCKMAN,F.E. & IVERSON,W.P. , 1975. "Marine Chemistry in the
Coastal Environment" (Church, ed.), pp 319-342.
Am. Chem. Soc., Washington D.C.

BROECKER,W.S., 1966. J. Geophys. Res. , 71 , 5827-5836

BROECKER,W.S., 1971. "Radioactivity in the Marine Environment" p 68. N.A.S., Washington D.C.

BROECKER,W.S. , 1975. "Chemical Oceanography". Harcourt Brace Jovanovich , New York.

BROECKER,W.S., EWING,M. & HEEZEN,B.C., 1960. Am. J. Sci. , 258 , 429.

BROOM,M.J., GRIMWOOD,P.D. & BELLINGER,E.G., 1975 Mar. Poll. Bull. , 6 , 24-26.

BRULAND,K., BERTINE,K., KOIDE,K. & GOLDBERG,E.D. , 1974. Environ. Sci. Tech. , 8 , 425.

BRYAN,G.W., PRESTON,A. & TEMPLETON,W.L. , 1966. "Disposal of Radioactive Wastes into Seas,Oceans and Surface Waters." I.A.E.A. proceedings STI/PUB/126 pp 623-637.

BURTON,J.D. , 1965. "Chemical Oceanography" (Riley & Skirrow, Eds.), 1st. ed., Vol. 2, pp425-475.

BURTON,J.D. , 1975. "Chemical Oceanography" (Riley & Skirrow, Eds.), 2nd. ed., Vol. 3, pp 91-191.

CAMBRAY,R.S., JEFFERIES,D.F. & TOPPING,G., 1975. U.K.A.E.A. Publication AERE-R7733. H.M.S.O.

CHERRY,R.D., GERICKE,I.H. & SHANNON,L.V., 1969. Earth Planet. Sci. Lett. , 6 , 451-456.

CHESTER,R. & ASTON,S.R., 1976. "Chemical Oceanography" (Riley & Chester,Eds.), 2nd. ed., Vol.6, pp 281-390. Academic Press , London.

CHUNG,Y-C., 1973. Earth Planet. Sci. Lett. , 17 , 319-323.

CHUNG,Y-C., 1974. Earth Planet. Sci. Lett. , 21 , 295-300.

CHUNG,Y-C. & CRAIG,H., 1973. Earth Planet. Sci. Lett., 17 , 306-318.

C.R.P.B.,1973. C.R.P.B. Annual Report No.17 for year 1972.
C.R.P.B.,1974a. " " " " 18 " " 1973.
C.R.P.B.,1975. " " " " 19 " " 1974.
C.R.P.B.,1976. " " " " 20 " " 1975.

CLYDE RIVER PURIFICATION BOARD, 1974b.
N.E.R.C. publications series C, no. 11, pp 24-27.

COLLAR,R.H.F., 1974. N.E.R.C. publications series C,no.11, pp 24-27.

COVELL,D.F., 1959. Anal. Chem. , 31 , 1785-1790.

COX,R.A., McCARTNEY,M.J. & CULKIN,F., 1970.
Deep-Sea Res. , 17 , 679-689.

CRAIB,J.S., 1965. J. Cons. Perm. Int. Explor. Mer.,30, 34-39.

CRAIG,R.E., 1956. Ann. Biol. Copenh. , 11 , 34-36.

CRAIG,R.E., 1959. Mar. Res. ,1958(2). H.M.S.O., Edinburgh.

CROUTHAMEL,C.E., ADAMS,F. & DAMS,R., 1970. "Applied Gamma-ray Spectrometry", 2nd. ed. Pergamon , Oxford.

CURRIE,R.I., 1972. Symp. Zool. Soc. Lond. , 29 , 285-296.

DANIELS,F. & ALBERTY,R.A., 1966. "Physical Chemistry", 3rd. ed. Wiley International ,New York.

DEEGAN,C.E., 1974. N.E.R.C. publications series C, no. 11, pp 6-9.

DEGENS,E.T. & MOPPER,K., 1976. "Chemical Oceanography" (Riley & Chester, eds.), 2nd. ed. Vol. 6, pp 59-113.

DE GROOT,A.J., SALOMENS,W. & ALLERSMA,E., 1976.
"Estuarine Chemistry" (Burton & Liss,eds.) Academic Press, London.

DOOLEY,H.D. & STEELE,J.H., 1969.
Dt. Hydrogr. Z. , 22 , 213-223.

DRAKE,C.L., IMBRIE,J., KNAUSS,J.A. & TUREKIAN,K.K., 1978. "Oceanography". Holt, Rinehart & Winston, New York.

DUNSTER,H.J., 1978. Mar. Poll. Bull. , 9 , 118-122.

DUTTON,J.W.R., 1977; 1978a. Personal Communication.

DUTTON ,J.W.R., 1978b. Unpublished paper in "Radioactivity in the Marine Environment", a conference of the Marine Chemistry Discussion Group, Liverpool.

DUTTON,J.W.R. & STEELE,A.K., 1966. "The detection of Radioactivity from Nuclear Shipping waste discharges in the Marine Environment at the U.S.N. Nuclear Submarine Base, HolyLoch, Scotland." M.A.F.F. report, F.R.L., Lowestoft.

DUURSMA,E.K., 1972. Oceanogr. Mar. Biol. Ann. Rev., 10 , 137-223.

DUURSMA,E.K., 1976. "Estuarine Chemistry" (Burton & Liss,eds.) pp 159-183.

DUURSMA,E.K. & HOEDE,C., 1967. Neth. J. Sea Res. , 3 , 423-457.

DUURSMA,E.K. & BOSCH,C.J., 1970. Neth. J. Sea Res. , 4 , 395-469.

DUURSMA,E.K. & GROSS,M.G., 1971. "Radioactivity in the Marine Environment" pp 147-160. N.A.S., Washington D.C.

DUURSMA,E.K. & EISMA,D., 1973. Neth. J. Sea Res. , 6 , 265-324.

DUURSMA,E.K. & MARCHAND,D., 1974. Oceanogr. Mar. Biol. Ann. Rev. , 12 , 315-431.

EDWARDS,A. & EDELSTEN,D.J., 1976a. Proc. Roy. Soc. Edin. , 75 , B207-221.

EDWARDS,A. & EDELSTEN,D.J., 1976b. Hydrological Sciences Bulletin, XXI , 445-450.

EDWARDS,A. & EDELSTEN,D.J., 1977.
Est. Coast. Mar. Sci., 5 .

EISENBUD,M., 1963. "Environmental Radioactivity". McGraw-Hill, New York.

ELLETT,D.J., 1977a. Ann. Biol. Copenh. , 33 , 28-30.

ELLETT,D.J., 1977b. Ann. Biol. Copenh. , 33 , 27-28.

ELLETT,D.J., 1977c. Cruise Report,R.R.S. Challenger Cruise 10/1977, S.M.B.A., Dunstaffnage.

ELLETT,D.J., 1978a. Proc. Roy. Soc. Edin. (B). In Press.

ELLETT,D.J., 1978b. Personal Communication.

EVANS,D.W. & CUTSHALL,N.H., 1973. "Radioactive contamination of the Marine Environment." I.A.E.A. proceedings, STI/PUB/313, Vienna pp 125-140.

FINKEL,R., KRISHNASWAMI,S. & CLARK,D.L., 1977.
Earth Planet. Sci. Lett. , 31 , 199.

FOLSOM,T.R., FELDMAN,C. & RAINS,T.C., 1964.
Science , 144 , 538-539.

FOLSOM,T.R. & SREEKUMARAN,C., 1970. "Reference Methods for Marine Radioactivity Studies." pp 129-186. I.A.E.A. Technical Reports Series No.118, STI/DOC/10/118,Vienna.

FRANCIS,C.W. & BRINKLEY,F.S., 1976.
Nature , 260 , 511-513.

FRIEDLANDER,G., KENNEDY,J.W. & MILLER,J.M., 1964.
"Nuclear and Radiochemistry," 2nd. ed. Wiley International, Singapore.

FUKAI,R. & MURRAY,C.N., 1973. "Environmental behaviour of radionuclides released in the nuclear industry," pp217-242. I.A.E.A. proceedings, STI/PUB/345, Vienna.

GILAT,E., LAICHTER,Y. & SHAFRIR,N.H., 1975. "Impacts of nuclear releases into Aquatic environments," pp 63-76. I.A.E.A. proceedings, STI/PUB/406, Vienna.

GOLDBERG,E.D., 1975. "Chemical Oceanography" (Riley & Skirrow, eds.) 2nd. ed., Vol.3, pp 39-89.

GOLDBERG,E.D. & KOIDE,M., 1962. Geochim. Cosmochim. Acta., 26 , 417-450.

GOLDBERG,E.D., BROECKER,W.S., GROSS,M.G. & TUREKIAN,K.K., 1971. "Radioactivity in the Marine Environment",pp 137-146. N.A.S., Washington D.C.

GOLDBERG,E.D. & BRULAND,K., 1974. "The Sea". (Goldberg,ed.), Vol. 5, pp 451-489.

GOODAIR,A., 1967. "The distribution of particulate isotopes derived from pressurised water reactor effluent from nuclear submarines in a sea loch." N.R.P.S. report, I.N.S., Alverstoke.

GREVE,P.A., 1971. Science , 173 , 1021.

GROSS,M.G., 1972. Mar. Poll. Bull., 3 , 61.

GROSS,M.G., BARNES,C.A. & RIEL,G.K., 1965. Science , 149 , 1088-1090.

GROSS,M.G. & NELSON,V.A., 1966. Science , 154 , 879.

GUINASSO,N.L. & SCHINK,D.R., 1975. J. Geophys. Res. , 80 , 3032-3043.

HAKANSON,L., 1976. Limnol. Oceanog. , 21 , 170.

HALCROW,W., MACKAY,D.W. & THORNTON,I., 1973. J. Mar. Biol. Ass. U.K. , 53 , 721-739.

HAMMOND,D.E., SIMPSON,H.J. & MATHIEU,G.,1975. "Marine Chemistry in the coastal environment." (Church,ed.), pp119-132. Am. Chem. Soc., Washington D.C.

HARDY,J.A., 1969. Unpublished lecture presented to the 24th. annual electronics,instruments,controls and components exhibition and convention, Manchester.

HARRISON,G.C.A., 1974. Earth Sci. Rev. , 10 , 1-36.

HEATH,R.L. & SCHROEDER,F., 1957. "Quantitative techniques of scintillation spectrometry as applied to calibration of standard sources." Idaho Operations Office,IDO-16149.

HEATH,G.W., 1974. N.E.R.C. publications series C,No.11,pp1-2.

HEDGES,R., 1978. New Scientist , 77 , 599-601.

HESS,C.T., SMITH,C.W. & PRICE,A.H., 1978. Nature , 272 , 807-809.

HETHERINGTON,J.A., 1976a. M.A.F.F. technical report FRL 11.

HETHERINGTON,J.A.,1976b. "Environmental Toxicity of Aquatic Radionuclides:Models and Mechanisms", pp81-106. Ann Arbor Science, Michigan.

HETHERINGTON,J.A. & JEFFERIES,D.F., 1974. Neth. J. Sea Res. , 8 , 319-338.

HETHERINGTON,J.A. & HARVEY,B.R., 1978. Mar. Poll. Bull. , 9 , 102-106.

HOWELLS,H., 1966. "Disposal of radioactive wastes into Seas, Oceans and Surface Waters", pp 769-785. I.A.E.A. proceedings, STI/PUB/126, Vienna.

HOWELLS,H., 1978. Personal Communication.

I.A.E.A., 1970. "Reference methods for marine radioactivity studies." I.A.E.A. technical report series No.118, STI/DOC/10/118, Vienna.

ISHIGURO,S., 1972. Oceanogr. Mar. Biol. Ann. Rev., 10 ,27-96.

ITO,N., FUKADA,M. & TANIGAWA,Y., 1966. "Disposal of radioactive wastes into Seas ,Oceans and Surface Waters," pp 471-482. I.A.E.A. proceedings,STI/PUB/126, Vienna.

JEFFERIES,D.F., 1968. Helgolander Wiss. Meeresunters , 17 , 280-290.

JEFFERIES,D.F., 1976;1978. Personal Communications.

JEFFERIES,D.F. & HEWETT,C.J., 1971. J. Mar. Biol. Ass. U.K. , 51 , 411-422.

JEFFERIES,D.F., PRESTON,A. & STEELE,A.K., 1973. Mar. Poll. Bull. , 4 , 118-122.

JERNELOV,A., 1974. "The Sea." (Goldberg,ed.), Vol.5, pp799-815. Wiley Interscience, New York.

JOHNSTON,R., ADAMS,J.A. & DOOLEY,H.D., 1974. N.E.R.C. publications series C,No.11, pp 16-21.

JOLY,J., 1908. Phil. Mag. , 15 , 385-395.

JOLY,J., 1912. Phil. Mag. , 24 , 694-705.

JOSEPH,A.B., GUSTAFSON,P.F., RUSSEL,I.R., SCHUERT,E.A., VOLCHOK, H.L. & TAMPLIN,A., 1971. "Radioactivity in the Marine Environment", pp 6-41. N.A.S., Washington D.C.

KAUFMAN,A., BROECKER,W.S., KU,T-L. & THURBER,D.L., 1971. Geochim. Cosmochim. Acta , 35 , 1155.

KAUTSKY,H., 1976. Dt. Hydrogr. Z. , 29 , 217-221.

KAWAMURA,S., SHIBATA,S. & KUROTAKI,K., 1971. Anal. Chim. Acta , 56 , 405-413.

KINNEL,B.L., AXLER,R.P. & GOLDMAN,C.R., 1977. Limnol. Oceanogr. , 23 , 768-772.

KOIDE,M., SOUTAR,A. & GOLDBERG,E.D., 1972. Earth Planet. Sci. Lett. , 14 , 442-446.

KOIDE,M., BRULAND,K.W. & GOLDBERG,E.D., 1973. Geochim. Cosmochim. Acta , 73 , 1171-1187.

KOIDE,M., BRULAND,K.W. & GOLDBERG,E.D., 1976.
Earth Planet. Sci. Lett. , 31 , 31-36.

KRISHNASWAMI,S., LAL,D., MARTIN,J.M. & MEYBECK,M., 1971.
Earth Planet. Sci. Lett. , 11 , 407.

KRISHNASWAMI,S. & LAL,D., 1972. "The Changing Chemistry of the Oceans." (Dyrssen & Jagner,eds.), pp 307-320. Wiley Interscience, New York.

KU,T-L., 1976. Ann. Rev. Earth Planet. Sci. , 4 , 347-380.

KU,T-L. & BROECKER,W.S., 1967. Progress in Oceanography, 4 , 95-104.

LAL,D., 1962. J. Oceanogr. Soc. Japan , 20 , 600.

LEATHERLAND,T., 1976;1977. Personal Communications.

LENNIE,D., 1978. B.Sc. Thesis, Glasgow University.

LERMAN,A. & LIETZKE,T.A., 1975.
Limnol. Oceanogr. , 20 , 497-500.

LIBBY,W.F., 1946. Phys. Rev. , 69 , 671.

LIETZKE,T.A., LERMAN,A. & TANIGUCHI,H., 1973.
Trans. Am. Geophys. Union, 54 , 341.

LIVINGSTON,D.A., 1963. Geol. Surv. Prof. Paper 440-G,U.S.A.

LIVINGSTON,H.D. & BOWEN,V.T., 1977.
Nature , 269 , 586-588.

LOVETT,M.B. & NELSON,D.M., 1978. "Symposium on the determination of radionuclides in environmental and biological materials", paper 14. C.E.G.B., London.

LOWMAN,F.G., PHELPS,D.K., McCLIN,R., ROMAN DE VEGA,V., OLIVER DE PADOVANI,I. & GARCIA,R.J., 1966. "Disposal of radioactive wastes into seas,oceans and surface waters", pp 249-266. I.A.E.A. proceedings STI/PUB/126, Vienna.

LOWMAN,F.G., RICE,T.R. & RICHARDS,F.A., 1971. "Radioactivity in the Marine Environment", pp161-199. N.A.S. Washington D.C.

MACKAY,D.W. & LEATHERLAND,T.M., 1976. "Estuarine Chemistry" (Burton & Liss,eds.), pp 185-218. Academic Press, London.

MACKENZIE,A.B., 1977. Ph.D. Thesis, Glasgow University.

MAUCHLINE,J., 1966. "Encyclopaedia of Oceanography" (Fairbridge,ed.),Vol.1,pp726-730. Reinhold, U.S.A.

MAUCHLINE,J., 1978. "Marginal Seas of Northeastern Europe" (Banner & Massie,eds.), In Press. Elsevier, London.

MAUCHLINE,J. & TEMPLETON,W.L., 1963. Nature , 198 , 623-626.

MAUCHLINE,J. & TEMPLETON,W.L., 1964. Oceanogr. Mar. Biol. Ann. Rev. , 2 , 229-279.

McKINLEY,I.G., 1975. B.Sc. Thesis, Glasgow University.

McLELLAN,H.J., 1965. "Elements of Physical Oceanography." Pergamon, Oxford.

MEYER,P.L., 1972. "Introductory probability and statistical applications." Addison-Wesley, Massachusetts.

MICHOLET-COTE,C.M., KIRCHMANN,R., CANTLLAN,G., COLLARD,J. & KOCH,G., 1973. "Environmental behaviour of radionuclides released in the nuclear industry," pp413-427. I.A.E.A. proceedings STI/PUB/345, Vienna.

MILL,H.R., 1892. Trans. Roy. Soc. Edin. , 36 , 641-729.

MILLERD,F.J. & LEPPLE,F.K., 1973. Mar. Chem. , 1,89

MILNE,P.H., 1972. Mar. Res., 1972(3) , 50pp.

MILNE,P.H., 1974. N.E.R.C. publications series C, no. 11 , pp 14-15.

MITCHELL,N.T.,1973. M.A.F.F. technical report FRL9, Lowestoft.
,1975. " " " FRL 10, "
,1977a. " " " FRL 12, "
,1977b. " " " FRL 13, "
,1978. " " " FRL 14, "

MOLCARD,R., 1972. Mem. Soc. Roy. De Sci. De Liege.
6e serie, Tome IV, pp 191-200.

MOORE,H.B., 1931. J. Mar. Biol. Ass. U.K., 17 , 325.

MOORE,W.S., 1972. Earth Planet. Sci. Lett. , 16 , 421-422.

MOORE,W.S. & KRISHNASWAMI,S., 1972.
Earth Planet. Sci. Lett. , 15 , 187.

MORGAN,K.Z., 1974. "Handbook of Chemistry and Physics",
(Weast,ed.), pp B406-415. C.R.C. Press, Ohio.

MURRAY,C.N. & KAUTSKY,H., 1977.
Est. Coast.Mar. Sci. , 5 , 319-328.

MURRAY,C.N., KAUTSKY,H, HOPPENHEIT,M., DOMIAN,M., 1978.
Nature , 276 , 225-230.

NATIONAL ACADEMY OF SCIENCES, 1971. "Radioactivity in the
Marine Environment." N.A.S., Washington D.C.

NATIONAL RESEARCH COUNCIL, 1973. N.R.C. Food Protection
Committee Report"Radionuclides in Food". N.A.S.
Washington D.C.

NATURAL ENVIRONMENT RESEARCH COUNCIL, 1974.
N.E.R.C. publications series C, No. 11.

NIHOUL,J.C.J., 1973. Mem. Soc. Roy. De Sci. De Liege.,
6e serie, Tome VI, pp 9-15.

NISBET,I.C.C. & SAROFIM,A.F., 1972.
Environ. Health Persp. , 1 , 21.

NOSHKIN,V.E., 1972. Health Physics , 22 , 537-549.

NOSHKIN,V.E. & BOWEN,V.T., 1973. "Radioactive contamination of the Marine Environment", pp 671-686. I.A.E.A. proceedings, STI/PUB/313, Vienna.

OESCHGER,H., SIEGENTHALER,U., SHOTTERER,U. & GUGELMANN,A.,1975. Tellus, XXVII , 168-192.

OFFICER,C.B., 1978. "Physical Oceanography of Estuaries." Wiley-Interscience, New York.

OSTERBERG,C., PATTULLO,J. & PERCY,W., 1964. Limnol. Oceanogr. , 9 , 249.

OSTERBERG,C., CUTSHALL,N. & CRONIN,J., 1975. Science , 150 , 1585.

OSTERBERG,C., CUTSHALL,N., JOHNSON,V., CRONIN,J., JENNINGS,D. & FREDERICK,L., 1966. "Disposal of radioactive wastes into seas,oceans and surface waters", pp 321-335. I.A.E.A. proceedings, STI/PUB/126, Vienna.

PARK,K., GEORGE,M.J., MUJAKE,Y., SARUKUSHI,K., KATSAURAGI,Y. & KANAZUYA,T., 1965. Nature , 208 , 1084-1085.

PATEL,B., MULAY,C.D. & GANGULY,A.K., 1975. Est. Coast. Mar. Sci. , 3 , 13-42.

PATEL,B., PATEL,S. & PAWAR,S., 1978. Est. Coast. Mar. Sci. , 7 , 49-58.

PENNINGTON,W., CAMBRAY,R.S. & FISHER,E.M., 1973. Nature , 242 , 324-326.

PENREATH,R.J., 1977. Oceanogr. Mar. Biol. Ann. Rev.,15, 365-460.

PERSSON,R.B.R., 1968. Health Physics , 14 , 241-250.

PETTERSSON,H., 1937. Mitt. Inst. Radiumforsch.,Wien, 400a.

PICKARD,G.L., 1975. "Descriptive Physical Oceanography.", 2nd. ed. Pergamon ,Oxford.

PIGGOT,C.S. & URRY,W.D., 1939. J. Wash. Acad. Sci. , 29 , 405-415.

PIGGOT,C.S. & URRY,W.D., 1941.
Am. J. Sci. , 239 , 81-91.

PLATO,P.A. & JACOBSON,A.P., 1976.
Environ. Pollut. , 10 , 19-34.

POLIKARPOV,G.G., 1966. "Radioecology of Aquatic Organisms."
Amsterdam.

POLLARD,R.T., 1973. Mem. Soc. Roy. De Sci. De Liege, 6^{e} serie,
Tome VI , pp 17-34.

PRESTON,A., 1973. Nature , 242 , 95-97.

PRESTON,A., 1974. "The Sea." (Goldberg,ed.), Vol. 5,
pp 817-836. Wiley- Interscience, New York.

PRESTON,A., 1975. "Impacts of Nuclear Releases into the
Aquatic Environment", pp 3-23. I.A.E.A. proceedings
STI/PUB/406, Vienna.

PRESTON,A., JEFFERIES,D.F. & MITCHELL,N.T., 1971.
"Nuclear Techniques in Environmental Pollution", pp 629-
644. I.A.E.A. proceedings, STI/PUB/268, ,Vienna.

PRESTON,A., JEFFERIES,D.F. & PENREATH,R.J., 1972.
Symp. Zool. Soc. Lond. , 29 , 271-284.

PRESTON,A., WOODHEAD,D.S., MITCHELL,N.T. & PENREATH,R.J., 1972
Proc. Roy. Soc. Edin. , 72 , B411-423.

PRICE,N.B., 1976. "Chemical Oceanography", (Riley & Chester,
eds.),2nd. ed., Vol. 6, pp 1-58. Academic Press,London.

PRITCHARD,D.W., OKUBO,A. & CARTER,H.H., 1966. "Disposal of
radioactive wastes into seas,oceans and surface waters",
pp 397-424. I.A.E.A. proceedings, STI/PUB/126, Vienna.

PRITCHARD,D.W., RIED,R.D., OKUBO,A. & CARTER,H.H., 1971.
"Radioactivity in the Marine Environment", pp 90-136.
N.A.S., Washington D.C.

PROSPERO,J.M. & KOCZY,F.F., 1966.
"Encyclopedia of Oceanography." (Fairbridge,ed.), Vol. 1, pp 730-739,740-748. Reinhold, U.S.A.

PROUDMAN,J., 1948. Proc. Roy. Soc. Lond. , 195 , A300-309.

PROUDMAN,J., 1953. "Dynamical Oceanography." Methuen,London.

PROUT,W.E., RUSSEL,E.R. & GROH,H.J., 1965.
J. Inorg. Nucl. Chem. , 27 , 473-479.

QUITTNER,P., 1969. Anal. Chem. , 41 , 1504-6.

RILEY,J.P., 1975. "Chemical Oceanography", (Riley & Skirrow, eds.), 2nd. ed., Vol. 3, pp 193-514. Academic Press, London.

RILEY,J.P. & TONGUDAI,M., 1966.
Chem. Geol. , 1 , 291294.

RILEY,J.P. & SKIRROW,G., 1975. "Chemical Oceanography", 2nd. ed., Vol. 3. Academic Press, London.

RITCHIE,J.C., McHENRY,R. & GILL,A.C., 1973.
Limnol. Oceanogr. , 18 , 254-263.

ROBBINS,J.A. & EDGINGTON,D.N., 1975.
Geochim. Cosmochim. Acta , 39 , 285-304.

ROBBINS,J.A., KREZOSKI,J.R. & MOZLEY,S.C., 1977.
Earth Planet. Sci. Lett. , 36 , 325-333.

ROBERTSON,D.E., SILKER,W.B., LANGFORD,J.C., PETERSON,M.R. & PERKINS,R.W., 1973. "Radioactive Contamination of the Marine Environment", pp 141-158. I.A.E.A. proceedings STI/PUB/313, Vienna.

ROSHOLT,J.N., EMILIANI,C., GEISS,J., KOCZY,F.F. & WANGERSKI, P.J., 1962. J. Geophys. Res. , 67 , 2907-2911.

RUTHERFORD,F. & CHURCH,T.M., 1975. "Marine Chemistry in the Coastal Environment", (Church,ed.), pp440-452. Am. Chem. Soc. , Washington D.C.

SAAD,A., 1978. Personal Communication.

SANDERS,P.M., 1973. Mem. Soc. Roy. De Sci. De Liege, 6^{e} serie Tome VI, pp99-108.

SCHINK,D.R. & GUINASSO,N.L., 1978. Mar. Geol. , 23 , 133-154.

SCHUERT,E.A., 1971. "Radioactivity in the Marine Environment", p 69. N.A.S., Washington D.C.

SHANNON,L.V., 1973. Investl. Rep. Div. Sea Fish. S. Afr., No. 100.

SMALES,A.A. & SALMON,L., 1955. Analyst , 80 , 37.

SOMAYAJULU,B.L.K., 1977. Geochim. Cosmochim. Acta , 41 , 909.

SPENCER,D.W., ROBERTSON,D.E., TUREKIAN,K.K. & FOLSOM,T.R.,1970 J. Geophys. Res. , 75 , 7688-7696.

SPENCER,C.P., 1975. "Chemical Oceanography", (Riley & Skirrow eds.), 2nd. ed. ,Vol. 2, pp 245-300.

STEANS,C.E. & THURBER,D.L., 1965. Progress in Oceanography, 4 , 293-305.

STEEL,J.A., 1972. Symp. Zool. Soc. Lond. , 29 , 41-67.

STEELE,J.H., McINTYRE,A.D., JOHNSTON,R., BAXTER,I.G., TOPPING, G. & DOOLEY,H.D., 1973. Mar. Poll. Bull. , 4 ,153-157.

STERLINSKI,S., 1968. Anal. Chem. , 40 , 1995-1998.

STERLINSKI,S., 1970 Anal. Chem. , 42 , 151-5.

STOMMEL,H., 1953. Coll. Repr. Woods Hole Oceanogr. Instn.No.655.

SUESS,H.E., 1959. Ann. Rev. Nucl. Sci. , 8 , 243-256.

SVERDRUP,H.U., JOHNSON,M.W. & FLEMING,R.H., 1942 "The Oceans." Prentice-Hall, New York.

SWAN,D.S., 1978. Ph.D. Thesis, Glasgow University.

TAMURA,T. & JACOBS,B.G., 1960. Health Physics , 2 , 391-398.

TEMPLETON,W.L. & PRESTON,A., 1966. "Disposal of Radioactive Wastes into seas ,oceans and surface waters", pp267-289. I.A.E.A. proceedings, STI/PUB/126, Vienna.

THOMSON,J. & WALTON,A., 1972. Proc. Roy. Soc. Edin. , 72/73 , B167-182.

THURBER,D.L., 1965. "Marine Geochemistry." (Schink & Corless, eds.), University of Rhode Island.

TILL,R., 1974. "Statistical Methods for the Earth Scientist." Macmillan, London.

TOPPING,G., 1974. I.C.E.S. report CM 1974/E32.

TUREKIAN,K.K., 1976. "The Oceans." Prentice-Hall, New Jersey.

TUREKIAN,K.K., 1977. Earth Planet. Sci. Lett. , 41 , 1139-1144.

TUREKIAN,K.K. & SCHUTZ,D.F., 1965. "Marine Geochemistry", (Schink & Corless,eds.), pp 41-89. University of Rhode Island.

VOLCHOK,H.L., BOWEN,V.T., FOLSOM,T.R., BROECKER,W.S., SCHUERT, E.A. & BIEN,G.S., 1971. "Radioactivity in the Marine Environment", pp 42-89. N.A.S., Washington D.C.

WALLACE,W.J., 1974 "The Development of the Chlorinity/Salinity Concept in Oceanography" Elsevier, Amsterdam.

WASSON,J.T., 1968. Personal Communication dicussed by Baedecker(1971).

WEAST,R.C.(Ed.), 1974. "Handbook of Chemistry and Physics", 55th. ed. C.R.C. Press, Ohio.

WILLIAMS,J.A. & DAVIDGE,P.C., 1962. J. Brit. Nucl. Energy Soc. , 1 , 14-29.

WILLIAMS,P.J. le B., 1975. "Chemical Oceanography", (Riley & Skirrow,eds.), 2nd. ed. , Vol.2, pp 301-383.

WILSON,T.R.S., 1974. Nature , 248 , 125-127.

WILSON,T.R.S., 1975. "Chemical Oceanography", (Riley & Skirrow,eds.), 2nd. ed. , Vol. 1, pp 365-413 .

WOODHEAD,D.S., 1973. "Radioactive Contamination of the Marine Environment", pp 499-525. I.A.E.A. proceedings, STI/PUB/313, Vienna.

YOUNG,D.R. & FOLSOM,T.R., 1973. "Radioactive Contamination of the Marine Environment", pp 633-650. I.A.E.A. proceedings, STI/PUB/313, Vienna.

YOUNG,D.R., McDERMOTT,D.J., HEESON,T.C. & JAN,J.K., 1975. "Marine Chemistry in the Coastal Environment", (Church,ed.), pp 424-439. Am. Chem. Soc.,Washington D.C.

YULE,H.P., 1968. Anal. Chem. , 40 , 1480-1486.

YULE,H.P., 1971. Proc. Conf. Activation Analysis in Geochemistry and Cosmochemistry. Scandinavian University Books, Denmark.

APPENDICES

Much of the following data tabulation comprises photocopied computer printout and thus is somewhat faint with uneven lettering. In view of the large volume of data accumulated, however, this was found to be the only commercially feasible manner of presentation. The actual programs which output these tables (and plot some of the figures contained in the text) are listed in Appendix II.2 .

APPENDIX I
****

IN THIS SECTION RESULTS OBTAINED IN THIS PROJECT WILL BE LISTED DIRECTLY AS OUTPUT FROM THE COMPUTER PROGRAMS DESCRIBED IN APPENDIX II. RESULTS ARE SUBDIVIDED BY REGION OF INTEREST THUS:-

I,1 CLYDE SEA AREA

I,2 L.GOIL/L.LONG DEEP SITES

I,3 ADDITIONAL SEA LOCH SITES

I,4 HEBRIDEAN SEA AREA

I,5 SEDIMENTS

I,6 MISCELLANEOUS

ABBREVIATIONS USED ARE:-

137(DPM/L) - CS-137 CONCENTRATION IN D,P,M, PER LITRE

134(DPM/L) - CS-134 CONCENTRATION IN D,P,M, PER LITRE

RATIO - CS-134/CS-137 ACTIVITY RATIO

SC7(DPM/L) - SALINITY CORRECTED CS-137 CONCENTRATION

SAL(PM) - SALINITY IN 0/00 (PER MIL)

D,O,(PM) - DISSOLVED OXYGEN IN 0/00

TEMP(C) - TEMPERATURE IN DEGREES CELSIUS.

DRY/WET - DRY/WET WEIGHT RATIO (SEDIMENTS)

****** - UNMEASURED PARAMETER

APPENDIX I.1 CLYDE SEA AREA SAMPLES
****

SAMPLES OBTAINED IN THE AREAL STUDY OF THE CSA DURING CRUISE JM/16/77 OF THE RESEARCH SHIP 'JOHN MURRAY' ARE LISTED ON PAGES A3 AND A4. SAMPLE DATES ARE:-

JM 1- 7 - 8/12/77

JM 8-14 - 9/12/77

JM15-26 - 14/12/77

JM27-32 - 15/12/77

SAMPLES FROM L.FYNE COLLECTED ON RV 'ENDRICK II' ON 7/12/77 ARE LISTED ON PAGE A5 WHILE SAMPLES FROM L.LONG/L.GOIL COLLECTED ON 28/12/77 ARE SHOWN ON PAGE A6.

STATION COORDINATES CORRESPONDING TO THE SAMPLE CODES USED ARE GIVEN ON TABLE 3.1 AND PLOTTED ON FIG. 3.1 OF CHAPTER 3

JOHN MURRAY CRUISE
****

CODE	DEPTH(M)	137(DPM/L)	134(DPM/L)	RATIO	SC7(DPM/L)	SAL(PM)	TEMP(C)	D.O.(PM)
JM1	3.0	130.0 +/- 2.3	12.0 +/- 0.4	0.092 +/- 0.003	137.0	33.21	9.80	0.0
JM2	3.0	131.7 +/- 2.3	11.8 +/- 0.4	0.090 +/- 0.003	139.0	33.16	9.60	0.0
JM3	1.0	122.8 +/- 2.2	11.4 +/- 0.4	0.093 +/- 0.003	130.1	33.02	10.80	0.0
JM4	17.0	133.3 +/- 2.3	12.9 +/- 0.4	0.096 +/- 0.003	141.4	33.00	9.80	0.0
JM5	37.0	116.6 +/- 2.1	10.3 +/- 0.4	0.088 +/- 0.004	123.5	33.03	9.50	0.0
JM6	3.0	127.7 +/- 2.2	11.7 +/- 0.4	0.091 +/- 0.003	135.0	33.10	10.40	0.0
JM7	3.0	127.4 +/- 2.2	12.0 +/- 0.4	0.094 +/- 0.003	134.8	33.06	10.60	0.0
JM8	3.0	129.2 +/- 2.3	14.6 +/- 0.4	0.113 +/- 0.003	136.7	33.09	11.80	0.0
JM9	3.0	126.3 +/- 2.2	11.2 +/- 0.4	0.089 +/- 0.003	133.4	33.14	10.50	0.0
JM10	3.0	132.1 +/- 2.3	12.2 +/- 0.4	0.092 +/- 0.003	137.2	33.72	10.70	8.10
JM11	25.0	110.5 +/- 2.0	11.1 +/- 0.4	0.101 +/- 0.004	114.2	33.89	9.90	8.00
JM12	45.0	135.4 +/- 2.4	12.0 +/- 0.4	0.089 +/- 0.003	139.3	34.01	9.20	6.60
JM13	3.0	127.0 +/- 2.2	11.0 +/- 0.4	0.087 +/- 0.003	133.5	33.30	10.30	0.0
JM14	3.0	122.1 +/- 2.2	11.5 +/- 0.4	0.095 +/- 0.003	126.0	33.91	10.90	0.0
JM15	1.0	124.1 +/- 2.2	9.2 +/- 0.4	0.074 +/- 0.003	131.3	33.08	9.50	7.40
JM16	10.0	131.2 +/- 2.3	13.8 +/- 0.4	0.106 +/- 0.003	138.9	33.06	9.30	7.60

JOHN MURRAY (CONT)
****

CODE	DEPTH(M)	137(DPM/L)	134(DPM/L)	RATIO	SC7(DPM/L)	SAL(PM)	TEMP(C)	D.O.(PM)
JM17	30.0	125.7 +/- 2.2	11.4 +/- 0.4	0.091 +/- 0.003	132.7	33.15	9.40	7.50
JM18	50.0	122.0 +/- 2.1	11.0 +/- 0.3	0.090 +/- 0.002	128.6	33.21	10.20	8.40
JM19	70.0	114.4 +/- 2.0	8.6 +/- 0.4	0.075 +/- 0.004	120.5	33.22	9.80	7.50
JM20	90.0	125.6 +/- 2.2	12.3 +/- 0.4	0.098 +/- 0.003	132.0	33.30	9.50	8.50
JM21	110.0	129.9 +/- 2.3	10.6 +/- 0.4	0.082 +/- 0.003	135.3	33.59	9.30	7.90
JM22	5.0	126.8 +/- 2.2	10.9 +/- 0.4	0.086 +/- 0.003	134.8	32.94	8.00	8.40
JM23	20.0	123.4 +/- 2.2	9.8 +/- 0.4	0.079 +/- 0.003	131.2	32.93	9.80	8.90
JM24	40.0	124.2 +/- 2.2	11.5 +/- 0.4	0.093 +/- 0.003	131.9	32.94	9.50	8.90
JM25	60.0	125.6 +/- 2.2	12.1 +/- 0.5	0.096 +/- 0.004	133.1	33.02	9.40	8.40
JM26	80.0	127.2 +/- 2.2	11.7 +/- 0.4	0.092 +/- 0.003	134.4	33.11	9.40	8.50
JM27	5.0	129.6 +/- 2.3	11.4 +/- 0.4	0.088 +/- 0.003	138.5	32.73	9.80	6.30
JM28	25.0	128.1 +/- 2.3	9.1 +/- 0.4	0.071 +/- 0.003	136.8	32.79	9.50	6.60
JM29	50.0	126.5 +/- 2.2	11.8 +/- 0.4	0.093 +/- 0.003	134.0	33.06	10.30	6.60
JM30	75.0	125.3 +/- 2.2	11.9 +/- 0.4	0.095 +/- 0.003	131.1	33.45	10.60	5.90
JM31	100.0	121.7 +/- 2.1	10.8 +/- 0.4	0.089 +/- 0.003	127.0	33.55	10.70	7.50
JM32	125.0	119.0 +/- 2.1	11.1 +/- 0.4	0.093 +/- 0.004	124.1	33.57	11.20	5.80

L.FYNE RESULTS
****

CODE	DEPTH(M)	137(DPM/L)	134(DPM/L)	RATIO	SC7(DPM/L)	SAL(PM)	TEMP(C)	D.O.(PM)
SLF1	1.0	133.0 +/- 2.3	11.5 +/- 0.4	0.086 +/- 0.003	141.8	32.82	9.05	9.50
NLF1	1.0	129.5 +/- 2.3	11.6 +/- 0.4	0.090 +/- 0.003	137.9	32.87	10.09	8.60
NLF2	10.0	124.8 +/- 2.2	11.4 +/- 0.4	0.092 +/- 0.003	132.8	32.89	10.10	8.70
NLF3	25.0	129.2 +/- 2.3	11.6 +/- 0.4	0.090 +/- 0.003	137.5	32.89	9.70	8.50
NLF4	35.0	134.9 +/- 2.4	12.0 +/- 0.4	0.089 +/- 0.003	143.5	32.89	9.80	8.50
NLF5	50.0	136.0 +/- 2.4	11.5 +/- 0.4	0.084 +/- 0.003	144.7	32.88	10.17	8.60
NLF6	75.0	133.7 +/- 2.4	12.4 +/- 0.4	0.093 +/- 0.003	142.2	32.91	10.18	8.50
NLF7	100.0	142.7 +/- 2.5	13.0 +/- 0.4	0.091 +/- 0.003	151.4	32.99	8.89	5.70
NLF8	110.0	137.2 +/- 2.4	10.5 +/- 0.4	0.077 +/- 0.003	145.5	32.99	8.60	5.50
NLF9	125.0	130.3 +/- 2.3	11.9 +/- 0.4	0.091 +/- 0.003	138.1	33.02	8.28	5.30
NLF10	135.0	121.2 +/- 2.1	10.6 +/- 0.4	0.088 +/- 0.004	128.4	33.02	******	5.50

L.GOIL RESULTS
****

CODE	DEPTH(M)	137(DPM/L)	134(DPM/L)	RATIO	SC7(DPM/L)	SAL(PM)	TEMP(C)	O.O.(PM)
LL1-1	1,0	109,3 +/- 1,9	9,5 +/- 0,3	0,087 +/- 0,003	130,3	29,35	7,30	8,80
LL1-2	10,0	109,6 +/- 1,9	9,5 +/- 0,3	0,086 +/- 0,003	119,1	32,21	9,56	7,70
LL1-3	30,0	118,7 +/- 2,1	10,9 +/- 0,3	0,092 +/- 0,003	126,3	32,87	9,51	7,88
LL1-4	50,0	126,6 +/- 2,2	11,0 +/- 0,3	0,087 +/- 0,003	134,7	32,91	9,33	8,08
LL1-5	65,0	126,5 +/- 2,2	10,8 +/- 0,3	0,085 +/- 0,003	134,5	32,92	9,40	8,05
LG1-5	1,0	103,1 +/- 1,8	9,7 +/- 0,3	0,094 +/- 0,003	121,2	29,78	7,83	8,70
LG1-4	10,0	123,3 +/- 2,1	10,4 +/- 0,3	0,084 +/- 0,002	138,2	31,21	9,06	7,82
LG1-3	30,0	131,1 +/- 2,3	11,4 +/- 0,3	0,087 +/- 0,002	140,3	32,72	10,03	6,11
LG1-2	50,0	134,4 +/- 2,3	11,2 +/- 0,3	0,083 +/- 0,002	143,1	32,87	9,91	3,10
LG1-1	70,0	123,6 +/- 2,1	10,5 +/- 0,3	0,085 +/- 0,002	131,5	32,89	9,58	1,15

APPENDIX I.2 L.GOIL/L.LONG DEEP SITES

****

RESULTS OF THE ANALYSIS OF SAMPLES FROM THE LOCH GOIL DEEP SITE (LG1) OVER THE PERIOD DECEMBER 1975 - FEBRUARY 1978 ARE LISTED ON PAGES A8 - A29 . RESULTS FROM THE LOCH LONG DEEP SITE (LL1) ARE LISTED ON PAGES A30 - A43 . THE LOCATIONS OF THESE SITES ARE PLOTTED ON FIG. 4.1 .

A8

L.GOIL 1 04/12/75

****

CODE	DEPTH(M)	137(DPM/L)	134(DPM/L)	RATIO	SC7(DPM/L)	SAL(PM)	TEMP(C)	D.O.(PM)
L.GIL	5.0	102.1 +/- 3.8	17.2 +/- 0.6	0.168 +/- 0.004	113.4	31.50	11.00	7.00
L.GIL	20.0	110.0 +/- 4.1	16.9 +/- 0.6	0.153 +/- 0.004	117.6	32.75	11.00	6.60
L.GIL	30.0	107.6 +/- 4.1	16.7 +/- 0.6	0.155 +/- 0.004	114.7	32.83	11.00	6.40
L.GIL	40.0	90.0 +/- 3.4	13.9 +/- 0.5	0.154 +/- 0.004	96.0	32.82	10.80	4.80
L.GIL	50.0	96.2 +/- 3.6	14.2 +/- 0.5	0.148 +/- 0.004	102.4	32.86	10.10	3.10
L.GIL	60.0	89.5 +/- 3.4	12.6 +/- 0.5	0.141 +/- 0.004	95.4	32.86	9.80	2.80
L.GIL	70.0	90.6 +/- 3.4	13.5 +/- 0.5	0.149 +/- 0.004	96.5	32.87	9.80	1.90

L,GOIL 1 08/01/76

CODE	DEPTH(M)	137(DPM/L)	134(DPM/L)	RATIO	SC7(DPM/L)	SAL(PM)	TEMP(C)	D,O,(PM)
L,GIL	0,0	82,8 +/- 3,1	12,4 +/- 0,5	0,150 +/- 0,005	112,9	25,68	8,50	9,38
L,GIL	10,0	105,6 +/- 4,0	17,4 +/- 0,6	0,165 +/- 0,004	127,4	29,00	8,23	8,62
L,GIL	20,0	116,9 +/- 4,4	18,1 +/- 0,6	0,155 +/- 0,003	126,6	32,30	9,47	7,30
L,GIL	30,0	112,2 +/- 4,2	18,0 +/- 0,6	0,160 +/- 0,004	121,0	32,48	9,60	7,15
L,GIL	40,0	108,6 +/- 4,1	17,9 +/- 0,6	0,165 +/- 0,004	116,5	32,63	9,90	5,61
L,GIL	60,0	105,3 +/- 4,0	15,8 +/- 0,6	0,150 +/- 0,004	112,8	32,68	9,82	4,70
L,GIL	75,0	100,3 +/- 3,8	15,1 +/- 0,6	0,151 +/- 0,004	107,2	32,75	9,82	4,28

L.GOIL 1 03/03/76

****

CODE	DEPTH(M)	137(DPM/L)	134(DPM/L)	RATIO	SC7(DPM/L)	SAL(PM)	TEMP(C)	D.O.(PM)
L.GIL	0.0	86.9 +/- 3.3	13.3 +/- 0.5	0.153 +/- 0.005	104.9	29.00	6.75	9.80
L.GIL	10.0	95.9 +/- 3.6	13.8 +/- 0.5	0.144 +/- 0.004	110.7	30.30	8.50	8.55
L.GIL	20.0	105.2 +/- 4.0	15.2 +/- 0.6	0.144 +/- 0.004	113.3	32.50	9.20	8.05
L.GIL	30.0	103.4 +/- 3.9	15.7 +/- 0.6	0.152 +/- 0.004	110.9	32.62	8.80	7.65
L.GIL	40.0	103.6 +/- 3.9	14.8 +/- 0.6	0.142 +/- 0.004	111.0	32.67	8.80	7.80
L.GIL	50.0	96.8 +/- 3.7	15.4 +/- 0.6	0.159 +/- 0.004	103.6	32.70	9.00	7.70
L.GIL	60.0	101.9 +/- 3.8	15.6 +/- 0.6	0.153 +/- 0.004	109.1	32.71	8.80	7.78
L.GIL	70.0	101.5 +/- 3.8	15.3 +/- 0.6	0.151 +/- 0.004	108.4	32.77	8.80	7.77

A11

L,GOIL 1 01/04/76

****

CODE	DEPTH(M)	137(DPM/L)	134(DPM/L)	RATIO	SC7(DPM/L)	SAL(PM)	TEMP(C)	D,O,(PM)
L,GIL	0,0	74,3 +/- 2,8	10,6 +/- 0,5	0,142 +/- 0,005	95,2	27,33	6,60	11,30
L,GIL	10,0	88,4 +/- 3,3	13,2 +/- 0,5	0,149 +/- 0,004	102,8	30,11	6,90	9,80
L,GIL	20,0	99,9 +/- 3,8	14,4 +/- 0,5	0,144 +/- 0,004	108,3	32,28	7,45	8,45
L,GIL	30,0	94,7 +/- 3,6	14,4 +/- 0,5	0,152 +/- 0,004	101,6	32,62	7,50	8,50
L,GIL	40,0	93,8 +/- 3,5	13,5 +/- 0,5	0,144 +/- 0,004	99,9	32,85	7,80	8,10
L,GIL	50,0	91,6 +/- 3,5	13,8 +/- 0,5	0,151 +/- 0,004	97,9	32,74	7,65	8,20
L,GIL	60,0	92,4 +/- 3,5	13,4 +/- 0,5	0,145 +/- 0,004	98,7	32,75	7,65	8,10

L.GOIL 1 31/05/76

****

CODE	DEPTH(M)	137(DPM/L)	134(DPM/L)	RATIO	SC7(DPM/L)	SAL(PM)	TEMP(C)	O,O,(PM)
L.GIL	0,0	71,7 +/- 2,7	9,9 +/- 0,5	0,138 +/- 0,005	102,9	24,40	11,90	116,00
L.GIL	10,0	90,4 +/- 3,4	13,6 +/- 0,5	0,150 +/- 0,004	98,8	32,03	8,00	84,00
L.GIL	20,0	97,4 +/- 3,7	13,9 +/- 0,5	0,143 +/- 0,004	104,8	32,53	7,90	79,00
L.GIL	30,0	97,2 +/- 3,7	14,7 +/- 0,6	0,151 +/- 0,004	104,0	32,70	7,70	77,00
L.GIL	40,0	83,1 +/- 3,2	12,2 +/- 0,5	0,147 +/- 0,005	88,7	32,80	7,30	73,00
L.GIL	50,0	91,5 +/- 3,5	13,2 +/- 0,5	0,145 +/- 0,004	97,4	32,88	7,10	71,00
L.GIL	60,0	89,6 +/- 3,4	13,1 +/- 0,5	0,146 +/- 0,005	95,2	32,95	7,10	68,00

L.GOIL 1 10/08/76

****

CODE	DEPTH(M)	137(DPM/L)	134(DPM/L)	RATIO	SC7(DPM/L)	SAL(PM)	TEMP(C)	D.O.(PM)
L.GIL	0.0	108.5 +/- 4.1	15.1 +/- 0.6	0.139 +/- 0.004	118.9	31.94	15.50	12.69
L.GIL	10.0	107.8 +/- 4.1	14.6 +/- 0.5	0.136 +/- 0.004	117.3	32.17	13.40	12.91
L.GIL	20.0	111.0 +/- 4.2	15.8 +/- 0.6	0.143 +/- 0.004	119.1	32.61	11.60	6.37
L.GIL	30.0	103.7 +/- 3.9	14.3 +/- 0.5	0.138 +/- 0.004	110.8	32.78	9.80	4.82
L.GIL	40.0	99.4 +/- 3.7	12.9 +/- 0.5	0.130 +/- 0.004	105.9	32.85	8.60	40.40
L.GIL	50.0	99.7 +/- 3.8	13.3 +/- 0.5	0.134 +/- 0.004	106.0	32.92	8.40	3.61
L.GIL	60.0	95.8 +/- 3.6	12.7 +/- 0.5	0.132 +/- 0.004	101.8	32.92	8.00	3.32
L.GIL	70.0	87.8 +/- 3.3	11.4 +/- 0.5	0.130 +/- 0.004	93.3	32.93	8.00	3.20

L.GOIL 1 28/09/76

****

CODE	DEPTH(M)	137(DPM/L)	134(DPM/L)	RATIO	SC7(DPM/L)	SAL(PM)	TEMP(C)	D.O.(PM)
L.GIL	0.0	130.7 +/- 4.9	17.5 +/- 0.6	0.134 +/- 0.003	143.1	31.95	12.10	8.21
L.GIL	10.0	127.7 +/- 4.8	17.3 +/- 0.6	0.136 +/- 0.003	136.4	32.75	11.50	7.10
L.GIL	20.0	119.5 +/- 4.5	16.4 +/- 0.6	0.137 +/- 0.003	126.9	32.95	11.24	6.09
L.GIL	30.0	126.8 +/- 4.8	16.8 +/- 0.6	0.132 +/- 0.003	134.4	33.02	10.62	5.13
L.GIL	40.0	106.3 +/- 4.0	13.8 +/- 0.5	0.130 +/- 0.004	113.1	32.89	9.90	2.96
L.GIL	50.0	102.5 +/- 3.9	13.4 +/- 0.5	0.131 +/- 0.004	109.1	32.88	8.95	2.21
L.GIL	60.0	96.9 +/- 3.7	12.3 +/- 0.5	0.127 +/- 0.004	103.1	32.90	8.90	1.98
L.GIL	70.0	101.8 +/- 3.8	12.9 +/- 0.5	0.126 +/- 0.004	108.3	32.92	8.48	1.53

L.GOIL 22/11/76

****

CODE	DEPTH(M)	137(DPM/L)	134(DPM/L)	RATIO	SC7(DPM/L)	SAL(PM)	TEMP(C)	D.O.(PM)
LG1 -1	1.0	139.1 +/- 4.6	15.4 +/- 0.8	0.111 +/- 0.003	151.5	32.13	10.00	6.75
LG1 -2	10.0	117.9 +/- 3.9	13.8 +/- 0.7	0.117 +/- 0.003	127.0	32.51	11.04	6.00
LG1 -3	20.0	122.1 +/- 4.0	14.4 +/- 0.7	0.118 +/- 0.003	130.0	32.87	11.00	5.58
LG1 -4	30.0	124.4 +/- 4.1	14.9 +/- 0.8	0.120 +/- 0.003	132.3	32.92	11.00	4.78
LG1 -5	40.0	118.9 +/- 3.9	14.0 +/- 0.7	0.118 +/- 0.003	126.4	32.93	10.50	3.39
LG1 -6	50.0	113.0 +/- 3.7	12.9 +/- 0.7	0.114 +/- 0.003	119.9	32.98	9.90	2.02
LG1 -7	60.0	114.1 +/- 3.8	11.9 +/- 0.6	0.104 +/- 0.003	121.5	32.87	9.54	1.47

L.GOIL 1 21/12/76

****

CODE	DEPTH(M)	137(DPM/L)	134(DPM/L)	RATIO	SC7(DPM/L)	SAL(PM)	TEMP(C)	D.O.(PM)
L.GIL	1.0	115.5 +/- 4.5	13.3 +/- 0.8	0.115 +/- 0.006	140.2	28.84	7.00	8.22
L.GIL	10.0	126.6 +/- 4.9	16.0 +/- 0.8	0.126 +/- 0.006	136.9	32.37	10.67	5.74
L.GIL	20.0	123.3 +/- 4.7	14.8 +/- 0.8	0.120 +/- 0.006	131.3	32.87	10.40	5.29
L.GIL	30.0	131.5 +/- 5.0	16.3 +/- 0.8	0.124 +/- 0.005	140.0	32.88	10.40	6.82
L.GIL	40.0	136.3 +/- 5.2	15.4 +/- 0.8	0.113 +/- 0.005	144.9	32.91	10.05	6.60
L.GIL	50.0	103.8 +/- 4.0	11.6 +/- 0.7	0.112 +/- 0.007	110.6	32.90	10.00	2.67
L.GIL	60.0	111.3 +/- 4.3	12.6 +/- 0.8	0.113 +/- 0.006	118.4	32.90	9.79	1.71
L.GIL	70.0	100.3 +/- 3.9	11.0 +/- 0.7	0.109 +/- 0.007	106.7	32.91	9.58	1.28
L.GIL	80.0	109.1 +/- 4.2	12.7 +/- 0.8	0.117 +/- 0.006	116.1	32.90	9.42	0.52

L.GOIL 12/01/77

****

CODE	DEPTH(M)	137(DPM/L)	134(DPM/L)	RATIO	SC7(DPM/L)	SAL(PM)	TEMP(C)	D.O.(PM)
LG1 -1	1.0	126.6 +/- 4.2	13.9 +/- 0.7	0.110 +/- 0.003	138.8	31.93	6.70	7.90
LG1 -2	10.0	132.4 +/- 4.3	15.0 +/- 0.8	0.113 +/- 0.003	142.6	32.49	8.97	7.28
LG1 -3	20.0	135.6 +/- 4.4	14.9 +/- 0.8	0.110 +/- 0.003	144.3	32.90	9.52	6.20
LG1 -4	30.0	123.1 +/- 4.0	13.4 +/- 0.7	0.109 +/- 0.003	130.9	32.91	9.50	5.52
LG1 -5	40.0	133.6 +/- 4.4	15.2 +/- 0.8	0.114 +/- 0.003	142.5	32.83	9.05	6.78
LG1 -6	50.0	137.7 +/- 4.5	14.0 +/- 0.7	0.102 +/- 0.003	146.5	32.90	8.40	6.62
LG1 -7	60.0	136.5 +/- 4.5	13.7 +/- 0.7	0.100 +/- 0.003	145.9	32.74	8.70	7.21
LG1 -8	70.0	140.9 +/- 4.6	15.2 +/- 0.8	0.108 +/- 0.003	150.0	32.89	9.06	5.70

L.GOIL 17/02/77

CODE	DEPTH(M)	137(DPM/L)	134(DPM/L)	RATIO	SC7(DPM/L)	SAL(PM)	TEMP(C)	D.O.(PM)
LG1 -1	1.0	124.1 +/- 4.1	14.1 +/- 0.7	0.113 +/- 0.003	170.3	25.50	4.50	10.35
LG1 -2	10.0	147.9 +/- 4.8	16.3 +/- 0.8	0.111 +/- 0.003	177.7	29.14	5.36	9.30
LG1 -3	20.0	148.2 +/- 4.8	16.8 +/- 0.8	0.113 +/- 0.003	159.4	32.53	7.63	7.95
LG1 -4	30.0	152.4 +/- 5.0	16.9 +/- 0.9	0.111 +/- 0.003	163.6	32.61	7.71	8.05
LG1 -5	40.0	146.6 +/- 4.8	16.2 +/- 0.8	0.111 +/- 0.003	156.9	32.70	7.80	7.75
LG1 -6	50.0	148.7 +/- 4.9	16.0 +/- 0.8	0.108 +/- 0.003	158.8	32.78	7.90	7.45
LG1 -7	60.0	157.9 +/- 5.2	17.0 +/- 0.9	0.107 +/- 0.003	168.5	32.80	7.94	7.70
LG1 -8	66.0	145.7 +/- 4.8	15.6 +/- 0.8	0.107 +/- 0.003	155.3	32.82	8.20	8.52

L.GOIL 22/03/77

****

CODE	DEPTH(M)	137(DPM/L)	134(DPM/L)	RATIO	SC7(DPM/L)	SAL(PM)	TEMP(C)	D.O.(PM)
LG1 -1	1.0	146.7 +/- 4.8	15.8 +/- 0.8	0.108 +/- 0.003	179.5	28.61	6.70	9.60
LG1 -2	10.0	153.9 +/- 5.0	16.1 +/- 0.8	0.104 +/- 0.003	169.3	31.82	6.78	8.67
LG1 -3	20.0	178.6 +/- 5.8	18.8 +/- 0.9	0.105 +/- 0.003	193.9	32.24	6.78	8.62
LG1 -4	30.0	148.9 +/- 4.9	16.2 +/- 0.8	0.109 +/- 0.003	160.6	32.46	6.80	8.40
LG1 -5	40.0	159.0 +/- 5.2	16.6 +/- 0.8	0.104 +/- 0.003	170.2	32.68	7.30	7.71
LG1 -6	50.0	161.6 +/- 5.3	16.9 +/- 0.9	0.105 +/- 0.003	172.9	32.71	7.10	8.01
LG1 -7	60.0	156.0 +/- 5.1	16.4 +/- 0.8	0.105 +/- 0.003	166.8	32.73	7.13	8.10
LG1 -8	69.0	158.7 +/- 5.2	16.3 +/- 0.8	0.102 +/- 0.003	169.3	32.82	7.11	8.00

L.GOIL 18/04/77

CODE	DEPTH(M)	137(DPM/L)	134(DPM/L)	RATIO	SC7(DPM/L)	SAL(PM)	TEMP(C)	D.O.(PM)
LG1 -1	1.0	165.4 +/- 5.5	16.3 +/- 1.0	0.098 +/- 0.004	188.3	30.73	7.40	11.79
LG1 -2	10.0	181.9 +/- 6.0	16.3 +/- 1.0	0.090 +/- 0.004	197.5	32.24	7.17	9.15
LG1 -3	20.0	168.5 +/- 5.6	18.5 +/- 1.1	0.110 +/- 0.004	181.0	32.58	6.83	8.40
LG1 -4	30.0	156.7 +/- 5.2	16.3 +/- 1.0	0.104 +/- 0.005	168.2	32.62	7.21	8.51
LG1 -5	40.0	172.4 +/- 5.7	17.5 +/- 1.0	0.101 +/- 0.004	184.6	32.68	6.70	8.82
LG1 -6	50.0	165.5 +/- 5.5	18.0 +/- 1.1	0.109 +/- 0.004	177.2	32.68	6.70	8.95
LG1 -7	60.0	168.1 +/- 5.6	18.3 +/- 1.1	0.109 +/- 0.004	179.9	32.70	6.69	8.97
LG1 -8	66.0	160.5 +/- 5.4	17.0 +/- 1.0	0.106 +/- 0.005	171.7	32.72	6.69	8.90

L.GOIL 06/06/77
****

CODE	DEPTH(M)	137(DPM/L)	134(DPM/L)	RATIO	SC7(DPM/L)	SAL(PM)	TEMP(C)	D.O.(PM)
LG1-1	1.0	154.4 +/- 2.7	16.1 +/- 0.4	0.104 +/- 0.003	166.1	32.52	8.40	9.07
LG1-2	10.0	157.2 +/- 2.8	16.5 +/- 0.4	0.105 +/- 0.003	168.0	32.74	7.79	8.30
LG1-3	20.0	158.4 +/- 2.8	16.5 +/- 0.4	0.104 +/- 0.003	169.1	32.78	7.67	8.02
LG1-4	30.0	153.6 +/- 2.7	17.5 +/- 0.5	0.114 +/- 0.003	163.9	32.80	7.03	7.61
LG1-5	40.0	155.9 +/- 2.7	16.5 +/- 0.4	0.106 +/- 0.003	166.2	32.84	7.05	7.48
LG1-6	50.0	154.2 +/- 2.7	17.3 +/- 0.5	0.113 +/- 0.003	164.3	32.85	7.08	7.56
LG1-7	60.0	145.3 +/- 2.5	16.3 +/- 0.4	0.112 +/- 0.003	154.7	32.88	6.87	7.55
LG1-8	65.0	160.1 +/- 2.8	17.4 +/- 0.5	0.109 +/- 0.003	170.2	32.91	7.15	7.45

L.GOIL 28/06/77
****

CODE	DEPTH(M)	137(DPM/L)	134(DPM/L)	RATIO	SC7(DPM/L)	SAL(PM)	TEMP(C)	D.O.(PM)
LG1-1	1.0	152.6 +/- 2.8	16.9 +/- 1.2	0.111 +/- 0.008	164.5	32.46	12.65	11.89
LG1-3	40.0	159.1 +/- 3.0	17.4 +/- 1.2	0.109 +/- 0.008	168.9	32.97	7.46	6.69
LG1-4	60.0	151.7 +/- 2.8	17.0 +/- 1.2	0.112 +/- 0.008	160.8	33.01	7.50	6.70
LG1-5	80.0	151.7 +/- 3.1	17.9 +/- 1.8	0.118 +/- 0.012	160.7	33.04	7.50	6.27

L.GOIL 19/07/77
****

CODE	DEPTH(M)	137(DPM/L)	134(DPM/L)	RATIO	SC7(DPM/L)	SAL(PM)	TEMP(C)	D.O.(PM)
LG1-1	1,0	145,5 +/- 2,6	14,6 +/- 0,4	0,100 +/- 0,003	159,5	31,93	15,40	9,41
LG1-2	10,0	144,1 +/- 2,5	15,8 +/- 0,4	0,110 +/- 0,003	156,2	32,28	12,57	9,01
LG1-3	20,0	146,0 +/- 2,6	15,9 +/- 0,4	0,109 +/- 0,003	155,3	32,89	9,52	6,80
LG1-4	30,0	147,9 +/- 2,6	15,8 +/- 0,4	0,107 +/- 0,003	157,0	32,97	8,59	6,11
LG1-5	40,0	152,1 +/- 2,7	15,5 +/- 0,4	0,102 +/- 0,003	161,4	32,99	8,20	5,80
LG1-6	50,0	153,8 +/- 2,7	16,4 +/- 0,4	0,107 +/- 0,003	163,3	32,97	7,79	5,75
LG1-7	60,0	154,3 +/- 2,7	15,7 +/- 0,4	0,102 +/- 0,003	163,8	32,96	7,59	5,41

L.GOIL 16/08/77
****

CODE	DEPTH(M)	137(DPM/L)	134(DPM/L)	RATIO	8C7(DPM/L)	SAL(PM)	TEMP(C)	D.O.(PM)
LG1-1	1.0	121.7 +/- 2.1	12.4 +/- 0.3	0.102 +/- 0.003	138.5	30.76	16.10	9.80
LG1-2	10.0	133.2 +/- 2.3	11.2 +/- 0.3	0.084 +/- 0.002	142.4	32.75	11.05	6.28
LG1-3	20.0	138.7 +/- 2.4	13.4 +/- 0.3	0.097 +/- 0.002	147.4	32.93	10.50	5.66
LG1-4	30.0	141.6 +/- 2.4	13.9 +/- 0.3	0.099 +/- 0.002	150.1	33.01	9.56	4.87
LG1-5	40.0	138.9 +/- 2.4	11.7 +/- 0.3	0.084 +/- 0.002	147.5	32.95	8.68	4.35
LG1-6	50.0	138.6 +/- 2.4	11.7 +/- 0.3	0.085 +/- 0.002	147.5	32.89	8.28	4.10
LG1-7	60.0	132.1 +/- 2.3	11.4 +/- 0.3	0.086 +/- 0.002	140.3	32.95	8.05	3.75
LG1-8	67.0	140.1 +/- 2.4	11.7 +/- 0.3	0.084 +/- 0.002	148.8	32.96	7.98	3.70

L.GOIL 11/10/77
****

CODE	DEPTH(M)	137(DPM/L)	134(DPM/L)	RATIO	SC7(DPM/L)	SAL(PM)	TEMP(C)	D.O.(PM)
LG1-1	1.0	102.9 +/- 1.8	9.2 +/- 0.4	0.089 +/- 0.004	138.1	26.06	10.67	8.48
LG1-2	10.0	131.2 +/- 2.3	12.4 +/- 0.4	0.095 +/- 0.003	144.9	31.09	11.78	6.45
LG1-3	20.0	136.8 +/- 2.4	12.6 +/- 0.4	0.092 +/- 0.003	146.5	32.09	11.82	6.77
LG1-4	30.0	130.0 +/- 2.3	12.2 +/- 0.4	0.094 +/- 0.003	138.6	32.81	11.76	5.03
LG1-5	40.0	137.3 +/- 2.4	13.2 +/- 0.4	0.096 +/- 0.003	146.2	32.87	11.70	5.03
LG1-6	50.0	140.8 +/- 2.5	13.5 +/- 0.4	0.096 +/- 0.003	149.9	32.87	10.20	3.00
LG1-7	60.0	133.2 +/- 2.3	12.7 +/- 0.4	0.095 +/- 0.003	141.6	32.92	9.32	2.60
LG1-8	70.0	140.2 +/- 2.5	13.4 +/- 0.4	0.096 +/- 0.003	149.0	32.93	9.10	2.30

L.GOIL 15/11/77
****

CODE	DEPTH(M)	137(DPM/L)	134(DPM/L)	RATIO	SC7(DPM/L)	SAL(PM)	TEMP(C)	D.O.(PM)
LG1-1	1.0	120.8 +/- 2.1	11.2 +/- 0.4	0.092 +/- 0.003	136.7	30.92	10.92	6.97
LG1-2	10.0	118.9 +/- 2.1	11.3 +/- 0.4	0.096 +/- 0.003	134.4	30.97	11.04	6.91
LG1-3	20.0	117.0 +/- 2.1	11.6 +/- 0.4	0.099 +/- 0.004	128.9	31.76	11.25	5.98
LG1-4	30.0	126.7 +/- 2.2	11.7 +/- 0.4	0.093 +/- 0.003	137.0	32.39	11.12	4.91
LG1-5	40.0	133.5 +/- 2.3	12.1 +/- 0.4	0.091 +/- 0.003	142.1	32.88	9.80	1.80
LG1-6	50.0	133.1 +/- 2.3	12.5 +/- 0.4	0.094 +/- 0.003	141.6	32.90	9.31	1.17
LG1-7	60.0	125.2 +/- 2.2	12.6 +/- 0.4	0.100 +/- 0.003	133.1	32.92	9.06	0.73
LG1-8	63.0	134.5 +/- 2.4	12.1 +/- 0.4	0.090 +/- 0.003	143.0	32.93	9.02	0.69

L.GOIL 28/12/77
****

CODE	DEPTH(M)	137(DPM/L)	134(DPM/L)	RATIO	SC7(DPM/L)	SAL(PM)	TEMP(C)	D.O.(PM)
LG1-5	1.0	103.1 +/- 1.8	9.7 +/- 0.3	0.094 +/- 0.003	121.2	29.78	7.83	8.70
LG1-4	10.0	123.3 +/- 2.1	10.4 +/- 0.3	0.084 +/- 0.002	138.2	31.21	9.06	7.82
LG1-3	30.0	131.1 +/- 2.3	11.4 +/- 0.3	0.087 +/- 0.002	140.3	32.72	10.03	6.11
LG1-2	50.0	134.4 +/- 2.3	11.2 +/- 0.3	0.083 +/- 0.002	143.1	32.87	9.91	3.10
LG1-1	70.0	123.6 +/- 2.1	10.5 +/- 0.3	0.085 +/- 0.002	131.5	32.89	9.58	1.15

L.GOIL 17/01/78
****

CODE	DEPTH(M)	137(DPM/L)	134(DPM/L)	RATIO	SC7(DPM/L)	SAL(PM)	TEMP(C)	O.D.(PM)
LG1-1	1.0	115.1 +/- 2.0	10.5 +/- 0.3	0.091 +/- 0.003	133.9	30.10	6.66	9.80
LG1-2	10.0	121.3 +/- 2.1	11.5 +/- 0.3	0.095 +/- 0.003	132.6	32.02	8.80	8.25
LG1-3	30.0	119.3 +/- 2.1	11.2 +/- 0.4	0.094 +/- 0.004	127.4	32.76	9.39	5.80
LG1-4	50.0	125.9 +/- 2.2	11.6 +/- 0.3	0.092 +/- 0.003	134.5	32.75	9.22	6.00
LG1-5	70.0	127.6 +/- 2.2	11.4 +/- 0.3	0.089 +/- 0.002	136.4	32.74	9.16	6.30

L.GOIL 21/02/78
****

CODE	DEPTH(M)	137(DPM/L)	134(DPM/L)	RATIO	SC7(DPM/L)	SAL(PM)	TEMP(C)	D.O.(PM)
LG1-1	1.0	123.6 +/- 2.2	10.8 +/- 0.3	0.088 +/- 0.003	137.7	31.42	4.20	9.55
LG1-2	10.0	125.5 +/- 2.2	11.4 +/- 0.3	0.091 +/- 0.003	136.3	32.22	5.80	8.76
LG1-3	30.0	125.3 +/- 2.2	11.5 +/- 0.3	0.092 +/- 0.002	133.7	32.81	7.62	8.20
LG1-4	50.0	121.7 +/- 2.1	10.9 +/- 0.3	0.090 +/- 0.003	129.7	32.82	7.50	8.15
LG1-5	70.0	125.0 +/- 2.2	11.6 +/- 0.3	0.092 +/- 0.002	133.3	32.82	7.50	8.15

L.LONG 07/12/76

CODE	DEPTH(M)	137(DPM/L)	134(DPM/L)	RATIO	SC7(DPM/L)	SAL(PM)	TEMP(C)	D.O.(PM)
LL1 -1	1.0	111.4 +/- 3.7	12.7 +/- 0.7	0.114 +/- 0.004	141.3	27.60	7.60	8.51
LL1 -2	10.0	118.9 +/- 3.9	14.3 +/- 0.8	0.120 +/- 0.004	137.3	30.30	9.40	7.68
LL1 -3	20.0	133.9 +/- 4.4	15.6 +/- 0.8	0.117 +/- 0.003	147.4	31.80	10.20	7.22
LL1 -4	30.0	138.4 +/- 4.5	16.1 +/- 0.8	0.116 +/- 0.003	152.8	31.70	10.20	7.78
LL1 -5	40.0	139.7 +/- 4.6	15.4 +/- 0.8	0.110 +/- 0.003	167.2	31.10	10.20	7.89
LL1 -6	50.0	136.6 +/- 4.5	15.2 +/- 0.8	0.111 +/- 0.003	149.9	31.90	10.20	7.96
LL1 -7	60.0	141.1 +/- 4.6	16.8 +/- 0.9	0.119 +/- 0.003	154.3	32.00	10.20	7.90
LL1 -8	70.0	148.6 +/- 4.9	16.9 +/- 0.9	0.114 +/- 0.003	163.5	31.80	10.20	7.90

L,LONG 12/01/77

****

CODE	DEPTH(M)	137(DPM/L)	134(DPM/L)	RATIO	SC7(DPM/L)	SAL(PM)	TEMP(C)	D,O,(PM)
LL1 -1	1.0	127.6 +/- 4.2	14.9 +/- 0.8	0.117 +/- 0.003	140.0	31.89	6.80	8.05
LL1 -2	10.0	153.2 +/- 5.0	16.5 +/- 0.8	0.107 +/- 0.003	165.9	32.32	7.81	8.10
LL1 -3	20.0	147.7 +/- 4.8	16.4 +/- 0.8	0.111 +/- 0.003	156.8	32.96	8.28	8.05
LL1 -4	30.0	139.5 +/- 4.6	15.6 +/- 0.8	0.112 +/- 0.003	148.0	33.00	8.00	8.15
LL1 -5	40.0	147.2 +/- 4.8	17.3 +/- 0.9	0.117 +/- 0.003	156.3	32.95	8.00	8.55
LL1 -6	50.0	146.7 +/- 4.8	16.5 +/- 0.8	0.112 +/- 0.003	155.8	32.97	7.93	8.20
LL1 -7	60.0	156.1 +/- 5.1	17.0 +/- 0.9	0.109 +/- 0.003	165.5	33.01	7.90	8.58
LL1 -8	70.0	153.8 +/- 5.0	17.1 +/- 0.9	0.111 +/- 0.003	162.3	33.16	7.98	8.55

L,LONG 17/02/77

CODE	DEPTH(M)	137(DPM/L)	134(DPM/L)	RATIO	SC7(DPM/L)	SAL(PM)	TEMP(C)	D,O,(PM)
LL1 -1	1.0	137.5 +/- 4.5	14.8 +/- 0.8	0.108 +/- 0.00	168.9	28.50	5.40	9.00
LL1 -2	10.0	147.6 +/- 4.8	15.6 +/- 0.8	0.105 +/- 0.00	180.7	28.60	5.71	9.40
LL1 -3	20.0	155.4 +/- 5.1	17.1 +/- 0.9	0.110 +/- 0.00	167.9	32.40	7.00	9.69
LL1 -4	30.0	154.1 +/- 5.0	16.2 +/- 0.8	0.105 +/- 0.00	165.2	32.64	7.10	8.55
LL1 -5	40.0	151.5 +/- 5.0	16.8 +/- 0.8	0.111 +/- 0.00	161.7	32.79	7.08	8.80
LL1 -6	50.0	166.0 +/- 5.4	18.1 +/- 0.9	0.109 +/- 0.00	176.9	32.83	6.93	8.95
LL1 -7	60.0	157.9 +/- 5.2	16.8 +/- 0.8	0.106 +/- 0.00	167.7	32.95	6.90	8.95
LL1 -8	69.0	154.2 +/- 5.0	16.8 +/- 0.8	0.109 +/- 0.00	164.2	32.86	6.93	8.92

L.LONG 22/03/77

CODE	DEPTH(M)	137(DPM/L)	134(DPM/L)	RATIO	SC7(DPM/L)	SAL(PM)	TEMP(C)	D.O.(PM)
LL1 -1	1.0	145.4 +/- 4.8	15.8 +/- 0.8	0.109 +/- 0.003	175.8	28.96	6.80	9.59
LL1 -2	10.0	157.8 +/- 5.2	17.1 +/- 0.9	0.108 +/- 0.003	170.9	32.31	6.72	8.75
LL1 -3	20.0	175.7 +/- 5.7	18.7 +/- 0.9	0.106 +/- 0.003	189.8	32.40	6.80	8.90
LL1 -4	30.0	151.0 +/- 4.9	17.1 +/- 0.9	0.113 +/- 0.003	162.9	32.45	6.70	8.96
LL1 -5	40.0	186.2 +/- 6.1	19.8 +/- 1.0	0.106 +/- 0.003	200.4	32.53	6.70	8.69
LL1 -6	50.0	171.0 +/- 5.6	18.6 +/- 0.9	0.109 +/- 0.003	183.5	32.62	6.70	8.65
LL1 -7	60.0	165.1 +/- 5.4	17.5 +/- 0.9	0.106 +/- 0.003	176.6	32.72	6.80	8.40
LL1 -8	69.0	168.0 +/- 5.5	18.3 +/- 0.9	0.109 +/- 0.003	179.4	32.76	6.80	8.35

L.LONG 18/04/77

CODE	DEPTH(M)	137(DPM/L)	134(DPM/L)	RATIO	SC7(DPM/L)	SAL(PM)	TEMP(C)	D.O.(PM)
LL1 -1	1.0	168.9 +/- 5.6	17.7 +/- 1.1	0.105 +/- 0.004	191.6	30.85	7.30	12.15
LL1 -2	10.0	156.9 +/- 5.2	15.9 +/- 1.0	0.101 +/- 0.005	168.9	32.52	6.90	8.96
LL1 -3	20.0	168.3 +/- 5.6	17.7 +/- 1.1	0.105 +/- 0.004	179.0	32.90	6.65	9.00
LL1 -4	30.0	167.2 +/- 5.6	17.7 +/- 1.1	0.106 +/- 0.004	177.5	32.95	6.65	9.00
LL1 -5	40.0	166.0 +/- 5.5	17.7 +/- 1.1	0.107 +/- 0.004	175.7	33.08	6.68	9.05
LL1 -6	50.0	175.3 +/- 5.8	18.4 +/- 1.1	0.105 +/- 0.004	185.4	33.10	6.89	9.06
LL1 -7	60.0	158.0 +/- 5.3	17.0 +/- 1.0	0.107 +/- 0.005	167.0	33.11	6.93	8.98
LL1 -8	66.0	169.0 +/- 5.6	18.0 +/- 1.1	0.106 +/- 0.004	178.6	33.12	6.72	8.95

L.LONG 06/06/77
****

CODE	DEPTH(M)	137(DPM/L)	134(DPM/L)	RATIO	SC7(DPM/L)	SAL(PM)	TEMP(C)	D.O.(PM)
LL1-1	1.0	153.6 +/- 2.7	16.9 +/- 0.5	0.110 +/- 0.003	167.5	32.09	9.20	10.00
LL1-2	10.0	156.7 +/- 2.7	17.1 +/- 0.5	0.109 +/- 0.003	167.7	32.70	8.38	8.95
LL1-3	20.0	147.4 +/- 2.6	16.3 +/- 0.5	0.111 +/- 0.003	156.7	32.92	7.80	8.05
LL1-5	40.0	159.5 +/- 2.8	16.8 +/- 0.5	0.105 +/- 0.003	168.6	33.11	7.20	8.12
LL1-6	50.0	147.4 +/- 2.6	16.4 +/- 0.5	0.111 +/- 0.003	155.7	33.13	7.20	7.88
LL1-7	60.0	158.3 +/- 2.8	16.8 +/- 0.5	0.106 +/- 0.003	167.3	33.13	7.22	7.95

L.LONG 19/07/77
****

CODE	DEPTH(M)	137(DPM/L)	134(DPM/L)	RATIO	SC7(DPM/L)	SAL(PM)	TEMP(C)	D.O.(PM)
LL1-1	1.0	143.9 +/- 2.5	14.3 +/- 0.4	0.099 +/- 0.003	155.8	32.32	14.80	11.50
LL1-2	10.0	137.7 +/- 2.4	14.5 +/- 0.4	0.105 +/- 0.003	147.8	32.62	12.11	8.94
LL1-3	20.0	130.4 +/- 2.3	15.1 +/- 0.4	0.116 +/- 0.003	138.3	32.99	9.85	6.78
LL1-4	30.0	134.9 +/- 2.3	14.5 +/- 0.4	0.107 +/- 0.003	142.0	33.23	9.00	5.95
LL1-5	40.0	140.3 +/- 2.4	14.5 +/- 0.4	0.103 +/- 0.003	147.8	33.21	9.71	5.90
LL1-6	50.0	141.7 +/- 2.4	14.2 +/- 0.4	0.100 +/- 0.003	149.1	33.27	9.12	5.95
LL1-7	60.0	130.4 +/- 2.3	14.2 +/- 0.4	0.109 +/- 0.003	137.0	33.29	8.89	5.90

L.LONG 16/08/77
****

CODE	DEPTH(M)	137(DPM/L)	134(DPM/L)	RATIO	SC7(DPM/L)	SAL(PM)	TEMP(C)	D.O.(PM)
LL1-1	1.0	131.5 +/- 2.3	13.5 +/- 0.3	0.103 +/- 0.002	142.9	32.20	13.52	8.75
LL1-2	15.0	131.8 +/- 2.3	13.2 +/- 0.3	0.100 +/- 0.003	140.0	32.96	10.55	5.55
LL1-3	30.0	136.0 +/- 2.4	13.2 +/- 0.3	0.097 +/- 0.002	143.7	33.13	10.10	5.14
LL1-4	50.0	133.2 +/- 2.3	13.2 +/- 0.3	0.099 +/- 0.003	140.5	33.20	9.71	4.58
LL1-5	66.0	121.3 +/- 2.1	12.6 +/- 0.3	0.103 +/- 0.003	127.9	33.20	9.47	4.00

L.LONG 27/09/77
****

CODE	DEPTH(M)	137(DPM/L)	134(DPM/L)	RATIO	SC7(DPM/L)	SAL(PM)	TEMP(C)	D.O.(PM)
LL1-1	1.0	119.5 +/- 2.1	12.4 +/- 0.5	0.104 +/- 0.004	136.5	30.64	12.32	0.0
LL1-2	10.0	123.2 +/- 2.2	13.3 +/- 0.5	0.108 +/- 0.004	131.9	32.69	11.98	0.0
LL1-3	20.0	131.0 +/- 2.3	13.1 +/- 0.5	0.100 +/- 0.004	138.7	33.06	11.81	0.0
LL1-4	30.0	127.1 +/- 2.2	13.1 +/- 0.5	0.103 +/- 0.004	134.1	33.17	11.81	0.0
LL1-5	40.0	126.0 +/- 2.2	13.0 +/- 0.5	0.103 +/- 0.004	133.0	33.16	11.80	0.0
LL1-6	50.0	131.0 +/- 2.3	13.1 +/- 0.5	0.100 +/- 0.004	138.1	33.22	11.85	0.0
LL1-7	60.0	130.6 +/- 2.3	13.1 +/- 0.5	0.100 +/- 0.004	138.0	33.14	11.60	0.0
LL1-8	70.0	128.3 +/- 2.3	13.4 +/- 0.5	0.104 +/- 0.004	135.5	33.16	11.63	0.0
LL2-1	1.0	124.6 +/- 2.2	13.8 +/- 0.5	0.111 +/- 0.004	138.3	31.53	12.50	0.0
LL2-2	10.0	128.3 +/- 2.3	12.8 +/- 0.5	0.100 +/- 0.004	141.3	31.77	12.24	0.0
LL2-3	20.0	137.2 +/- 2.4	15.1 +/- 0.6	0.110 +/- 0.004	147.0	32.67	12.12	0.0
LL2-4	30.0	132.3 +/- 2.3	12.9 +/- 0.5	0.098 +/- 0.004	139.8	33.11	11.92	0.0
LL2-5	40.0	131.0 +/- 2.3	12.8 +/- 0.5	0.098 +/- 0.004	138.5	33.11	11.87	0.0
LL2-6	50.0	131.3 +/- 2.3	13.8 +/- 0.4	0.105 +/- 0.003	138.8	33.12	11.82	0.0
LL2-7	60.0	133.1 +/- 2.3	13.6 +/- 0.5	0.102 +/- 0.004	140.3	33.20	11.81	0.0
LL2-8	65.0	130.4 +/- 2.3	12.9 +/- 0.5	0.099 +/- 0.004	137.3	33.25	11.81	0.0

L.LONG 11/10/77
****

CODE	DEPTH(M)	137(DPM/L)	134(DPM/L)	RATIO	SC7(DPM/L)	SAL(PM)	TEMP(C)	D.O.(PM)
LL1-1	1.0	101.1 +/- 1.8	10.4 +/- 0.4	0.102 +/- 0.004	133.2	26.55	10.78	8.04
LL1-2	10.0	107.8 +/- 1.9	10.6 +/- 0.4	0.098 +/- 0.004	120.9	31.22	11.50	6.50
LL1-3	20.0	132.7 +/- 2.3	12.4 +/- 0.3	0.093 +/- 0.002	142.2	32.65	11.90	5.70
LL1-4	30.0	131.3 +/- 2.3	12.4 +/- 0.3	0.094 +/- 0.002	139.7	32.89	11.90	5.40
LL1-5	40.0	130.4 +/- 2.3	12.6 +/- 0.3	0.097 +/- 0.002	138.3	33.00	11.87	5.40
LL1-6	50.0	126.9 +/- 2.2	12.3 +/- 0.3	0.097 +/- 0.002	134.5	33.04	11.83	5.30
LL1-7	60.0	115.6 +/- 2.0	13.2 +/- 0.3	0.114 +/- 0.003	122.4	33.06	11.82	5.30
LL1-8	65.0	134.6 +/- 2.3	13.5 +/- 0.3	0.100 +/- 0.002	142.4	33.08	11.81	5.20

L.LONG 15/11/77
****

CODE	DEPTH(M)	137(DPM/L)	134(DPM/L)	RATIO	SC7(DPM/L)	SAL(PM)	TEMP(C)	D.O.(PM)
LL1-1	1.0	98.5 +/- 1.8	10.2 +/- 0.4	0.104 +/- 0.004	140.0	24.62	9.18	9.45
LL1-2	10.0	119.9 +/- 2.1	12.2 +/- 0.4	0.102 +/- 0.003	129.8	32.33	11.49	7.28
LL1-3	20.0	124.7 +/- 2.2	13.2 +/- 0.3	0.106 +/- 0.002	134.3	32.52	11.61	6.97
LL1-4	30.0	113.9 +/- 2.0	11.8 +/- 0.4	0.104 +/- 0.004	122.4	32.58	11.66	6.88
LL1-5	40.0	120.3 +/- 2.1	12.8 +/- 0.4	0.106 +/- 0.003	129.1	32.60	11.72	6.49
LL1-6	50.0	124.4 +/- 2.2	11.3 +/- 0.4	0.091 +/- 0.003	133.4	32.63	11.76	6.36

L.LONG 28/12/77
****

CODE	DEPTH(M)	137(DPM/L)	134(DPM/L)	RATIO	SC7(DPM/L)	SAL(PM)	TEMP(C)	D.O.(PM)
LL1-1	1.0	109.3 +/- 1.9	9.8 +/- 0.3	0.090 +/- 0.003	130.3	29.38	7.30	8.80
LL1-2	10.0	109.6 +/- 1.9	9.8 +/- 0.3	0.089 +/- 0.003	119.1	32.21	9.56	7.70
LL1-3	30.0	118.7 +/- 2.1	11.3 +/- 0.3	0.095 +/- 0.003	126.3	32.87	9.51	7.88
LL1-4	50.0	126.6 +/- 2.2	11.3 +/- 0.3	0.089 +/- 0.003	134.7	32.91	9.33	8.08
LL1-5	65.0	126.5 +/- 2.2	11.1 +/- 0.3	0.088 +/- 0.003	134.5	32.92	9.40	8.05

L.LONG 17/01/78
****

CODE	DEPTH(M)	137(DPM/L)	134(DPM/L)	RATIO	SC7(DPM/L)	SAL(PM)	TEMP(C)	D.O.(PM)
LL1-1	1.0	114.6 +/- 2.0	10.7 +/- 0.4	0.093 +/- 0.003	136.7	29.34	6.04	9.85
LL1-3	30.0	128.1 +/- 2.3	12.1 +/- 0.3	0.095 +/- 0.003	136.2	32.90	8.69	8.45
LL1-4	50.0	119.8 +/- 2.1	10.3 +/- 0.3	0.086 +/- 0.003	127.5	32.87	8.19	8.50
LL1-5	70.0	131.5 +/- 2.3	11.9 +/- 0.3	0.091 +/- 0.002	139.9	32.89	8.06	8.50

L.LONG 21/02/78
****

CODE	DEPTH(M)	137(DPM/L)	134(DPM/L)	RATIO	SC7(DPM/L)	SAL(PM)	TEMP(C)	D.O.(PM)
LL1-1	1.0	117.5 +/- 2.1	11.6 +/- 0.3	0.099 +/- 0.003	129.6	31.72	5.20	9.22
LL1-2	10.0	124.2 +/- 2.2	11.5 +/- 0.3	0.093 +/- 0.003	133.8	32.48	6.59	8.63
LL1-3	30.0	117.7 +/- 2.1	10.8 +/- 0.3	0.092 +/- 0.003	125.1	32.93	7.11	8.65
LL1-4	50.0	116.2 +/- 2.1	10.5 +/- 0.3	0.090 +/- 0.003	122.8	33.12	7.11	8.58
LL1-5	65.0	122.2 +/- 2.2	11.2 +/- 0.3	0.092 +/- 0.003	128.9	33.17	7.12	8.66

APPENDIX I.3 ADDITIONAL SEA LOCH SITES

****

RESULTS OF THE ANALYSIS OF SAMPLES FROM SEA LOCH SITES OTHER THAN THE L.GOIL/L.LONG DEEP SITES ARE LISTED IN THIS SECTION. LOCH GOIL SHALLOW SITES LG2 & LG3 ARE LISTED ON PAGES A45 - 49 AND PAGE A50 RESPECTIVELY (LOCATIONS SHOWN ON FIG. 4.1) . SAMPLES FROM L.LONG SITES (PLOTTED ON FIG. 4.12) ARE LISTED ON PAGES A51 - 53 , FROM GARELOCH ON PAGES A54 & 55 AND FROM L.FYNE ON PAGES A56 - 58 . ADDITIONAL SAMPLES FROM L.FYNE OBTAINED DURING THE CLYDE SEA AREA SURVEY HAVE BEEN PREVIOUSLY LISTED IN APPENDIX I.1 (PAGES A4 & 5) .

L,GOIL 2 04/12/75

****

CODE	DEPTH(M)	137(DPM/L)	134(DPM/L)	RATIO	SC7(DPM/L)	SAL(PM)	TEMP(C)	D,O,(PM)
L,GIL	1,0	113,9 +/- 4,3	18,3 +/- 0,6	0,161 +/- 0,003	130,8	30,46	10,60	7,80
L,GIL	20,0	114,1 +/- 4,3	17,7 +/- 0,6	0,156 +/- 0,003	122,2	32,68	10,90	7,00
L,GIL	30,0	111,5 +/- 4,2	17,2 +/- 0,6	0,154 +/- 0,004	119,1	32,76	10,80	7,00
L,GIL	40,0	107,2 +/- 4,0	17,0 +/- 0,6	0,159 +/- 0,004	114,3	32,83	7,80	7,90

L.GOIL 2 08/01/76

****

CODE	DEPTH(M)	137(DPM/L)	134(DPM/L)	RATIO	SC7(DPM/L)	SAL(PM)	TEMP(C)	D.O.(PM)
L.GIL	1.0	101.6 +/- 3.8	15.8 +/- 0.6	0.156 +/- 0.004	136.8	26.00	8.10	9.60
L.GIL	10.0	100.9 +/- 4.1	17.2 +/- 0.6	0.158 +/- 0.004	131.3	29.03	8.50	9.08
L.GIL2	20.0	119.8 +/- 4.5	18.3 +/- 0.7	0.153 +/- 0.004	130.0	32.23	9.47	7.41
L.GIL	30.0	116.2 +/- 4.4	18.3 +/- 0.6	0.157 +/- 0.003	125.1	32.50	9.60	7.25
L.GIL	40.0	109.2 +/- 4.1	17.2 +/- 0.6	0.158 +/- 0.004	117.1	32.62	9.72	6.28
L.GIL	50.0	117.4 +/- 4.4	18.3 +/- 0.6	0.156 +/- 0.003	124.7	32.93	9.82	4.95

L.GOIL 2 03/03/76

****

CODE	DEPTH(M)	137(DPM/L)	134(DPM/L)	RATIO	SC7(DPM/L)	SAL(PM)	TEMP(C)	D.O.(PM)
L.GIL	1.0	85.5 +/- 3.2	13.2 +/- 0.5	0.154 +/- 0.004	104.9	28.53	8.35	9.40
L.GIL	10.0	96.7 +/- 3.7	14.9 +/- 0.5	0.154 +/- 0.004	108.3	31.27	8.55	8.42
L.GIL	20.0	100.4 +/- 3.8	14.9 +/- 0.5	0.149 +/- 0.004	108.2	32.46	8.50	8.10
L.GIL	30.0	97.7 +/- 3.7	15.2 +/- 0.6	0.156 +/- 0.004	105.0	32.57	8.80	7.87
L.GIL	40.0	103.8 +/- 3.9	15.4 +/- 0.6	0.149 +/- 0.004	110.2	32.95	8.80	7.90

L.GOIL 2 01/04/76

****

CODE	DEPTH(M)	137(DPM/L)	134(DPM/L)	RATIO	SC7(DPM/L)	SAL(PM)	TEMP(C)	D.O.(PM)
L.GIL	1.0	81.6 +/- 3.1	12.1 +/- 0.5	0.148 +/- 0.005	105.2	27.15	6.40	10.60
L.GIL	10.0	81.2 +/- 3.1	12.4 +/- 0.5	0.152 +/- 0.005	94.7	30.01	6.80	10.20
L.GIL	20.0	91.0 +/- 3.4	13.7 +/- 0.5	0.150 +/- 0.005	99.8	31.92	7.05	8.65
L.GIL	30.0	92.0 +/- 3.5	13.7 +/- 0.5	0.149 +/- 0.004	99.6	32.33	7.20	8.48
L.GIL	40.0	98.0 +/- 3.7	14.0 +/- 0.5	0.143 +/- 0.004	105.6	32.47	7.55	8.50
L.GIL	50.0	94.2 +/- 3.6	13.5 +/- 0.5	0.143 +/- 0.004	100.9	32.68	7.50	8.40

L,GOIL 07/12/76

CODE	DEPTH(M)	137(DPM/L)	134(DPM/L)	RATIO	SC7(DPM/L)	SAL(PM)	TEMP(C)	D.O.(PM)
LG2 -1	1.0	108.6 +/- 3.6	12.4 +/- 0.7	0.114 +/- 0.004	143.5	26.50	6.20	9.00
LG2 -2	10.0	131.0 +/- 4.3	15.0 +/- 0.8	0.114 +/- 0.003	152.4	30.10	9.10	7.32
LG2 -3	20.0	133.5 +/- 4.4	15.3 +/- 0.8	0.114 +/- 0.003	147.4	31.70	10.00	6.75
LG2 -4	30.0	132.0 +/- 4.3	14.6 +/- 0.8	0.111 +/- 0.003	145.7	31.70	10.10	6.75
LG2 -5	40.0	129.6 +/- 4.3	13.6 +/- 0.7	0.105 +/- 0.003	143.6	31.60	10.20	5.31

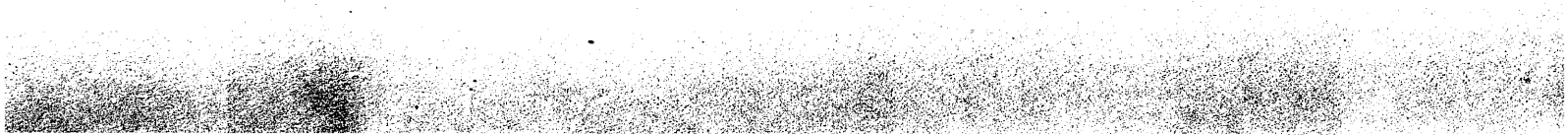

L.GOIL 01/04/76

****

CODE	DEPTH(M)	137(DPM/L)	134(DPM/L)	RATIO	SC7(DPM/L)	SAL(PM)	TEMP(C)	D.O.(PM)
L.GOIL 3	1.0	71.0 +/- 2.7	9.9 +/- 0.5	0.139 +/- 0.005	96.7	25.68	6.20	12.20
L.GOIL 3	10.0	80.9 +/- 3.1	11.4 +/- 0.5	0.141 +/- 0.005	95.3	29.70	6.60	10.00
L.GOIL 3	20.0	96.4 +/- 3.6	13.8 +/- 0.5	0.143 +/- 0.004	104.7	32.25	7.48	8.25
L.GOIL 3	30.0	100.8 +/- 3.8	14.9 +/- 0.6	0.148 +/- 0.004	107.8	32.71	7.80	8.25
L.GOIL 3	40.0	97.0 +/- 3.7	14.5 +/- 0.6	0.150 +/- 0.004	103.6	32.75	7.80	7.40

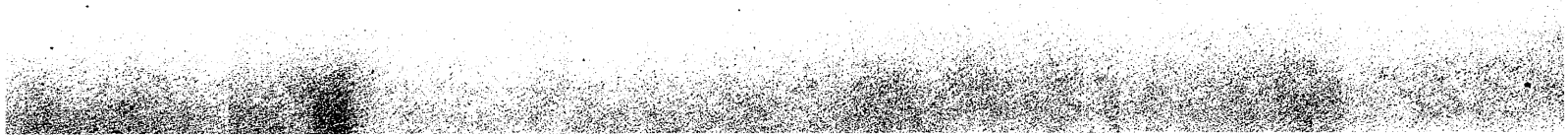

LL 08/01/76

****

CODE	DEPTH(M)	137(DPM/L)	134(DPM/L)	RATIO	SC7(DPM/L)	SAL(PM)	TEMP(C)	D.O.(PM)
L.LONG 3	1.0	100.7 +/- 4.1	16.9 +/- 0.6	0.155 +/- 0.004	131.7	28.80	9.35	9.05
L.LONG 2	1.0	101.8 +/- 3.8	15.8 +/- 0.6	0.156 +/- 0.004	133.2	26.75	8.05	9.43
L.LONG 1	1.0	101.9 +/- 3.8	15.3 +/- 0.6	0.150 +/- 0.004	137.2	26.00	8.30	9.43

LL-LG 04/02/76

****

CODE	DEPTH(M)	137(DPM/L)	134(DPM/L)	RATIO	SC7(DPM/L)	SAL(PM)	TEMP(C)	D.O.(PM)
LG1	25.0	113.1 +/- 4.3	17.3 +/- 0.6	0.153 +/- 0.003	123.9	31.94	7.00	8.47
LG2	25.0	93.5 +/- 3.6	14.6 +/- 0.5	0.153 +/- 0.004	105.5	31.70	8.00	9.52
LL3E	25.0	115.9 +/- 4.4	17.7 +/- 0.6	0.153 +/- 0.003	143.6	28.36	7.90	9.10
LL2E	25.0	113.5 +/- 4.3	17.4 +/- 0.6	0.154 +/- 0.003	124.1	32.03	7.50	8.95
LL1E	25.0	110.4 +/- 4.2	16.1 +/- 0.6	0.146 +/- 0.003	118.8	32.52	7.90	9.11
LL3W	25.0	110.8 +/- 4.2	16.8 +/- 0.6	0.151 +/- 0.003	124.6	31.12	6.50	8.90
LL2W	25.0	111.0 +/- 4.2	16.5 +/- 0.6	0.149 +/- 0.003	125.4	31.00	6.00	9.15
LL1W	25.0	108.6 +/- 4.1	16.5 +/- 0.6	0.152 +/- 0.004	118.6	32.06	7.20	9.35

LL 03/03/76

CODE	DEPTH(M)	137(DPM/L)	134(DPM/L)	RATIO	SC7(DPM/L)	SAL(PM)	TEMP(C)	D.O.(PM)
LL3E	2.0	81.0 +/- 3.1	12.0 +/- 0.5	0.148 +/- 0.005	103.6	27.35	7.10	9.22
LL2E	2.0	85.4 +/- 3.2	13.4 +/- 0.5	0.157 +/- 0.004	107.8	27.73	7.75	9.55
LL1E	2.0	91.8 +/- 3.5	13.9 +/- 0.5	0.152 +/- 0.004	113.6	28.28	7.35	9.50
LL3W	2.0	85.5 +/- 3.2	12.7 +/- 0.5	0.148 +/- 0.004	112.8	26.55	6.80	9.52
LL2W	2.0	90.9 +/- 3.4	13.7 +/- 0.5	0.150 +/- 0.004	112.2	28.36	7.05	9.35
LL1W	2.0	86.0 +/- 3.3	13.2 +/- 0.5	0.154 +/- 0.004	107.3	28.04	7.10	9.49

GAREL, 06/12/75

CODE	DEPTH(M)	137(DPM/L)	134(DPM/L)	RATIO	SC7(DPM/L)	SAL(PM)	TEMP(C)	D.O.(PM)
GARL.	20.0	85.3 +/- 3.2	13.2 +/- 0.5	0.155 +/- 0.004	98.6	30.29	11.30	6.90
GARL.	30.0	83.4 +/- 3.2	13.1 +/- 0.5	0.157 +/- 0.004	92.8	31.46	11.90	5.90

G.LOCH 03/08/76

CODE	DEPTH(M)	137(DPM/L)	134(DPM/L)	RATIO	SC7(DPM/L)	SAL(PM)	TEMP(C)	D.O.(PM)
G.LOCH	0.0	107.0 +/- 4.0	14.3 +/- 0.5	0.134 +/- 0.004	119.8	31.26	13.39	9.50
G.LOCH	10.0	119.7 +/- 4.5	16.4 +/- 0.6	0.137 +/- 0.003	132.6	31.60	13.00	7.30
G.LOCH	20.0	118.3 +/- 4.4	16.1 +/- 0.6	0.136 +/- 0.003	130.4	31.74	12.47	6.70
G.LOCH	30.0	104.1 +/- 3.9	14.3 +/- 0.5	0.137 +/- 0.004	114.4	31.84	12.30	6.60
G.LOCH	40.0	106.9 +/- 4.0	15.1 +/- 0.6	0.141 +/- 0.004	117.1	31.95	12.19	6.50

LF 17/02/76

****

CODE	DEPTH(M)	137(DPM/L)	134(DPM/L)	RATIO	SC7(DPM/L)	SAL(PH)	TEMP(C)	D.O.(PPM)
L.FYNE 2	1.0	104.2 +/- 3.9	16.5 +/- 0.6	0.158 +/- 0.004	116.8	31.22	6.50	9.42
L.FYNE 1	1.0	100.0 +/- 3.8	15.4 +/- 0.6	0.154 +/- 0.004	107.1	32.67	6.90	9.32

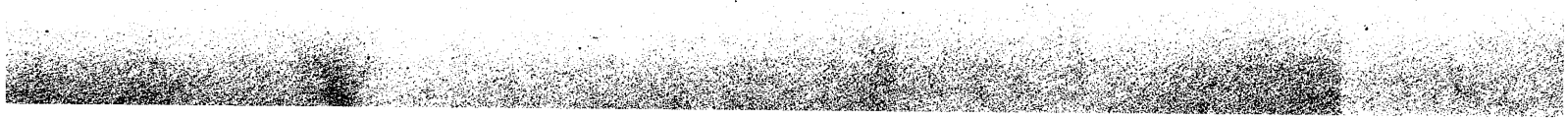

L.FYNE 17/02/76

****

CODE	DEPTH(M)	137(DPM/L)	134(DPM/L)	RATIO	SC7(DPM/L)	SAL(PM)	TEMP(C)	D.O.(PM)
L.FYNE 3	10.0	103.3 +/- 3.9	16.3 +/- 0.6	0.157 +/- 0.004	121.0	29.88	6.20	9.70
L.FYNE 3	10.0	105.7 +/- 4.0	16.3 +/- 0.6	0.154 +/- 0.004	113.5	32.59	8.30	8.92
L.FYNE 3	20.0	109.4 +/- 4.1	16.6 +/- 0.6	0.151 +/- 0.004	117.1	32.69	8.30	8.59
L.FYNE 3	30.0	112.1 +/- 4.2	17.0 +/- 0.6	0.152 +/- 0.003	119.9	32.74	8.39	8.41
L.FYNE 3	39.0	105.0 +/- 4.0	17.2 +/- 0.6	0.164 +/- 0.004	111.9	32.84	8.60	8.19

L.FYNE 24/11/76

****

CODE	DEPTH(M)	137(DPM/L)	134(DPM/L)	RATIO	SC7(DPM/L)	SAL(PM)	TEMP(C)	O.O.(PM)
LF1	1.0	128.9 +/- 4.2	14.5 +/- 0.8	0.112 +/- 0.003	137.4	32.85	10.20	77.50
LF3	150.0	132.0 +/- 4.3	15.4 +/- 0.8	0.117 +/- 0.003	137.3	33.65	11.50	76.50
LF5	1.0	115.8 +/- 3.8	13.2 +/- 0.7	0.114 +/- 0.004	131.2	30.90	9.60	88.90
LF7	125.0	91.2 +/- 3.0	9.4 +/- 0.6	0.103 +/- 0.004	97.0	32.91	8.21	51.10

****

APPENDIX I.4 THE HEBRIDEAN SEA AREA

****

IN THIS SECTION RESULTS FROM SAMPLES OBTAINED DURING CRUISES 8/1976 (PAGES A60 - 65) AND 10/1977 (PAGES A66 - 77) OF THE R.S. CHALLENGER ARE LISTED . DISSOLVED OXYGEN WAS NOT MEASURED IN ANY OF THESE SAMPLES . LOCATIONS CORRESPONDING TO SAMPLE CODES FOR EACH YEAR ARE PLOTTED ON FIG. 5.1 .

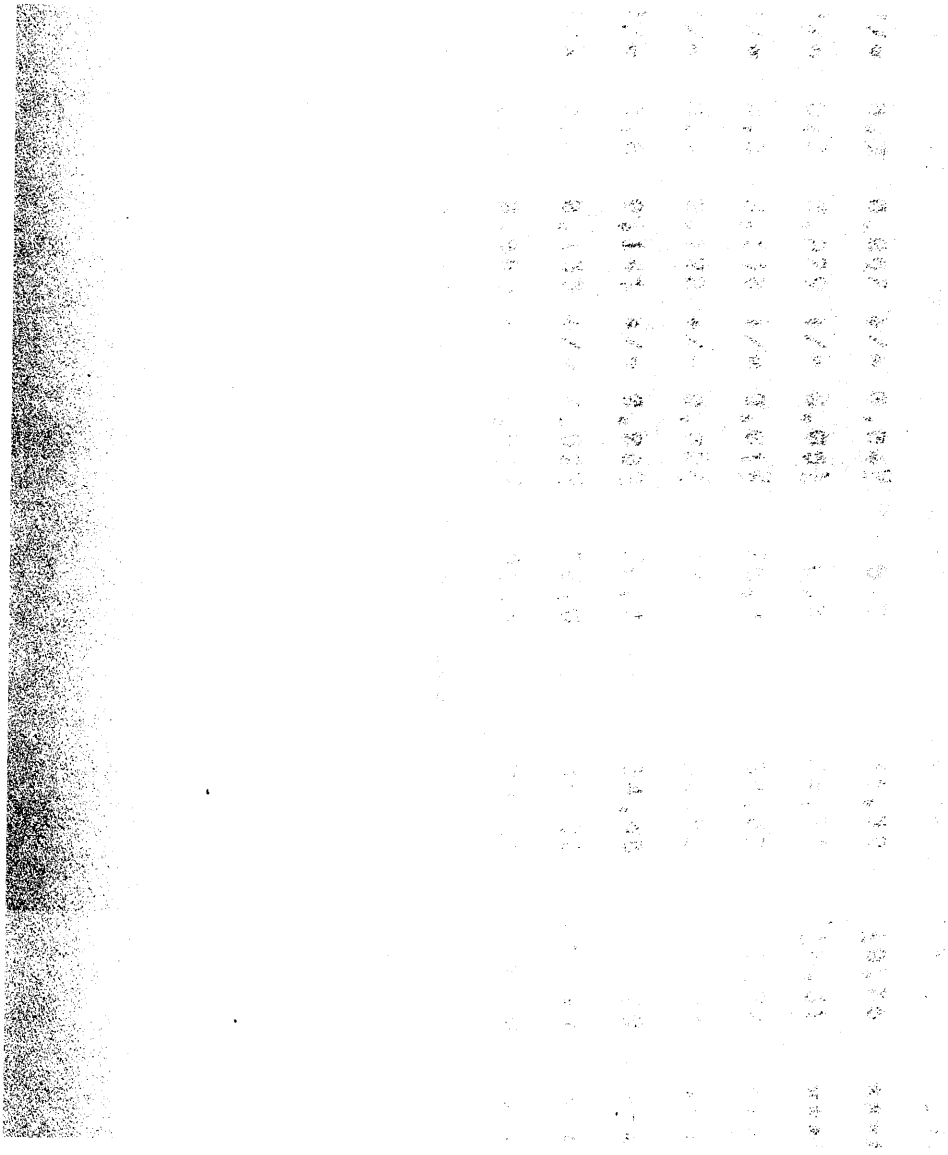

ATLANTIC RUN A

CODE	DEPTH(M)	137(DPM/L)	134(DPM/L)	RATIO	SC7(DPM/L)	SAL(PM)	TEMP(C)	D.O.(PM)
1A	1.0	5.2 +/- 0.3	0.3 +/- 0.3	0.067 +/- 0.04	5.3	34.32	10.76	******
2A	1.0	5.2 +/- 0.3	0.4 +/- 0.3	0.079 +/- 0.05	5.3	34.77	10.31	******
3A	1.0	25.6 +/- 0.9	3.5 +/- 0.3	0.138 +/- 0.01	25.8	34.67	9.77	******
4A	1.0	46.4 +/- 1.6	5.7 +/- 0.4	0.122 +/- 0.00	47.1	34.52	9.44	******
5A	1.0	69.6 +/- 2.3	9.8 +/- 0.6	0.141 +/- 0.00	70.7	34.46	9.29	******
6A	1.0	78.4 +/- 2.6	10.4 +/- 0.6	0.133 +/- 0.00	80.0	34.30	*****	******
7A	1.0	67.2 +/- 3.4	5.6 +/- 2.3	0.083 +/- 0.03	68.6	34.30	9.02	******

ATLANTIC RUN B

CODE	DEPTH(M)	137(DPM/L)	134(DPM/L)	RATIO	SC7(DPM/L)	SAL(PM)	TEMP(C)	D.O.(PM)
1B	1.0	69.8 +/- 2.3	9.3 +/- 0.6	0.134 +/- 0.005	71.0	34.39	9.06	******
2B	1.0	75.3 +/- 2.7	9.6 +/- 0.9	0.127 +/- 0.010	76.6	34.37	9.14	******
3B	1.0	67.9 +/- 2.3	9.4 +/- 0.6	0.138 +/- 0.005	69.1	34.38	9.14	******
4B	1.0	44.1 +/- 1.5	6.1 +/- 0.4	0.138 +/- 0.008	44.6	34.64	9.44	******
5B	1.0	0.9 +/- 0.2	0.1 +/- 0.3	0.147 +/- 0.304	0.9	35.10	10.08	******
6B	1.0	0.5 +/- 0.2	-0.1 +/- 0.2	-0.120 +/- -.454	0.5	35.16	10.18	******
7B	1.0	0.3 +/- 0.2	-0.1 +/- 0.3	-0.188 +/- -.967	0.3	35.29	9.30	******
8B	1.0	0.4 +/- 0.2	0.2 +/- 0.3	0.420 +/- 0.709	0.4	35.30	*****	******

ATLANTIC RUN C

CODE	DEPTH(M)	137(DPM/L)	134(DPM/L)	RATIO	SC7(DPM/L)	SAL(PM)	TEMP(C)	D.O.(PM)
2C	1.0	30.8 +/- 1.1	3.1 +/- 0.3	0.101 +/- 0.010	31.3	34.45	9.90	******
3C	1.0	13.8 +/- 0.6	1.6 +/- 0.3	0.114 +/- 0.021	13.8	34.99	9.67	******
4C	1.0	12.3 +/- 0.7	1.7 +/- 0.5	0.142 +/- 0.040	12.2	35.02	10.10	******
5C	1.0	4.1 +/- 0.8	0.4 +/- 1.0	0.093 +/- 0.241	4.1	35.04	*****	******
6C	1.0	5.5 +/- 0.3	0.7 +/- 0.3	0.129 +/- 0.049	5.5	35.10	9.04	******
7C	1.0	11.8 +/- 0.5	1.5 +/- 0.3	0.126 +/- 0.024	11.8	34.86	9.34	******
8C	1.0	9.4 +/- 0.4	1.4 +/- 0.3	0.149 +/- 0.030	9.2	35.92	*****	******
8AC	1.0	2.1 +/- 1.5	0.2 +/- 2.0	0.105 +/- 0.933	2.1	35.29	8.84	******
9AC	1.0	0.5 +/- 0.2	-0.0 +/- 0.3	-0.062 +/- -.484	0.5	35.30	9.00	******
10C	1.0	0.1 +/- 0.2	-0.1 +/- 0.3	-0.770 +/- *****	0.1	35.31	9.64	******

ATLANTIC BUOYS

CODE	DEPTH(M)	137(DPM/L)	134(DPM/L)	RATIO	SC7(DPM/L)	SAL(PM)	TEMP(C)	D.O.(PM)
'A'	1.0	39.6 +/- 1.4	5.3 +/- 0.4	0.135 +/- 0.009	40.2	34.48	9.78	******
'B'	1.0	20.7 +/- 0.8	2.7 +/- 0.3	0.131 +/- 0.014	20.8	34.82	10.22	******

ATLANTIC RUN D

CODE	DEPTH(M)	137(DPM/L)	134(DPM/L)	RATIO	SC7(DPM/L)	SAL(PM)	TEMP(C)	O.O.(PM)
1D	1.0	38.7 +/- 1.4	5.2 +/- 0.4	0.133 +/- 0.009	38.6	34.23	9.03	******
2D	1.0	43.5 +/- 1.5	5.6 +/- 0.4	0.129 +/- 0.008	44.8	34.23	8.99	******
4D	1.0	53.8 +/- 1.8	7.7 +/- 0.5	0.143 +/- 0.007	54.7	34.44	8.97	******
6D	1.0	45.3 +/- 1.6	6.2 +/- 0.4	0.136 +/- 0.008	45.9	34.57	10.07	******
6/7D	1.0	49.7 +/- 1.7	6.8 +/- 0.5	0.137 +/- 0.007	50.4	34.55	*****	******
8D	1.0	1.1 +/- 0.2	0.1 +/- 0.3	0.100 +/- 0.240	1.1	35.26	9.34	******
9D	1.0	0.9 +/- 0.2	0.0 +/- 0.3	0.032 +/- 0.283	0.9	35.29	9.41	******
10D	1.0	9.6 +/- 0.4	1.1 +/- 0.3	0.118 +/- 0.028	9.7	34.93	8.50	******
12D	1.0	4.7 +/- 0.3	0.6 +/- 0.3	0.132 +/- 0.059	4.7	35.13	8.42	******
14D	1.0	0.8 +/- 0.2	0.1 +/- 0.3	0.144 +/- 0.320	0.8	35.28	*****	******
15D	1.0	0.4 +/- 0.2	0.0 +/- 0.3	0.007 +/- 0.691	0.4	35.30	*****	******
16D	1.0	0.3 +/- 0.2	0.0 +/- 0.3	0.010 +/- 0.930	0.3	35.31	8.72	******

ATLANTIC RUN E

CODE	DEPTH(M)	137(DPM/L)	134(DPM/L)	RATIO	SC7(DPM/L)	SAL(PM)	TEMP(C)	D.O.(PM)
1E	1.0	28.5 +/- 1.0	3.9 +/- 0.4	0.138 +/- 0.011	29.5	33.89	9.50	******
2E	1.0	29.8 +/- 1.1	3.7 +/- 0.4	0.124 +/- 0.011	30.3	34.38	9.60	******
3E	1.0	30.9 +/- 1.1	3.7 +/- 0.4	0.119 +/- 0.010	31.4	34.53	9.66	******
4E	1.0	32.7 +/- 1.2	4.2 +/- 0.4	0.130 +/- 0.010	33.0	34.63	10.12	******
5E	1.0	13.1 +/- 0.5	1.7 +/- 0.3	0.130 +/- 0.022	13.1	34.96	*****	******

ATLANTIC RUN A
****

CODE	DEPTH(M)	137(DPM/L)	134(DPM/L)	RATIO	SC7(DPM/L)	SAL(PM)	TEMP(C)	D.O.(PM)
A1	1.0	109.9 +/- 1.9	12.2 +/- 0.2	0.111 +/- 0.002	113.2	34.00	*****	0.0
A2	1.0	95.3 +/- 1.7	11.1 +/- 0.5	0.117 +/- 0.005	98.1	34.01	*****	0.0
A3	1.0	98.2 +/- 1.7	11.2 +/- 0.2	0.114 +/- 0.002	100.9	34.08	*****	0.0
A4	1.0	101.2 +/- 1.8	11.3 +/- 0.2	0.111 +/- 0.002	104.0	34.09	*****	0.0
A5	1.0	100.8 +/- 1.8	10.7 +/- 0.2	0.106 +/- 0.002	103.5	34.08	*****	0.0
A6	1.0	85.8 +/- 1.5	9.8 +/- 0.2	0.114 +/- 0.003	88.1	34.09	*****	0.0

****

ATLANTIC RUN B
****

CODE	DEPTH(M)	137(DPM/L)	134(DPM/L)	RATIO	SC7(DPM/L)	SAL(PM)	TEMP(C)	D.O.(PM)
B1	1.0	86.1 +/- 1.5	9.6 +/- 0.3	0.111 +/- 0.003	88.8	33.95	*****	0.0
B2	1.0	99.7 +/- 1.7	10.8 +/- 0.3	0.109 +/- 0.003	102.8	33.96	*****	0.0
B3	1.0	105.6 +/- 1.8	11.3 +/- 0.3	0.107 +/- 0.003	108.8	33.98	*****	0.0
B4	1.0	96.7 +/- 1.7	11.0 +/- 0.3	0.114 +/- 0.003	99.7	33.97	*****	0.0
B5	1.0	98.9 +/- 1.7	10.8 +/- 0.3	0.109 +/- 0.003	101.7	34.03	*****	0.0
B6	1.0	109.5 +/- 1.9	11.4 +/- 0.3	0.104 +/- 0.003	112.8	33.99	*****	0.0

****

ATLANTIC RUN C
****

CODE	DEPTH(M)	137(DPM/L)	134(DPM/L)	RATIO	SC7(DPM/L)	SAL(PM)	TEMP(C)	D.O.(PM)
C1	1.0	90.9 +/- 1.6	10.2 +/- 0.2	0.112 +/- 0.002	93.3	34.10	11.64	0.0
C2	1.0	81.7 +/- 1.4	9.3 +/- 0.2	0.114 +/- 0.002	83.6	34.21	10.83	0.0
C3	1.0	73.9 +/- 1.3	8.4 +/- 0.2	0.113 +/- 0.002	75.4	34.29	10.96	0.0
C4	1.0	69.4 +/- 1.2	7.3 +/- 0.2	0.105 +/- 0.003	70.9	34.26	11.05	0.0
C5	1.0	81.7 +/- 1.4	8.4 +/- 0.2	0.103 +/- 0.002	83.5	34.24	11.08	0.0
C6	1.0	51.3 +/- 0.9	5.6 +/- 0.2	0.108 +/- 0.003	52.1	34.49	11.62	0.0
C7	1.0	10.1 +/- 0.2	0.8 +/- 0.2	0.075 +/- 0.015	10.2	34.72	12.42	0.0

****

ATLANTIC RUN D
****

CODE	DEPTH(M)	137(DPM/L)	134(DPM/L)	RATIO	SC7(DPM/L)	SAL(PM)	TEMP(C)	D.O.(PM)
01	1.0	81.0 +/- 1.4	9.1 +/- 0.2	0.113 +/- 0.002	82.9	34.20	±1.22	0.0
02	1.0	75.6 +/- 1.3	8.6 +/- 0.2	0.114 +/- 0.002	77.3	34.21	±1.13	0.0
03	1.0	79.1 +/- 1.4	8.5 +/- 0.2	0.107 +/- 0.002	80.9	34.21	±1.08	0.0
04	1.0	80.3 +/- 1.4	8.8 +/- 0.2	0.110 +/- 0.002	82.1	34.21	±1.15	0.0
05	1.0	81.3 +/- 1.4	8.3 +/- 0.2	0.102 +/- 0.002	83.2	34.20	±1.10	0.0
06	1.0	74.4 +/- 1.3	8.0 +/- 0.2	0.107 +/- 0.002	76.0	34.22	±1.18	0.0
07	1.0	25.0 +/- 0.4	2.7 +/- 0.1	0.109 +/- 0.006	25.1	34.80	±3.05	0.0

****

ATLANTIC RUN E
****

CODE	DEPTH(M)	137(DPM/L)	134(DPM/L)	RATIO	SC7(DPM/L)	SAL(PM)	TEMP(C)	D.O.(PM)
E1	1.0	76.8 +/- 1.3	8.8 +/- 0.2	0.114 +/- 0.002	78.7	34.16	±12.15	0.0
E2	1.0	86.7 +/- 1.5	9.3 +/- 0.2	0.107 +/- 0.002	89.0	34.11	±11.77	0.0
E3	1.0	66.3 +/- 1.1	7.1 +/- 0.2	0.108 +/- 0.002	67.6	34.35	±12.70	0.0
E4	1.0	69.8 +/- 1.2	7.6 +/- 0.2	0.107 +/- 0.002	71.1	34.34	±12.17	0.0
E5	1.0	73.9 +/- 1.3	8.1 +/- 0.2	0.110 +/- 0.002	75.5	34.26	±11.95	0.0
E6	1.0	59.8 +/- 1.0	6.9 +/- 0.2	0.116 +/- 0.003	60.8	34.41	±12.18	0.0
E7	1.0	65.8 +/- 1.1	7.2 +/- 0.2	0.110 +/- 0.003	67.0	34.38	±12.30	0.0
E8	1.0	61.6 +/- 1.1	6.2 +/- 0.2	0.101 +/- 0.003	62.6	34.45	±13.09	0.0
E9	1.0	47.5 +/- 0.8	5.2 +/- 0.2	0.110 +/- 0.003	48.1	34.58	±13.17	0.0
E10	1.0	35.5 +/- 0.6	4.2 +/- 0.2	0.118 +/- 0.004	35.8	34.69	±13.86	0.0

****

ATLANTIC RUN F
****

CODE	DEPTH(M)	137(DPM/L)	134(DPM/L)	RATIO	SC7(DPM/L)	SAL(PM)	TEMP(C)	D.O.(PM)
F1	1.0	59.5 +/- 1.0	6.9 +/- 0.2	0.116 +/- 0.003	******	******	±11.33	0.0
F2	1.0	63.5 +/- 1.1	6.9 +/- 0.2	0.109 +/- 0.003	******	******	±11.50	0.0
F3	1.0	62.5 +/- 1.1	6.8 +/- 0.2	0.109 +/- 0.003	63.6	34.38	±11.72	0.0
F4	1.0	62.6 +/- 1.1	6.5 +/- 0.2	0.105 +/- 0.003	******	******	±11.90	0.0
F5	1.0	56.2 +/- 1.0	6.0 +/- 0.2	0.106 +/- 0.003	57.0	34.46	±11.82	0.0

****

ATLANTIC RUN G
****

CODE	DEPTH(M)	137(DPM/L)	134(DPM/L)	RATIO	SC7(DPM/L)	SAL(PM)	TEMP(C)	D.O.(PM)
G1	1.0	58.6 +/- 1.0	7.2 +/- 0.2	0.122 +/- 0.003	59.8	34.30	±2.08	0.0
G3	1.0	61.6 +/- 1.1	6.7 +/- 0.2	0.109 +/- 0.003	62.8	34.35	±1.56	0.0
G5	1.0	45.8 +/- 0.8	5.0 +/- 0.2	0.109 +/- 0.003	46.4	34.58	±1.77	0.0
G7	1.0	45.9 +/- 0.8	4.9 +/- 0.2	0.106 +/- 0.003	46.4	34.60	±3.25	0.0
G9	1.0	42.9 +/- 0.8	5.1 +/- 0.2	0.119 +/- 0.004	43.5	34.56	±2.30	0.0

****

ATLANTIC RUN H
****

CODE	DEPTH(M)	137(DPM/L)	134(DPM/L)	RATIO	SC7(DPM/L)	SAL(PM)	TEMP(C)	D.O.(PM)
H1	1.0	59.2 +/- 1.0	6.1 +/- 0.2	0.103 +/- 0.003	60.3	34.39	±1.23	0.0
H2	1.0	58.5 +/- 1.0	6.3 +/- 0.2	0.108 +/- 0.003	59.5	34.41	±1.88	0.0
H3	1.0	55.7 +/- 1.0	5.8 +/- 0.2	0.103 +/- 0.003	******	******	±1.89	0.0
H4	1.0	56.1 +/- 1.0	5.9 +/- 0.2	0.104 +/- 0.003	56.9	34.47	±1.88	0.0
H5	1.0	52.6 +/- 0.9	5.8 +/- 0.2	0.109 +/- 0.003	53.4	34.48	±2.60	0.0
H6	1.0	55.0 +/- 1.0	5.9 +/- 0.2	0.107 +/- 0.003	55.8	34.49	±2.43	0.0
H7	1.0	50.5 +/- 0.9	4.3 +/- 0.2	0.084 +/- 0.003	51.2	34.54	±2.70	0.0
H8	1.0	48.0 +/- 0.8	5.1 +/- 0.2	0.107 +/- 0.004	48.6	34.58	±2.78	0.0
H9	1.0	48.4 +/- 0.8	5.0 +/- 0.2	0.103 +/- 0.004	48.9	34.60	±0.63	0.0

****

ATLANTIC RUN I
****

CODE	DEPTH(M)	137(DPM/L)	134(DPM/L)	RATIO	SC7(DPM/L)	SAL(PM)	TEMP(C)	D.O.(PM)
I2	1.0	45.5 +/- 0.8	5.4 +/- 0.2	0.119 +/- 0.004	46.1	34.54	±0.68	0.0
I3	1.0	50.1 +/- 0.9	5.2 +/- 0.2	0.103 +/- 0.004	50.8	34.54	±0.74	0.0
I4	1.0	51.6 +/- 0.9	5.3 +/- 0.2	0.102 +/- 0.003	52.3	34.53	±0.40	0.0
I5	1.0	52.1 +/- 0.9	5.4 +/- 0.2	0.104 +/- 0.003	52.8	34.52	±0.77	0.0
I6	1.0	52.3 +/- 0.9	5.2 +/- 0.2	0.100 +/- 0.003	53.0	34.52	±0.32	0.0

****

ATLANTIC RUN J
****

CODE	DEPTH(M)	137(DPM/L)	134(DPM/L)	RATIO	SC7(DPM/L)	SAL(PM)	TEMP(C)	D.O.(PM)
J1	1.0	52.5 +/- 0.9	5.4 +/- 0.2	0.103 +/- 0.003	53.2	34.52	*****	0.0
J2	1.0	48.2 +/- 0.8	5.3 +/- 0.2	0.110 +/- 0.004	48.9	34.46	*****	0.0
J3	1.0	55.1 +/- 1.0	5.4 +/- 0.2	0.097 +/- 0.003	57.7	33.44	*****	0.0
J4	1.0	50.4 +/- 0.9	5.1 +/- 0.2	0.100 +/- 0.003	51.1	34.55	*****	0.0
J5	1.0	52.6 +/- 0.9	3.9 +/- 0.2	0.075 +/- 0.003	53.2	34.56	*****	0.0

****

ATLANTIC RUN K
****

CODE	DEPTH(M)	137(DPM/L)	134(DPM/L)	RATIO	SC7(DPM/L)	SAL(PM)	TEMP(C)	D.O.(PM)
K2	1.0	30.7 +/- 0.5	2.9 +/- 0.2	0.095 +/- 0.005	30.8	34.88	11.70	0.0
K4	1.0	39.0 +/- 0.7	3.7 +/- 0.2	0.096 +/- 0.004	39.3	34.69	12.35	0.0

****

ATLANTIC RUN W
****

CODE	DEPTH(M)	137(DPM/L)	134(DPM/L)	RATIO	SC7(DPM/L)	SAL(PM)	TEMP(C)	D.O.(PM)
W4	1.0	50.6 +/- 0.9	5.1 +/- 0.2	0.101 +/- 0.003	51.2	34.58	11.79	0.0
W6	1.0	56.1 +/- 1.0	5.8 +/- 0.2	0.104 +/- 0.003	57.0	34.43	11.28	0.0
W8	1.0	50.0 +/- 0.9	5.6 +/- 0.2	0.112 +/- 0.004	50.6	34.52	*****	0.0

****

APPENDIX I.5 SEDIMENT PROFILES

****

IN THIS SECTION THE RESULTS OF ANALYSIS OF SEDIMENT CORES FROM THE CLYDE SEA AREA ARE LISTED IN CHRONOLOGICAL ORDER OF DATE OF CORING (PAGES A79 - 86) . FURTHER DETAILS OF THE CORES ARE LISTED IN THE MAIN TEXT (TABLE 6.1). CORING LOCATIONS ARE PLOTTED ON FIG. 6.1 . ADDITIONALLY , L.LOMOND MACKARETH CORE RESULTS ARE LISTED ON PAGE A87 . IN THIS SECTION ALL ACTIVITIES ARE REPORTED IN DISINTEGRATIONS PER MINUTE (DPM) PER GRAMME DRY WEIGHT .

GARELOCH GRAVITY CORE 1 14/01/74

SECTION	CS-137(DPM/G)	CS-134(DPM/G)	RATIO	DRY/WET	CODE NO.
GLG1-1	16.2 +/- 2.5	-6.7 +/- -8.2	-0.411+/--.511	0.330	398
GLG1-2	27.9 +/- 2.7	-4.7 +/- -5.3	-0.167+/--.189	0.360	399
GLG1-4	8.3 +/- 0.8	2.2 +/- 1.6	0.261+/-0.195	0.360	402
GLG1-6	4.8 +/- 1.7	-8.4 +/- -7.2	-1.777+/-*****	0.390	402
GLG1-7	1.9 +/- 0.8	-2.8 +/- -3.4	-1.484+/-*****	0.390	404
GLG1-9	1.1 +/- 0.5	-0.4 +/- -2.0	-0.401+/-*****	0.390	401

ERRORS QUOTED ARE 1 SIGMA TOTAL

GAIRLOCH CRAIB CORE 3 07/11/75

SECTION	CS-137(DPM/G)	CS-134(DPM/G)	RATIO	DRY/WET	CODE NO.
GLC3-2	68,5 +/- 6,2	12,6 +/- 4,6	0,183+/-0,066	0,277	332
GLC3-3	55,0 +/- 4,5	9,3 +/- 1,6	0,169+/-0,027	0,295	333
GLC3-4	38,2 +/- 3,1	5,2 +/- 0,9	0,135+/-0,023	0,319	334
GLC3-5	39,8 +/- 3,4	8,0 +/- 1,8	0,200+/-0,043	0,327	335
GLC3-6	29,5 +/- 2,4	4,0 +/- 0,8	0,135+/-0,026	0,343	336
GLC3-7	24,7 +/- 2,1	4,0 +/- 0,9	0,162+/-0,034	0,343	338
GLC3-8	24,5 +/- 2,0	2,9 +/- 0,9	0,119+/-0,034	0,334	339
GLC3-9	21,0 +/- 1,8	2,7 +/- 0,9	0,130+/-0,042	0,338	340
GLC3-10	15,5 +/- 1,4	2,2 +/- 0,9	0,144+/-0,055	0,337	341
GLC3-11	14,6 +/- 1,3	1,8 +/- 0,8	0,121+/-0,052	0,346	342
GLC3-12	12,8 +/- 1,2	3,6 +/- 1,0	0,284+/-0,072	0,351	343
GLC3-13	10,2 +/- 0,9	1,4 +/- 0,7	0,135+/-0,070	0,352	344
GLC3-14	9,8 +/- 1,5	0,9 +/- 2,6	0,086+/-0,267	0,366	346

ERRORS QUOTED ARE 1 SIGMA TOTAL

L.GOIL GRAVITY CORE 5 04/02/76

SECTION	CS-137(DPM/G)	CS-134(DPM/G)	RATIO	DRY/WET	CODE NO.
LGG5-1	5.6 +/- 1.4	1.5 +/- 3.0	0.263+/-0.528	0.125	393
LGG5-2	8.5 +/- 1.7	-2.1 +/- -3.2	-0.251+/--.382	0.213	394
LGG5-3	7.1 +/- 1.7	-4.8 +/- -3.6	-0.676+/--.530	0.314	395
LGG5-4	7.6 +/- 1.0	-1.7 +/- -1.7	-0.228+/--.230	0.228	396
LGG5-8	1.8 +/- 0.4	-0.1 +/- -0.9	-0.055+/--.502	0.268	397

ERRORS QUOTED ARE 1 SIGMA TOTAL

LOCH GOIL CRAIB CORE 4 03/03/76

SECTION	CS-137(DPM/G)	CS-134(DPM/G)	RATIO	DRY/WET	CODE NO.
LGC4-1	32,7 +/- 2,7	5,6 +/- 1,0	0,170+/-0,029	0,253	194
LGC4-2	50,2 +/- 4,1	6,8 +/- 1,0	0,136+/-0,016	0,310	195
LGC4-3	36,2 +/- 3,0	4,8 +/- 0,9	0,131+/-0,022	0,323	196
LGC4-4	34,1 +/- 2,8	5,3 +/- 0,8	0,156+/-0,022	0,332	197
LGC4-5	33,4 +/- 2,7	4,6 +/- 0,8	0,136+/-0,021	0,342	198
LGC4-6	30,3 +/- 2,5	4,3 +/- 0,8	0,140+/-0,023	0,357	199
LGC4-7	24,1 +/- 2,0	2,7 +/- 0,7	0,114+/-0,028	0,363	200
LGC4-8	17,5 +/- 1,5	2,1 +/- 0,7	0,119+/-0,039	0,367	201
LGC4-9	13,7 +/- 1,2	1,0 +/- 0,7	0,075+/-0,049	0,376	205
LGC4-10	9,3 +/- 0,9	1,2 +/- 0,6	0,127+/-0,059	0,383	210
LGC4-11	9,6 +/- 0,9	1,0 +/- 0,6	0,106+/-0,063	0,383	212
LGC4-12	9,3 +/- 0,9	1,5 +/- 0,6	0,159+/-0,067	0,383	213
LGC4-13	9,9 +/- 0,9	0,9 +/- 0,6	0,092+/-0,063	0,387	214
LGC4-14	10,8 +/- 1,0	1,8 +/- 0,6	0,168+/-0,055	0,386	215
LGC4-15	6,6 +/- 0,7	1,0 +/- 0,6	0,147+/-0,087	0,407	216
LGC4-16	3,2 +/- 0,5	0,9 +/- 0,6	0,280+/-0,206	0,430	217
LGC4-17	3,2 +/- 0,4	1,1 +/- 0,6	0,326+/-0,183	0,430	218

ERRORS QUOTED ARE 1 SIGMA TOTAL

LOCH GOIL CRAIB CORE 9 10/08/76

SECTION	CS-137(DPM/G)	CS-134(DPM/G)	RATIO	DRY/WET	CODE NO.
LGC9-1	48.9 +/- 4.1	5.3 +/- 1.1	0.108+/-0.020	0.233	147
LGC9-2	30.1 +/- 2.6	3.8 +/- 1.0	0.127+/-0.033	0.229	146
LGC9-3	29.5 +/- 2.4	2.5 +/- 0.6	0.086+/-0.020	0.273	145
LGC9-4	28.7 +/- 2.4	2.1 +/- 0.6	0.074+/-0.019	0.265	138
LGC9-5	21.7 +/- 1.8	2.0 +/- 0.6	0.094+/-0.028	0.297	148
LGC9-6	17.6 +/- 1.5	1.7 +/- 0.6	0.096+/-0.034	0.260	149
LGC9-7	14.7 +/- 1.3	1.1 +/- 0.5	0.072+/-0.030	0.300	151
LGC9-8	12.2 +/- 1.1	1.2 +/- 0.5	0.100+/-0.043	0.276	152
LGC9-9	6.8 +/- 0.6	1.3 +/- 0.4	0.184+/-0.056	0.324	153
LGC9-10	4.5 +/- 0.6	0.2 +/- 0.6	0.036+/-0.143	0.293	175
LGC9-11	4.6 +/- 0.6	-0.2 +/- -0.6	-0.041+/--.141	0.336	176
LGC9-12	4.3 +/- 0.6	0.1 +/- 0.7	0.034+/-0.159	0.277	177
LGC9-13	2.8 +/- 0.5	-0.4 +/- -0.7	-0.138+/--.237	0.317	179
LGC9-14	3.2 +/- 0.6	0.3 +/- 0.7	0.098+/-0.209	0.272	181
LGC9-15	3.1 +/- 0.6	-0.4 +/- -0.7	-0.134+/--.229	0.295	183
LGC9-16	3.3 +/- 0.6	0.4 +/- 0.7	0.121+/-0.212	0.273	184
LGC9-17	2.6 +/- 0.5	0.3 +/- 0.7	0.131+/-0.262	0.310	185

ERRORS QUOTED ARE 1 SIGMA TOTAL

HOLYLOCH CRAIB CORE 1 28/06/77

SECTION	CS-137(DPM/G)	CS-134(DPM/G)	RATIO	DRY/WET	CODE NO.
HLC1-1	47.5 +/- 3.9	7.1 +/- 0.9	0.150+/-0.016	0.287	408
HLC1-2	52.0 +/- 4.2	6.3 +/- 0.9	0.122+/-0.014	0.361	409
HLC1-3	53.4 +/- 4.3	6.7 +/- 0.9	0.126+/-0.014	0.390	410
HLC1-4	46.1 +/- 3.8	6.1 +/- 0.9	0.133+/-0.016	0.400	411
HLC1-5	40.8 +/- 3.4	5.1 +/- 0.9	0.124+/-0.019	0.407	412
HLC1-6	34.7 +/- 2.9	5.4 +/- 0.9	0.156+/-0.022	0.406	413
HLC1-7	30.9 +/- 2.6	5.6 +/- 0.9	0.183+/-0.025	0.406	414
HLC1-8	23.0 +/- 2.0	4.6 +/- 0.8	0.198+/-0.034	0.420	415
HLC1-9	16.4 +/- 1.5	2.4 +/- 0.7	0.146+/-0.040	0.425	416
HLC1-10	15.5 +/- 1.4	2.7 +/- 0.7	0.177+/-0.045	0.393	417

ERRORS QUOTED ARE 1 SIGMA TOTAL

LOCH GOIL CRAIB CORE 11 28/06/77

SECTION	CS-137(DPM/G)	CS-134(DPM/G)	RATIO	DRY/WET	CODE NO.
LGC11-1	13,1 +/- 2,1	3,6 +/- 2,5	0,272+/-0,192	0,031	370
LGC11-2	63,0 +/- 5,2	8,6 +/- 1,5	0,137+/-0,021	0,118	353
LGC11-3	55,6 +/- 4,5	7,1 +/- 1,0	0,127+/-0,014	0,194	355
LGC11-4	29,8 +/- 2,5	3,0 +/- 0,8	0,101+/-0,025	0,253	358
LGC11-5	22,6 +/- 1,9	2,3 +/- 0,7	0,104+/-0,029	0,279	359
LGC11-6	17,1 +/- 1,5	1,3 +/- 0,6	0,079+/-0,037	0,277	371
LGC11-7	16,1 +/- 1,5	1,4 +/- 0,7	0,086+/-0,046	0,286	361
LGC11-8	10,8 +/- 1,1	1,1 +/- 0,7	0,098+/-0,063	0,292	363
LGC11-9	7,7 +/- 0,8	-0,1 +/- -0,5	-0,018+/--,071	0,304	362
LGC11-10	7,2 +/- 0,8	0,9 +/- 0,6	0,124+/-0,082	0,310	372
LGC11-11	5,0 +/- 0,6	0,6 +/- 0,5	0,129+/-0,107	0,318	366
LGC11-12	4,1 +/- 0,5	0,0 +/- 0,5	0,009+/-0,130	0,313	367
LGC11-13	2,0 +/- 0,4	1,5 +/- 0,6	0,732+/-0,327	0,302	368
LGC11-14	3,2 +/- 1,4	-0,2 +/- -1,9	-0,064+/--,592	0,301	369

ERRORS QUOTED ARE 1 SIGMA TOTAL

LOCH GOIL CRAIB CORE 12 28/06/77

SECTION	CS-137(DPM/G)	CS-134(DPM/G)	RATIO	DRY/WET	CODE NO.
LGC12-1	60.5 +/- 5.1	6.9 +/- 1.5	0.115+/-0.024	0.127	283
LGC12-2	66.6 +/- 5.5	8.2 +/- 1.3	0.123+/-0.018	0.140	284
LGC12-3	57.5 +/- 4.7	4.9 +/- 0.7	0.086+/-0.011	0.199	286
LGC12-4	46.3 +/- 3.8	4.2 +/- 0.7	0.092+/-0.013	0.238	287
LGC12-5	26.0 +/- 2.2	3.4 +/- 0.7	0.131+/-0.026	0.265	288
LGC12-6	17.8 +/- 1.5	2.1 +/- 0.6	0.119+/-0.031	0.264	308
LGC12-7	17.7 +/- 1.6	1.8 +/- 0.6	0.101+/-0.032	0.267	309
LGC12-8	12.3 +/- 1.1	1.7 +/- 0.5	0.139+/-0.044	0.275	310
LGC12-9	10.0 +/- 1.0	1.5 +/- 0.5	0.153+/-0.051	0.292	311
LGC12-10	6.6 +/- 0.7	0.6 +/- 0.5	0.088+/-0.073	0.311	312

ERRORS QUOTED ARE 1 SIGMA TOTAL

L.LOMOND MACKARETH CORE 22/08/76

SECTION	CS-137(DPM/G)	CS-134(DPM/G)	RATIO	DRY/WET	CODE NO.
LLRP1-1	72.7 +/- 6.0	0.6 +/- 1.2	0.009+/-0.016	0.158	33
LLRP1-2	62.2 +/- 5.3	0.9 +/- 1.5	0.014+/-0.023	0.197	34
LLRP1-3	24.7 +/- 2.4	-0.8 +/- -1.3	-0.034+/--.054	0.205	35
LLRP1-4	8.4 +/- 1.2	0.3 +/- 1.2	0.040+/-0.137	0.219	36
LLRP1-5	4.8 +/- 1.0	2.0 +/- 1.2	0.418+/-0.262	0.226	37
LLRP1-7	0.1 +/- 0.7	0.6 +/- 1.0	4.700+/-*****	0.237	38
LLRP1-10	-1.6 +/- -0.7	1.5 +/- 1.0	-0.911+/--.717	0.274	39

ERRORS QUOTED ARE 1 SIGMA TOTAL

APPENDIX I.6 MISCELLANEOUS SAMPLES

****

IN THIS SECTION THE RESULTS OF ANALYSES PERFORMED ON WATER AND SEDIMENT SAMPLES NOT DISCUSSED IN THE MAIN TEXT ARE LISTED . INSUFFICIENT BACKGROUND OR SUPPORT DATA IS AVAILABLE FOR MEANINGFUL INTERPRETATION OF THESE RESULTS AND THUS THEY ARE REPORTED WITHOUT COMMENT . THE LOCATIONS OF THE EAST COAST SAMPLES (PAGE A89) ARE:

S1 56 3.8' N 3 8.8' W 10/1/78

S2 56 9.6' N 2 37.8' W 27/1/78

DECCA COORDINATES (DECCA CHARTS CHAIN 3B) FOR THE ISLE OF MAN (P.A90) RUN ARE:-

IOM1	KEPPEL PIER , I.O.M.	
IOM4	RED - D23.5	PURPLE - G77.7
IOM7	RED - D0.0	PURPLE - C54
IOM10	RED - B11	GREEN - C32

N.B. DISSOLVED OXYGEN WAS NOT MEASURED IN ANY OF THESE SAMPLES .

RESULTS FROM A CORE FROM THE CILICIA BASIN (SHAKLETON 118) ARE LISTED ON PAGE A91 . THIS CORE IS DISCUSSED IN SOME DETAIL BY SWAN (1978).

EAST COAST SAMPLES
****

CODE	DEPTH(M)	137(DPM/L)	134(DPM/L)	RATIO	SC7(DPM/L)	SAL(PM)	TEMP(C)	D.O.(PM)
S1	20.0	25.4 +/- 0.5	0.2 +/- 0.2	0.009 +/- 0.009	******	******	*****	0.0
S2	23.0	28.6 +/- 0.5	0.6 +/- 0.2	0.020 +/- 0.008	******	******	*****	0.0

ISLE OF MAN RUN 06/7
****

CODE	DEPTH(M)	137(DPM/L)	134(DPM/L)	RATIO	SC7(DPM/L)	SAL(PM)	TEMP(C)	D.O.(PM)
IOM 1	1.0	131.6 +/- 2.3	15.6 +/- 0.4	0.118 +/- 0.003	142.8	32.27	*****	0.0
IOM 4	1.0	146.8 +/- 2.5	15.6 +/- 0.4	0.106 +/- 0.003	153.6	33.45	*****	0.0
IOM 7	1.0	149.2 +/- 2.6	16.6 +/- 0.4	0.111 +/- 0.003	153.2	34.09	*****	0.0
IOM 10	1.0	192.4 +/- 3.3	22.4 +/- 0.4	0.116 +/- 0.002	197.6	34.09	*****	0.0

CILICIA BASIN GRAVITY CORE 118 12/09/72

SECTION	CS-137(DPM/G)	CS-134(DPM/G)	RATIO	DRY/WET	CODE NO.
CBGC-1	2.2 +/- 1.9	5.1 +/- 10.2	2.308+/-4.997	0.621	262
CBGC-2	0.2 +/- 0.6	-1.8 +/- -3.2	-10.082+/-*****	0.615	263
CBGC-3	0.9 +/- 0.4	0.0 +/- 0.0	0.0 +/-0.0	0.616	264
CBGC-4	0.4 +/- 0.6	0.6 +/- 3.1	1.324+/-7.550	0.623	265
CBGC-5	0.3 +/- 0.4	2.2 +/- 2.1	6.342+/-9.115	0.624	266
CBGC-6	0.2 +/- 0.3	-0.1 +/- -1.8	-0.664+/-*****	0.625	267
CBGC-7	0.1 +/- 0.4	1.1 +/- 2.1	15.291+/-*****	0.621	268
CBGC-8	0.2 +/- 0.4	3.7 +/- 2.0	21.707+/-*****	0.625	269
CBGC-9	0.1 +/- 0.3	2.3 +/- 1.9	18.188+/-*****	0.618	270
CBGC-10	0.9 +/- 0.4	0.2 +/- 2.2	0.175+/-2.425	0.636	271
CBGC-11	0.3 +/- 0.4	-0.8 +/- -2.1	-2.299+/-*****	0.988	272

ERRORS QUOTED ARE 1 SIGMA TOTAL

Appendix II · 1

Box-Model Program.

The two alternative methods of quantitatively modelling a system are via either digital or analogue simulation. In digital methods examination of the model allows the formulation of a set of equations involving both measured and unknown parameters. The unknown parameters may then be calculated, if at least an equal number of independant equations are formulated, by the iterative solution of simultaneous equations. This iterative method of solution may readily be expressed as an algorithm and the solution of a very large set of simultaneous equations performed by a digital computer.

Alternatively, in an analogue method, the model or a representation of it is physically constructed and its response evaluated. Normally this is most conveniently done by constructing an electronic circuit which alters an input waveform in a manner similar to the alteration of an input parameter by the actual model. Optimum configuration of circuit elements to duplicate measured responses may, on calibration, be related to unknown parameters. This process is normally carried out on an analogue computer which simply consists of a function generator, a circuit representation of the desired model with variable components corresponding to unknown parameters and an output device, usually a plotter or oscilloscope. In some cases, however, an analogue-type model may be evaluated by a digital program by formulating an algorithm for the model response and inputing a waveform as a discrete set of points. Variable parameters may thus be stepped through a series of values by use of 'do-loops' and the resulting number stream output may be plotted automatically to give families of curves.

In this project a digital program has been devised to examine the perturbation of input curves corresponding to ^{137}Cs concentration and $^{134}Cs/^{137}Cs$ ratios on passage through simple mixing boxes.

In the listed sample program (List A1.1), the mixing algarithm is evaluated as a subroutine (BXMX) and the main program consists of a series of setup and input steps (Cards 1-17) followed by the first call to the subroutine (Card 18). The second mixing box is obtained by feeding the first J of the curves produced by the first box back through the subroutine (Cards 19-25), where the upper limit of J is determined by the number of curves generated by the subroutine. The remaining cards (26-29) simply terminate the program. In the subroutive BXMX after setup (Cards 1-7), the input curves are transformed into a series of K curves corresponding to values of the box residence half time of 1 - K months. Integral values of $\tau_{\frac{1}{2}}$ in months were chosen as the step size as this was the minimum value which could be reasonably chosen bearing in mind the monthly sampling frequency determining the input curves. After setting initial parameters (Cards 8-14), the first loop (Cards 15-27) calculate and store the derived ^{137}Cs content and $^{134}Cs/^{137}Cs$ ratio in the box over a series of monthly increments taking into account the fraction of original content lost each month, the corresponding amount input during that month, and in the case of ^{134}Cs, the extent of decay during the one month period (decay of ^{137}Cs being regarded as insignificant over the periods studied). The second loop (Cards 34-40) outputs the data streams as a series of curves drawn by an interfaced plotter with an additional option of alternating curve colour between black and red (Cards 30-32) for ease of analysis. In this program, although both values of derived ^{137}Cs concentration and ratio are output on the

lineprinter, only one or other of these parameters may be output on the plotter during any one run, the parameter output being determined by the content of the A matrix. Inputing TOT values into this matrix results in plotting of ^{137}Cs curves while input of RTT results in plots of ratio curves.

By the use of the BXMX subroutive, the program is rendered very versatile, e.g. the program could be expanded to include a third box by a further level of do-loop in the main program (external to the Do 200 loop) and expansion of the X and Y matrices to 3 dimensions, the main limit to this procedure being the vast amount of data generated - in particular with respect to plotter-time as even a 2-box model requires plot time of ~1 hour.

```
0001              COMMON A(100),B(100),C7(100),CR(100),N,X(10,100),Y(10,100)
0002              COMMON JZ
0003              CALL PAPER(1)
0004              JZ=1
0005              RN=1.0
0006              READ(5,10)N
0007              WRITE(6,15)N
0008           10 FORMAT(I3)
0009           15 FORMAT(1H0,10X,I3)
0010              DO50 I=1,N
0011              READ(5,20) C7(I),CR(I)
0012              WRITE(6,30)C7(I),CR(I)
0013           50 CONTINUE
0014              WRITE(6,40)
0015           20 FORMAT(F4.1,F4.3)
0016           30 FORMAT(1H ,10X,F8.2,5X,F8.4)
0017           40 FORMAT(1H1,80(1H*))
0018              CALL BXMX
0019              DO 200 J=1,3
0020              DO 250 K=1,N
0021              C7(K)=X(J,K)
0022              CR(K)=Y(J,K)
0023          250 CONTINUE
0024              CALL BXMX
0025          200 CONTINUE
0026          999 CONTINUE
0027              CALL GREND
0028              STOP
0029              END
```

```
0001            SUBROUTINE BXMX
0002            COMMON A(100),B(100),C7(100),CR(100),N,X(10,100),Y(10,100)
0003            COMMON JZ
0004            CALL BLKPEN
0005            CALL CTRMAG (12)
0006            CALL MAP(0.0,75.0,0.0,0.0,0.27)
0007            CALL SCALSI(12.0,0.05)
0008            DO60 K=1,16
0009            RN=FLOAT(K)
0010            TOT=20.0
0011            RTT=0.175
0012            FN=-0.693/RN
0013            FR=EXP(FN)
0014            FR=1.0-FR
0015            DO100 I=1,N
0016            RTT=0.974*(((1.0-FR)*RTT*TOT)+(FR*C7(I)*CR(I)))
0017            TOT=((1.0-FR)*TOT)+(FR*C7(I))
0018            RTT=RTT/TOT
0019            WRITE(6,30)TOT,RTT
0020         30 FORMAT(1H ,10X,F8.2,5X,F8.4)
0021            A(I)=RTT
0022            B(I)=TOT
0023            IF(JZ.GE.2) GOTO 90
0024            X(K,I)=TOT
0025            Y(K,I)=RTT
0026         90 CONTINUE
0027        100 CONTINUE
0028            WRITE(6,40)
0029         40 FORMAT(1H1,80(1H*))
0030            IF(K.EQ.5)CALL REDPEN
0031            IF(K.EQ.9)CALL BLKPEN
0032            IF(K.EQ.13) CALL REDPEN
0033            NJ=N-1
0034            DO120 I=1,NJ
0035            F=FLOAT(I)
0036            CALL POINT (F,A(I))
0037            J=I+1
0038            G=F+1.0
```

```
0039            CALL JOIN(G,A(J))
0040          120 CONTINUE
0041           60 CONTINUE
0042              JZ=JZ+1
0043              CALL FRAME
0044              RETURN
0045              END
```

Appendix II.2 Calculation and Presentation Programs

A suite of computer programs were written in FORTRAN IV to perform the basic calculations described in Chapter 2. In addition, these programs input all relevant data on each sample allowing comprehensive results tabulation in the form presented in Appendix I. A further set of subroutines have been devised to allow selected data to be output graphically on a plotter. While details of the program vary according to the detector (flat-top NaI (Tl), well NaI (Tl), Ge (Li)) and sample (water, sediment, organics), there is a common basis. This is illustrated by describing, in turn, programs for the calculation of results from water samples counted on the flat-top NaI (Tl) and sediment samples on the Ge (Li), both of which are listed at the end of this section.

After an identifying comment card, the first two lines of the flat-top program assign variable names to a common block and dimension matrices. Line 3 switches on the plotter if graphical output is desired. Lines 4-6 read in the number of water profiles (MCT) and define a default. Lines 7 and 8 read in a title (TITLE) for graphical output. The main loop (lines 9-48) is passed once for each profile and consists of title and table headings output (lines 11-16) followed by a calculations loop (lines 18-45) passed once for each sample in the profile, the number of which (NX) is read in line 10. Within the calculation loop, input data includes the number of counts in the Cs-137 window (C7), the number in the Cs-134 window (C4), the number of days between sampling and counting (DY), printout code number (IW), sample volume (VL), count time (TM), sample position and date (T1-6), depth (D), salinity (S), temperature (T) and dissolved oxygen concentration (O). Output data calculated by the program are Cs-137 activity (A), Cs-134 activity (B), 134/137 ratio (R), the errors ($1\sigma_{TOTAL}$) on these measurements (E, F and G respectively) and the salinity corrected Cs-137 activity (X).

The drawing subroutine (DRAW) graphs each data point in depth/activity space, draws error bars and connects points on each profile. Lines 1-9 set up the subroutine, define plot space, draw and label axes and output graph title. The loop defined by lines 10-24 is passed once for each sample in the profile while loop DO15 connects the data points. This program is very flexible and may be readily altered to output graphically profiles (with or without error bars) of any input or calculated parameter while multiple graphs may be handled via the CALL FRAME command - controlled either internally or externally.

The Ge (Li) program is essentially similar to that for the NaI (Tl) although, as discussed in Chapter 2, the calculation steps are somewhat simpler. The drawing subroutine in this program, however, plots a separate graph of the variation of Cs-137 (full line) and Cs-134 (broken line) activity with depth for each profile - in this particular case plotting salinity corrected activities against depth in mg cm^{-2} (cf Chapter 6) without error bars. Again this program may be readily converted to plot profiles of any included parameter while, if not required, the salt correction steps (38-48) may be omitted.

Finally, it must be noted that, prior to transfer of these programs to a compiler outside the NUMAC system, a list of variable names (List A2.3) together with any dummy variable used must be checked against those prohibited (system used) by that particular assembly to prevent I.D. conflict failures.

```
      C  CS137/134 PEAK INTEGRATION PROGRAM
0001     CALL PAPER(1)
      C
      C     CORE INTEGRATION PROGRAM
      C
      C     DIMENSION STATEMENT
0002     DIMENSION A7(20),A4(20),WT(20),TM(20),KN(20),DW(20),TIT(20),RAT(20
        1),ERT(20),AB(20,2),DP(20),B7(20),B4(20),BB(20,5),E7(20),E4(20),F7(
        220),F4(20)
0003     DIMENSION WW(99),CW(99),CC(99),FF(99),PW(99)
0004     COMMON A(100),B(100),E(100),F(100),JD(100),I,TITLE(15)
0005     COMMON ZD(100)
      C     READ LOOP CONTROLER  1=START  0=STOP
0006    1 READ(5,10)ILC
0007   10 FORMAT(I2)
0008     IF(ILC.EQ.0) GOTO 999
      C     READ IDENTIFIER
0009     READ(5,20)(TIT(IJ),IJ=1,20)
0010   20 FORMAT(20A4)
0011     READ(5,25)AA,ZZ
0012   25 FORMAT(2F5.3)
0013     ZW=0.0
0014     DO 15 KX=1,15
0015     TITLE(KX)=TIT(KX)
0016   15 CONTINUE
      C     READ NUMBER OF SAMPLES
0017     READ(5,10)JN
0018     I=JN
      C     DATA INPUT - IDENT,WT.,137,134,DRY/WET,G=NO.,EXTRA DATA.
0019     DO 100 JX=1,JN
0020     READ(5,30)(AB(JX,J),J=1,2),WT(JX),A7(JX),A4(JX),TM(JX),DW(JX),KN(J
        1X),JD(JX),(BB(JX,J),J=1,5)
0021     READ(5,40)DD,WW(JX)
0022   30 FORMAT(2A4,F6.4,F10.2,F7.2,F5.1,F8.5,I4,I7,5X,5A4)
0023   40 FORMAT(A4,4X,F6.4)
0024  100 CONTINUE
0025     WRITE(6,110)
0026  110 FORMAT(1H1,2X,'RED.WT.',4X,'RED.137',4X,'RED.134')
      C     CALCULATIONS
0027     DO 200 JY=1,JN
```

```
0028                BC7=(A7(JY)-352.2)
0029                BC4=(A4(JY)-381.0)
0030                B7(JY)=(0.06614*BC7/WT(JY))*EXP(0.000633*TM(JY))
0031                B4(JY)=(0.07711*BC4/WT(JY))*EXP(0.000941*TM(JY))
0032                E4(JY)=(SQRT(A4(JY)+381.0)/BC4)
0033                E7(JY)=(SQRT(A7(JY)+352.2)/BC7)
0034                F7(JY)=(SQRT((E7(JY)**2)+0.00624)*B7(JY))
0035                F4(JY)=(SQRT((E4(JY)**2)+0.00624)*B4(JY))
0036                RAT(JY)=(B4(JY)/B7(JY))
0037                ERT(JY)=(SQRT((E7(JY)**2)+(E4(JY)**2))*RAT(JY))
                C       SALT CORRECTION OPTION
0038                V=(WW(JY)/DW(JY))-WW(JY)
0039                SW=(WW(JY)-(0.0318*V))
0040                ZW=ZW+SW
0041                QW=ZW+(0.5*SW)
0042                ZD(JY)=QW/25.52
0043                CC(JY)=((B7(JY)*WW(JY))-(AA*V))/SW
0044                FF(JY)=((B4(JY)*WW(JY))-(ZZ*V))/SW
0045                A(JY)=CC(JY)
0046                B(JY)=FF(JY)
0047                QW=QW/25.52
0048                WRITE(6,120)QW,A(JY),B(JY)
0049              120 FORMAT (1H0,4F10.4)
0050              200 CONTINUE
                C       OUTPUT
0051                WRITE(6,410)(TIT(IJ),IJ=1,20)
0052              410 FORMAT(1H1,10X,80(1H*)/30X,20A4/11X,80(1H*)//11X,'SECTION',3X,'CS-
                    1137(DPM/G)',5X,'CS-134(DPM/G)',5X,'RATIO',7X,'DRY/WET',2X,'CODE NO
                    2,')
0053                DO 500 JW=1,JN
0054                WRITE(6,420)(AB(JW,J),J=1,2),B7(JW),F7(JW),B4(JW),F4(JW),RAT(JW),E
                    1RT(JW),DW(JW),KN(JW)
0055              500 CONTINUE
0056              420 FORMAT(1H0,10X,2A4,2X,F5.1,' +/- ',F4.1,2X,F5.1,' +/- ',F4.1,F8.3,
                    1'+/-',F5.3,3X,F5.3,4X,I4)
0057                WRITE(6,510)
0058                WRITE(6,555)
0059              510 FORMAT(1H0,20X,'ERRORS QUOTED ARE 1 SIGMA TOTAL')
0060              555 FORMAT(1H0,10X,80(1H*))
0061                CALL DRAW
0062                GOTO 1
0063              999 CONTINUE
0064                CALL GREND
0065                STOP
0066                END
```

A101

```
0001              SUBROUTINE DRAW
0002              COMMON A(100),B(100),E(100),F(100),JD(100),I,TITLE(15)
0003              COMMON ZD(100)
0004              CALL CTRMAG(14)
0005              CALL PLOTCS(0.3,0.90,TITLE,60)
0006              CALL CTRMAG(12)
0007              CALL PSPACE(0.2,0.8,0.2,0.8)
0008              CALL SCALE(0.8,0.8)
0009              CALL MAP(0.0,90.0,6.0,-0.5)
0010              CALL SCALES
0011              CALL CTRMAG(10)
0012              I=I-1
0013              DO30 KM=1,I
0014              CALL POINT(A(KM),ZD(KM))
0015              KK=KM+1
0016              CALL JOIN (A(KK),ZD(KK))
0017           30 CONTINUE
0018              CALL BROKEN(5,5,4,4)
0019              DO50 KM=1,I
0020              CALL POINT(B(KM),ZD(KM))
0021              KK=KM+1
0022              CALL JOIN (B(KK),ZD(KK))
0023           50 CONTINUE
0024              CALL FULL
0025              CALL FRAME
0026              CALL PSPACE (0.05,0.95,0.05,0.95)
0027              RETURN
0028              END
```

```
C       NAI (FLAT-TOP) SPECTRUM
0001    COMMON YSCS(20,20),XSCS(20,20),XERS(20,20),NX(20),TITLE(15),MCT
0002    DIMENSION A(99),B(99),C(99),S(99),T(99),O(99),T1(99),D(99),E(99),F
       1(99),G(99),R(99),X(99)
0003    CALL PAPER(1)
0004     10 READ(5,99) MCT
0005     99 FORMAT(I2)
0006    IF(MCT.EQ.0.0) GOTO999
0007    READ(5,110)(TITLE(KX),KX=1,15)
0008    110 FORMAT(15A4)
0009    DO 800 IX=1,MCT
0010    READ(5,99) NX(IX)
0011    READ(5,110)(TT(K),K=1,15)
0012    WRITE(6,120)(TT(K),K=1,15)
0013    120 FORMAT(1H1,20X,15A4/20X,60(1H*))
0014    WRITE(6,130)
0015    130 FORMAT(//10X,'CODE',4X,'DEPTH(M)',3X,'137(DPM/L)',5X,'134(DPM/L)',
       15X,'RATIO',7X,'SC7(DPM/L)  SAL(PM)  TEMP(C)  D.O.(PM)')
0016    KQ=NX(IX)
0017    DO 100 J=1,KQ
0018    READ(5,20) C7,C4,DY,IW,VL,TM,T1,T2,T3,T4,T5,T6,D(J),S(J),T(J),O(J)
0019     20 FORMAT(2(F10.2,10X),F10.2,I8,F12.5,F5.2/3A4,2X,3A4/4F10.2)
0020    IF(TM.EQ.0.0) TM=800.0
0021    IF(S(J).EQ.0.0) S(J)=0.0001
0022    IF(VL.EQ.0.0) VL=10.0
0023    B7=13.778375*TM
0024    B4=8.098*TM
0025    FC=EXP(0.0000628*DY)/(0.057218*TM*VL)
0026    FD=EXP(0.0009255*DY)/(0.048000*TM*VL)
0027    A(J)=(((C7-B7)-1.3532*(C4-B4))/0.99732)
0028    B(J)=((C4-B4)-0.00198*A(J))*FD
0029    A(J)=A(J)*FC
0030    R(J)=B(J)/A(J)
0031    X(J)=A(J)*(35.0/S(J))
0032    C7=C7+B7
0033    C4=C4+B4
0034    EC=SQRT((C7+1.83115*C4)**(FC/0.99732)
0035    ED=SQRT(C4)*FD
0036    ER=SQRT(((EC/A(J))**2)+((ED/B(J))**2) )
0037    E(J)=SQRT((EC**2)+((0.07*A(J))**2))
```

```
0038            F(J)=SQRT((ED**2)+((0.0E7*B(J))**2))
0039            G(J)=ER*R(J)
0040            XSCS(IX,J)=X(J)
0041            YSCS(IX,J)=D(J)
0042            XERS(IX,J)=E(J)
0043            WRITE(6,60)T1,T2,D(J),A(J),E(J),B(J),F(J),R(J),G(J),X(J),S(J),T(J)
               1,O(J)
0044             60 FORMAT(/10X,2A4,F5.1,2(F6.1,' +/= ',F4.1),F7.3,' +/= ',F5.3,F7.1,6
               1X,3(F6.2,3X))
0045            100 CONTINUE
0046                WRITE (6,560)
0047            560 FORMAT(1H1,99(1H*))
0048            800 CONTINUE
0049                CALL DRAW
0050            999 CONTINUE
0051                CALL GREND

0001                SUBROUTINE DRAW
0002                COMMON YSCS(20,20),XSCS(20,20),XERS(20,20),NX(20),TITLE(15),MCT
0003                CALL CTRMAG(14)
0004                CALL PLOTCS(0.3,0.97,TITLE,60)
0005                CALL CTRMAG(12)
0006                CALL PLOTCS(0.75,0.05,'CS=137    PCI/L',15)
0007                CALL PLOTCS(0.05,0.96,'DEPTH (M)',9)
0008                CALL MAP (75.0,150.0,85.0,-5.0)
0009                CALL SCALES
0010                DO20 I=1,MCT
0011                INX=NX(I)
0012                DO10 J=1,INX
0013                XU=XSCS(I,J)-XERS(I,J)
0014                XV=XSCS(I,J)+XERS(I,J)
0015                CALL POINT (XU,YSCS(I,J))
0016                CALL JOIN  (XV,YSCS(I,J))
0017             10 CONTINUE
0018                IMX=INX-1
0019                DO15 K=1,IMX
0020                CALL POINT (XSCS(I,K),YSCS(I,K))
0021                IK=K+1
0022                CALL JOIN (XSCS(I,IK),YSCS(I,IK))
0023             15 CONTINUE
0024             20 CONTINUE
0025                RETURN
0026                END
```

LIST A2.3 VARIABLE NAMES

1) Flat-top NaI (Tl), water samples.

MCT	number of water profiles
TITLE	graph title
NX	number of samples in particular profile
TT	table heading
C7	number of counts in Cs-137 window
C4	" " " " Cs-134 "
DY	decay time (days)
IW	printout number
VL	sample volume (litres)
TM	count time (minutes)
T1 - T6	location and date
D	sample depth (metres)
S	" salinity (°/oo)
T	" temperature (C)
O	" D.O. concentration (°/oo)
B7	background in Cs-137 window (c.p.m.)
B4	" " Cs-134 " "
A	Cs-137 concentration ($d.p.m.l^{-1}$)
E	error on Cs-137 "
B	Cs-134 concentration "
C	error on Cs-134 "
R	Cs-134/Cs-137 ratio
G	error on ratio
X	salinity corrected Cs-137 concentration ($d.p.m.l^{-1}$)

2) Ge (Li), sediment samples

ILC	loop controller (external)
TIT	title
AA	concentration of Cs-137 in ambient sea water ($d.p.m.l^{-1}$)
ZZ	" " Cs-134 " " " " "
JN	number of samples in profile
AB	sample code
WT	sample weight (g)
A7	number of counts in Cs-137 window
A4	" " " " Cs-134 "
TM	decay time (days)
DW	dry/wet ratio
KN	printout number
JD	sample depth (cm)
BB	sample location and date
DD	check code
WW	dry weight of core section
QW	salinity corrected sample depth ($mg.cm^{-2}$)
A	" " Cs-137 activity ($d.p.m.g^{-1}$)
B	" " Cs-134 " "
B7	Cs-137 activity ($d.p.m.g^{-1}$)
B4	Cs-134 " "
F7	total error (1) on Cs-137 ($d.p.m.g^{-1}$)
F4	" " " " Cs-134 "
RAT	Cs-134/Cs-137 ratio
ERT	total error on ratio